

# Single Phase Heat Exchangers

PERFORMANCE  
TEST CODES



**AN AMERICAN NATIONAL STANDARD**

**ASME  
PTC 12.5-2000**

# Single Phase Heat Exchangers



The American Society of  
Mechanical Engineers

**PERFORMANCE  
TEST CODES**

Date of Issuance: December 31, 2001

This Standard will be revised when the Society approves the issuance of a new edition. There will be no addenda issued to ASME PTC 12.5-2000.

Please note: ASME issues written replies to inquiries concerning interpretation of technical aspects of this document.

ASME is the registered trademark of The American Society of Mechanical Engineers.

This code or standard was developed under procedures accredited as meeting the criteria for American National Standards. The Standards Committee that approved the code or standard was balanced to assure that individuals from competent and concerned interests have had an opportunity to participate. The proposed code or standard was made available for public review and comment that provides an opportunity for additional public input from industry, academia, regulatory agencies, and the public-at-large.

ASME does not "approve," "rate," or "endorse" any item, construction, proprietary device, or activity.

ASME does not take any position with respect to the validity of any patent rights asserted in connection with any items mentioned in this document, and does not undertake to insure anyone utilizing a standard against liability for infringement of any applicable letters patent, nor assume any such liability. Users of a code or standard are expressly advised that determination of the validity of any such patent rights, and the risk of infringement of such rights, is entirely their own responsibility.

Participation by federal agency representative(s) or person(s) affiliated with industry is not to be interpreted as government or industry endorsement of this code or standard.

ASME accepts responsibility for only those interpretations of this document issued in accordance with the established ASME procedures and policies, which precludes the issuance of interpretations by individuals.

No part of this document may be reproduced in any form,  
in an electronic retrieval system or otherwise,  
without the prior written permission of the publisher.

The American Society of Mechanical Engineers  
Three Park Avenue, New York, NY 10016-5990

Copyright © 2001 by  
THE AMERICAN SOCIETY OF MECHANICAL ENGINEERS  
All Rights Reserved  
Printed in U.S.A.

## FOREWORD

Performance tests of industrial heat exchangers are often conducted to compare test results with manufacturer's rating data, to evaluate the cause(s) of degradation, to verify regulatory compliance, or to assess process improvements. All tests have associated costs. Those costs can be great if the test results are inconclusive. Historically, testing heat exchanger performance in operating processes was not conducted according to standard, acceptable methods; therefore, the results were inconsistent. Many of the unacceptable results have been attributed to small deviations in test conditions and measurement practices. In other cases, analysis of the data did not consider all factors which affect performance.

As industry implements improvements to reduce costs and increase output, performance margins of process streams tend to be reduced. The need for accurate performance test methods is increasing to meet the commercial demand. A single consistent test philosophy and methodology including measurement and analysis techniques for delivery of accurate and repeatable heat exchanger test data would provide a foundation to assess performance. Such a test standard has wide applicability in the power, food-processing, chemical and petroleum industries, among others. It was with the intent of satisfying these industry needs that the Board on Performance Test Codes (BPTC) authorized the formation of the PTC 12.5 Committee to explore the development of the present Code.

The PTC 12.5 Committee began its deliberations late in 1994. An early version of the draft code was subjected to a thorough review by industry, including members of the BPTC. Comments were incorporated in the version which was approved by the Committee on 11 August 1999. PTC 12.5-2000 on Single Phase Heat Exchangers was then approved as a Standard practice of the Society by action of the Board on Performance Test Codes on 8 May 2000. It was approved as an American National Standard by the ANSI Board of Standards Review on September 26, 2000.

(Revised 26 September 2000)

## NOTICE

All Performance Test Codes **MUST** adhere to the requirements of **PTC 1, GENERAL INSTRUCTIONS**. The following information is based on that document and is included here for emphasis and for the convenience of the user of this Code. It is expected that the Code user is fully cognizant of Parts I and III of PTC 1 and has read them prior to applying this Code.

ASME Performance Test Codes provide test procedures which yield results of the highest level of accuracy consistent with the best engineering knowledge and practice currently available. They were developed by balanced committees representing all concerned interests. They specify procedures, instrumentation, equipment operating requirements, calculation methods, and uncertainty analysis.

When tests are run in accordance with this Code, the test results themselves, without adjustment for uncertainty, yield the best available indication of the actual performance of the tested equipment. ASME Performance Test Codes do **not** specify means to compare those results to contractual guarantees. Therefore, it is recommended that the parties to a commercial test agree **before starting the test and preferably before signing the contract** on the method to be used for comparing the test results to the contractual guarantees. It is beyond the scope of any Code to determine or interpret how such comparisons shall be made.

Approved by Letter Ballot #95-1 and BPTC Administrative Meeting of March 13–14, 1995.

**PERSONNEL OF PERFORMANCE TEST CODE COMMITTEE NO. 12.5  
ON SINGLE PHASE HEAT EXCHANGERS**

**OFFICERS**

**Thomas G. Lestina**, *Chair*  
**Benjamin H. Scott**, *Vice Chair*  
**George Osolobe**, *Secretary*

**COMMITTEE PERSONNEL**

**Fernando J. Aguirre**, Heat Transfer Research, Inc.  
**Kenneth J. Bell**, Oklahoma State University  
**Charles F. Bowman**, Chuck Bowman Associates  
**William H. Closser, Jr.**, C&A Consulting Service  
**Samuel J. Korellis**, Dynegy Midwest Generation  
**Thomas G. Lestina**, MPR Associates  
**Jayesh Modi**, Yuba Heat Transfer  
**Kalyan K. Niyogi**, Holtec International  
**Matthew M. Pesce**, Consultant  
**Joseph M. Pundyk**, PFR Engineering Systems  
**Benjamin H. Scott**, Calvert Cliffs Nuclear Power Plant, Inc.  
**Euan F. Somerscales**, Consultant

## BOARD ON PERFORMANCE TEST CODES

### OFFICERS

**P. M. Gerhart**, *Chair*  
**S. J. Korellis**, *Vice Chair*  
**W. O. Hays**, *Secretary*

### COMMITTEE PERSONNEL

R. P. Allen	Y. Goland	A. L. Plumley
R. L. Bannister	R. S. Hecklinger	R. R. Priestley
D. S. Beachler	T. C. Heil	J. W. Siegmund
B. Bornstein	D. R. Keyser	J. A. Silvaggio
J. M. Burns	P. M. McHale	W. G. Steele
A. J. Egli	J. W. Milton	J. C. Westcott
J. R. Friedman	G. H. Mittendorf	J. G. Yost
G. J. Gerber	S. P. Nuspl	

## CONTENTS

Foreword . . . . .		iii
Notice . . . . .		iv
Committee Roster . . . . .		v
Board Roster . . . . .		vi
<b>Section</b>		
0	Introduction . . . . .	1
1	Object and Scope. . . . .	3
2	Definitions and Description of Terms . . . . .	5
3	Guiding Principles . . . . .	13
4	Instruments and Methods of Measurement. . . . .	19
5	Computation of Results. . . . .	23
6	Report of Results . . . . .	33
7	References . . . . .	35
<b>Figure</b>		
5.1	Comparison of Measured Hot and Cold Stream Heat Loads . . . . .	25
<b>Tables</b>		
3.1	Typical Heat Exchanger Mechanical Data Needed for Performance Analysis . . . . .	15
3.2	Typical Heat Exchanger Thermal Model Parameters Needed for Performance Analysis . . . . .	15
<b>Nonmandatory Appendices</b>		
A	Steady State Criteria . . . . .	39
B	Equations and Coefficients for Uncertainty Analysis. . . . .	43
C	The Delaware Method for Shell-Side Performance. . . . .	47
D	Mean Temperature Difference. . . . .	75
E	Derivation of Performance Equations . . . . .	97
F	Tube-Side Performance Methods. . . . .	103
G	Fouling Resistance . . . . .	107
H	Plate Frame Performance Methods . . . . .	111
I	Thermal Physical Properties . . . . .	113
J	Room Cooler Performance Methods . . . . .	115
K	Examples . . . . .	119

This page intentionally left blank.

## SECTION 0 — INTRODUCTION

Performance testing of industrial heat exchangers is conducted to compare installed capability with design specifications, assess degradation, and evaluate the benefit of performance improvements such as cleanings, heat transfer surface enhancements and unit replacement. Industrial and experimental experience indicates that results can vary significantly with small changes in the test and analysis methods. Application of detailed and consistent test practices is needed for reliable and accurate results. A commercial standard for heat exchanger testing provides a basis for comparison of results from different test organizations and designs.

This Test Code provides comprehensive guidance to plan, conduct, and analyze results for accurate performance tests of single phase heat exchangers. The key test requirements are applicable to most heat exchanger designs with two single phase fluid streams in a wide variety of industrial applications.

Guidance is sufficiently detailed for a test engineer to estimate the cost and benefit of performing an accurate test. Step-by-step examples are provided for shell-and-tube, plate-frame, and room air cooler designs. Even though the guidance is comprehensive, flexibility is provided to permit a variety of analysis methods. The user may perform Code calculations using the data provided, proprietary computer software, or other analytic tools.

During the development of this Code, data from the open literature has been compiled and evaluated in order to establish a basis for the accuracy of test results. The appendices provide a description of these evaluations for technical topics including steady state criteria, uncertainty analysis, shell-side performance methods, mean temperature difference, tube-side performance methods, fouling resistance, plate-frame performance methods, room cooler analysis, and thermal physical properties. These appendices provide valuable background material for the user.

This page intentionally left blank.

## SECTION 1 — OBJECT AND SCOPE

### 1.1 OBJECT

This Code provides methods and procedures for testing single phase heat exchangers. The Code presents and describes the methods for determining heat exchanger performance, for measuring fluid conditions and related phenomena, and for projecting performance parameters to reference conditions. Performance parameters included are overall heat transfer coefficient, heat transfer rate, and pressure drop. Guidelines are provided for recommended instrumentation and accuracy.

### 1.2 SCOPE

The scope of this Code includes instruments, calculation techniques, and methods to determine the steady state performance of single phase heat exchangers at both test conditions and reference conditions. This Code applies to, but is not limited to, the following types of heat exchangers:

- (a) Shell-and-tube;
- (b) Plate-frame;
- (c) Plate-fin;
- (d) Tube-in-plate fin.

Single-phase fluid streams, including liquid-to-liquid, gas-to-liquid, and gas-to-gas are included. Excluded from this Code are heat exchangers used in condensation, vaporization, fired, direct contact, non-newtonian fluid, and more than two-fluid applications.

### 1.3 EXPECTED UNCERTAINTY

The values of the overall uncertainty of performance parameters determined in accordance with this Code are expected to lie within the band described by the overall uncertainty interval stated below.

Performance Parameter [Note (1)]	Expected Uncertainty [Note (2)]
Overall Heat Transfer Coefficient, $U^*$	$\pm 3-10\%$
Heat Transfer Rate, $Q^*$	$\pm 3-10\%$
Nozzle-to-Nozzle Pressure Loss, $\Delta P_{n-n}^*$	$\pm 3-12\%$

#### NOTES:

- (1) At reference conditions.
- (2) Based on 95% confidence.

This page intentionally left blank.

## SECTION 2 — DEFINITIONS AND DESCRIPTION OF TERMS

### 2.1 TERMS

In this Section, only those terms are defined which are characteristic of single-phase heat exchangers and the requirements for testing them. For the definition of all other physical terms, or the description of instruments used in this Code, reference is made to the literature and particularly to PTC 2, Definitions and Values, and to the PTC 19 Series on Instruments and Apparatus.

*calibration uncertainty*: the uncertainty attributed to instrument calibration practices including the instrument linearity, hysteresis, and repeatability along with the accuracy of the calibration equipment.

*cold stream*: flow stream with the lower heat exchanger inlet temperature.

*cold stream temperature change*: the difference between the outlet and inlet temperatures of the cold stream ( $t_o - t_i$ ).

*design conditions*: performance conditions upon which the design of the heat exchanger was based.

*effective mean temperature difference*: the log mean temperature difference corrected for deviations from true countercurrent flow conditions.

*fouling*: accumulated foreign material such as corrosion products or any other deposits on the heat transfer surface.

*heat transfer area*: the area of the wall surface over which heat is transferred from the hot fluid to the cold fluid (see para. 3.2.3).

*heat transfer rate*: the amount of heat transferred from the hot stream to the cold stream per unit of time.

*hot stream*: flow stream with the higher heat exchanger inlet temperature.

*hot stream temperature change*: the difference between the inlet and outlet temperatures of the hot stream ( $T_i - T_o$ ).

*hydraulic resistance*: resistance to flow due to form losses and friction in the heat exchanger.

*log mean temperature difference*: the logarithmic average temperature difference defined by Eqs. (D.1.) and (D.2). Except where otherwise noted, the log mean temperature difference for countercurrent flow is used in this Code.

*overall heat transfer coefficient*: the heat transfer rate per unit of heat transfer area per unit of effective mean temperature difference.

*overlap of error bar*: that portion of the uncertainty interval in which the true value must lie and still fall within the uncertainty interval of two or more measurements of the same value.

*pressure loss*: loss of total pressure across the heat exchanger due to hydraulic resistance.

*process variables*: hot and cold stream inlet and outlet temperatures and flow rates.

*reference conditions*: process operating conditions defined by fixing four of the six variables (see para. 3.2.2).

*sensitivity coefficient*: the change in the calculated result due to an incremental change in a contributing factor. For an arbitrary result  $Y$  and contributing factor  $x$ , the sensitivity coefficient is  $\Theta_{Y,x} = \partial Y / \partial x$ .

*temperature difference*: the difference between a hot stream temperature and the corresponding cold stream temperature.

*test run*: a complete set of performance data that will allow analysis of heat exchanger capability per this Code.

*total measurement uncertainty*: the uncertainty in measurement due to the combined effects of all systematic error (or bias) and random error associated with instrument calibration, spatial variation, installation practices, data acquisition, and process variations (see para. 5.2.3).

*uncertainty*: the uncertainty is the interval about the measurement or result that contains the true value for a given confidence level (see ASME PTC 19.1).

## 2.2 LETTER SYMBOLS

Symbols used in multiple sections of this Code are described here. Symbols which are not in this list are defined in the text immediately following

their usage. The equations in this Code are based on any consistent set of units. The units in the following list are one example of consistent units both for U.S. Customary and SI/metric systems.

Symbol	Definition	Units	
		U.S. Customary	SI
$A$	Reference heat transfer area (see para. 3.2.3)	ft <sup>2</sup>	[m <sup>2</sup> ]
$A_c$	Cold side heat transfer area	ft <sup>2</sup>	[m <sup>2</sup> ]
$A_h$	Hot side heat transfer area	ft <sup>2</sup>	[m <sup>2</sup> ]
$A_{i, pipe}$	Flow area of inlet pipe	ft <sup>2</sup>	[m <sup>2</sup> ]
$A_{o, pipe}$	Flow area of outlet pipe	ft <sup>2</sup>	[m <sup>2</sup> ]
$A_w$	Heat transfer area of wall	ft <sup>2</sup>	[m <sup>2</sup> ]
$b_{cal}$	Systematic uncertainty attributed to calibration	Units of measurement parameter	
$b_{DataAcq}$	Systematic uncertainty attributed to data acquisition	Units of measurement parameter	
$b_{EMTD, mixing}$	Systematic uncertainty attributed to a non-uniform temperature distribution over a flow cross section	°F	[°C]
$b_{EMTD, U}$	Systematic uncertainty attributed to a variable heat transfer coefficient along the flow length	°F	[°C]
$b_{install}$	Systematic uncertainty attributed to instrument installation practices	Units of measurement parameter	
$b_{SpatVar}$	Systematic uncertainty attributed to spatial variation	Units of measurement parameter	
$c_p$	Constant pressure specific heat	Btu/(lbm-°F)	[J/(kg-°C)]
$c_{p, c}$	Constant pressure specific heat of the cold stream	Btu/(lbm-°F)	[J/(kg-°C)]
$c_{p, h}$	Constant pressure specific heat of the hot stream	Btu/(lbm-°F)	[J/(kg-°C)]
$d_i$	Inside tube diameter	ft	[m]
$d_o$	Outside tube diameter	ft	[m]
	Outside diameter of unfinned portion of tube	ft	[m]
$EMTD$	Effective mean temperature difference	°F	[°C]
$F$	Configuration correction factor for deviation from true countercurrent flow (see Appendix D)	Dimensionless	

Symbol	Definition	Units	
		U.S. Customary	SI
$g$	Gravitational acceleration	ft/hr <sup>2</sup>	[m/s <sup>2</sup> ]
$g_c$	Units conversion constant, 4.17(10 <sup>8</sup> ) in U.S. Customary units, [1 in metric units]	lbm-ft/lbf-hr <sup>2</sup>	[kg-m/N-s <sup>2</sup> ]
$H_R$	Calculated hydraulic resistance = $\Delta P/m^n$ (see para. 5.4.7)	(lbf/ft <sup>2</sup> )(hr/lbm) <sup>n</sup>	[Pa/(s/kg) <sup>n</sup> ]
$h$	Individual heat transfer coefficient	Btu/(hr-ft <sup>2</sup> -°F)	[W/(m <sup>2</sup> -°C)]
$h_c$	Cold side heat transfer coefficient	Btu/(hr-ft <sup>2</sup> -°F)	[W/(m <sup>2</sup> -°C)]
$h_h$	Hot side heat transfer coefficient	Btu/(hr-ft <sup>2</sup> -°F)	[W/(m <sup>2</sup> -°C)]
$k$	Thermal conductivity	Btu/(hr-ft-°F)	[W/(m-°C)]
$k_w$	Thermal conductivity of wall	Btu/(hr-ft-°F)	[W/(m-°C)]
$K_{i, pipe}$	Loss coefficient of inlet pipe and fittings	Dimensionless	
$K_{o, pipe}$	Loss coefficient of outlet pipe and fittings	Dimensionless	
$\ell$	Effective length of tubes between tubesheets	ft	[m]
$L$	Length of tubes	ft	[m]
$LMTD$	Log mean temperature difference	°F	[°C]
$m$	Mass flow rate	lbm/hr	[kg/s]
$m_c$	Cold stream mass flow rate	lbm/hr	[kg/s]
$m_h$	Hot stream mass flow rate	lbm/hr	[kg/s]
$N_t$	Number of tubes	Dimensionless	
$Nu$	Nusselt number = $hd/k$	Dimensionless	
$P_u$	Measured upstream pressure	lbf/ft <sup>2</sup> absolute	[Pa] absolute
$Pr$	Prandtl Number = $\mu_c \rho / k$	Dimensionless	
$Q$	Heat transfer rate for the heat exchanger	Btu/hr	[W]
$Q_{ave}$	Average heat transfer rate for a test run based on the hot and cold stream heat transfer rates	Btu/hr	[W]
$Q_{ave}^*$	Average heat transfer rate at reference conditions based on multiple test runs	Btu/hr	[W]
$Q_c$	Cold stream heat transfer rate	Btu/hr	[W]

Symbol	Definition	Units	
		U.S. Customary	SI
$Q_h$	Hot stream heat transfer rate	Btu/hr	[W]
$R_c$	Thermal resistance of the cold stream film based on the heat transfer rate $Q$ , $R_c = 1/(\eta_c h_c A_c)$	(hr-°F)/Btu	[°C/W]
$Re$	Reynolds number = $\rho V d / \mu$	Dimensionless	
$R_h$	Thermal resistance of the hot stream film based on the heat transfer rate $Q$ , $R_h = 1/(\eta_h h_h A_h)$	(hr-°F)/Btu	[°C/W]
$R_f$	Thermal resistance of fouling on both the hot and cold stream sides based on the heat transfer rate $Q$	(hr-°F)/Btu	[°C/W]
$r_f$	Average thermal resistance due to fouling on both the hot and cold stream sides based on the heat transfer rate per unit area, $r_f = R_f A$	(hr-ft <sup>2</sup> -°F)/Btu	[(m <sup>2</sup> -°C)/W]
$R_w$	Thermal resistance of the wall separating the hot and cold stream based on the heat transfer rate $Q$	(hr-°F)/Btu	[°C/W]
$T_i$	Hot stream inlet temperature	°F	[°C]
$T_o$	Hot stream outlet temperature	°F	[°C]
$t_i$	Cold stream inlet temperature	°F	[°C]
$t_o$	Cold stream outlet temperature	°F	[°C]
$t_w$	Wall temperature	°F	[°C]
$\hat{t}$	Student $t$	Dimensionless	
$U$	Overall heat transfer coefficient	Btu/(hr-ft <sup>2</sup> -°F)	[W/(m <sup>2</sup> -°C)]
$u_{cp}$	Uncertainty of specific heat (see para. 5.3.1.1)	Btu/(lbm-°F)	[J/(kg-°C)]
$u_{1/h}$	Uncertainty of average thermal resistance of film based on heat transfer rate per unit area	(hr-ft <sup>2</sup> -°F)/Btu	[(m <sup>2</sup> -°C)/W]
$u_{1/h^*-1/h}$	Uncertainty of the difference in average thermal resistance of film between reference and test conditions based on heat transfer rate per unit area	(hr-ft <sup>2</sup> -°F)/Btu	[(m <sup>2</sup> -°C)/W]
$U_{HR^*/HR^+}$	Uncertainty interval of hydraulic resistance ratio greater than the best estimate [see Eq. (5.19)]	Dimensionless	

Symbol	Definition	Units	
		U.S. Customary	SI
$u_{HR^*/HR}$	Uncertainty interval of hydraulic resistance ratio less than the best estimate [see Eq. (5.19)]	Dimensionless	
$u_{pv}$	Uncertainty attributed to process variations	Units of measurement parameter	
$u_{Qc}$	Uncertainty of cold side heat transfer rate at test conditions	Btu/hr	[W]
$u_{Qh}$	Uncertainty of hot side heat transfer rate at test conditions	Btu/hr	[W]
$u_{Q1}$	Uncertainty of heat transfer rate at reference conditions for test run 1	Btu/hr	[W]
$u_{Q2}$	Uncertainty of heat transfer rate at reference conditions for test run 2	Btu/hr	[W]
$u_U$	Uncertainty of overall heat transfer coefficient	Btu/(hr-ft <sup>2</sup> -°F)	[W/(m <sup>2</sup> -°C)]
$v$	Fluid velocity	ft/hr	[m/s]
$v_i$	Fluid velocity in inlet piping	ft/hr	[m/s]
$v_o$	Fluid velocity in outlet piping	ft/hr	[m/s]
$v_t$	Fluid velocity in heat exchanger tubes	ft/hr	[m/s]
$z_i$	Elevation of inlet wall pressure tap	ft	[m]
$z_o$	Elevation of outlet wall pressure tap	ft	[m]
$z_u$	Elevation of upstream pressure instrument	ft	[m]
$\Delta P$	Measured differential pressure	lbf/ft <sup>2</sup>	[Pa]
$\Delta P_{n-n}$	Total nozzle-to-nozzle pressure loss	lbf/ft <sup>2</sup>	[Pa]
$\Delta T_1$	Hot stream inlet temperature minus cold stream outlet temperature	°F	[°C]
$\Delta T_2$	Hot stream outlet temperature minus cold stream inlet temperature	°F	[°C]
$\Delta X_w$	Wall thickness (plate or tube)	ft	[m]
$\eta$	Surface effectiveness or measure of the reduction in temperature potential between the extended surface and the fluid. The surface effectiveness is related to the fin efficiency as described in Appendix E.	Dimensionless	
$\mu$	Dynamic (or absolute) viscosity	lbm/(ft-hr)	[kg/(m-s)]
$\mu_b$	Dynamic (or absolute) viscosity at the average bulk temperature	lbm/(ft-hr)	[kg/(m-s)]

Symbol	Definition	Units	
		U.S. Customary	SI
$\mu_w$	Dynamic (or absolute) viscosity at the wall surface temperature	lbm/(ft-hr)	[kg/(m-s)]
$\phi_Q$	Heat transfer rate correction factor to account for reference flow and temperature conditions different from test conditions	Dimensionless	
$\phi_U$	Overall heat transfer coefficient correction factor to account for reference flow and temperature conditions different from test conditions	Btu/(hr-ft <sup>2</sup> -°F)	[(m <sup>2</sup> -°C)/W]
$\phi_{\Delta P}$	Pressure loss correction factor to account for reference flow and temperature conditions different from test conditions	Dimensionless	
$\rho$	Fluid density	lbm/ft <sup>3</sup>	[kg/m <sup>3</sup> ]
$\rho_{ave}$	Average fluid density in heat exchanger	lbm/ft <sup>3</sup>	[kg/m <sup>3</sup> ]
$\rho_{gage}$	Fluid density in pressure gage or impulse tubing	lbm/ft <sup>3</sup>	[kg/m <sup>3</sup> ]
$\rho_{i, pipe}$	Fluid density in inlet pipe	lbm/ft <sup>3</sup>	[kg/m <sup>3</sup> ]
$\rho_{o, pipe}$	Fluid density in outlet pipe	lbm/ft <sup>3</sup>	[kg/m <sup>3</sup> ]

### 2.3 SUBSCRIPTS

<b>Abbreviation</b>	<b>Term</b>
<i>b</i>	Bulk fluid
<i>c</i>	Cold stream
<i>h</i>	Hot stream
<i>i</i>	Inlet end of heat exchanger
<i>o</i>	Outlet end of heat exchanger
<i>s</i>	Shell-side
<i>t</i>	Tube-side
<i>w</i>	Wall

### 2.4 SUPERScript

<b>Abbreviation</b>	<b>Term</b>
*	Reference conditions (see para. 3.2.2)

This page intentionally left blank.

## SECTION 3 — GUIDING PRINCIPLES

### 3.1 GENERAL TEST REQUIREMENTS

The key procedural steps are:

- (a) measure temperatures, flow rates and pressures accurately;
- (b) obtain a heat balance between hot and cold fluids streams and confirm steady state conditions;
- (c) perform calculations to predict performance at reference conditions;
- (d) analyze uncertainty of test measurements and performance calculations.

**3.1.1 Accurate Measurements.** The measurement uncertainty of the hot and cold stream flow rates, inlet temperatures, outlet temperatures, and pressures shall be appropriate to ensure that the uncertainties of  $U^*$ ,  $Q^*$ , and  $\Delta P_{n-n}^*$  are within the range specified in para. 1.3. Consideration for instrument calibration, spatial variation, installation practices, data acquisition methods, process variations and random instrument error is needed to ensure that the measurements conform to this requirement (see para. 5.2.3). As a benchmark, the calibration uncertainty for temperature measurements shall be less than  $\pm 0.2^\circ\text{F}$  ( $\pm 0.1^\circ\text{C}$ ), the total flow measurement uncertainty shall be less than  $\pm 5\%$  of measured flow, and the total pressure measurement uncertainty shall be less than  $\pm 1\%$  of reading (see paras. 4.4, 4.5, and 4.7). Lower uncertainties may be needed to meet the uncertainty range for  $U^*$ ,  $Q^*$ , and  $\Delta P_{n-n}^*$  specified in para. 1.3. Measurement of outlet temperatures with the appropriate uncertainty requires careful examination of spatial variation since outlet temperatures are not uniform for most heat exchangers (see para. 4.2.4).

**3.1.2 Heat Balance.** Steady state conditions shall be maintained during a test. The cold stream heat transfer rate shall be calculated based on the cold stream measurements, and the hot stream heat transfer rate shall be calculated based on the hot stream measurements. The differences in the cold stream heat transfer rate and hot stream heat transfer rate shall be assessed to confirm a heat balance is maintained as specified in para. 5.3.1.4.

**3.1.3 Performance Calculation.** A performance parameter (overall heat transfer coefficient, heat transfer

rate, or pressure loss) shall be calculated based on average test measurements and adjusted to reference conditions. Reference conditions represent design or baseline conditions and are typically different than test conditions. The adjustments of overall heat transfer coefficient, heat transfer rate and pressure loss are expressed as follows:

$$\frac{1}{U^*} = \frac{1}{U} + \phi_U \quad (3.1)$$

$$Q^* = \phi_Q Q \quad (3.2)$$

$$\Delta P_{n-n}^* = \phi_{\Delta P} \Delta P_{n-n} \quad (3.3)$$

where  $U$ ,  $Q$ , and  $\Delta P_{n-n}$  are the overall heat transfer coefficient, heat transfer rate, and pressure loss based on average measurements at test conditions.  $U^*$ ,  $Q^*$ , and  $\Delta P_{n-n}^*$  are the overall heat transfer coefficient, heat transfer rate, and pressure loss at reference conditions.  $\phi_U$ ,  $\phi_Q$ , and  $\phi_{\Delta P}$  are the associated correction factors that adjust test conditions to reference conditions.

These correction factors are derived in Appendix E or alternatively may be calculated using computer programs. (See para. 3.2.6).

**3.1.4 Uncertainty Analysis.** Calculation of uncertainty shall be performed before the test (pre-test) and after the test (post-test) in accordance with the methods and guidelines provided in ASME PTC 19.1, Reference 1. The uncertainty analysis shall include assessment of factors which affect the accuracy of test measurements, and factors which affect the accuracy of the performance calculation. As a minimum, the following elemental sources of error shall be considered:

- (a) inlet and outlet temperature measurements of the hot and cold streams;
- (b) flow measurements of the hot and cold streams;
- (c) pressure measurements;
- (d) specific heats of the hot and cold streams;

(e) heat transfer coefficients of the hot and cold streams;

(f) idealizations used in the calculation of mean temperature difference (such as variable heat transfer coefficient along flow length and nonuniform temperature distribution); and

(g) adjustment of pressure loss from test to reference conditions including contributions attributed to flow measurements, roughness (i.e., friction factor), and pressure loss correlations.

The uncertainty of the temperature, flow and pressure measurements shall be propagated through all calculations for overall heat transfer coefficient, heat transfer rate, and pressure loss including any intermediate calculations of mean temperature difference.

The test uncertainty varies for different heat exchanger designs and operating conditions. The expected uncertainties in para. 1.3 are for a range of typical single phase heat exchanger applications based on 95% confidence. For overall heat transfer coefficient and heat transfer rate, an uncertainty of  $\pm 3\%$  is considered to be the best attainable based on idealized conditions where the temperature measurement uncertainty is  $\pm 0.2^\circ\text{F}$ , flow measurement uncertainty is within  $\pm 2\%$ , mean temperature difference is greater than  $10^\circ\text{F}$ , fluid stream temperature changes are greater than  $10^\circ\text{F}$ , and the properties of the fluids are well known. These idealized conditions can be attained in full scale test beds where thermal mixers and flow straighteners can be used to reduce spatial variation, where steady process conditions can be established near reference conditions, and where environmental effects are stable. Since it is often not practical to meet these ideal conditions for many process applications, a range of uncertainties is provided for overall heat transfer coefficient and heat transfer rate. For pressure loss, the  $\pm 3\%$  uncertainty is based on flow measurement uncertainty within about  $\pm 1\%$ , pressure measurement uncertainty within  $\pm 1\%$ , and test conditions near reference conditions. Since it is often not practical to meet these conditions, a range of uncertainties is provided for pressure loss.

## 3.2 PREPARATION FOR THE TEST

**3.2.1 Test Plan.** A test plan shall be prepared to document the pre-test agreements. The parties to the test shall agree upon the following prior to the test:

(a) Test objectives, methods, and performance parameters,

(b) Organization and responsibilities including test director responsible for overall test quality;

(c) Heat exchanger operating conditions including constraints on test conditions;

(d) Definition of reference conditions (four of the six process variables);

(e) System alignment and steady state criteria;

(f) Cleanliness condition of heat exchanger;

(g) Scope and criteria for equipment inspections prior to test;

(h) Identification of known damage or deficiency (e.g., plugged tubes);

(i) Schedule for performing pre-test inspections, calibrations, preliminary testing, and performance testing;

(j) Number, use, installation, and location of temperature, pressure, and flow sensors;

(k) Instrument accuracy, calibration methods, storage and handling practices;

(l) Configuration of data acquisition system including type of equipment used and frequency of measurements, number of test runs, and duration of test runs;

(m) Acceptance of test results including acceptable deviations;

(n) Heat exchanger mechanical data (see Table 3.1);<sup>1</sup>

(o) Methods of calculation and associated uncertainty for heat exchanger thermal model parameters including all thermal physical properties (see Table 3.2).

**3.2.2 Definition of Reference Conditions.** Test conditions cannot be controlled to the extent that a specified set of conditions can be duplicated. To allow comparison of measured performance to the desired performance, the results must be adjusted to specified reference conditions. Adjustment of the results to a set of reference conditions is also necessary if it is intended to trend the results of a series of tests.

The reference conditions shall be defined and agreed by all parties to the test in accordance with para. 3.2.1. The definition of the reference conditions shall include four of the six basic thermal performance parameters, i.e., hot and cold side mass flow rates,  $m_h^*$  and  $m_c^*$ , and hot and cold side inlet and outlet temperatures,  $T_i^*$ ,  $T_o^*$ ,  $t_i^*$ , and  $t_o^*$ . The remaining two parameters will be calculated based on measured heat exchanger performance. In many

<sup>1</sup> Table 3.1 contains typical data and is not intended to be a complete list of data needed. The complete set of mechanical data depends upon the method of calculating the individual heat transfer coefficients.

**TABLE 3.1  
TYPICAL HEAT EXCHANGER MECHANICAL DATA NEEDED FOR  
PERFORMANCE ANALYSIS**

<b>Shell and Tube Heat Exchangers</b>	
Shell inside diameter	Tube diameter, layout, material and thickness
Diameter of the outer tube limit	Number of tubes, number of tubes plugged
Baffle spacing, cut and thickness (Inlet and outlet spacing also)	Tube length
Pass partition clearances, number and orientation	Finned tube geometry
Tube-to-baffle clearance	Tube sheet thickness
Shell-to-baffle clearance	
<b>Plate-Frame Heat Exchangers</b>	
Number of plates	Effective plate length
Effective area per plate	Plate width
Chevron angle and pattern	Channel spacing
Plate material and thickness	Number of passes
<b>Room Air Coolers</b>	
Coil geometry (length and width of coil and frame, depth in number of tube rows, number of tube circuits)	Fin geometry (fin spacing, thickness, height, width and root diameter)
Tube layout and geometry (transverse and longitudinal tube spacing, tube diameter and thickness, number of tubes in a coil, length of tubes)	

**TABLE 3.2  
TYPICAL HEAT EXCHANGER THERMAL MODEL PARAMETERS NEEDED FOR  
PERFORMANCE ANALYSIS**

Convective heat transfer coefficients for hot and cold streams	Thermal conductivity of the wall (tube or plate)
Mean temperature difference	Fouling resistance
Specific heats of the hot and cold streams	Thermal conductivity of fin and contact resistance between fin and tube
Cold side, hot side, and reference heat transfer areas	Surface effectiveness of enhancements such as fins

cases, the heat exchanger design conditions will provide the basis for the selected reference conditions. However, the two sets of parameters will differ because the actual fouling resistance at the time of the test probably will not equal the fouling resistance assumed in the design.

The following are two examples of reference conditions:

(a) The maximum heat exchanger inlet temperatures ( $T_{i,*}$  and  $t_{i,*}$ ) are defined by plant operating constraints. The mass flow rates ( $m_{h,*}$  and  $m_{c,*}$ ) are established by the pump and system operating conditions.

These four values are selected as reference conditions for the evaluation of the test results. The two outlet temperatures ( $T_{o,*}$  and  $t_{o,*}$ ) will be calculated during the evaluation based on the measured test performance and fouling resistance.

(b) The hot side of a heat exchanger is designed with a temperature controller in the outlet piping. Therefore, hot side flow will vary depending on the inlet temperature and the heat transfer capacity of the exchanger. The maximum heat exchanger inlet temperatures ( $T_{i,*}$  and  $t_{i,*}$ ) are defined by plant operating constraints. In this case, the defined reference condi-

tions would be the hot side temperatures ( $T_{i^*}$ ,  $T_{o^*}$ ) and cold side inlet temperature ( $t_i^*$ ) and the cold side mass flow rate ( $m_c^*$ ). The resulting hot side mass flow rate and cold side outlet temperatures at reference conditions will be calculated using the four defined conditions and the measured heat exchanger performance characteristics.

**3.2.3 Heat Transfer Area.** The heat transfer area is the wall surface area over which heat is transferred from the hot fluid to the cold fluid. The heat transfer areas on the hot and cold sides of the heat exchanger are calculated based on the mechanical data. The heat transfer area on the hot side is often different than the heat transfer area on the cold side such as with shell-and-tube heat exchangers and with finned surfaces. A reference heat transfer area is assigned to correspond with the overall heat transfer coefficient. The reference heat transfer area usually corresponds to either the hot or cold side area. For shell-and-tube heat exchangers, the shell side heat transfer area is typically selected as the reference area.

The hot side and cold side heat transfer areas shall be the best estimate of the surface area available for heat transfer (based on the mechanical data and results of equipment inspections). The area of plugged tubes and blocked flow shall not be included in the heat transfer area. The hot side, cold side and reference heat transfer areas shall be agreed to by the parties to the test.

**3.2.4 Pre-Test Uncertainty Analysis.** Prior to the test, an uncertainty analysis shall be performed based on the requirements in Section 5 and the guidelines in Reference 1. The purpose of the pre-test uncertainty analysis is to verify that the test objectives can be met with the prescribed testing methods. The results of the pre-test uncertainty analysis should be used to confirm:

- (a) Permissible test limits and steady state criteria;
- (b) Number, location and accuracy of instrumentation; and
- (c) Frequency of measurements, number of test runs, and duration of test runs.

As necessary, the test plan should be modified based on results of the uncertainty analysis.

**3.2.5 Provisions for Equipment Inspection.** The parties to the test shall agree to the scope and criteria of equipment inspection performed before the test. The scope of the inspection should include confirmation of heat exchanger geometry data, mate-

rial condition of the heat exchanger, and status of installed instrumentation ports. The following actions are recommended, as appropriate:

- (a) Determine if the equipment conforms with the as-built drawings (including thermal insulation) to the extent practical.
- (b) Determine the number of plugged tubes or blocked flow passages.
- (c) Verify the adequacy of the tube-to-tubesheet seals, if practical.
- (d) Assess the cleanliness of the heat exchanger. Heat exchanger surfaces should be cleaned to conditions agreed to prior to the test.
- (e) Check if the test ports (e.g., temperature, pressure, flow) or sample taps are present and adequate for the required test instrumentation.
- (f) Check the condition of the baffle plates, shell pass divider plates, longitudinal sealing strips, and gaskets, if practical.

**3.2.6 Use of Computer Programs for Performance Calculations.** The use of computer programs is appropriate for calculation of the correction factors  $\phi_U$ ,  $\phi_Q$ , and  $\phi_{\Delta P}$ , individual heat transfer coefficients and mean temperature difference. If used, the basis for the calculation methods used by the computer program shall be agreed upon by the parties to the test. In particular, the following criteria should be agreed to:

- (a) the definition and method of input for reference conditions;
- (b) the basis for the correlations of convective heat transfer coefficients (see para. 5.3.4);
- (c) the method of determining mean temperature difference;
- (d) the basis for determining fluid physical properties; and
- (e) the method for determining pressure loss; including correlations for friction factor and loss coefficients.

The uncertainty of the results of the computer program shall be estimated. This may be accomplished by performing a sensitivity analysis of key assumptions and correlations.

### 3.3 TEST METHODS

**3.3.1 Test Procedures.** Testing shall be performed in accordance with written test procedures consistent with the conditions agreed upon prior to the test.

**3.3.2 Preliminary Testing.** Preliminary test runs should be performed to:

(a) Check the operation of the instrumentation and data acquisition system;

(b) Validate the test procedure, including verifying system operating alignment, ensuring operating conditions can be met, and orienting test personnel; and

(c) Verify pre-test uncertainties, including effects attributed to instrument installation methods and spatial variation.

**3.3.3 Calibration of Instruments.** Instruments used to measure the parameters in para. 3.3.4 shall be calibrated before the test to ensure that the measurements are accurate. After initial calibration, controlled practices shall be used to handle the instruments so that calibration is not adversely affected. The storage practices of the instruments should be agreed to prior to the test based on the characteristics of the instrument.

**3.3.4 Test Parameters.** Test parameters shall include, as a minimum, the following:

- (a) Cold stream inlet temperature;
- (b) Cold stream outlet temperature;
- (c) Cold stream flow rate;
- (d) Cold stream differential pressure;
- (e) Cold stream inlet pressure;
- (f) Hot stream inlet temperature;
- (g) Hot stream outlet temperature;
- (h) Hot stream flow rate;
- (i) Hot stream differential pressure;
- (j) Hot stream inlet pressure.

Additional parameters may be measured, as desired, to use as additional validity checks. Special considerations required in the selection, calibration, and placement of test instrumentation are described in Section 4.

**3.3.5 Constraints on Test Conditions.** The parties to the test shall agree to the constraints and test limits prior to the test. The test limits shall be consistent with the system operating conditions so that the overall test uncertainty is acceptable. The following conditions should be met:

(a) The flow regime at test conditions should be the same as at reference conditions so that testing is not performed in the laminar regime when reference conditions are in the turbulent regime or vice versa.<sup>2</sup>

(b) The cold stream temperature change, hot stream temperature change, and mean temperature

difference should be more than 5 times the uncertainties in their measured values.

Other constraints should be established as appropriate.

**3.3.6 System Operating Alignment.** The system operating alignment shall be established to ensure that hot stream and cold stream measurement locations do not include fluid which has not passed through the heat exchanger. The parties to the test shall agree upon the system operating alignment prior to the test. When establishing the alignment requirements, consideration should be given to the operation of automatic control valves, flow in heat exchanger bypass lines, excessive throttling of flow control valves and the changes in operating alignment of other equipment in the hot and cold fluid systems. These factors may prevent steady state heat exchanger test conditions from being established.

**3.3.7 Constancy of Test Conditions.** The test shall be performed with the heat exchanger at steady state. The parties to the test shall agree to specific steady state criteria prior to the test. Following the test, the test data shall be evaluated to confirm that the steady state criteria have been met. Steady state criteria are described in Appendix A.

**3.3.8 Number and Frequency of Test Readings.** The parties to the test shall agree upon the number and frequency of test readings prior to the test consistent with the pre-test uncertainty analysis. Instrument readings shall be recorded for all test points during conditions, which meet steady state criteria. For example, 30 sets of readings should be recorded at a fixed frequency for each test run.

**3.3.9 Number and Duration of Test Runs.** Each test shall be conducted in accordance with the predetermined schedule. The parties to the test shall agree upon the number and duration of test runs. The duration of each test run shall be sufficient to ensure steady state conditions are established. The minimum duration of each steady state test run is 15 min, except for gas-gas heat exchangers, which require a minimum 30 min test run. A minimum of two test runs should be conducted to ensure repeatability of results.

**3.3.10 Acceptability of Test Runs.** Test data from each run shall be evaluated to ensure acceptability. The parties to the test shall agree upon criteria for acceptance of test data. As a minimum, the following conditions should be checked for acceptability:

- (a) Qualifications of test personnel are acceptable.

<sup>2</sup> The flow regime should be checked at the inlet and outlet temperatures for fluids where large variations in properties are expected (such as lube oil).

(b) Constraints on operating conditions are met, including environmental and atmospheric temperature and humidity conditions.

(c) System operating alignment is correct, including assumptions regarding the leak tightness of valves.

(d) Steady state criteria are met.

(e) Cleanliness and material condition of heat exchanger is acceptable, including condition of insulation.

(f) Pre-test inspections have been performed as agreed to.

(g) Calibration, location, and installation of instruments is consistent with the assumptions in the pre-test uncertainty analysis or the differences can be explained.

(h) Composition and properties of fluids are consistent with pre-test assumptions or the differences can be agreed to.

(i) Duration of the test run is adequate and variations in test data are within pre-test uncertainty limits or the differences can be explained.

(j) The heat balance can be verified based on the criteria in para. 5.3.1.4.

(k) The results of the calculations are consistent with assumptions as discussed in para. 5.5.1.

Test data, which do not meet the acceptance criteria, shall not be used to evaluate performance under the requirements of this Code.

### 3.4 ANALYSIS METHODS

The parties to the test shall agree upon the analysis methods prior to the test. Requirements for performance calculations are included in Section 5.

## SECTION 4 — INSTRUMENTS AND METHODS OF MEASUREMENT

### 4.1 GENERAL

This Section describes the choice of instruments, their required sensitivity or precision, and calibration corrections to readings and measurements. Included are requirements on methods of measurements, location of measuring systems, and precautions to be taken, including critical timing of measurements to minimize error attributed to changing conditions. The Supplements on Instruments and Apparatus (PTC 19 series) describe details of methods of measurement, instrument types, limits, sources of error, corrections, and calibrations. Where appropriate, this Code refers to, and makes mandatory, the application of the Supplements on Instruments and Apparatus, PTC 19 series.

For any of the measurements necessary under this Code, instrumentation systems or methods other than those prescribed herein may be used provided they do not increase the measurement uncertainty. Other methods may be employed if agreed by the parties to the test. Any departure from prescribed methods and its associated uncertainty shall be described in the test report.

The measurement uncertainty shall consider all aspects of the methods of measurement, including calibration, installation practices, spatial variation, and data acquisition. References 2 to 9 provide a discussion of sources of error for typical temperature, flow, and pressure instruments and industrial installation practices.

### 4.2 GENERAL MEASUREMENTS

**4.2.1 Measurement of Physical Dimensions.** Physical data shall be obtained for use in performance testing and evaluation. Specific physical data should be measured to minimize overall test uncertainty. Drawing or design information can be used to verify measurements. Data that should be measured are the dimensions of the heat exchanger and associated piping (or flow conduits) and information that affects the measurement of properties and the calculation

of results. These include data of the design geometry of the heat exchanger as described in Table 3.1 and data of the instrument installation, which affects the accuracy of the measurements.

In general, the uncertainty of the measurement of physical dimensions need not be considered explicitly in the calculation of test uncertainty. Instead, discrepancies between measured heat exchanger geometry and design data should be included in the uncertainty of individual heat transfer coefficient.

**4.2.2 Calibration of Instruments.** Instruments used to measure the parameters in para. 3.3.4 shall be calibrated before the test. The specific calibration data, duration and procedure for each instrument shall be provided to the parties to the test. Instruments used for flow, temperature, pressure and data acquisition shall be calibrated to physical standards or to standards traceable to those maintained by the National Institute of Standards and Technology. The calibration method shall be appropriate to the range of parameter values during the test, to the conditions to which the instrument will be exposed, and to the configuration of the instrument, wiring, and data acquisition system. An appropriate measurement uncertainty shall be included for all factors not included in the calibration.

**4.2.3 Data Acquisition Systems.** Automated data acquisition systems should have the capability to record data accurately at a high sampling rate with minimal increase of total measurement uncertainty. To follow these guidelines, the data acquisition system must minimize noise that may distort the signals or recorded values. The sampling rate should be chosen to record information throughout the entire cycle of process variations. An overall system calibration is preferred over a calibration of the individual components comprising a data acquisition system. For a system calibration, the uncertainty attributed to the data acquisition system is included with the calibration uncertainty of the instruments.

**4.2.4 Spatial Variations.** The effect of spatial variations should be evaluated for every measurement. The effect of spacing of duplicate instrumentation should be determined to ensure that arithmetic averaging of their output results in acceptable uncertainty. Otherwise, it is possible to account for spatial variations by applying weighting factors to data prior to determining an average. As an example, the effect of temperature stratification can be compensated by utilizing flow areas, each represented by temperature measurements.

#### 4.3 MEASUREMENT OF ENVIRONMENTAL EFFECTS

Prior to the test, a survey of the area surrounding the unit shall be conducted jointly by the parties to the test. Environmental conditions that may contribute to variations in performance shall be investigated. Potential environmental effects include:

- (a) Nonuniform ambient heat input, e.g., solar heat input, seasonal variation;
- (b) Vibration;
- (c) Electrical noise;
- (d) Thermal radiation;
- (e) Nonuniform ambient air flow, e.g., area ventilation fan exhausts near heat exchanger.

Measurements necessary to record these effects during the test shall be determined by agreement, and test data shall be obtained as necessary. If such measurements are not feasible or the area surrounding the heat exchanger contains elements which can significantly affect those measurements, effort should be made to remove or reduce the environmental effect, or a suitable estimation of its effect should be made.

#### 4.4 MEASUREMENT OF TEMPERATURE

The calibration uncertainty for measurement devices shall be less than  $\pm 0.2^\circ\text{F}$  ( $\pm 0.1^\circ\text{C}$ ). The total uncertainty should be less than  $\pm 0.6^\circ\text{F}$  ( $\pm 0.3^\circ\text{C}$ ). For tests with small changes in the cold or hot fluid stream temperatures, and for tests with a small mean temperature difference, lower uncertainty of the temperature measurements may be needed to obtain acceptable total uncertainty of heat exchanger performance. Uncertainties greater than  $\pm 0.6^\circ\text{F}$  ( $\pm 0.3^\circ\text{C}$ ) can be acceptable provided that the total uncertainty limits for heat exchanger performance in Section 1 are met.

Measurement locations shall be chosen to minimize the effect of thermal stratification in the outlet temperature. Measurement locations shall be close enough to the heat exchanger to prevent appreciable error attributed to temperature change associated with heat transfer to the surroundings. Where stratification is a possibility, preliminary tests shall be conducted to determine the magnitude of the possible resultant error. These preliminary tests shall be made part of the test report.

If the effect of temperature stratification on total uncertainty is unacceptable, measurement techniques should be modified. A properly placed static mixer can reduce the stratification and the associated uncertainty in spatial variation, but can also affect differential pressure and flow measurements. Traversing the flow area, multiple depth thermowells, and increased number of instruments are recommended options to minimize the consequences of stratification.

Instruments may be installed in a thermowell, directly immersed, or surface mounted. Thermowell instruments are preferred since they are less likely to have thermal gradients attributed to ambient surface contact resistance. The tip of the temperature element should be in contact with the bottom of the thermowell. Thermal grease or paste may be used during testing to facilitate heat transfer and improve the temperature measurement. It should be removed after testing is complete since thermal grease can harden in time, causing interference or increasing thermal resistance to the tips of the thermowell.

Surface mounted instruments shall be covered with insulation to minimize the thermal gradient between the bulk fluid temperature and the sensing element. The temperature bias caused by the use of surface-mounted instruments should be determined by analysis as discussed in References 8 and 9. The installation bias should be determined and included in the measurement uncertainty. To avoid thermal "wicking" (caused by heat conduction along the thermocouple wire) place insulation over the surface-mounted thermocouples and over at least 6 in., of sensor lead wire.

Instrument selection and details of measurement techniques should be in accordance with PTC 19.3. Satisfactory instruments include thermocouples, platinum resistance temperature devices, and thermistors. For large measurement areas, instruments may be traversed or ganged together. In cases where stratification of inlet and outlet fluid is small in comparison to the total uncertainty, temperature differences may be accurately measured directly.

Thermocouples, joined together in a series to form a thermopile, may be used to measure the difference of multiple inlet and outlet locations.

#### 4.5 MEASUREMENT OF FLOW

The total uncertainty shall be less than  $\pm 5\%$  of measured flow. If it is necessary to minimize this contribution to the total uncertainty of heat exchanger performance, the total uncertainty of the flow measurement should be less than  $\pm 2\text{--}3\%$ . It is considered possible to meet this lower uncertainty with a variety of flowmeters in most industrial applications. With differential pressure instruments such as orifice meters, this lower uncertainty can be obtained by applying standard industry guidance. With ultrasonic flowmeters, a calibration in a flow loop may be needed to meet this lower uncertainty.

##### 4.5.1 Flow Instrument Selection and Installation.

Instrument selection and details of measurement techniques shall be in accordance with PTC 19.5. Satisfactory instruments include venturi meters, orifice meters, flow nozzles, pitot tubes, turbine meters, annubars, ultrasonic flowmeters, mass flow meters, and other equivalent devices. Additional recommended installation practices and instrument applications for specific instrument types are outlined in the following paragraphs.

Measurements shall be made in the piping leading to, and as close as possible to, the test unit. If this is not practical, an alternate location shall be selected by agreement, and corrections made as necessary to determine the actual flow into the unit. References 2 to 5 provide installation guidance for various flow instruments. Measurements must account for leaking valve seals, bypass lines, and non-uniform flow profiles.

Temperature measurement errors and fluid property measurement errors can increase the error in fluid density, which directly affects the mass flow rate error (for instruments which measure flow velocity or volumetric flow rate). The temperature measured closest in proximity to the flow element should be used (not the average bulk fluid temperature) when calculating density for mass flow determination.

**4.5.2 Gas Flow.** Flow areas that are not symmetrical, or of a size to produce a wide variation in gas velocities, or characterized by a non-developed flow

profile, are candidates for a complete traverse. Suitable instruments for the traverse include the propeller anemometer, rotating vane anemometer, and pitot tube. Instruments may also be "ganged together."

The selection of the most suitable area for anemometer traverses shall be determined by the general physical arrangement, accessibility, obstruction, wind conditions (if applicable), and gas temperature rise. Pitot tubes may be used for fan ring traverses, as described in PTC 11. Instructions provided with the instruments should be followed to keep the overall test uncertainty within the prescribed limits. A minimum period of observation of 30 sec for individual readings is recommended for hand-held measurements.

A velocity traverse may be required at the exit plane in order to account for spatial variation of the outlet temperatures. Physical constraints might also require a velocity traverse at the inlet. For additional information on traversing methods, instrumentation, and evaluation of data, refer to PTC 18, PTC 19.5, and PTC 30.

#### 4.6 MEASUREMENT OF LIQUID AND GAS PROPERTIES

Gas and fluid composition is needed to determine thermodynamic and transport properties of materials passing through the heat exchanger. Methods and accuracy of analysis shall be agreed upon by the parties to the test. Sufficient samples of fluid should be obtained to enable determination of the composition of inlet and outlet streams, as discussed in Appendix I. Appendix I contains a list of the physical properties required.

#### 4.7 MEASUREMENT OF PRESSURE

The calibration uncertainty of pressure measurement devices shall be less than  $\pm 0.3\%$  of reading. The total uncertainty shall be less than  $\pm 1.0\%$  of reading. Instrument selection and details of measurement techniques shall be made in accordance with PTC 19.2. Satisfactory instruments for ambient and differential pressures include manometers, gages, and pressure transducers.

Pressure taps shall be located as close to the heat exchanger as possible. The pressure loss between the taps and the heat exchanger nozzle should be determined and appropriately applied to the pressure

measurement (see para. 5.3.6). This includes losses associated with the inlet and outlet piping. The pressure tap should be located in a straight run of pipe or a wall of a component with near constant hydraulic diameter. Placement of a tap in an accelerating flow field, e.g., a reducer, will create a bias to the expected static pressure measurement.

To minimize the errors contributed by sensor tubing (which connects the process tap to the instrument):

(a) Minimize the length of sensor tubing between the process tap and the instrument.

(b) Ensure the sensor tubing is blown down in advance of the test to ensure that non-condensibles are

removed for liquid measurements and condensibles (or contaminating liquids) are removed for gas measurements.

(c) Measure the elevations of the process taps and pressure instrument.

(d) Consistently and correctly apply the fluid elevation correction to all pressure measurements based on the measured elevation differences, temperature of fluid in the sensor tubing, and temperature of the fluid in the piping.

Differential pressure measurements should be made with one instrument. Utilizing two separate pressure gages substantially increases the uncertainty.

## SECTION 5 — COMPUTATION OF RESULTS

### 5.1 GENERAL

This Section describes the procedure to reduce the test data, calculate the performance parameters, adjust the results to reference conditions, and calculate the uncertainty of the test results. The procedure and equations are based on a F-LMTD heat transfer model as developed in Appendix E. The basic procedure for computation of performance capability is outlined below. Each step is described in more detail in paras. 5.2 through 5.5.

#### (a) Data reduction:

- (1) Review the raw test data (see para. 5.2.1);
- (2) Average the selected data (see para. 5.2.2);
- (3) Evaluate the uncertainty of the temperature, flow and pressure measurements (see para. 5.2.3).

#### (b) Heat exchanger performance at test conditions:

- (1) Compute the heat transfer rate at test conditions (see para. 5.3.1);
- (2) Compute the effective mean temperature difference at test conditions (see para. 5.3.2);
- (3) Compute the overall heat transfer coefficient at test conditions (see para. 5.3.3);
- (4) Determine individual heat transfer coefficients at test conditions (see para. 5.3.4);
- (5) Determine the wall resistance at test conditions (see para. 5.3.5);
- (6) Determine the nozzle-to-nozzle pressure loss (see para. 5.3.6).

#### (c) Heat exchanger performance at reference conditions:

- (1) Solve the heat transfer equations at reference conditions (see para. 5.4.1);
- (2) Determine the individual heat transfer coefficients at reference conditions (see para. 5.4.2);
- (3) Determine the wall resistance at reference conditions (see para. 5.4.3);
- (4) Compute the overall heat transfer coefficient at reference conditions (see para. 5.4.4);
- (5) Compute the heat transfer rate at reference conditions (see para. 5.4.5);
- (6) Calculate the uncertainty of thermal performance results (see para. 5.4.6);
- (7) Calculate the pressure loss at reference conditions (see para. 5.4.7).

#### (d) Evaluation of calculated results:

- (1) Verify that all analytical assumptions have been satisfied (see para. 5.5.1);
- (2) Compare multiple test runs (see para. 5.5.2);
- (3) Compare performance at reference conditions to independent criteria (see para. 5.5.3).

### 5.2 DATA REDUCTION

**5.2.1 Review the Raw Test Data.** The raw test data shall be carefully reviewed to ensure acceptability based on the agreement of the parties to the test. This review should be started at the beginning of the test, providing an opportunity for immediate discovery of possible errors in instruments, procedures, and methods of measurement. Guidance for the review of data and test conditions is given in para. 3.3.10.

**5.2.2 Average the Selected Data.** The purpose of averaging the raw test data is to give a single set of numbers, which is representative of the collected data to be used in calculations to determine performance. In general, multiple readings taken over time should be arithmetically averaged. A weighted average of measurements of the same parameter by multiple instruments at a given location should be used to establish a representative value to be used in the evaluation. Typically, the weighting factors would be equal; however, asymmetric weighting factors can be used if the specific test configuration warrants. In all cases, the parties to the test shall agree, in advance, to the averaging methods to be used for each parameter.

**5.2.3 Evaluate the Uncertainty of Temperature, Flow and Pressure Measurements.** The uncertainty of the temperature, flow and pressure measurements contributes to the uncertainty of heat transfer rate at test conditions  $Q$ , the mean temperature difference  $EMTD$ , and overall heat transfer coefficient at test conditions  $U$ . Assessment of measurement uncertainty shall include the following factors.

(a) *Instrument Calibration.* The uncertainty attributed to instrument calibration is based on the instru-

ment linearity, hysteresis, and repeatability, calibration methods and tolerances and accuracy of calibration instruments.

(b) *Spatial Variation.* The uncertainty attributed to spatial variation is based on the measured or estimated nonuniform distribution of the parameter in the flow cross section.

(c) *Installation.* The uncertainty attributed to installation is based on nonideal installation practices (such as with temperature measurement on the outside surface of the pipe).

(d) *Data Acquisition.* The uncertainty attributed to data acquisition is based on signal conditioning, gain and zero offset errors for the equipment used to measure and record output of the instrument.

(e) *Almost Steady Conditions.* The uncertainty attributed to non-steady or almost steady conditions is based on variations in process fluid conditions during the test period.

(f) *Random Error.* The uncertainty attributed to random error is estimated by calculating the standard deviation, and is based on variations in readings from a single instrument while system conditions remain constant.

References identified in Section 7 describe the sources of error for typical industrial instrumentation practices. Based on the review of the sources of error, averaged data can be corrected to compensate for bias related to calibration, spatial variation, installation, data acquisition, and drift in process conditions. However, correcting data does not eliminate the uncertainty, it only reduces the bias.

### 5.3 HEAT EXCHANGER PERFORMANCE AT TEST CONDITIONS

**5.3.1 Compute the Heat Transfer Rate at Test Conditions.** Heat transfer rates shall be calculated for both the hot and cold streams. The objectives of these calculations are two-fold; (1) to determine a representative average heat transfer rate of the heat exchanger under the test conditions, and (2) to confirm the heat balance.

**5.3.1.1 Specific Heat.** The specific heat of the hot and cold fluid streams is needed for the calculation of heat transfer rate.<sup>1</sup> Since specific heat is a function of temperature, the specific heat selected should be

<sup>1</sup> For some fluids such as moist air, the change in enthalpy is used to determine heat transfer rate. For these instances, a value for specific heat is not used explicitly; however, the use of tabulated enthalpy as a function of temperature is considered to be equivalent to the methods in this Code.

based on a representative temperature. For many fluids, it is acceptable to evaluate the specific heat based on the average of the inlet and outlet temperatures. If the variation in specific heat is large, the specific heat at the inlet and outlet temperatures should be evaluated so that the change in enthalpy is calculated.

The uncertainty in average specific heat ( $u_{cp}$ ) for the hot and cold streams shall be included. The uncertainty is attributed to variation in fluid properties and to uncertainty of experimental measurements, which are the basis of the values used. Based on the discussion and references identified in Appendix I, the following uncertainties may be considered bounding for many applications:

- (a)  $u_{cp}/c_p$  is equal to  $\pm 0.01$  for water;
- (b)  $u_{cp}/c_p$  is equal to  $\pm 0.05$  for other liquids;
- (c)  $u_{cp}/c_p$  is equal to  $\pm 0.01$  for steam and dry air;
- (d)  $u_{cp}/c_p$  is equal to  $\pm 0.02$  for other gases.

**5.3.1.2 Hot Stream Heat Transfer Rate.** The heat transfer rate for the hot stream at test conditions is:

$$Q_h = m_h c_{p,h} (T_i - T_o) \quad (5.1)$$

where

- $m_h$  = mass flow rate of the hot stream
- $c_{p,h}$  = average (or representative) specific heat of the hot stream
- $T_i$  = hot stream inlet temperature
- $T_o$  = hot stream outlet temperature

The uncertainty of the hot stream heat transfer rate shall be determined based on the uncertainty of the inlet and outlet temperature measurements, mass flow rate and specific heat. (See Eq. (B.6) for an acceptable method.)

**5.3.1.3 Cold Stream Heat Transfer Rate.** The heat transfer rate for the cold stream at test conditions is:

$$Q_c = m_c c_{p,c} (t_o - t_i) \quad (5.2)$$

where

- $m_c$  = mass flow rate of the cold stream
- $c_{p,c}$  = average (or representative) specific heat of the cold stream
- $t_i$  = cold stream inlet temperature
- $t_o$  = cold stream outlet temperature

The uncertainty of the cold stream heat transfer rate shall be determined based on the uncertainty of the inlet and outlet temperature measurements, mass flow rate and specific heat. (See Eq. (B.5) for an acceptable method.)

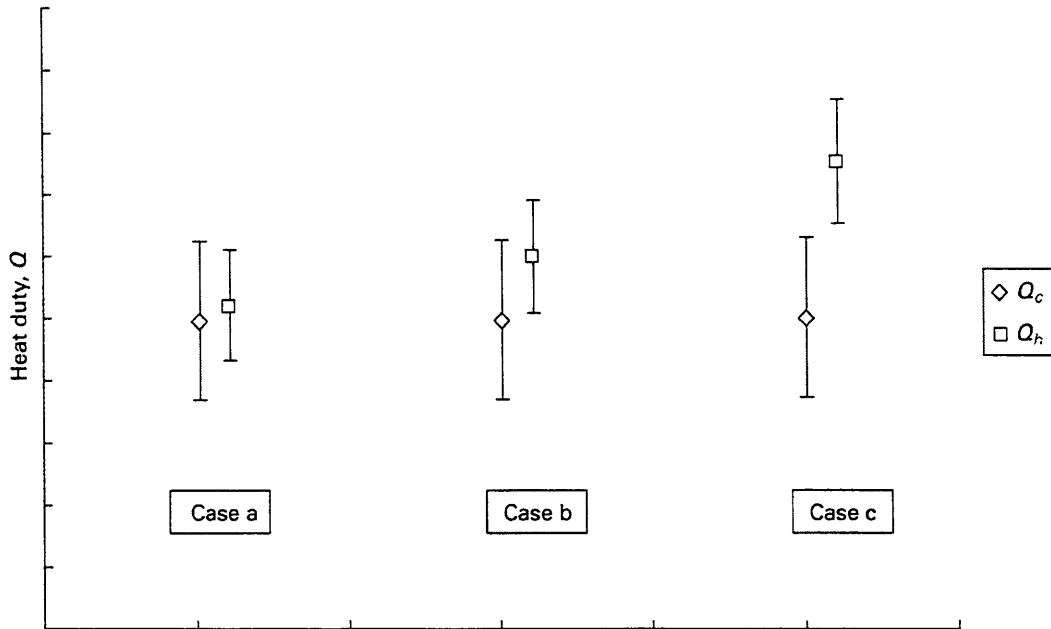


FIG. 5.1 COMPARISON OF MEASURED HOT AND COLD STREAM HEAT LOADS

**5.3.1.4 Evaluation of Heat Balance.** The differences between the cold stream heat transfer rate and the hot stream heat transfer rate shall be assessed to confirm a heat balance. The parties to the test shall agree upon criteria to confirm that a heat balance is maintained between the hot and cold streams. Two methods to evaluate heat balance are described below. Other methods are acceptable as agreed.

(a) *Overlap of Uncertainty Bars.* Comparing the heat loads and their uncertainties can result in one of three cases as shown in Fig. 5.1. In case a, the uncertainty intervals completely overlap. In this case, a heat balance has been achieved within the limitations of the test and installed instrumentation. In case c, there is no overlap between uncertainty intervals. In this case, a problem with the data or test configuration clearly exists or the uncertainties have been underestimated. The problem must be resolved and, if necessary, the test rerun before continuing with the evaluation. Case b is the most difficult to evaluate. A partial overlap of the uncertainty intervals exists. Judgment is needed to determine the acceptability of partial overlap, and the parties to the test should agree to criteria of acceptability for partial overlap. (See Reference 1.)

(b) *Hypothesis Testing.* The evaluation of the significance of the difference between the two heat loads

may be performed using hypothesis testing methodology. (Reference 10 provides a description of standard methods to compare the averages of two processes.) With hypothesis testing, the engineer, knowing the statistical character of the two observed heat loads from their respective standard deviations, investigates the likelihood that the difference between the mean values of the heat loads is due to chance or is due to a non-random effect. In the first case, there is no significant difference between the heat loads, and they can be considered equal within the measurement uncertainty. In the second case, a significant difference is considered to exist between the heat loads, so that the two values differ because of some non-random cause, such as instrument malfunction, lack of steady state, or operator error. Hypothesis testing requires for its application a judgment on the part of the test engineer as to the level of statistical probability that will be acceptable if the difference between the two heat load values is to be due to a non-random cause. An example of hypothesis testing is provided in Appendix K.

**5.3.1.5 Weighted Average Heat Transfer Rate.** To minimize the impact of any difference in measured heat loads, a weighted average shall be used in the projection of results to reference conditions:

$$Q_{ave} = \left( \frac{u_{Qh}^2}{u_{Qc}^2 + u_{Qh}^2} \right) Q_c + \left( \frac{u_{Qc}^2}{u_{Qc}^2 + u_{Qh}^2} \right) Q_h \quad (5.3)$$

where

$u_{Qc}$  = uncertainty of cold side heat transfer rate at test conditions [Eq. (B.5)]

$u_{Qh}$  = uncertainty of hot side heat transfer rate at test conditions [Eq. (B.6)]

**5.3.2 Compute Effective Mean Temperature Difference at Test Conditions.** The effective mean temperature difference,  $EMTD$ , shall be calculated. The mean temperature difference is needed to calculate the overall heat transfer coefficient from the weighted average heat transfer rate. This Code is based on the  $F$ - $LMTD$  method where the log mean temperature difference,  $LMTD$ , is calculated using the terminal temperatures measured during the test and  $F$  is the configuration correction factor for deviation from true countercurrent flow:

$$EMTD = (F)(LMTD) \quad (5.4)$$

Appendix D provides guidance on the evaluation of  $EMTD$ . Methods and idealizations used in the traditional development of  $LMTD$  and  $F$  are described along with alternative methods. Alternative methods may be used if traditional methods result in the uncertainties of  $Q^*$  and  $U^*$  which exceed the values specified in para. 1.3.

The uncertainty analysis shall consider sources of error attributed to the determination of  $EMTD$ . The sources of error which shall be considered include the uncertainty of the measurements used and the uncertainty of the idealizations used in the calculation of  $EMTD$ . For the traditional method of determining  $EMTD$ , the uncertainty analysis shall consider the uncertainty in temperature measurements and analytic uncertainties due to the variable heat transfer coefficient along the flow length ( $b_{EMTD,U}$ ) and non-uniform temperature distribution over a flow cross section ( $b_{EMTD,mixing}$ ). Appendix D provides a discussion of these two uncertainties.

**5.3.3 Compute the Overall Heat Transfer Coefficient at Test Conditions.** The overall heat transfer coefficient at test conditions,  $U$ , can be determined from the test parameters and the values calculated above.

$$U = \frac{Q_{ave}}{A(EMTD)} \quad (5.5)$$

where

$A$  = reference heat transfer area (see para. 3.2.3)

**5.3.4 Determine Individual Heat Transfer Coefficients at Test Conditions.** The individual heat transfer coefficients at test conditions shall be calculated for both the hot and cold stream fluids. Appendices C and F provide common methods for evaluating shell and tube side heat transfer coefficients, and Appendix H provides a method for evaluating plate-frame heat exchanger coefficients. Other methods are acceptable for use in the evaluation provided the following conditions are satisfied:

(a) Both parties shall agree to the use of the selected correlation or computer code.

(b) The accuracy of the correlation shall be agreed upon.

(c) Assumptions critical to the validity of the correlation shall be valid at test conditions.

(d) Assumptions critical to the validity of the correlation shall be valid at reference conditions.

(e) The same correlation or computer code shall be used for evaluation at both test and reference conditions. The evaluation shall not use different correlations for determining a heat transfer coefficient at the two conditions. Care should be taken when using computer codes to verify that this requirement is satisfied since the program may contain criteria to select an appropriate correlation for each given set of conditions.

To meet these conditions when using computer codes, it may be necessary to obtain prior agreements with the software vendor since the data and correlations used are often proprietary.

The uncertainty of the heat transfer coefficients shall be evaluated. The uncertainty is attributed to variations in flow distributions, variations in flow geometry, variations in fluid properties, and uncertainty in experimental measurements, which are the basis of the heat transfer correlation. Use of a computer program, which models the heat exchanger with multiple heat transfer elements does not eliminate this uncertainty but may reduce the uncertainty depending on the data used to validate the model. Estimating the uncertainty of individual heat transfer coefficients is difficult. This difficulty is primarily attributed the possibility that the correlations are used for tests outside the limits of the original experimental data and the methods used to reduce the experimental data. A review of open literature

and industrial experience has identified the following uncertainties for typical heat exchanger flow geometries:

$$\frac{u_{1/h}}{1/h} = \pm 0.10 \text{ for tube-side of shell and tube, Appendix F and References 11, 12}$$

$$\frac{u_{1/h}}{1/h} = \pm 0.20 - 0.50 \text{ for shell-side of shell and tube, Reference 13}$$

$$\frac{u_{1/h}}{1/h} = \pm 0.10 - 0.30 \text{ for plate-frame, Appendix H}$$

$$\frac{u_{1/h}}{1/h} = \pm 0.20 \text{ for plate-fin, References 14 and 15}$$

where

$1/h$  = inverse of the individual heat transfer coefficient = average thermal resistance of the film based on the heat transfer per unit area

$u_{1/h}$  = uncertainty of average thermal resistance of the film

Use of these uncertainties is considered reasonable for an initial assumption in the pre-test uncertainty analysis. If the overall uncertainty is dominated by factors other than the heat transfer coefficient, use of these uncertainties is acceptable in the final analysis. If the overall uncertainty is dominated by these coefficient uncertainties, additional data should be obtained (such as test data at various operating points) to verify their acceptability or to reduce their contribution to the uncertainty of  $U^*$  and  $Q^*$ , as necessary.

**5.3.5 Determine the Wall Resistance at Test Conditions.** The resistance of the wall which separates the hot and cold fluids shall be calculated for a representative temperature during the test. The wall temperature is between the hot and cold fluid temperature and may be estimated using the ratio of the individual hot and cold stream heat transfer coefficients. For circular tubes:

$$R_w = \frac{\ln(d_o/d_i)}{2\pi k_w \ell N_t} \quad (5.6)$$

where

$k_w$  = thermal conductivity of the wall

$\ell$  = effective length of tube

$N_t$  = number of tubes

$d_o$  = outside diameter of tubes

$d_i$  = inside diameter of tubes

For plates:

$$R_w = \frac{\Delta X}{A_w k_w} \quad (5.7)$$

where

$\Delta X$  = plate thickness

$A_w$  = total heat transfer area of all plates

**5.3.6 Determine the Nozzle-to-Nozzle Pressure Loss.** Evaluation of differential pressure data shall be based on nozzle-to-nozzle locations. The pressure measurements shall be corrected to account for losses in piping and fittings, which are between the pressure tap and the nozzle, elevation differences between the pressure tap and the nozzle, velocity head differences, and fluid density differences. For differential pressure measurements using wall taps, the nozzle-to-nozzle pressure loss is derived in Appendix E:

$$\Delta P_{n-n} = \rho_{ave} \left[ \begin{aligned} & \frac{\Delta P}{\rho_{o, pipe}} + \left( \frac{1}{\rho_{i, pipe}} - \frac{1}{\rho_{o, pipe}} \right) \\ & \left( P_u + \rho_{gage} \frac{g}{g_c} (z_u - z_i) \right) \\ & + \left( 1 - \frac{\rho_{gage}}{\rho_{o, pipe}} \right) \frac{g}{g_c} (z_i - z_o) \\ & + \left( 1 - K_{i, pipe} - (1 + K_{o, pipe}) \right. \\ & \left. \left( \frac{\rho_{i, pipe} A_{i, pipe}}{\rho_{o, pipe} A_{o, pipe}} \right)^2 \right) v_i^2 / 2g_c \end{aligned} \right] \quad (5.8)$$

where

$\Delta P_{n-n}$  = nozzle-to-nozzle pressure loss

$\Delta P$  = measured differential pressure

$P_u$  = measured upstream pressure

$\rho_{ave}$  = average fluid density in the heat exchanger<sup>2</sup>

$\rho_{gage}$  = fluid density in the gage or impulse tubing<sup>3</sup>

$\rho_{i, pipe}$  = fluid density in inlet piping

$\rho_{o, pipe}$  = fluid density in outlet piping

$g$  = gravitational acceleration

$g_c$  = units conversion constant

$z_i$  = elevation of the inlet pressure tap

$z_o$  = elevation of the outlet pressure tap

$z_u$  = elevation of the inlet pressure instrument

<sup>2</sup> When the change in fluid density is small, the average fluid density is given by  $(\rho_{i, pipe} + \rho_{o, pipe})/2$ . The change in fluid density is small if the second term in Eq. (5.8) is less than the uncertainty in  $\Delta P_{n-n}$ . If the change in fluid density is significant, a pre-test agreement for the method of determining average fluid density should be attained.

<sup>3</sup> For small diameter uninsulated gage tubing, the fluid density is typically at ambient temperature.

$K_{i, pipe}$  = loss coefficient for the fittings and pipe between the inlet pressure instrument and nozzle

$v_i$  = inlet pipe flow velocity

$K_{o, pipe}$  = loss coefficient for the fittings and pipe between the outlet pressure instrument and nozzle

$A_{i, pipe}$  = flow area of the inlet piping

$A_{o, pipe}$  = flow area of the outlet piping

Use of pressure taps in the tapered section of the nozzle results in erroneous measurements and is not acceptable.

#### 5.4 HEAT EXCHANGER PERFORMANCE AT REFERENCE CONDITIONS

The calculated performance parameters at test conditions, the defined reference conditions and the heat exchanger geometry and characteristics shall be used to adjust the heat exchanger thermal performance to the pre-selected reference conditions.

**5.4.1 Solve the Heat Transfer Equations at Reference Conditions.** The thermal performance characteristics of the heat exchanger are calculated by solving the following equations simultaneously:

$$Q^* = m_c^* c_{p,c}^* (t_o^* - t_i^*) \quad (5.9)$$

$$Q^* = m_h^* c_{p,h}^* (T_i^* - T_o^*) \quad (5.10)$$

$$Q^* = U^* A (EMTD^*) \quad (5.11)$$

$$\frac{1}{U^* A} = \frac{1}{\eta_c h_c^* A_c} + R_f^* + \frac{1}{\eta_h h_h^* A_h} + R_w^* \quad (5.12)$$

where

$Q^*$  = heat transfer rate at reference conditions

$m_c^*$  = mass flow rate of the cold stream at reference conditions

$c_{p,c}^*$  = average (or representative) specific heat of the cold stream at reference conditions

$t_i^*$  = cold stream inlet temperature at reference conditions

$t_o^*$  = cold stream outlet temperature at reference conditions

$m_h^*$  = mass flow rate of the hot stream at reference conditions

$c_{p,h}^*$  = average (or representative) specific heat of the hot stream at reference conditions

$T_i^*$  = hot stream inlet temperature at reference conditions

$T_o^*$  = hot stream outlet temperature at reference conditions

$U^*$  = overall heat transfer coefficient at reference conditions

$A$  = reference heat transfer area (see para. 3.2.3)

$h_c^*$  = average individual heat transfer coefficient for the cold side at reference conditions

$\eta_c$  = surface temperature effectiveness of the cold side

$A_c$  = cold side heat transfer area

$h_h^*$  = average individual heat transfer coefficient for the hot side at reference conditions

$\eta_h$  = surface temperature effectiveness of the hot side

$A_h$  = hot side heat transfer area

$R_f^*$  = fouling resistance at reference conditions

$R_w^*$  = wall resistance at reference conditions

Four of the six process variables are defined by the reference conditions (para. 3.2.2), the individual heat transfer coefficients are functions of the flow geometry, fluid properties and process variables (para. 5.4.2), the effective mean temperature difference is a function of the flow geometry and process variables (Appendix D) and the wall resistance is a function of the wall geometry, material properties, and wall temperatures (para. 5.4.3). It is assumed that fouling resistance at reference conditions is equal to the fouling resistance at test conditions:

$$R_f^* = R_f \quad (5.13)$$

**5.4.2 Determine the Individual Heat Transfer Coefficients at Reference Conditions.** The heat transfer coefficients at reference conditions shall be calculated for both the hot and cold side of the heat exchanger using the same correlations or computer codes selected in para. 5.3.4.

The uncertainty of the individual heat transfer coefficients at reference conditions shall be considered. It should be noted that the overall uncertainty attributed to the individual heat transfer coefficients is negligible for tests where the coefficient at test conditions is approximately equal to the coefficient at reference conditions. To estimate the effect of the uncertainty in heat transfer coefficients without "double-counting," the following method should be used to estimate the uncertainty of  $1/h^* - 1/h$ , Reference 17:

$$u_{1/h^* \cdot 1/h} = u_{1/h}(1 - X) \quad (5.14)$$

where

$$X = h^*/h \text{ for } h^* < h$$

$$X = h/h^* \text{ for } h < h^*$$

### 5.4.3 Determine the Wall Resistance at Reference Conditions.

The resistance of the wall, which separates the hot and cold fluids, shall be calculated for a representative temperature at reference conditions. [See Eqs. (5.6) and (5.7)].

### 5.4.4 Overall Heat Transfer Coefficient at Reference Conditions.

The overall heat transfer coefficient at reference conditions is calculated by solving Eqs. (5.8) through (5.11) simultaneously as discussed in para. 5.4.1. The overall heat transfer coefficient at reference conditions is represented by the following function of test parameters:

$$U^* = \frac{1}{\frac{1}{U} + \frac{A}{\eta_h A_h} \left[ \frac{1}{h_h^*} - \frac{1}{h_h} \right] + \frac{A}{\eta_c A_c} \left[ \frac{1}{h_c^*} - \frac{1}{h_c} \right] + (R_w^* - R_w)} \quad (5.15)$$

This expression is derived in Appendix E and is the basis for uncertainty calculations in Appendix B.

### 5.4.5 Compute the Heat Transfer Rate at Reference Conditions.

The heat transfer rate at reference conditions is calculated by solving Eqs. (5.8) through (5.11) simultaneously as discussed in para. 5.4.1. The heat transfer rate at reference conditions is represented by the following function of test parameters:

$$Q^* = \frac{Q_{ave}(EMTD^*/EMTD)}{1 + U \left[ \frac{A}{\eta_c A_c} \left( \frac{1}{h_c^*} - \frac{1}{h_c} \right) + \frac{A}{\eta_h A_h} \left( \frac{1}{h_h^*} - \frac{1}{h_h} \right) + R_w^* - R_w \right]} \quad (5.16)$$

This expression is derived in Appendix E and is the basis for uncertainty calculations in Appendix B.

### 5.4.6 Calculate the Uncertainty of Thermal Performance Results.

The uncertainty of the heat exchanger performance at reference conditions shall be calculated before the test (pre-test) and after the test (post-test) based on the sources of error in para. 3.1.4 and the guidelines in ASME PTC 19.1, Reference 1. As agreed by the parties to the test, evaluation of other sources of error may be needed to ensure that the assessment is adequate. Other sources of error include:

(a) *Heat Transfer Area.* For instances where flow blockage or tube plugging are not known, uncertainty in heat transfer area should be considered.

(b) *Wall Resistance.* For instances where the change in wall resistance is significant, an uncertainty due to thermal conductivity and approximation of wall temperatures should be considered.

(c) *Longitudinal Conduction.* For high effectiveness and high temperature gradient applications such as recuperators, bias due to longitudinal conduction along the flow length should be considered. The effect of longitudinal conduction can be calculated based on the approach discussed in Reference 18.

(d) *Change in Average Fouling Resistance.* The analysis method used in this Code assumes that the average fouling resistance at test conditions is the same as at reference conditions. As discussed in Appendix G, the difference in average fouling resistance at test conditions and at reference conditions may be significant for instances where both the fouling resistance is high and the test conditions are substantially different than the reference conditions. For these conditions, a bounding calculation which integrates the heat transfer across the heat exchanger area (based on fouling conditions which vary spatially) can be used to estimate the uncertainty.

(e) *Heat Loss to Ambient.* For applications where the calculated heat loss to the surroundings is a significant fraction of uncertainty in heat transfer rate, the bias due to this heat loss should be considered.

The recommended approach to calculate the uncertainty of  $U^*$ ,  $Q^*$ , and  $\Delta P_{n-n}^*$  consists of the following:

(a) establishing an equation (or other suitable calculation method) which describes  $U^*$ ,  $Q^*$ , and  $\Delta P_{n-n}^*$  based on test measurements;

(b) estimating the magnitude of the uncertainty for each elemental source of error, and;

(c) propagating the elemental uncertainties to an overall result.

Using this recommended approach, the uncertainty of  $U^*$ ,  $Q^*$ , and  $\Delta P_{n-n}^*$  is dominated by the contributions of only a few elemental uncertainties. In general, the uncertainty is dominated by the contributions of temperature measurements (and particularly outlet temperatures) and flow measurements. As a result, most of the elemental uncertainties can be approximated with upper bound limits without increasing the uncertainty of  $U^*$ ,  $Q^*$ , and  $\Delta P_{n-n}^*$  significantly.

Appendix B contains a procedure to propagate the uncertainty of measurements into an uncertainty of performance results. Other methods to propagate uncertainty are acceptable. For example, use of a computer program to identify the sensitivity coefficients for each of the measurements and parameters

used (by incrementing each parameter individually) is an acceptable approach as long as all sources of error listed in para. 3.1.4 are considered.

**5.4.7 Calculate the Pressure Loss at Reference Conditions.** The nozzle-to-nozzle pressure loss shall be adjusted to reference conditions based on the following:

$$\Delta P_{n-n}^* = \phi_{\Delta P} \Delta P_{n-n} \quad (5.17)$$

where  $\phi_{\Delta P}$  is the correction factor to account for reference flow and temperature conditions different than test conditions. This correction factor is calculated based on a model of the pressure loss through the unit:

$$\phi_{\Delta P} = \frac{(\Delta P_{n-n})_{\text{calculated at reference conditions}}}{(\Delta P_{n-n})_{\text{calculated at test conditions}}} \quad (5.18)$$

The method to calculate the correction factor shall be agreed by the parties to the test. Guidance for shell side pressure loss calculations is provided in Appendix C. Guidance for calculating tube side pressure loss is provided in Appendix F.

The uncertainty in pressure loss adjustment shall be evaluated. This uncertainty is attributed to the uncertainty in flow measurements, uncertainty in pressure loss correlations and uncertainty in roughness and internal condition of flow surface. To calculate the contribution due to flow measurement separate from the pressure loss correlation and roughness contributions, the following equation can be used:

$$\phi_{\Delta P} = \frac{H_R^*}{H_R} \frac{m^*}{m^n} \quad (5.19)$$

where

$H_R^*$  = calculated hydraulic resistance at reference conditions =  $\Delta P_{n-n}^* / (m^*)^n$

$H_R$  = calculated hydraulic resistance at test conditions =  $\Delta P_{n-n} / m^n$

$m^*$  = mass flow rate at reference conditions

$m$  = mass flow rate at test conditions

$n$  = flow rate exponent depending on flow regime and assumptions regarding roughness

$n = 2$  in fully roughened turbulent regime

$n = 1.6 - 1.8$  for turbulent flow in smooth regime

$n = 1$  for laminar flow

A generalized expression for the uncertainty in pressure loss correlations and roughness contribu-

tions has not been developed since it is not considered practical to bound these effects in a generalized manner for all test applications. Instead, the uncertainty may be based on an upper and lower limit for the calculated pressure loss adjustment:

$$\begin{aligned} u_{HR^*/HR} + &= (H_R^*/H_R)_{\max} - H_R^*/H_R \quad (5.20) \\ u_{HR^*/HR} - &= H_R^*/H_R - (H_R^*/H_R)_{\min} \end{aligned}$$

where

$H_R^*/H_R$  = best estimate of the hydraulic resistance ratio

$(H_R^*/H_R)_{\max}$  = upper estimate of hydraulic resistance ratio

$(H_R^*/H_R)_{\min}$  = lower estimate of hydraulic resistance ratio

## 5.5 EVALUATION OF CALCULATED RESULTS

**5.5.1 Verify All Analytical Assumptions Have Been Satisfied.** To ensure the validity of the correlations, methodologies, or computer codes selected for determination of individual heat transfer coefficients during the evaluation, it should be verified that each flow stream was in the required flow regime and that the same flow regime exists at both test and reference conditions. It should be verified that the test and reference flow rates satisfy the appropriate assumptions or limitations of the selected heat transfer correlations or codes. In addition, any assumptions implicit in the computer code, if applicable, should be validated for the test and reference conditions.

**5.5.2 Compare Multiple Test Runs.** If multiple test runs were conducted, the results for each test shall be evaluated as described in paras. 5.3 and 5.4. The projected results calculated for all test runs shall agree within the uncertainty of the results, or the differences shall be explained. If the difference in results exceeds the uncertainty of the tests and cannot be explained, the results shall be considered inconclusive.

The average of more than one test run should be calculated as described in Reference 1, para. 7.3.2. The uncertainty of the average test result is less than that for one test run because of the reduction in random uncertainty of the average. Systematic uncertainty will remain the same as for a single test run. For heat exchanger performance testing, most of the uncertainty is typically systematic (such as instrument

calibration and spatial variation) and therefore the overall uncertainty for multiple test runs is not substantially less than the uncertainty for one test run.

**5.5.3 Compare Performance at Reference Conditions to Independent Criteria.** After the performance

of the heat exchanger and its associated uncertainty is calculated for reference conditions, comparison with independent criteria can be performed. Independent criteria include design specifications and minimum process requirements. Methods for comparison with independent criteria are outside the scope of this Code.

This page intentionally left blank.

## SECTION 6 — REPORT OF RESULTS

### 6.1 COMPOSITION OF REPORT

The report for the performance test shall include the following:

#### 6.1.1 General Information

- (a) Identification of the heat exchanger to be tested.
- (b) Identification of the plant where the heat exchanger is located, and general information regarding the facility and the particular heat exchanger under test.
- (c) The name of the owner of the heat exchanger.
- (d) The name of the manufacturer of the heat exchanger.
- (e) A statement of who conducted the test and who observed the test.
- (f) Dates(s) and time(s) of the test.
- (g) Date of first commercial operation of the heat exchanger.
- (h) The design conditions and reference conditions required of the heat exchanger.
- (i) A statement of the heat exchanger performance criteria.
- (j) Run numbers included in the test report.

**6.1.2 Object of the Test.** This shall describe the purpose of the test.

**6.1.3 Background.** This shall include a brief history of the operation of the heat exchanger and any pertinent background information. It shall list all prior agreements with regard to the test. It shall also discuss any inspection prior to or following the test and state what was inspected and what was found. It shall describe when and how the heat exchanger was last cleaned and its condition during the test. This shall include a description of any degraded conditions including fouling discovered during the inspections of the heat exchanger. (See para. 3.2.5.)

**6.1.4 Test Methods and Procedures.** This shall describe how the test was actually conducted including system alignments and data acquisition methods including the location of each measurement instrument and any unusual occurrences during the test. It shall include a summary of the types of instruments used during the test. It shall identify analytical corre-

lations used for data reduction. The test report shall include a description of preliminary and special tests.

**6.1.5 Test Data and Results at Actual Test Conditions.** This shall include a listing of the test results for each test run at actual test conditions after all corrections are applied.

**6.1.6 Test Result Adjusted to Design Conditions.** This shall include a listing of the test results for each run projected to reference conditions after all corrections are applied.

**6.1.7 Multiple Test Run Comparisons.** Multiple test runs shall be compared and shown to meet the requirements of para. 5.5.2.

**6.1.8 Conclusions.** The report shall state the performance parameters at reference conditions (overall heat transfer coefficient, heat transfer rate, and/or pressure losses) and the total uncertainty of each. There shall be a statement of the conclusions derived from the test, including whether or not the heat exchanger met its performance criteria or fell short of that performance.

**6.1.9 Appendices.** As a minimum, the following appendices shall be included.

(a) *Sample Calculation.* This shall be included using the data from one run. The sample calculation shall illustrate all the calculations and adjustments that are made to that run so that the parties to the test could start with the data from any run and make all necessary calculations to verify the results of any of the other runs. Software input and output should be included.

(b) *List of Instrumentation.* This shall list all the instrumentation used on the test, including manufacturer, model number, and serial number and calibration record.

(c) *List of all Participating Personnel.* This shall list the participating personnel, their function, and the parties to the test that they represent.

(d) *Uncertainty Analysis Sample Calculation.* A sample calculation for one run should be included. It should use the same run that was used for the results sample calculation, per (a) above.

- (e) *Mechanical Data and Specification Sheets and Drawings.* (See Table 3.1).  
 (f) *Raw Test Data.*

## 6.2 REPORT DATA

A list of typical data to be included in the report follows

- (a) Heat transfer areas,  $A$ ,  $A_c$ ,  $A_h$ .  
 (b) Cold stream mass flow rate,  $m_c$ .  
 (c) Hot stream mass flow rate,  $m_h$ .  
 (d) Hot stream inlet temperature,  $T_i$ .  
 (e) Hot stream outlet temperature,  $T_o$ .  
 (f) Cold stream inlet temperature,  $t_i$ .  
 (g) Cold stream outlet temperature,  $t_o$ .  
 (h) Hot stream differential pressure if measured directly,  $\Delta P_h$ .  
 (i) Hot stream inlet pressure,  $P_{hi}$ .  
 (j) Hot stream outlet pressure,  $P_{ho}$ .  
 (k) Cold stream differential pressure if measured directly,  $\Delta P_c$ .  
 (l) Cold stream inlet pressure,  $P_{ci}$ .  
 (m) Cold stream outlet pressure,  $P_{co}$ .  
 (n) Hot stream physical properties used in the evaluation, either tabulated or graphed over the temperature range encountered in the test.  
 (o) Cold stream physical properties used in the evaluation, either tabulated or graphed over the temperature range encountered in the test.  
 (p) Effective mean temperature difference,  $EMTD$ .  
 (q) Hot side and cold side heat transfer rates,  $Q_c$  and  $Q_h$ .  
 (r) Hot side and cold side convection film coefficients,  $h_c$  and  $h_h$ .  
 (s) Overall heat transfer coefficient,  $U$ .  
 (t) Average heat transfer rate,  $Q_{ave}$ .

## SECTION 7 — REFERENCES

- [1] ASME PTC 19.1-1998. "Test Uncertainty."<sup>1</sup>
- [2] ASME MFC 3M-1989. "Measurement of Fluid Flow in Pipes Using Orifice, Nozzle and Venturi."
- [3] ISO 5167-1. "Measurement of Fluid Flow by Means of Pressure Differential Devices — Part 1: Orifice Plates, Nozzles, and Venturi Tubes Inserted in Circular Cross-Section Conduits Running Full," 1991.
- [4] ASME MFC 5M-1985. "Measurement of Liquid Flow in Closed Conduits Using Transit-Time Ultrasonic Flowmeters."
- [5] Miller, R.W. "Fluid Measurement Engineering Handbook," McGraw-Hill Book Company, Third Edition, 1996.
- [6] Benedict, R.P. "Fundamentals of Temperature, Pressure and Flow Measurements," John Wiley & Sons, Third Edition, 1984.
- [7] Nicholas, J. and White, D. "Traceable Temperatures," John Wiley & Sons, 1994.
- [8] Hennecke, D.K. and Sparrow, E.M., "Local Heat Sink on a Convectively Cooled Surface — Application to Temperature Measurement Error," *International Journal of Heat and Mass Transfer*, Vol. 13, No. 2, February 1970, pp. 287–303.
- [9] Sparrow, E.M. "Error Estimates in Temperature Measurement," *Measurements in Heat Transfer*, ed. E.R. Eckert and R.J. Goldstein, McGraw Hill Book Company, Second Edition, 1976, pp. 1–22.
- [10] Natrella, Mary G. "Experimental Statistics," National Institute of Standards and Technology Handbook 91, 1966.
- [11] Bhatti, M. and Shah, R.K. "Turbulent and Transition Flow Convective Heat Transfer in Ducts," Chapter 4 of *Handbook of Single-Phase Convective Heat Transfer*, editors S. Kakac, R.K. Shah and W. Aung, John Wiley & Sons, 1987.
- [12] Petukhov, B. "Heat Transfer and Friction in Turbulent Pipe Flow with Variable Physical Properties," *Advances in Heat Transfer*, editors J.P. Hartnett and T.F. Irvine, Academic Press, 1970, Vol. 6, pp. 503–564.
- [13] Palen, J.W. and Taborek, J. "Solution of Shell Side Flow, Pressure Drop and Heat Transfer by Stream Analysis Method," *Chemical Engineering Progress — Symposium Series No. 92*, Vol. 65, 1969, pp. 53–63.
- [14] Manglik, R.M. and Bergles, A.E. "The Thermal Hydraulic Design of Rectangular Offset Strip Fin Compact Heat Exchanger," *Compact Heat Exchangers*, Eds. R.K. Shah, A.D. Kraus, and D. Metzger, Hemisphere Publishing Corp., 1990, pp. 123–150.
- [15] Webb, R.L. "Principles of Enhanced Heat Transfer," John Wiley & Sons, 1994.
- [16] Crane Technical Paper No. 410, "Flow of Fluids Through Valves, Fittings, and Pipe," Crane Company 1982.
- [17] Lestina, T. and Scott, B. "Assessing the Uncertainty of Thermal Performance Measurements of Industrial Heat Exchangers," *Engineering Foundation Conference — Compact Heat Exchangers for the Process Industries*, June 1997.
- [18] Shah, R.K. "A Review of Longitudinal Wall Heat Conduction in Recuperators," *Journal of Energy, Heat and Mass Transfer*, Vol. 16, 1994, pp. 15–25.
- [19] Bendat, J.S. and Piersol, A.G. "Random Data Analysis and Measurement Procedures," John Wiley & Sons, Inc., Second Edition, 1986.
- [20] Cao, S. and Rhinehart, R.R. "An Efficient Method for On-Line Identification of Steady State," *Journal of Process Control*, Vol. 5, No. 6, December 1995, pp. 363–374.
- [21] Cima, R.M. and London, A.L. "The Transient Response of a Two-Fluid Counterflow Heat Exchanger — The Gas Turbine Regenerator," *ASME Transactions* Vol. 80, No. 1, 1958, pp. 1169–1179.
- [22] Kays, W. M. and London, A. L. "Compact Heat Exchangers," McGraw Hill Book Co., Second Edition, 1964.
- [23] Shah, R. K. "The Transient Response of Heat Exchangers," *Heat Exchangers: Thermal Hy-*

<sup>1</sup> Reference 1 is mandatory. Other references are nonmandatory and are provided for information only.

- draulic Fundamentals and Design*, Eds. S. Kakac, A.E. Bergles, and F. Mayinger, Hemisphere Publishing Corp., 1981, pp. 915–953.
- [24] Kerlin, T.W. and Shepard, R.L. "Industrial Temperature Measurement," Instrument Society of America, 1982.
- [25] Green, S.J. and Hunt, T.W. "Accuracy and Response of Thermocouples for Surface and Fluid Temperature Measurements," *Temperature, Its Measurement and Control in Science and Industry*, Reinhold Publishing Corporation, Vol. 3, Part 2, 1962, pp. 695–722.
- [26] Handbook of Heat Exchanger Design, edited by G.F. Hewitt et al., Begell House, Inc., 1992.
- [27] Tinker, T. "Shell-Side Characteristics of Shell and Tube Heat Exchangers," Proceedings of the General Discussion on Heat Transfer, Institution of Mechanical Engineers, London, England, 1951, pp. 97–116.
- [28] Standards of Tubular Exchanger Manufacturers Association (TEMA), Tarrytown, NY, Seventh Edition, 1988.
- [29] Bowman, R.A. Mueller, A.C. and Nagle. "Mean Temperature Differences in Design," *ASME Transactions*, Vol. 62, May 1940, pp. 283–294.
- [30] Colburn, A.P. "Mean Temperature Difference and Heat Transfer Coefficient in Liquid Heat Exchangers," *Industrial Engineering and Chemistry*, Vol. 25, No. 8, August 1933, pp. 873–877.
- [31] Sieder, E. and Tate, G. "Heat Transfer and Pressure Drop of Liquids in Tubes," *Industrial Engineering and Chemistry*, Vol. 28 No. 12, December 1936, pp. 1429–1435.
- [32] Gardner, K. and Taborek, J. "Mean Temperature Difference: A Reappraisal," *AIChE Journal*, Vol. 23, No. 6, November 1977, pp. 777–786.
- [33] Gardner, K. "Variable Heat Transfer Rate Correction in Multipass Exchangers, Shell-Side Film Controlling," *ASME Transactions*, Vol. 67, January 1945, pp. 31–38.
- [34] Whistler, A. "Effect of Leakage Around Cross-Baffles in a Heat Exchanger," *Petroleum Refiner*, Vol. 26 No. 10, 1947, pp. 114–118.
- [35] Fisher, J. and Parker, R. "New Ideas on Heat Exchanger Design," *Hydrocarbon Processing*, Vol. 48, July 1969, pp. 147–154.
- [36] Bell, K. and Kegler, W. "Analysis of Bypass Flow Effects in Tube Banks and Heat Exchangers," *AIChE Symposium Series*, Vol. 74, No. 174, 1978, pp. 47–52.
- [37] Shah, R.K. and Pignotti, A. "The Influence of a Finite Number of Baffles on the Shell-and-Tube Heat Exchanger Performance," *Heat Transfer Engineering*, Vol. 18, No. 1, 1997, pp. 82–94.
- [38] Mueller, A. and Chiou, J. "Review of Various Types of Flow Maldistribution in Heat Exchangers," *Heat Transfer Engineering* Vol. 9, No. 2, 1988, pp. 36–50.
- [39] Heat Exchange Institute (HEI) Standard for Power Plant Heat Exchangers, Second Edition, 1990.
- [40] Whistler, A.M. "Correction for Heat Conduction Through Longitudinal Baffle of Heat Exchanger," *ASME Transactions*, Vol. 69, 1947, pp. 683–685.
- [41] Rozenman, T. and Taborek, J. "The Effect of Leakage Through the Longitudinal Baffle on the Performance of Two-Pass Shell Exchangers," *AIChE Symposium Series*, Vol. 68, No. 118, 1971, pp. 12–20.
- [42] Handbook of Heat Transfer Applications, eds. W.M. Rohsenow, J.P. Hartnett, and Y.I. Cho, McGraw Hill Book Company, Third Edition, 1998.
- [43] Kern, D.Q. and Kraus, A.D. "Extended Surface Heat Transfer," McGraw Hill Book Company, 1972.
- [44] Watkinson, A. P. Miletti, D. L. and Tarsoff, P. "Turbulent Heat Transfer and Pressure Drop in Internally Finned Tubes," *AIChE Symposium Series*, Vol. 69, No. 131, 1973, pp. 94–103.
- [45] Bergles, A. E. "Augmentation of Heat Transfer," *Heat Exchanger Design Handbook*, ed. E. U. Schlünder, Section 2.5.11-6, Hemisphere, Washington, D.C., 1983.
- [46] Carnavos, T. C. "Heat Transfer Performance of Internally Finned Tubes in Turbulent Flow," *Advances in Enhanced Heat Transfer*, eds. J. M. Chenoweth, J. Kaellis, J. W. Michel, and S. Shenkman, ASME, New York, 1979, pp. 61–67.
- [47] Filonenko, G.K. "Hydraulic Resistance in Pipes," (in Russian), *Teploenergetika*, Vol. 1 No. 4, 1954, pp. 40–44.
- [48] Gnielinski, V. "New Equations for Heat and Mass Transfer in Turbulent Pipe and Channel Flow," *International Chemical Engineering*, Vol. 16, No. 2, April 1976, pp. 359–368.
- [49] Colburn, A.P. "A Method of Correlating Forced Convection Heat Transfer Data and a Compar-

- ison with Fluid Friction," *Transactions of AIChE*, Vol. 29, pp. 174–210.
- [50] Metais, B. and Eckert, E.R.G. "Forced, Mixed, and Free Convection Regimes," *ASME Journal of Heat Transfer*, Vol. 86, No. 2, May 1964, pp. 295–296.
- [51] Ghajar, A.J. and Tam, L.M. "Flow Regime Map for a Horizontal Pipe with Uniform Wall Heat Flux and Three Different Inlet Configurations," *ASME HTD-Vol. 247, Mixed Convection Heat Transfer*, 1993, pp. 43–52.
- [52] Palen, J.W. and Taborek, J. "An Improved Heat Transfer Correlation for Laminar Flow of High Prandtl Number Liquids in Horizontal Tubes," *AIChE Symposium Series*, Vol. 81, No. 245, 1985, pp. 90–96.
- [53] Depew, C.A. and August, S.E. "Heat Transfer Due to Combined Free and Forced Convection in a Horizontal and Isothermal Tube," *ASME Journal of Heat Transfer*, Vol. 93, 1971, pp. 380–384.
- [54] Marner, W. J. and McMillan, H. K. "Combined Free and Forced Laminar Non-Newtonian Convection in a Vertical Tube with Constant Wall Temperature," *Chemical Engineering Science*, Vol. 27, 1972, pp. 473–488.
- [55] Pigford, R. L. "Nonisothermal Flow and Heat Transfer Inside Vertical Tubes," *Chemical Engineering Progress Symposium Series*, Vol. 51, 1959, pp. 79–92.
- [56] Jackson, T. W. Harrison, W. B, and Boteler, W. C. "Combined Free and Forced Convection in a Constant Temperature Vertical Tube," *ASME Journal Heat Transfer*, Vol. 79, 1958, pp. 739–745.
- [57] Herbert, L. S. and Sterns, V. J. "Heat Transfer in Vertical Tubes — Interaction of Forced and Free Convection," *Chemical Engineering Journal*, Vol. 4, 1972, pp. 46–52.
- [58] Colebrook, C.F. "Turbulent Flow in Pipes with Particular Reference to the Transition Region Between Smooth and Rough Pipe Laws," *Journal of the Institution of Civil Engineers*, Vol. 11, 1939, pp. 133–156.
- [59] Moody, L.F. "Friction Factors for Pipe Flow," *Transactions of the ASME*, Vol. 66, pp. 671–684.
- [60] Handbook of Heat Transfer Applications, eds. W.M. Rohsenow, J.P. Hartnett, and Y.I. Cho, McGraw Hill Book Company, Third Edition, 1998.
- [61] Fryer, P.J. and Slater, N.K.H. "A Direct Simulation Procedure for Chemical Reaction Fouling in Heat Exchangers," *The Chemical Engineering Journal*, Vol. 31, 1985, pp. 97–107.
- [62] Somerscales, E.C. Sanatagar, H. and Khartabil, H.F. "The Uncertainty of Fouling Thermal Resistance Measurements," to be published in *Experimental Thermal and Fluid Science*.
- [63] Cooper, A. and Usher, J.D. "Plate Arrangement and Correction Factors," *Handbook of Heat Exchanger Design*, Chapter 3.7.8, Begell House, Inc., New York, 1992.
- [64] Arpaci, Vedat S. "Microscales of Turbulent Heat and Mass Transfer," *Advances in Heat Transfer*, Academic Press, 1997, pp. 1–91.
- [65] Bowman, C. F. and Craig, E. F. "Plate Heat Exchanger Performance in Nuclear Safety Related Service Water Applications," 1995 International Joint Power Generation Conference.
- [66] ASME Steam Tables, ASME Press, New York, Seventh Edition.
- [67] Reid, R.C. Prausnitz, J.M. and Poling, B.E. "The Properties of Liquids and Gases," McGraw Hill Book Company, Fourth Edition, 1987.
- [68] Vargaftik, N.B. et al., "Handbook of Physical Properties of Liquids and Gases," Third Edition, Begell House, 1996.
- [69] ASHRAE Handbook of Fundamentals, American Society of Heating, Refrigerating, and Air Conditioning Engineers, Atlanta GA, 1985.
- [70] GPA Standard 2174-93, "Obtaining Liquid Hydrocarbon Samples for Analysis by Gas Chromatography," Gas Processors Association, Tulsa OK, 1993.
- [71] GPA Standard 2166-86, "Obtaining Natural Gas Samples for Analysis by Gas Chromatography," Gas Processors Association, Tulsa OK, 1986.
- [72] ASTM D 4057, "Standard Practice for Manual Sampling of Petroleum and Petroleum Products," from Section 1, Chapter 8 of the *Manual of Petroleum Measurement Standards*, American Petroleum Institute, Third Edition, October 1995.
- [73] ASTM D 5842, "Standard Practice for Manual Sampling and Handling of Fuels for Volatility Measurement," from Section 4, Chapter 8 of the *Manual of Petroleum Measurement Standards*, American Petroleum Institute, Third Edition, October 1995.
- [74] ANSI/ARI 410-91, "Forced-Circulation Air-Cooling and Air-Heating Coils," 1991.
- [75] ASHRAE SPC 33-1992, "Methods of Testing Forced Circulation Air Cooling and Air Heating Coils," 1992.

- [76] Kim, N.H. Youn, B. and Webb, R.L. "Air-Side Heat Transfer and Friction Correlations for Plain Fin-and-Tube Heat Exchangers With Staggered Tube Arrangements," *ASME Journal of Heat Transfer*, Vol. 121, pp. 662–667.
- [77] Schenck, H. "Theories of Engineering Experimentation," Chapter 9, Third Edition. Washington D.C. and New York: Hemisphere Publishing Corporation and McGraw Hill Book Company, 1979.

# NONMANDATORY APPENDIX A — STEADY STATE CRITERIA

Testing shall be performed at steady state conditions. Testing under transient conditions can be used to perform an accurate assessment of performance but the methods used to analyze the results are not included in this Code. If tests performed under transient conditions are analyzed in accordance with the methods of this Code, the results may be different and the overall uncertainty will be greater than if transient analysis methods are used.

Industrial process streams typically do not operate under completely steady conditions. Instead, interactions between the pumps, valves, heat exchangers and tanks result in process variations described as “almost steady.” To ensure conditions adequately approximate steady state, limits of variation for the measurements are often specified in the test procedures. Limiting variations during a test is often not practical and is not necessary for high accuracy testing. Instead, an assessment of the significance and uncertainty due to these process variations is performed. The use of limits of variation may be used in the test procedures to control test conditions, but an evaluation of the variations of the data is required to assess the acceptability and uncertainty of the steady state assumption.

This Appendix describes guidelines to assess the significance of almost steady conditions and methods to estimate the uncertainty of the measurements attributed to process variations. The uncertainty of flow, temperature, and pressure measurements attributed to process variations is estimated as the difference between the calculated average values over the test period and their true, unbiased representative values over the test period. This assessment includes evaluation of transient conditions prior to the test, evaluation of the random process variations during the test, and non-random drift over the test period.<sup>1</sup>

As discussed in Section 3, parties to the test shall agree to steady state criteria. Specific criteria depend

upon particular conditions of the industrial facility and are not discussed in this appendix. For an ideal test, data during the test period should not contain a drift or other non-random component, and random process variations during the test period should be kept to a minimum. Data with some drift and larger process variations are acceptable provided that the uncertainty attributed to these non-ideal effects is adequately bounded. Steady state criteria consist of qualitative and/or quantitative measures of acceptable random and non-random variations along with methods to estimate their uncertainty.

## A.1 NON-STEADY CONDITIONS PRIOR TO THE TEST PERIOD

Prior to the test, non-steady conditions are expected due to startup of pumps, positioning of valves, and heat-up of the heat exchanger. The transient, non-random behavior of the data should be completely dampened at the beginning of the test period. The impact of most pre-test events such as pump starts and valve operation can be confirmed by reviewing the data traces for temperatures and flows, and performing a qualitative visual evaluation of the data traces to confirm that pretest transients have dampened. Quantitative evaluation of pre-test conditions can be performed by comparing the average and variance of data in sample windows prior to the test as discussed in para. A.2 below.

## A.2 RANDOM PROCESS VARIATIONS

Random variation of process measurements is expected during the test period due to variations in temperature, pressure and flow conditions, and random instrument effects which cannot be controlled or eliminated. A heat exchanger test at steady state conditions is comprised primarily of random process variations (random variations are substantially greater than non-random variations). There are a number of methods to test the conditions for steady state,

<sup>1</sup> The guidelines included in the Code are general for application to heat exchanger testing; references to more complete discussion are included.

and two methods are introduced here. The first method is based on the test for stationarity from Reference 19.

(a) Divide the data measured over the test period into  $M$  equal time intervals with  $N$  data measurements in each time interval. Time intervals of 1 to 3 minutes are considered acceptable for most industrial tests.

(b) Calculate the average value,  $\bar{x}$ , and variance,  $s_x^2$ , for each interval in accordance with Eqs. (A.1) and (A.2).

$$\bar{x} = \frac{1}{N} \sum_{i=1}^N x_i \quad (\text{A.1})$$

$$s_x^2 = \frac{1}{N-1} \sum_{i=1}^N (x_i - \bar{x})^2 \quad (\text{A.2})$$

(c) Evaluate the calculated sample average and variance for trends or variations other than those expected. This evaluation can be performed with a statistical test, but qualitative inspection of the interval data is often sufficient to identify trends.

Several statistical tests discussed in Reference 19 can be considered. For example, evaluation to establish the randomness of observed variations in the data can be performed with a run test or reverse arrangements test. A t-statistic test can determine if the average changes significantly for successive intervals. An F-statistic test evaluates the ratio of the variances, where the numerator is the mean of the squared differences of the measured data and the average over the time window and the denominator is the mean of the squared differences between successive data. If the time series is stationary, the ratio will be near unity. For non-steady processes, the value of the ratio will be substantially greater than unity.

The second method introduced in this Section is a variation of the F-statistic test suited for implementation with an automated data acquisition and control system, Reference 20. The ratio of variances is determined with the variance in the numerator calculated based on the mean of the squared differences between the measured data and the filtered value, and the variance in the denominator calculated based on the mean of the squared differences between successive measured data. As with the F-statistic test, the ratio will be near unity for a stationary process, and the ratio will be substantially greater than unity for non-steady processes. As discussed in Reference 20, the value of the ratio is

dependent upon the filtering constants, and a critical threshold should be established based on preliminary test runs as agreed by the parties to the test.

If randomness of the observed variations can be established, the standard deviation of  $M$  sample time intervals due to these random process variations can be estimated:

$$s_{\bar{x}} = \frac{s_x}{\sqrt{M}} \quad (\text{A.3})$$

This value can be used to estimate the uncertainty based on Eq. (A.4).

### A.3 NON-RANDOM PROCESS VARIATIONS

Non-random variations consist of periodic or transient non-periodic changes in measurement conditions. For heat exchanger testing, non-random variations typically consist of drift in the measurements attributed to conditions, which cannot be stabilized during the test period (such as cooldown or heat up of a tank, or slow changes in environmental conditions). Unlike random variations, the bias due to drift may not be reduced by extending the test period. Data sampling rate and instrument accuracies should be sufficient to measure drift in test conditions such that the calculated average does not contain a bias, which is greater than the calibration bias of the associated instrument. The bias in the measurements is attributed to the thermal lag in the response of the instrument and heat exchanger to the changing inlet conditions. A model of the thermal response of the instrument and heat exchanger can be used to calculate the thermal lag. The bias is represented by the difference between the calculated response and the ideal response without thermal lag.

Development of methods to calculate the thermal lag in measurements due to the instrument and heat exchanger is beyond the scope of this Code. Models to calculate the thermal response of instruments and heat exchangers are available in the open literature. The references in Section 7 contain methods to estimate the thermal lag of instrumentation. In addition, References 24 and 25 provide a model for the response of a temperature element. A model of a counterflow heat exchanger element is developed in References 21, 22 and 23. References 22 and 23 provide solutions for response to step changes in inlet temperature and flow conditions.

Once a calculation of the thermal lag of the instruments and heat exchanger has been performed, data can be corrected to reduce the bias. However, some bias contribution to the total measurement uncertainty should be retained for tests with drift in measurements.

#### A.4 UNCERTAINTY ATTRIBUTED TO PROCESS VARIATIONS

An estimate of the uncertainty of process variations is required. The uncertainty due to almost steady conditions of an averaged measurement  $x$ ,  $u_{x,pv}$ ,

consists of a bias component due to drift,  $b_{x, drift}$ , and a random component  $s_{\bar{x}}$ , which are combined based on the guidelines provided in ASME PTC 19.1, Reference 1:

$$u_{x, pv} = 2 \sqrt{(b_{x, drift}/2)^2 + (s_{\bar{x}})^2} \quad (\text{A.4})$$

where

$M$  = number of sample time intervals over the test period

$s_{\bar{x}}$  = standard deviation of the mean of  $M$  time intervals

$b_{x, drift}$  = bias component due to drift of the data over the interval

This page intentionally left blank.

# NONMANDATORY APPENDIX B — EQUATIONS AND COEFFICIENTS FOR UNCERTAINTY ANALYSIS

This Appendix describes a procedure to propagate elemental uncertainties and calculate the uncertainty of performance parameters at reference conditions consistent with the requirements of this Code and methods in ASME PTC 19.1. The method described in this appendix is suitable for spreadsheet implementation. Alternate approaches consistent with the requirements of this Code are acceptable.

The equations for propagating elemental sources of uncertainty used in this appendix are as follows:

$$U^* = \frac{1}{\frac{1}{U} + \frac{A}{(\eta A)_c} \left[ \frac{1}{h_c^*} - \frac{1}{h_c} \right] + \frac{A}{(\eta A)_h} \left[ \frac{1}{h_h^*} - \frac{1}{h_h} \right] + (R_w^* - R_w)} \quad (\text{B.1})$$

$$Q^* = \frac{Q_{ave} EMTD^*/EMTD}{1 + U \left[ \frac{A}{(\eta A)_c} \left( \frac{1}{h_c^*} - \frac{1}{h_c} \right) + \frac{A}{(\eta A)_h} \left( \frac{1}{h_h^*} - \frac{1}{h_h} \right) + R_w^* - R_w \right]} \quad (\text{B.2})$$

$$\Delta P_{n-n}^* = \phi_{\Delta P} \Delta P_{n-n} = \frac{H_{R^*}}{H_R} \left( \frac{m^*}{m} \right)^n \Delta P_{n-n} \quad (\text{B.3})$$

Equations (B.1), (B.2), and (B.3) are the same as Eqs. (5.15), (5.16), and (5.17) respectively. Refer to Section 5 and Section 2 for a description of the nomenclature.

## Step 1. Calculate the Uncertainty of Temperature, Flow, and Pressure Measurements

The overall uncertainty for 95% confidence of an individual temperature, pressure or flow measurement,  $u_x$ , with 31 or more measurement samples is given by Eq. (B.4):

$$u_x = 2 \left[ (b_{install}^2 + b_{cal}^2 + b_{SpatVar}^2 + b_{DataAcq}^2 + u_{pv}^2)/4 + s_{\bar{x}}^2 \right]^{1/2} \quad (\text{B.4})$$

where the terms are defined in Table B.1.

**TABLE B.1**  
**SENSITIVITY COEFFICIENTS FOR UNCERTAINTY OF TEMPERATURE, FLOW, AND PRESSURE MEASUREMENTS [Note (1)]**

Contributing Factor	Sensitivity Coefficient
Uncertainty attributed to calibration, $b_{cal}$	1
Uncertainty attributed to spatial variation, $b_{SpatVar}$	1
Uncertainty attributed to installation, $b_{install}$	1
Uncertainty attributed to data acquisition, $b_{DataAcq}$	1
Uncertainty attributed to almost steady conditions, $u_{pv}$	1
Uncertainty attributed to random error (standard deviation of the mean, based on measurement variations while system conditions remain constant), $s_{\bar{x}}$	N/A

NOTE:

(1) The sensitivity coefficient is the change in the calculated result due to an incremental change in a contributing factor. For an arbitrary result  $Y$  and contributing factor  $x$ , the sensitivity coefficient is  $\Theta_{Y,x} = \partial Y / \partial x$ .

## Step 2. Calculate the Uncertainty of Heat Transfer Rate at Test Conditions

The uncertainties of the cold stream heat transfer rate,  $u_{Qc}$ , hot stream heat transfer rate,  $u_{Qh}$ , and weighted average heat rate,  $u_{Qave}$ , are given by Eqs. (B.5), (B.6), and (B.7) where the terms are defined in Table B.2:

$$u_{Qc} = [(\theta_{Q,ti} u_{ti})^2 + (\theta_{Q,to} u_{to})^2 + (\theta_{Q,mc} u_{mc})^2 + (\theta_{Q,cpc} u_{cpc})^2]^{1/2} \quad (\text{B.5})$$

$$u_{Qh} = [(\theta_{Q,Ti} u_{Ti})^2 + (\theta_{Q,To} u_{To})^2 + (\theta_{Q,mh} u_{mh})^2 + (\theta_{Q,cph} u_{cph})^2]^{1/2} \quad (\text{B.6})$$

$$u_{Qave} = [u_{Qc}^4 u_{Qh}^2 + u_{Qh}^4 u_{Qc}^2]^{1/2} / (u_{Qc}^2 + u_{Qh}^2) \quad (\text{B.7})$$

**TABLE B.2**  
**SENSITIVITY COEFFICIENTS FOR UNCERTAINTY OF HEAT TRANSFER RATE**  
**AT TEST CONDITIONS**

Contributing Factor	Sensitivity Coefficient
Uncertainty attributed to cold stream inlet temperature, $u_{ti}$	$\theta_{Q,ti} = -m_c c_{p,c}$
Uncertainty attributed to cold stream outlet temperature, $u_{to}$	$\theta_{Q,to} = m_c c_{p,c}$
Uncertainty attributed to cold stream flow rate, $u_{mc}$	$\theta_{Q,mc} = c_{p,c}(t_o - t_i)$
Uncertainty attributed to cold stream specific heat, $u_{cpc}$	$\theta_{Q,cpc} = m_c(t_o - t_i)$
Uncertainty attributed to hot stream inlet temperature, $u_{Ti}$	$\theta_{Q,Ti} = m_h c_{p,h}$
Uncertainty attributed to hot stream outlet temperature, $u_{To}$	$\theta_{Q,To} = -m_h c_{p,h}$
Uncertainty attributed to hot stream flow rate, $u_{mh}$	$\theta_{Q,mh} = c_{p,h}(T_i - T_o)$
Uncertainty attributed to hot stream specific heat, $u_{cph}$	$\theta_{Q,cph} = m_h(T_i - T_o)$

**TABLE B.3**  
**SENSITIVITY COEFFICIENTS FOR UNCERTAINTY OF OVERALL HEAT**  
**TRANSFER COEFFICIENT AT TEST CONDITIONS**

Contributing Factor	Sensitivity Coefficient
Uncertainty attributed to mean temperature difference at test conditions, $u_{EMTD}$	$\theta_{U,EMTD} = \frac{Q_{ave}}{A EMTD^2}$
Uncertainty attributed to average heat transfer rate at test conditions, $u_{Qave}$	$\theta_{U,Q} = \frac{1}{A EMTD}$

### Step 3. Calculate the Uncertainty of the Mean Temperature Difference at Test Conditions

The uncertainty in mean temperature difference at test conditions,  $u_{EMTD}$ , can be calculated by analytic methods or graphical methods as discussed in Appendix D.

### Step 4. Calculate the Uncertainty of the Overall Heat Transfer Coefficient at Test Conditions

The uncertainty in overall heat transfer coefficient at test conditions,  $u_U$ , is given by Eq. (B.8) where the terms are defined in Table B.3:

$$u_U = [(\theta_{U,Q} u_{Qave})^2 + (\theta_{U,EMTD} u_{EMTD})^2]^{1/2} \quad (B.8)$$

### Step 5. Calculate the Uncertainty of the Overall Heat Transfer Coefficient at Reference Conditions

The uncertainty in overall heat transfer coefficient at reference conditions,  $u_{U^*}$ , is given by Eq. (B.9) where the terms are defined in Table B.4:

$$u_{U^*} = [(\theta_{U^*,U} u_U)^2 + (\theta_{U^*,(1/h^* - 1/h)c} u_{(1/h^* - 1/h)c})^2 + (\theta_{U^*,(1/h^* - 1/h)h} u_{(1/h^* - 1/h)h})^2]^{1/2} \quad (B.9)$$

### Step 6. Calculate the Uncertainty of the Heat Transfer Rate at Reference Conditions

**TABLE B.4**  
**SENSITIVITY COEFFICIENTS FOR UNCERTAINTY OF**  
**OVERALL HEAT TRANSFER COEFFICIENT AT REFERENCE CONDITIONS**

Contributing Factor	Sensitivity Coefficient
Uncertainty attributed to overall heat transfer coefficient at test conditions, $u_U$	$\theta_{U^*,U} = (U^*/U)^2$
Uncertainty attributed to adjustment in cold stream convective thermal resistance, $u_{(1/h^* - 1/h)c}$	$\theta_{U^*,(1/h^* - 1/h)c} = \frac{A}{(\eta A)_c} (U^*)^2$
Uncertainty attributed to adjustment in hot stream heat transfer coefficient, $u_{(1/h^* - 1/h)h}$	$\theta_{U^*,(1/h^* - 1/h)h} = \frac{A}{(\eta A)_h} (U^*)^2$

**TABLE B.5**  
**SENSITIVITY COEFFICIENTS FOR UNCERTAINTY OF HEAT TRANSFER RATE**  
**AT REFERENCE CONDITIONS**

Contributing Factor	Sensitivity Coefficient
Uncertainty attributed to the mean temperature difference at test conditions, $u_{EMTD}$	$\theta_{Q^*,EMTD} = \frac{-Q^*}{EMTD}$
Uncertainty attributed to heat transfer rate at test conditions, $u_{Q_{ave}}$	$\theta_{Q^*,Q} = \frac{Q^*}{Q_{ave}}$
Uncertainty attributed to overall heat transfer coefficient at test conditions, $u_U$	$\theta_{Q^*,U} = \frac{Q^*}{U} \left(1 - \frac{U^*}{U}\right)$
Uncertainty attributed to change in cold stream convective thermal resistance, $u_{(1/h^* - 1/h)c}$	$\theta_{Q^*,(1/h^* - 1/h)c} = Q^* U^* \frac{A}{(\eta A)_c}$
Uncertainty attributed to change in hot stream convective thermal resistance, $u_{(1/h^* - 1/h)h}$	$\theta_{Q^*,(1/h^* - 1/h)h} = Q^* U^* \frac{A}{(\eta A)_h}$

The uncertainty in heat transfer rate at reference conditions,  $u_{Q^*}$ , is given by Eq. (B.10) and the terms are defined in Table B.5:

$$u_{Q^*} = [(\theta_{Q^*,Q} u_{Q_{ave}})^2 + (\theta_{Q^*,EMTD} u_{EMTD})^2 + ((\theta_{Q^*,U} u_U)^2 + (\theta_{Q^*,(1/h^* - 1/h)c} u_{(1/h^* - 1/h)c})^2 + (\theta_{Q^*,(1/h^* - 1/h)h} u_{(1/h^* - 1/h)h})^2]^{1/2} \quad (B.10)$$

#### Step 7. Calculate the Uncertainty of the Nozzle-to-Nozzle Pressure Loss at Test Conditions

Assuming that the uncertainty of the fluid density is small because the change in fluid density is small, the uncertainty of the nozzle-to-nozzle pressure loss is calculated based on contributions due to the pressure measurement, the loss coefficients of the pipe and fittings between the inlet and outlet nozzles and associated pressure taps, and the pipe fluid velocity. The uncertainty in nozzle-to-nozzle pres-

sure loss at test conditions is given by Eq. (B.11) and the terms are defined in Table B.6:

$$u_{\Delta P_{n-n}} = \left[ \begin{aligned} &(\theta_{\Delta P_{n-n}, \Delta P} u_{\Delta P})^2 + (\theta_{\Delta P_{n-n}, P_U} u_{P_U})^2 \\ &+ (\theta_{\Delta P_{n-n}, i, K_{pipe}} u_{i, K_{pipe}})^2 \\ &+ (\theta_{\Delta P_{n-n}, o, K_{pipe}} u_{o, K_{pipe}})^2 \\ &+ (\theta_{\Delta P_{n-n}, v} u_{v})^2 \end{aligned} \right]^{1/2} \quad (B.11)$$

#### Step 8. Calculate the Uncertainty of Nozzle-to-Nozzle Pressure Loss at Reference Conditions

The uncertainty in the pressure loss at reference conditions,  $\Delta P_{n-n}^*$ , is given by Eq. (B.12) and the terms are defined in Table B.7:

$$u_{\Delta P_{n-n}^*} = [(\theta_{\Delta P_{n-n}^*, HR^*/HR} u_{HR^*/HR})^2 + (\theta_{\Delta P_{n-n}^*, m} u_m)^2 + (\theta_{\Delta P_{n-n}^*, \Delta P_{n-n}} u_{\Delta P_{n-n}})^2]^{1/2} \quad (B.12)$$

**TABLE B.6**  
**SENSITIVITY COEFFICIENTS FOR UNCERTAINTY OF**  
**NOZZLE-TO-NOZZLE PRESSURE LOSS AT TEST CONDITIONS**

Contributing Factor	Sensitivity Coefficient
Uncertainty attributed to the differential pressure measurement, $u_{\Delta P}$	$\theta_{\Delta P_{n-n}, \Delta P} = \frac{\rho_{ave}}{\rho_{o, pipe}}$
Uncertainty attributed to the upstream pressure measurement, $u_{P_u}$	$\theta_{\Delta P_{n-n}, P_u} = \rho_{ave} \left( \frac{1}{\rho_{i, pipe}} - \frac{1}{\rho_{o, pipe}} \right)$
Uncertainty attributed to the loss coefficient for the pipe and fittings between the inlet nozzle and pressure tap, $u_{\Delta P_{n-n}, i, K_{pipe}}$	$\theta_{\Delta P_{n-n}, i, K_{pipe}} = -\rho_{ave} v_i^2 / 2g_c$
Uncertainty attributed to the loss coefficient for the pipe and fittings between the outlet nozzle and pressure tap, $u_{\Delta P_{n-n}, o, K_{pipe}}$	$\theta_{\Delta P_{n-n}, o, K_{pipe}} = -\rho_{ave} \left( \frac{\rho_{i, pipe} A_{i, pipe}}{\rho_{o, pipe} A_{o, pipe}} \right)^2 v_i^2 / 2g_c$
Uncertainty attributed to inlet pipe velocity, $u_{v_i}$	$\theta_{\Delta P_{n-n}, v_i} = \rho_{ave} \left[ \begin{array}{c} 1 - K_{pipe, i} \\ - (1 + K_{o, pipe}) \left( \frac{\rho_{i, pipe} A_{pipe, i}}{\rho_{o, pipe} A_{pipe, o}} \right)^2 \end{array} \right] v_i / g_c$

**TABLE B.7**  
**SENSITIVITY COEFFICIENTS FOR UNCERTAINTY OF**  
**NOZZLE-TO-NOZZLE PRESSURE LOSS AT REFERENCE CONDITIONS**

Contributing Factor	Sensitivity Coefficient
Uncertainty attributed to the hydraulic resistance ratio, $u_{HR^*/HR}$	$\theta_{\Delta P_{n-n}^*, HR^*/HR} = \Delta P_{n-n} \left( \frac{m^*}{m} \right)^n$
Uncertainty attributed to flow rate measurement, $u_m$	$\theta_{\Delta P_{n-n}^*, m} = -\frac{n \Delta P_{n-n}^*}{m}$
Uncertainty attributed to nozzle-to-nozzle pressure loss test conditions, $u_{\Delta P_{n-n}}$	$\theta_{\Delta P_{n-n}^*, \Delta P_{n-n}} = \phi_{\Delta P}$

# NONMANDATORY APPENDIX C — THE DELAWARE METHOD FOR SHELL-SIDE PERFORMANCE

## C.1 INTRODUCTION

The Delaware Method for calculating shell-side heat transfer and pressure loss for shell and tube heat exchangers was first developed from the results of the University of Delaware research program on shell and tube heat exchangers carried out under ASME sponsorship from 1947 to 1963. The first publication of the rating method was in 1961 and there have been a number of subsequent publications (with slight variations and extensions) in the years since. The Delaware Method is generally regarded as the most accurate and comprehensive shell and tube design method in the open literature and has been selected for inclusion in this document because it is available to all users without restriction. The version given here is consistent with the version in Reference 26. The present form is quite feasible for hand calculations, but can be readily converted to a computer-based procedure if frequency warrants.

The application of the Delaware Method for the purposes of this Code is to "rate" the performance of a (nominally) completely specified shell and tube heat exchanger under specified operating conditions, i.e., to calculate the heat transfer characteristics (film and overall heat transfer coefficients, stream outlet temperatures and heat duty) and shell-side and tube-side pressure losses.

There are more accurate proprietary computer-based methods available. Most of these are based on Tinker's Stream Analysis Method (see para. C.2) and require the use of a computer and some expertise in running and interpreting the program.

## C.2 SIMPLIFIED MECHANISMS OF SHELL-SIDE FLOW

In Fig. C-2.1, a diagram of the shell-side flow mechanisms in a highly idealized form is shown. This diagram has been modified from Palen and Taborek, Reference 13, who in turn borrowed it and modified it from the original version shown by Tinker, Reference 27. Five different streams on the

shell-side are identified. Stream B is the main cross-flow stream flowing through one window across the crossflow section and out through the opposite window. This is the stream that is desired on the shell-side of the exchanger.

However, because of the mechanical clearances required in a shell and tube exchanger, there are four other streams which compete with the B stream. First, there is the A stream leaking through the clearances between the tubes and the baffle, from one baffle compartment to the next. Then there is the C stream, the bundle bypass stream, flowing around the tube bundle between the outermost tubes in the bundle and the inside of the shell. The E stream is the shell-to-baffle leakage stream flowing through the clearance between the baffles and the inside diameter of the shell. The last of the identified major streams is the F stream, which flows through any channels within the tube bundle caused by the provision of pass dividers in the exchanger header (i.e., only in multiple tubepass configurations). (It should be noted that, for a two tubepass configuration as shown here, the pass divider ordinarily would be oriented perpendicular to the direction of the main crossflow stream and would not provide an internal bypass stream; however, it is shown here because it can have a very serious effect in multiple tubepass configurations, where at least some of the pass lanes may be parallel to the direction of flow.)

These streams do not, of course, exist as precisely defined streams as shown in Fig. C-2.1. They form and mix and interact with one another, and a more complete mathematical analysis of the shell-side flow would take this into account. However, these analyses are also quite complicated (see Reference 13) and cannot be carried out exactly in any case, simply because of a lack of knowledge of the turbulent flow structures on the shell-side. Therefore, Fig. C-2.1 is an idealized representation but does allow us to talk in terms of the major effects modifying the idealized flow pattern.

In the Delaware Method, the B stream is regarded as the essential stream in the exchanger with the

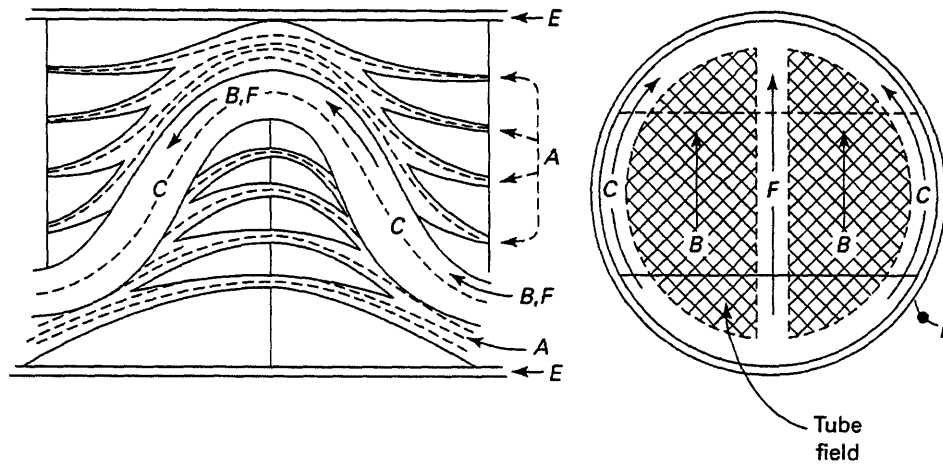


**FIG. C.2-1 IDEALIZED DIAGRAM OF SHELL-SIDE FLOW STREAMS**  
 (Adapted from Palen and Taborek (13) and Tinker (27)  
 (Courtesy of Kenneth J. Bell))

other streams exerting various modifying effects upon the performance as predicted for the B stream alone. The various leakage and bypass streams affect the heat transfer rate in two separate ways:

(a) They reduce the B stream and therefore the local heat transfer coefficient;

(b) They alter the shell-side temperature profile. The Delaware Method in effect lumps these two effects together into a single correction.

Not all of the leakage and bypass streams have the same relative magnitude of effect and, of course, they respond differently to various geometrical parameters of the shell-side. For example, the A stream (tube-to-baffle leakage) has only a relatively small effect upon the heat transfer coefficient and the pressure loss. The C stream has a relatively large effect, but there are mechanical ways of partially blocking this flow to minimize that effect. The E stream (shell-to-baffle leakage) has an extremely serious effect and unfortunately there is relatively little one can do to help. Finally, the pass divider bypass stream (F stream) has a moderate effect and responds to some of the same treatments that the bundle bypass stream does.

### C.3 DETERMINATION OF SHELL-SIDE GEOMETRICAL PARAMETERS<sup>1</sup>

The Delaware Method assumes that the flow rate and the inlet and outlet temperatures (also pressures

for a gas or vapor) of the shell-side fluid are specified and that the density, viscosity, thermal conductivity, and specific heat of the shell-side fluid are known or can be reasonably estimated as a function of temperature. The method also assumes that the following minimum set of shell-side geometry data is known or specified:

- (a) Tube outside diameter,  $d_o$ ;
- (b) Tube geometrical arrangement (unit cell geometry and tube pitch);
- (c) Shell inside diameter,  $D_i$ ;
- (d) Diameter of the outer tube limit,  $D_{oli}$ ;
- (e) Effective tube length (between tube sheets),  $\ell$ ;
- (f) Baffle cut,  $\ell_c$ ;
- (g) Baffle spacing  $\ell_s$  (also the inlet and outlet baffle spacings,  $\ell_{s,i}$  and  $\ell_{s,o}$ , if different from  $\ell_s$ );
- (h) Number of sealing strips/side,  $N_{ss}$ ;
- (i) Number of pass partition lanes parallel to the direction of flow,  $N_p$ , and the width of these lanes,  $W_p$ ;
- (j) Number of fins per unit length,  $N_f$ , the fin thickness,  $y_f$ , and fin height,  $h_f$ .

From this geometrical information, all remaining geometrical parameters needed in the shell-side calculations can be calculated or estimated by methods given here, assuming that Standards of the Tubular Exchanger Manufacturers Association, Reference 28, are met with respect to tube-to-baffle and shell-to-baffle clearances. However, if additional specific information is available (e.g., tube-to-baffle clearance), the exact values of certain parameters may be used in the calculation with some improvement

<sup>1</sup> The nomenclature for this appendix is in para. C.6.

in accuracy. The Delaware Method can be applied to a variety of shell-side geometries. Some modification to the equations presented in this section may be needed to apply the Delaware method to all shell geometries. Fig. C.3-1 shows shell-side geometry characteristics of a fully tubed E-shell to assist in application of equations provided in this section.

(a) *Total Number of Tubes in the Exchanger,  $N_t$ .* If not known by direct count, find in Table C.3-1, as a function of the diameter of the outer tube limit,  $D_{otl}$ , the tube pitch,  $p$ , and the layout. The shell diameter  $D_i$  and outer tube limit  $D_{otl}$ , given in the Table are those for a conventional fully tubed split-ring floating head design. For a given shell diameter, the value of  $D_{otl}$  will be greater than that shown for a fixed tube sheet design and smaller for a pull-through floating head. In any case, the tube count can be reasonably interpolated from Table C.3-1 using the known or specified  $D_{otl}$ , assuming that the tube count is proportional to  $(D_{otl})^2$ . All tube count tables are only approximate since the actual number of tubes that can be fitted into a given tubesheet depends upon the pass partition pattern, the thickness of the pass dividers and exactly where the drilling pattern is started relative to the dividers and the outer tube limit. Additional tubes will be lost from the bundle for a U-tube design because the minimum bending radius prevents tubes from being inserted in some or all of the possible drilling positions near the centerline of the U-tube pattern. Tubes will also be lost if an impingement plate is inserted underneath the nozzle; analysis of this case requires special care. For a no-tubes-in-the-window design, the actual number of tubes in the bundle can be estimated as  $F_c N_t$  (see para. C.3-4 for the definition of  $F_c$ ).

(b) *Tube Pitch Parallel to Flow,  $p_p$ , and Normal to Flow,  $p_n$ .* These quantities are needed only for the purpose of estimating other parameters. If a detailed drawing of the exchanger is available, or if the exchanger itself can be conveniently examined, it is better to obtain these other parameters by direct count or calculation. These quantities are described by Fig. C.3-2 and read from Table C.3-2 for the most common tube layouts.

(c) *Number of Tube Rows Crossed in One Crossflow Section (Between Baffle Tips),  $N_c$ .* Count from exchanger drawing or estimate from Eq. (C.3-1).

$$N_c = \frac{D_i \left[ 1 - 2 \left( \frac{\ell_c}{D_i} \right) \right]}{p_p} \quad (\text{C.3-1})$$

(d) *Fraction of Total Tubes in Crossflow,  $F_c$ .*

$$F_c = \frac{1}{\pi} \left\{ \pi + 2 \left( \frac{D_i - 2\ell_c}{D_{otl}} \right) \sin \left[ \cos^{-1} \left( \frac{D_i - 2\ell_c}{D_{otl}} \right) \right] - 2 \cos^{-1} \left( \frac{D_i - 2\ell_c}{D_{otl}} \right) \right\} \quad (\text{C.3-2})$$

where all the angles are read in radians. For convenience,  $F_c$  has been plotted to an acceptable degree of precision in Fig. C.3-3 as a function of percent baffle cut,  $(\ell_c/D_i)(100\%)$ , and shell diameter  $D_i$ . This figure is strictly applicable only to the  $(D_i - D_{otl})$  combinations shown in Table C.3-1 but may be used for other situations with minor error. For fixed tube sheet construction,  $F_c$  is a little lower than that shown, especially for the smaller shell diameters; for pull-through floating head construction,  $F_c$  is a little higher.

For no-tubes-in-the-window design, the actual number of tubes in the exchanger is  $F_c N_t$ , where  $F_c$  is given by Eq. (C.3-2), for all subsequent calculations for this design,  $F_c$  is then taken as 1.00.

(e) *Number of Effective Crossflow Rows in Each Window,  $N_{cw}$ .* If shop drawings are available,  $N_{cw}$  is the number of rows of tubes from the baffle cut to the shell that have at least half of the number of tubes in a row located at the centerline of the exchanger. Alternatively, estimate from Eq. (C.3-3).

$$N_{cw} = \frac{0.8\ell_c}{p_p} \quad (\text{C.3-3})$$

This equation assumes that the shell-side fluid on the average crosses about half of the tube rows in the window (but crosses each such row twice) and the tube rows extend about 0.8 of the distance from the baffle tip to the shell inside diameter. For no-tubes-in-the-window design,  $N_{cw} = 0$ .

(f) *Number of Baffles,  $N_b$ .* Count from the drawing, or calculate from Eq. (C.3-4).

$$N_b = \frac{\ell - \ell_{s,i} - \ell_{s,o}}{\ell_s} + 1 \quad (\text{C.3-4})$$

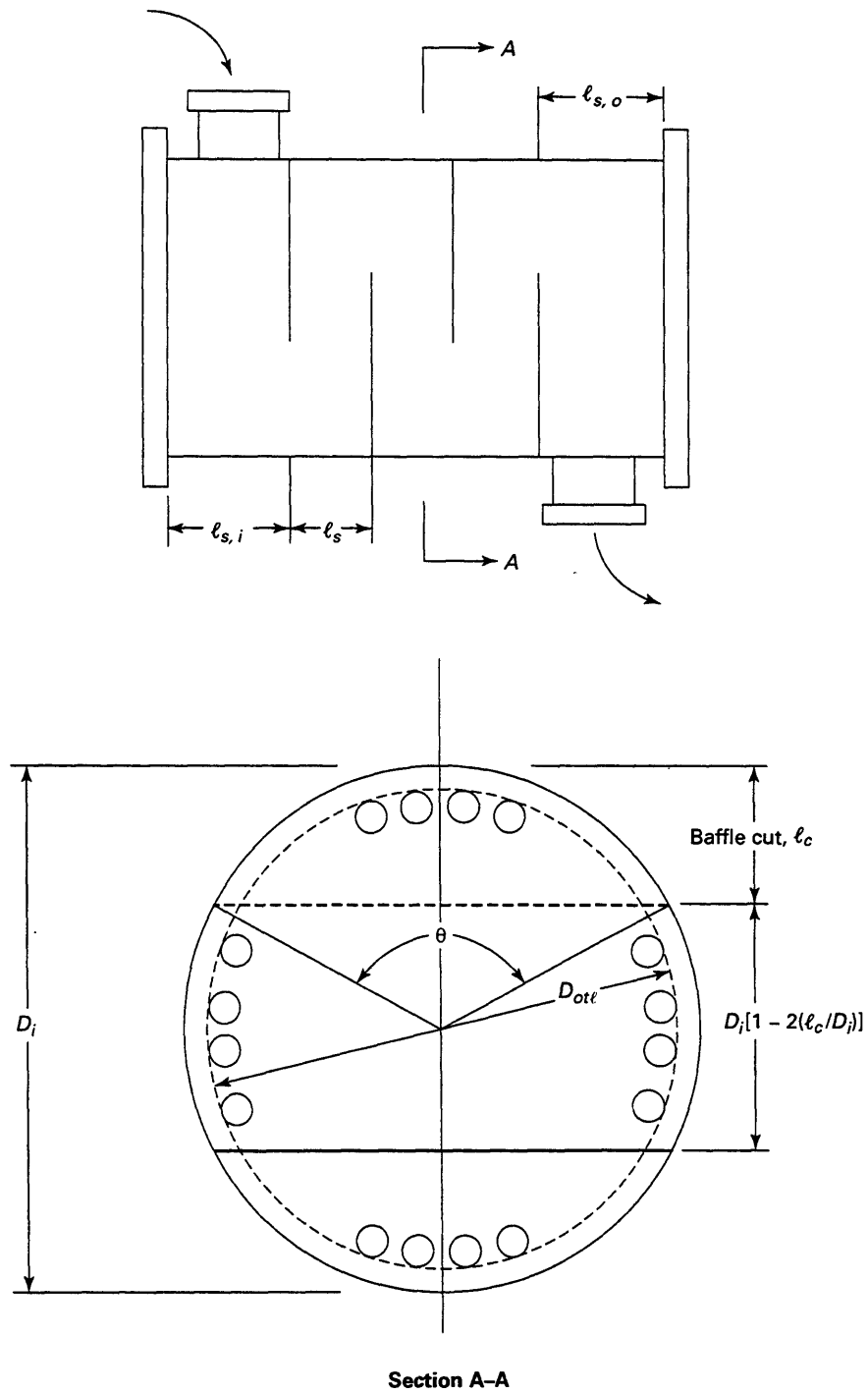


**FIG. C.3-1 SHELL-SIDE GEOMETRY CHARACTERISTICS FOR A FULLY-TUBED E-SHELL**  
 (Courtesy of Kenneth J. Bell)

**TABLE C.3-1 TUBE COUNTS**  
 (Adapted from Wolverine Tube Engineering Data Book and Perry's Handbook, 5th Edition)  
 (Courtesy of Kenneth J. Bell)

Shell ID in.	Dia. of Outer Tube Limit, in.	Tube OD, in.	Tube Pitch, in. Layout	Number of Tube Passes				
				1	2	4	6	8
8.07	6.82	$\frac{3}{4}$	$\frac{15}{16}$ $\Delta$	38	32	26	24	18
		$\frac{3}{4}$	1 $\square \diamond$	32	26	20	20	
		$\frac{3}{4}$	1 $\Delta$	37	30	24	24	
		1	$1\frac{1}{4}$ $\square \diamond$	21	16	16	14	
		1	$1\frac{1}{4}$ $\Delta$	22	18	16	14	
10.02	8.77	$\frac{3}{4}$	$\frac{15}{16}$ $\Delta$	62	56	47	42	36
		$\frac{3}{4}$	1 $\square \diamond$	52	52	40	36	
		$\frac{3}{4}$	1 $\Delta$	61	52	48	48	
		1	$1\frac{1}{4}$ $\square \diamond$	32	32	26	24	
		1	$1\frac{1}{4}$ $\Delta$	37	32	28	28	
12	$10\frac{3}{4}$	$\frac{3}{4}$	$\frac{15}{16}$ $\Delta$	109	98	86	82	
		$\frac{3}{4}$	1 $\square \diamond$	80	72	68	68	60
		$\frac{3}{4}$	1 $\Delta$	90	84	72	70	68
		1	$1\frac{1}{4}$ $\square \diamond$	48	44	40	38	36
		1	$1\frac{1}{4}$ $\Delta$	57	52	44	42	40
$13\frac{1}{4}$	12	$\frac{3}{4}$	$\frac{15}{16}$ $\Delta$	127	114	96	90	86
		$\frac{3}{4}$	1 $\square \diamond$	95	90	81	77	70
		$\frac{3}{4}$	1 $\Delta$	110	101	90	88	74
		1	$1\frac{1}{4}$ $\square \diamond$	60	56	51	46	44
		1	$1\frac{1}{4}$ $\Delta$	67	63	56	54	50
$15\frac{1}{4}$	14	$\frac{3}{4}$	$\frac{15}{16}$ $\Delta$	170	160	140	136	128
		$\frac{3}{4}$	1 $\square \diamond$	138	132	116	112	108
		$\frac{3}{4}$	1 $\Delta$	163	152	136	133	110
		1	$1\frac{1}{4}$ $\square \diamond$	88	82	75	70	64
		1	$1\frac{1}{4}$ $\Delta$	96	92	86	84	72
$17\frac{1}{4}$	16	$\frac{3}{4}$	$\frac{15}{16}$ $\Delta$	239	224	194	188	178
		$\frac{3}{4}$	1 $\square \diamond$	188	178	168	164	142
		$\frac{3}{4}$	1 $\Delta$	211	201	181	176	166
		1	$1\frac{1}{4}$ $\square \diamond$	112	110	102	98	82
		1	$1\frac{1}{4}$ $\Delta$	130	124	116	110	94
$19\frac{1}{4}$	18	$\frac{3}{4}$	$\frac{15}{16}$ $\Delta$	301	282	252	244	234
		$\frac{3}{4}$	1 $\square \diamond$	236	224	216	208	188
		$\frac{3}{4}$	1 $\Delta$	273	256	242	236	210
		1	$1\frac{1}{4}$ $\square \diamond$	148	142	136	129	116
		1	$1\frac{1}{4}$ $\Delta$	172	162	152	148	128

**TABLE C.3-1 TUBE COUNTS (CONT'D)**  
 (Adapted from Wolverine Tube Engineering Data Book and Perry's Handbook, 5th Edition)  
 (Courtesy of Kenneth J. Bell)

Shell ID, in.	Dia. of Outer Tube Limit, in.	Tube OD, in.	Tube Pitch, in. Layout	Number of Tube Passes				
				1	2	4	6	8
21	19 <sup>1</sup> / <sub>4</sub>	<sup>3</sup> / <sub>4</sub>	<sup>15</sup> / <sub>16</sub> Δ	361	342	314	306	290
		<sup>3</sup> / <sub>4</sub>	1 □◇	276	264	246	240	234
		<sup>3</sup> / <sub>4</sub>	1 Δ	318	308	279	269	260
		1	1 <sup>1</sup> / <sub>4</sub> □◇	170	168	157	150	148
		1	1 <sup>1</sup> / <sub>4</sub> Δ	199	188	170	164	160
23 <sup>1</sup> / <sub>4</sub>	21 <sup>1</sup> / <sub>2</sub>	<sup>3</sup> / <sub>4</sub>	<sup>15</sup> / <sub>16</sub> Δ	442	420	386	378	364
		<sup>3</sup> / <sub>4</sub>	1 □◇	341	321	308	296	292
		<sup>3</sup> / <sub>4</sub>	1 Δ	381	369	349	326	328
		1	1 <sup>1</sup> / <sub>4</sub> □◇	210	199	197	186	184
		1	1 <sup>1</sup> / <sub>4</sub> Δ	247	230	216	208	202
25	23 <sup>1</sup> / <sub>4</sub>	<sup>3</sup> / <sub>4</sub>	<sup>15</sup> / <sub>16</sub> Δ	531	506	468	446	434
		<sup>3</sup> / <sub>4</sub>	1 □◇	397	391	370	360	343
		<sup>3</sup> / <sub>4</sub>	1 Δ	470	452	422	394	382
		1	1 <sup>1</sup> / <sub>4</sub> □◇	250	248	224	216	210
		1	1 <sup>1</sup> / <sub>4</sub> Δ	294	282	256	252	242
27	25 <sup>1</sup> / <sub>4</sub>	<sup>3</sup> / <sub>4</sub>	<sup>15</sup> / <sub>16</sub> Δ	637	602	550	536	524
		<sup>3</sup> / <sub>4</sub>	1 □◇	465	452	427	418	408
		<sup>3</sup> / <sub>4</sub>	1 Δ	559	534	488	474	464
		1	1 <sup>1</sup> / <sub>4</sub> □◇	286	275	267	257	250
		1	1 <sup>1</sup> / <sub>4</sub> Δ	349	334	302	296	286
29	27 <sup>1</sup> / <sub>4</sub>	<sup>3</sup> / <sub>4</sub>	<sup>15</sup> / <sub>16</sub> Δ	721	692	640	620	594
		<sup>3</sup> / <sub>4</sub>	1 □◇	554	542	525	509	500
		<sup>3</sup> / <sub>4</sub>	1 Δ	630	604	556	538	508
		1	1 <sup>1</sup> / <sub>4</sub> □◇	348	340	322	314	313
		1	1 <sup>1</sup> / <sub>4</sub> Δ	397	376	354	334	316
31	29 <sup>1</sup> / <sub>4</sub>	<sup>3</sup> / <sub>4</sub>	<sup>15</sup> / <sub>16</sub> Δ	847	822	766	722	720
		<sup>3</sup> / <sub>4</sub>	1 □◇	633	616	590	586	570
		<sup>3</sup> / <sub>4</sub>	1 Δ	745	728	678	666	640
		1	1 <sup>1</sup> / <sub>4</sub> □◇	402	390	366	360	348
		1	1 <sup>1</sup> / <sub>4</sub> Δ	472	454	430	420	400
33	31 <sup>1</sup> / <sub>4</sub>	<sup>3</sup> / <sub>4</sub>	<sup>15</sup> / <sub>16</sub> Δ	974	938	872	852	826
		<sup>3</sup> / <sub>4</sub>	1 □◇	742	713	687	683	672
		<sup>3</sup> / <sub>4</sub>	1 Δ	856	830	774	760	732
		1	1 <sup>1</sup> / <sub>4</sub> □◇	460	453	430	420	414
		1	1 <sup>1</sup> / <sub>4</sub> Δ	538	522	486	470	454
35	33 <sup>1</sup> / <sub>4</sub>	<sup>3</sup> / <sub>4</sub>	<sup>15</sup> / <sub>16</sub> Δ	1102	1068	1004	988	958
		<sup>3</sup> / <sub>4</sub>	1 □◇	827	811	773	762	756
		<sup>3</sup> / <sub>4</sub>	1 Δ	970	938	882	864	848
		1	1 <sup>1</sup> / <sub>4</sub> □◇	517	513	487	486	480
		1	1 <sup>1</sup> / <sub>4</sub> Δ	608	592	566	546	532

**TABLE C.3-1 TUBE COUNTS (CONT'D)**  
 (Adapted from Wolverine Tube Engineering Data Book and Perry's Handbook, 5th Edition)  
 (Courtesy of Kenneth J. Bell)

Shell ID, in.	Dia. of Outer Tube Limit, in.	Tube OD, in.	Tube Pitch, in. Layout	Number of Tube Passes					
				1	2	4	6	8	
37	35 <sup>1</sup> / <sub>4</sub>	<sup>3</sup> / <sub>4</sub>	<sup>15</sup> / <sub>16</sub> Δ	1242	1200	1144	1104	1078	
			1 □◇	929	902	880	870	852	
		1	<sup>3</sup> / <sub>4</sub>	1 Δ	1090	1042	982	966	958
			<sup>3</sup> / <sub>4</sub>	1 <sup>1</sup> / <sub>4</sub> □◇	588	580	555	544	538
				1 <sup>1</sup> / <sub>4</sub> Δ	678	664	632	614	598
39	37 <sup>1</sup> / <sub>4</sub>	<sup>3</sup> / <sub>4</sub>	<sup>15</sup> / <sub>16</sub> Δ	1377	1330	1258	1248	1212	
			1 □◇	1025	1012	984	964	952	
		1	<sup>3</sup> / <sub>4</sub>	1 Δ	1206	1176	1128	1100	1078
			<sup>3</sup> / <sub>4</sub>	1 <sup>1</sup> / <sub>4</sub> □◇	645	637	619	610	605
				1 <sup>1</sup> / <sub>4</sub> Δ	766	736	700	688	672
42	40 <sup>1</sup> / <sub>4</sub>	<sup>3</sup> / <sub>4</sub>	<sup>15</sup> / <sub>16</sub> Δ	1611	1580	1498	1464	1456	
			1 □◇	1201	1171	1144	1109	1087	
		1	<sup>3</sup> / <sub>4</sub>	1 Δ	1409	1378	1314	1296	1280
			<sup>3</sup> / <sub>4</sub>	1 <sup>1</sup> / <sub>4</sub> □◇	745	728	708	686	680
				1 <sup>1</sup> / <sub>4</sub> Δ	890	878	834	808	800
44	42 <sup>1</sup> / <sub>4</sub>	<sup>3</sup> / <sub>4</sub>	<sup>15</sup> / <sub>16</sub> Δ	1782	1738	1650	1624	1592	
			1 □◇	1349	1327	1286	1270	1252	
		1	<sup>3</sup> / <sub>4</sub>	1 Δ	1562	1535	1464	1422	1394
			<sup>3</sup> / <sub>4</sub>	1 <sup>1</sup> / <sub>4</sub> □◇	856	837	809	778	763
				1 <sup>1</sup> / <sub>4</sub> Δ	990	966	921	888	871
48	46	<sup>3</sup> / <sub>4</sub>	<sup>15</sup> / <sub>16</sub> Δ	1965	1908	1834	1801	1766	
			1 □◇	1620	1598	1553	1535	1505	
		1	<sup>3</sup> / <sub>4</sub>	1 Δ	1872	1845	1766	1724	1690
			<sup>3</sup> / <sub>4</sub>	1 <sup>1</sup> / <sub>4</sub> □◇	1029	1010	975	959	940
				1 <sup>1</sup> / <sub>4</sub> Δ	1188	1163	1098	1076	1055
52	50	<sup>3</sup> / <sub>4</sub>	<sup>15</sup> / <sub>16</sub> Δ	2347	2273	2178	2152	2110	
			1 □◇	1918	1890	1848	1826	1790	
		1	<sup>3</sup> / <sub>4</sub>	1 Δ	2212	2183	2092	2050	2010
			<sup>3</sup> / <sub>4</sub>	1 <sup>1</sup> / <sub>4</sub> □◇	1216	1196	1167	1132	1110
				1 <sup>1</sup> / <sub>4</sub> Δ	1405	1375	1323	1287	1262
56	54	<sup>3</sup> / <sub>4</sub>	<sup>15</sup> / <sub>16</sub> Δ	2704	2660	2556	2526	2489	
			1 □◇	2241	2214	2167	2142	2110	
		1	<sup>3</sup> / <sub>4</sub>	1 Δ	2588	2545	2446	2409	2373
			<sup>3</sup> / <sub>4</sub>	1 <sup>1</sup> / <sub>4</sub> □◇	1420	1400	1371	1333	1307
				1 <sup>1</sup> / <sub>4</sub> Δ	1638	1605	1549	1501	1472
60	58	<sup>3</sup> / <sub>4</sub>	<sup>15</sup> / <sub>16</sub> Δ	3399	3343	3232	3195	3162	
			1 □◇	2587	2556	2510	2485	2460	
		1	<sup>3</sup> / <sub>4</sub>	1 Δ	2987	2945	2827	2798	2770
			<sup>3</sup> / <sub>4</sub>	1 <sup>1</sup> / <sub>4</sub> □◇	1639	1615	1587	1553	1522
				1 <sup>1</sup> / <sub>4</sub> Δ	1889	1851	1797	1761	1726

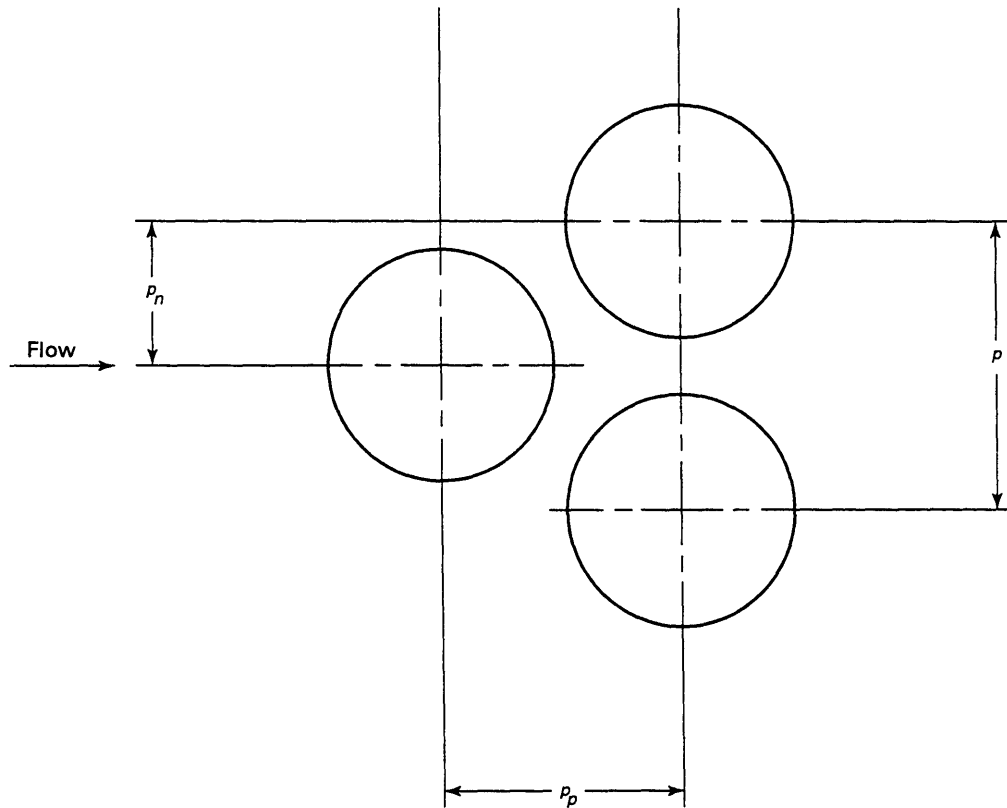


**FIG. C.3-2 TUBE PITCHES PARALLEL AND NORMAL TO FLOW (TYPICAL TRIANGULAR ARRANGEMENT SHOWN)**  
(Courtesy of Kenneth J. Bell)

This equation considers that the entrance and/or exit baffle spacings may be different than the central baffle spacing.

(g) *Crossflow Area at or Near Centerline for One Crossflow Section,  $S_m$ .* For plain tubes, estimate from Eq. (C.3-5a) and Eq. (C.3-5b):

$$S_m = \ell_s \left[ D_i - D_{ot\ell} + \left( \frac{D_{ot\ell} - d_o}{p_n} \right) (p - d_o) \right] \quad (\text{C.3-5a})$$

for rotated and inline square layouts use Eq. (C.3-5a)

$$S_m = \ell_s \left[ D_i - D_{ot\ell} + \left( \frac{D_{ot\ell} - d_o}{p} \right) (p - d_o) \right] \quad (\text{C.3-5b})$$

for triangular layouts use Eq. (C.3-5b).

These equations assume a nearly uniform tube field, except as required for tube pass partition lanes, and the difference between the shell inside diameter and the outer tube limit. (Those clearances are corrected for separately.) There is also no problem if the center line of the bundle normal to the crossflow is devoid of tubes, as required for U-tube or multiple tube pass construction; that is a minor disturbance of the uniformity of the tube field.

If low-finned tubes are used, the correct equations are Eq. (C.3-5c) and Eq. (C.3-5d).

$$S_m = \ell_s \left[ D_i - D_{ot\ell} + \left( \frac{D_{ot\ell} - d_r}{p_n} \right) [(p - d_o) - 2N_f h_f y_{fl}] \right] \quad (\text{C.3-5c})$$

TABLE C.3-2  
TUBE PITCHES PARALLEL AND NORMAL TO FLOW  
(Courtesy of Kenneth J. Bell)

Tube, O.D. $d_o$ , in.	Tube Pitch $p$ , in.	Layout	$p_p$ in.	$p_n$ in.
$1/2 = 0.500$	$5/8 = 0.625$	$\rightarrow \square$	0.625	0.625
$1/2 = 0.500$	$5/8 = 0.625$	$\rightarrow \diamond$	0.442	0.442
$1/2 = 0.500$	$5/8 = 0.625$	$\rightarrow \triangleleft$	0.541	0.3125
$5/8 = 0.625$	$13/16 = 0.812$	$\rightarrow \square$	0.812	0.812
$5/8 = 0.625$	$13/16 = 0.812$	$\rightarrow \diamond$	0.574	0.574
$5/8 = 0.625$	$13/16 = 0.812$	$\rightarrow \triangleleft$	0.704	0.406
$3/4 = 0.750$	$15/16 = 0.938$	$\rightarrow \square$	0.938	0.938
$3/4 = 0.750$	$15/16 = 0.938$	$\rightarrow \diamond$	0.663	0.663
$3/4 = 0.750$	$15/16 = 0.938$	$\rightarrow \triangleleft$	0.814	0.469
$3/4 = 0.750$	1	$\rightarrow \square$	1.000	1.000
$3/4 = 0.750$	1	$\rightarrow \diamond$	0.707	0.707
$3/4 = 0.750$	1	$\rightarrow \triangleleft$	0.866	0.500
$7/8 = 0.875$	1.094	$\rightarrow \square$	1.094	1.094
$7/8 = 0.875$	1.094	$\rightarrow \diamond$	0.773	0.773
$7/8 = 0.875$	1.094	$\rightarrow \triangleleft$	0.947	0.505
1	$1 1/4 = 1.250$	$\rightarrow \square$	1.250	1.250
1	$1 1/4 = 1.250$	$\rightarrow \diamond$	0.884	0.884
1	$1 1/4 = 1.250$	$\rightarrow \triangleleft$	1.082	0.625

for rotated and inline square layouts, use Eq. (C.3-5c).

$$S_m = \ell_s \left[ D_i - D_{otl} + \left( \frac{D_{otl} - d_r}{p} \right) (p - d_r) - 2N_f h_f y_f \right] \quad (\text{C.3-5d})$$

for triangular layouts use Eq. (C.3-5d).

In the above equations,  $d_r$  is the root diameter of the finned tube,  $N_f$  is the number of fins per unit length of tube,  $h_f$  is the height of the fin, and  $y_f$  is the fin thickness.

(h) *Fraction of Crossflow Area Available for Bypass Flow*,  $F_{sbp}$ . Estimate from Eq. (C.3-6).

$$F_{sbp} = \frac{\left[ D_i - D_{otl} + \frac{1}{2} (N_p W_p) \right] \ell_s}{S_m} \quad (\text{C.3-6})$$

where  $N_p$  is the number of pass partition lanes through the tube field parallel to the direction of the crossflow stream and  $W_p$  is the width of these lanes. This term accounts for the effect of flow that can bypass the tube field wholly or partially, with a great reduction of contact with heat transfer surface

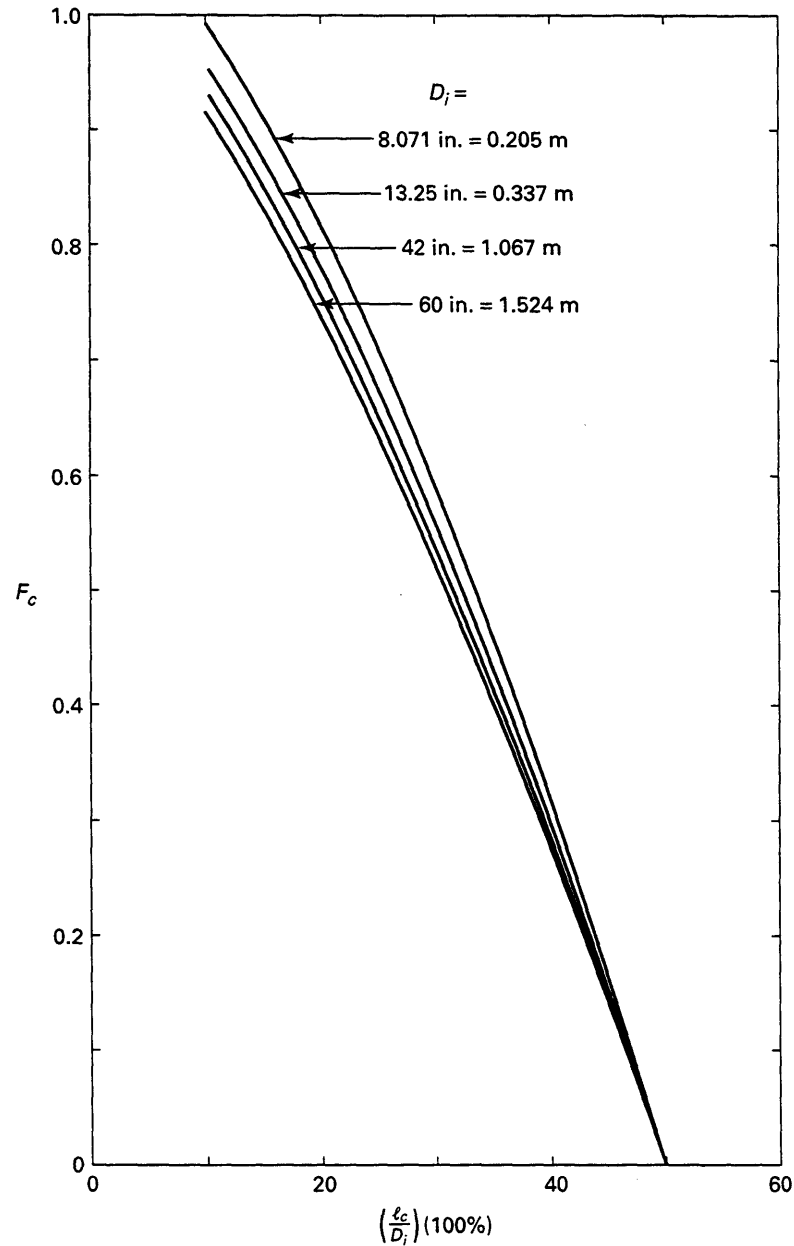
and distortion of the temperature profile.  $W_p$  can be measured if the tubesheet can be examined, or if a good layout drawing of the tube sheet is available. Otherwise,  $W_p$  can be estimated to be the TEMA minimum thickness of pass partition plates (see Table C.3-3) +  $1/4$  in.

(i) *Tube-to-Baffle Leakage Area for One Baffle*,  $S_{tb}$ . Estimate from Eq. (C.3-7).

$$S_{tb} = \pi d_o \delta_{tb} \left( \frac{1}{4} \right) (1 + F_c) N_t \quad (\text{C.3-7})$$

where  $\delta_{tb}$  is the diametral clearance between the tube and the baffle. TEMA Class R construction specifies a  $\delta_{tb}$  of  $1/32$  in. where maximum unsupported tube length (normally  $2\ell_s$ ) does not exceed 36 in., and a  $\delta_{tb}$  of  $1/64$  in., otherwise. If there is any fouling, these clearances may be partially or completely blocked; on the other hand, corrosion or tube vibration may have caused substantial enlargement. However, neither of these conditions can be confirmed without detailed inspection of the tube bundle and even then only superficially and qualitatively.

(j) *Baffle Cut Angle*,  $\theta$  is the angle subtended from the center of the shell cross-section by the intersection of the cut edge of the baffle with the inside surface



$$F_c = \frac{1}{\pi} \left\{ \pi + 2 \left( \frac{D_i - 2l_c}{D_{otl}} \right) \sin \left[ \cos^{-1} \left( \frac{D_i - 2l_c}{D_{otl}} \right) \right] - 2 \cos^{-1} \left( \frac{D_i - 2l_c}{D_{otl}} \right) \right\}$$

**FIG. C.3-3 ESTIMATION OF FRACTION OF TUBES IN CROSSFLOW**  
(Courtesy of Kenneth J. Bell)

**TABLE C.3-3**  
**NOMINAL PASS PARTITION PLATE THICKNESS**  
**(TEMA TABLE RCB-9.131)**

Reprinted by permission of (Tubular Exchanger Manufacturers Association)

Shell Inside Diameter, in.	Carbon Steel	Alloy Material
Less than 24	3/8 in.	1/4 in.
24-60	1/2 in.	3/8 in.

**TABLE C.3-4a**  
**MAXIMUM BAFFLE AND SUPPORT PLATE CLEARANCES**

(Taken from TEMA Tables RCB-4.3 and RGP-RCB-4.3, Seventh Edition (1988))

Reprinted by permission of (Tubular Exchanger Manufacturers Association)

Nominal Shell Inside Diameter, in.	$\delta_{sb}$ , in.	
6-17	1/8	These values may be doubled in applications where this would have no effect on shellside heat transfer or mean temperature difference.
18-39	3/16	
40-54	1/4	
55-60	5/16	
61-69	5/16	Recommended good practice
70-84	3/8	
85-100	7/16	

**TABLE C.3-4b**  
**MAXIMUM BAFFLE AND SUPPORT PLATE CLEARANCES**

(Taken from TEMA Tables R-4.3, C-4.3, B-4.3, and RGP-RCB-4.3 Sixth Edition (1978))

Reprinted by permission of (Tubular Exchanger Manufacturers Association)

Nominal Shell Inside Diameter, in.	$\delta_{sb}$ , in.	
8-13	0.100	These values may be doubled in applications where this would have no effect on shellside heat transfer or mean temperature difference.
14-17	0.125	
18-23	0.150	
24-39	0.175	
40-54	0.225	
55-60	0.300	
61-69	0.300	Recommended good practice
70-84	0.375	
85-100	0.438	

of the shell. In terms of previously-defined quantities see Eq. (C.3-8).

$$\theta = 2 \cos^{-1} \left( 1 - \frac{2\ell_c}{D_i} \right) \quad (\text{C.3-8})$$

where  $\theta$  is in radians. This equation is shown graphically in Fig. C.3-4.

(k) *Shell-to-Baffle Leakage Area for one Baffle,  $S_{sb}$ .* If diametral shell-baffle clearance,  $\delta_{sb}$ , is known,  $S_{sb}$  can be calculated from Eq. (C.3-9).

$$S_{sb} = \frac{\pi D_i \delta_{sb}}{2} \left[ 1 - \frac{\theta}{2\pi} \right] \quad (\text{C.3-9})$$

where the value of  $\theta$  is in radians and is between 0 and  $\pi$ . This area has been calculated and plotted in Fig. C.3-5 as a function of percent baffle cut,  $(\ell_c/D_i)$  (100%), and inside shell diameter,  $D_i$ . The standard diametral clearance between shell inside diameter and baffle outside diameter specified by TEMA Standards Seventh Edition (1988) is shown in Table C.3-4a. However, earlier editions of the TEMA Standards gave somewhat different values. These values are given in Table C.3-4b. For shells rolled from plate (which is the usual case for shells greater than 24 in., outside diameter), TEMA Standards allow an extra 1/8 in., inside diameter. Again, for heat exchangers that have been in service, these clearances may have become partially or totally blocked by even small amounts of fouling.

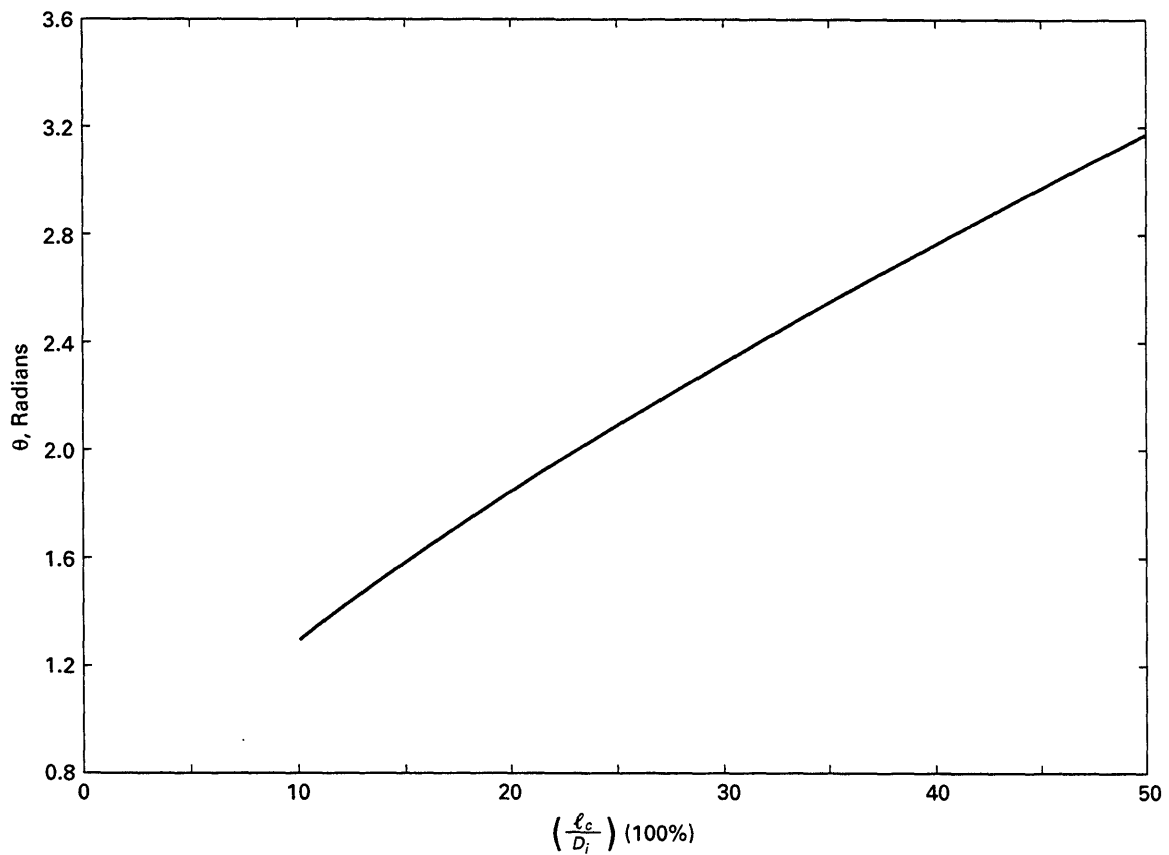
(l) *Area for Flow Through Window,  $S_w$ .* This area is obtained as the difference between the gross window area,  $S_{wg}$  and the window area occupied by tubes,  $S_{wt}$ , see Eq. (C.3-10a).

$$S_w = S_{wg} - S_{wt} \quad (\text{C.3-10a})$$

The value of  $S_{wg}$  can be calculated from Eq. (C.3-10b).

$$S_{wg} = \frac{D_i^2}{4} \left\{ \frac{\theta}{2} - \left[ 1 - 2 \left( \frac{\ell_c}{D_i} \right) \right] \sin \left( \frac{\theta}{2} \right) \right\} \quad (\text{C.3-10b})$$

The window area occupied by the tubes,  $S_{wt}$ , can be calculated from Eq. (C.3-10c).



$$\theta = 2 \cos^{-1} \left( 1 - \frac{2l_c}{D_i} \right)$$

FIG. C.3-4 BAFFLE CUT ANGLE  
(Courtesy of Kenneth J. Bell)

$$S_{wt} = \frac{N_t}{8} (1 - F_c) \pi d_o^2 \quad (\text{C.3-10c})$$

$$Re_s = \frac{d_o m_s}{\mu_s S_m} \quad (\text{C.4-1a})$$

(m) *Equivalent Diameter of Window,  $D_w$* . This value is required only if laminar flow, defined as  $Re_s \leq 100$ , exists. Calculate from Eq. (C.3-11).

For finned tubes, the shell-side Reynolds number is defined as Eq. (C.4-1b).

$$D_w = \frac{4S_w}{\frac{\pi}{2} N_t (1 - F_c) d_o + D_i \theta} \quad (\text{C.3-11})$$

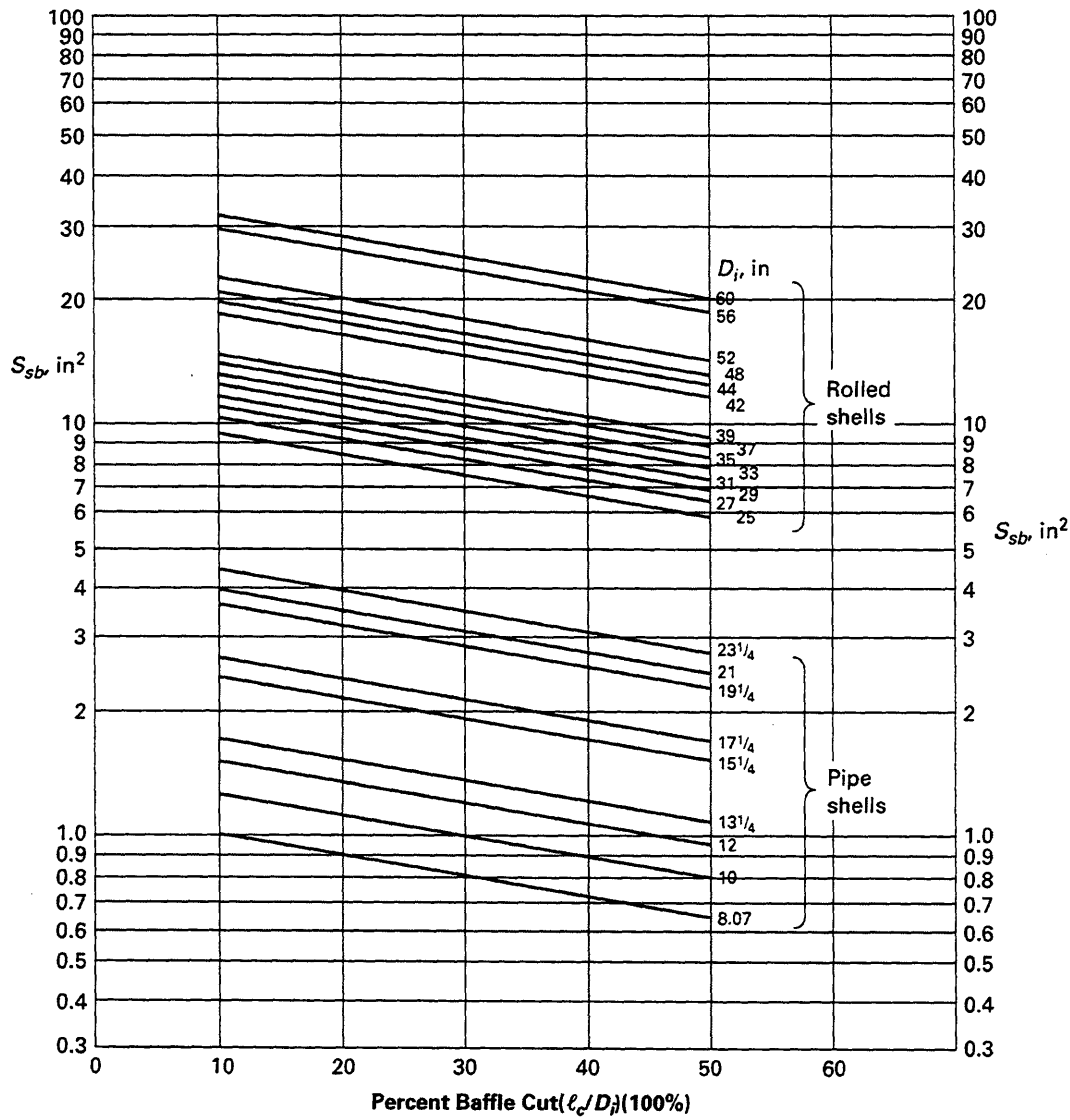
$$Re_s = \frac{d_r m_s}{\mu_s S_m} \quad (\text{C.4-1b})$$

where  $d_r$  is the root diameter of the tube.

#### C.4 CALCULATION OF SHELL-SIDE HEAT TRANSFER PERFORMANCE

(a) *Calculate Shell-Side Reynolds Number,  $Re_s$* . The shell-side Reynolds number is defined as Eq. (C.4-1a).

It is usually adequate to use the arithmetic mean bulk shell-side fluid temperature (i.e., halfway between the inlet and exit temperatures) to evaluate all bulk properties of the shell-side fluid. In the case of long temperature ranges or for a fluid whose viscosity is very sensitive to temperature change,



$$S_{sb} = \frac{\pi D_i \delta_{sb}}{2} \left[ 1 - \frac{\theta}{2\pi} \right]$$

**FIG. C.3-5 ESTIMATION OF SHELL-TO-BAFFLE LEAKAGE AREA**  
 (Based on TEMA Class R standards)  
 (Courtesy of Kenneth J. Bell)

special care must be taken (such as breaking the calculation into segments, each covering a more limited temperature range). Even then, the accuracy of the procedure is less than for more conventional cases.

(b) Find  $j_i$ . For plain tubes, use the ideal tube bank curve for a given tube layout at the calculated value of  $Re_s$ , using Fig. C.4-1a.

For finned tubes, limited data suggest that the  $j_i$  curves are somewhat lower for finned tubes than for plain ones at  $Re_s < 1000$ , as shown in Fig. C.4-1b. While the comparison given in Fig. C.4-1b is for curve 1 (equilateral triangular layouts), it seems reasonable to apply the same relative correction to curves 2 and 3 (rotated and inline square layouts).

(c) Calculate the Shell-Side Heat Transfer Coefficient for an Ideal Tube Bank,  $h_{ideal}$ . See Eq. (C.4-2).

$$h_{ideal} = j_i c_{p,s} \left( \frac{m_s}{S_m} \right) \left( \frac{k_s}{c_{p,s} \mu_s} \right)^{2/3} \left( \frac{\mu_s}{\mu_{s,w}} \right)^{0.14} \quad (C.4-2)$$

(d) Find the Correction Factor for Baffle Configuration Effects,  $J_c$ .  $J_c$  is read from Fig. C.4-2 as a function of  $F_c$ . For no-tubes-in-the-window designs,  $J_c = 1$ .

(e) Find the Correction Factor for Baffle Leakage Effects,  $J_R$ .  $J_R$  is found from Fig. C.4-3 as a function of the ratio of the total baffle leakage area,  $(S_{sb} + S_{tb})$ , to the crossflow area,  $S_m$ , and of the ratio of the shell-to-baffle leakage area,  $S_{sb}$ , to the total baffle leakage area,  $(S_{sb} + S_{tb})$ .

(f) Find the Correction Factor for Bundle Bypassing Effects,  $J_b$ .  $J_b$  is found from Fig. C.4-4 as a function of  $F_{sbp}$  and of  $N_{ss}/N_c$  (the ratio of the number of sealing strips per side to the number of rows crossed in one baffle crossflow section). The solid lines on Fig. C.4-4 are for  $Re_s > 100$ ; the dashed lines for  $Re_s < 100$ . If there are pass divider lanes through the tube field parallel to the crossflow stream, it is assumed that equivalent steps will be taken to block that flow (F stream) as for the bundle-shell bypass flow (C stream). This can be done by tie rods and spacers as well as by sealing strips.

(g) Find the Correction Factor for Adverse Temperature Gradient Build-up at Low Reynolds Numbers,  $J_r$ . This factor is equal to 1.00 if  $Re_s$  is equal to or greater than 100. For  $Re_s$  equal to or less than 20, the correction factor is fully effective and a function only of the total number of tube rows crossed. From  $Re_s$  between 20 and 100, a linear proportion rule is used.

(1) Therefore:

(a) If  $Re_s < 100$ , find  $J_r^*$  from Fig. C.4-5, knowing  $N_b$  and  $(N_c + N_{cw})$

(b) If  $Re_s \leq 20$ ,  $J_r = J_r^*$

(c) If  $20 < Re_s < 100$ , find  $J_r$  from Fig. C.4-6, knowing  $J_r^*$  and  $Re_s$

(h) Find the Correction Factor for Unequal Baffle Spacing at Inlet and/or Outlet,  $J_s$ . See Eq. (C.4-3).

$$J_s = \frac{(N_b - 1) + (\ell_{s,i}^*)^{1-n} + (\ell_{s,o}^*)^{1-n}}{(N_b - 1) + \ell_{s,i}^* + \ell_{s,o}^*} \quad (C.4-3)$$

where

$N_b$  = number of baffles

$\ell_{s,i}^* = \ell_{s,i}/\ell_s$

$\ell_{s,o}^* = \ell_{s,o}/\ell_s$

$\ell_s$  = internal (central) baffle spacing

$\ell_{s,i}$  = entrance baffle spacing

$\ell_{s,o}$  = exit baffle spacing

$n = 0.6$  for turbulent flow ( $Re_s > 100$ )

$n = 1/3$  for laminar flow ( $Re_s < 100$ )

Equation (C.4-3) is plotted in Fig. C.4-7a for turbulent flow and in Fig. C.4-7b for laminar flow, for the particular (but common) case that  $\ell_{s,i} = \ell_{s,o}$ .

(i) Calculate the Shell-Side Heat Transfer Coefficient for the Exchanger,  $h_s$ . See Eq. (C.4-4).

$$h_s = h_{ideal} J_c J_e J_b J_r J_s \quad (C.4-4)$$

## C.5 CALCULATION OF EXPECTED SHELL-SIDE PRESSURE LOSS

(a) Find  $f_i$  From the Ideal Tube Bank Friction Curve for the Given Tube Layout. At the calculated value of  $Re_s$ , use Fig. C.5-1a for triangular and rotated square arrays of plain tubes and Fig. C.5-1b for inline square arrays.

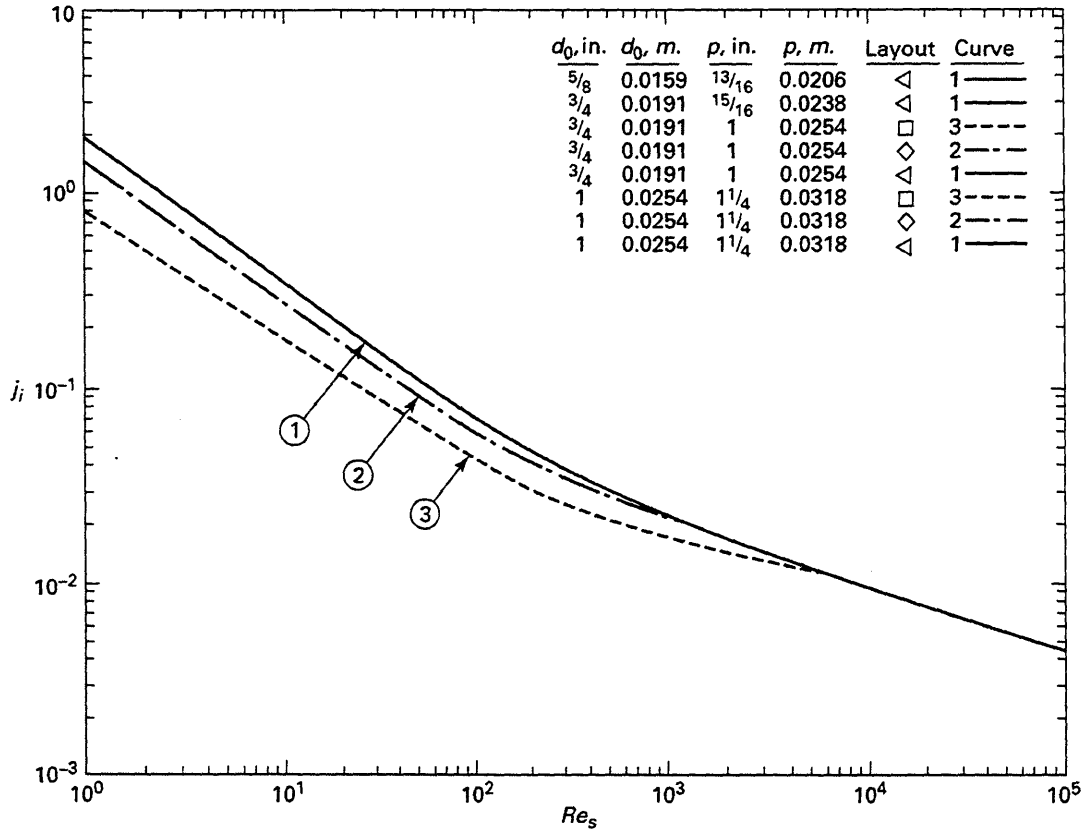
(b) Calculate the Pressure Loss for an Ideal Crossflow Section,  $\Delta P_{b,i}$ . See Eq. (C.5-1).

$$\Delta P_{b,i} = \frac{4 f_i m_s^2 N_c}{2 \rho_s g_c S_m^2} \left( \frac{\mu_{s,w}}{\mu_s} \right)^{0.14} \quad (C.5-1)$$

(c) Calculate the Pressure Loss for an Ideal Window Section,  $\Delta P_{w,i}$ . See Eqs. (C.5-2a) and (C.5-2b).

(1) If  $Re_s \geq 100$ :

$$\Delta P_{w,i} = \frac{m_s^2 (2 + 0.6 N_{cw})}{2 g_c S_m S_{w \rho_s}} \quad (C.5-2a)$$



Curve 1:

$$j_i = 1.73 Re_s^{-0.694} \quad 1.0 \leq Re_s \leq 100$$

$$j_i = 0.717 Re_s^{-0.507} \quad 100 \leq Re_s \leq 1000$$

$$j_i = 0.236 Re_s^{-0.346} \quad 1000 \leq Re_s$$

Curve 2:

$$j_i = 1.39 Re_s^{-0.691} \quad 1.0 \leq Re_s \leq 100$$

$$j_i = 0.414 Re_s^{-0.425} \quad 100 \leq Re_s \leq 1000$$

$$j_i = 0.257 Re_s^{-0.357} \quad 1000 \leq Re_s$$

Curve 3:

$$j_i = 0.817 Re_s^{-0.632} \quad 1.0 \leq Re_s \leq 100$$

$$j_i = 0.290 Re_s^{-0.418} \quad 100 \leq Re_s \leq 700$$

$$j_i = 0.059 Re_s^{-0.181} \quad 700 \leq Re_s \leq 4000$$

$$j_i = 0.185 Re_s^{-0.324} \quad 4000 \leq Re_s$$

FIG. C.4-1a CORRELATION OF  $j_i$  FOR IDEAL TUBE BANKS WITH PLAIN TUBES  
(Courtesy of Kenneth J. Bell)

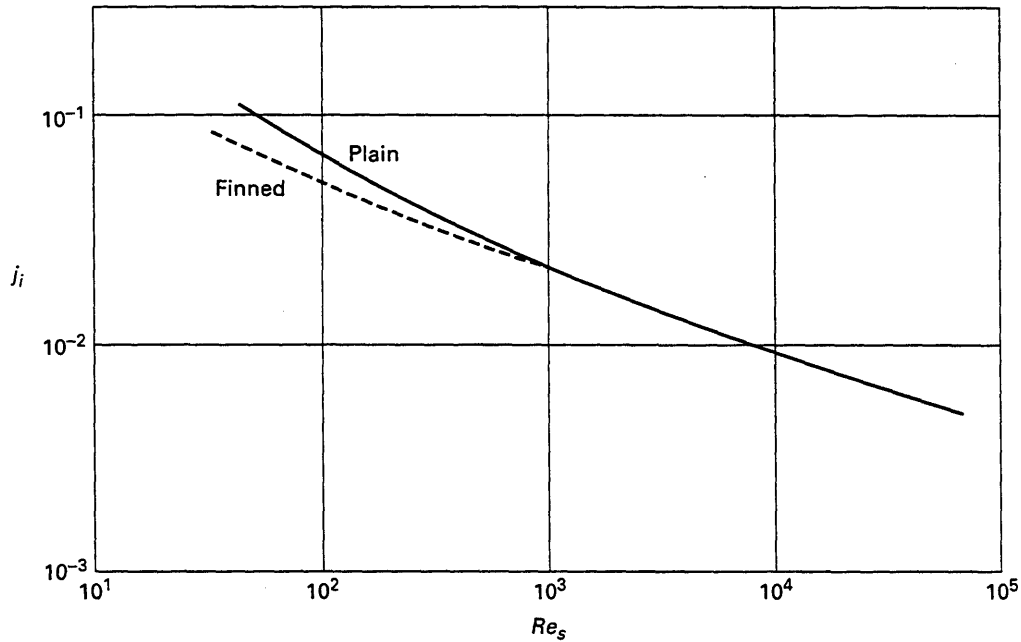


FIG. C.4-1b CORRELATION OF  $j_i$  VS.  $Re_s$  FOR TWO SIMILAR SHELL AND TUBE HEAT EXCHANGERS, ONE WITH FINNED TUBES AND ONE WITH PLAIN TUBES (Courtesy of Kenneth J. Bell)

(2) If  $Re_s < 100$ :

$$\Delta P_{w,i} = 26 \frac{\mu_s m_s}{g_c \rho_s \sqrt{S_m S_w}} \left[ \frac{N_{cw}}{p - d_o} + \frac{\ell_s}{D_w^2} \right] \quad (C.5-2b)$$

$$+ \frac{m_s^2}{g_c S_m S_w \rho_s}$$

(d) Find the Correction Factor for Effect of Baffle Leakage on Pressure Loss,  $R_R$ . Read from Fig. C.5-2 as a function of  $(S_{sb} + S_{tb})/S_m$  with parameter of  $S_{sb}/(S_{sb} + S_{tb})$ . Curves shown are not to be extrapolated beyond the points shown.

(e) Find the Correction Factor for Bundle Bypass,  $R_b$ . Read from Fig. C.5-3 as a function of  $F_{sbp}$  and  $N_{ss}/N_c$ . The solid lines are for  $Re_s > 100$ ; the dashed lines are for  $Re_s < 100$ .

(f) Find the Correction Factor for Unequal Baffle Spacing,  $R_s$ . See Eq. (C.5-3).

$$R_s = \frac{1}{2} [(\ell_{s,i}^*)^{-n'} + (\ell_{s,o}^*)^{-n}] \quad (C.5-3)$$

where

$$\ell_{s,i}^* = \ell_{s,i}/\ell_s$$

$$\ell_{s,o}^* = \ell_{s,o}/\ell_s$$

$n' = 1.6$  for turbulent flow ( $Re_s > 100$ )

$n' = 1$  for laminar flow ( $Re_s < 100$ )

(g) Calculate the Pressure Loss Across the Shell-Side (Excluding Nozzles),  $\Delta P_s$ , from Eq. (C.5-4).

$$\Delta P_s = [(N_b - 1)(\Delta P_{b,i})R_b + N_b \Delta P_{w,i}] R_e \quad (C.5-4)$$

$$+ 2 \Delta P_{b,i} R_b \left( 1 + \frac{N_{cw}}{N_c} \right) R_s$$

## C.6 NOMENCLATURE

$c_{p,s}$  = specific heat of shell-side fluid

$D_i$  = shell inside diameter

$D_{otl}$  = diameter of the outer tube limit

$D_w$  = equivalent diameter of the window

$d_o$  = tube outside diameter

$d_r$  = root diameter of low-finned tube

$F_c$  = fraction of the total tubes that are in cross flow

$F_{sbp}$  = fraction of total crossflow area that is available for bypass flow around tube bundle and through pass partition lanes

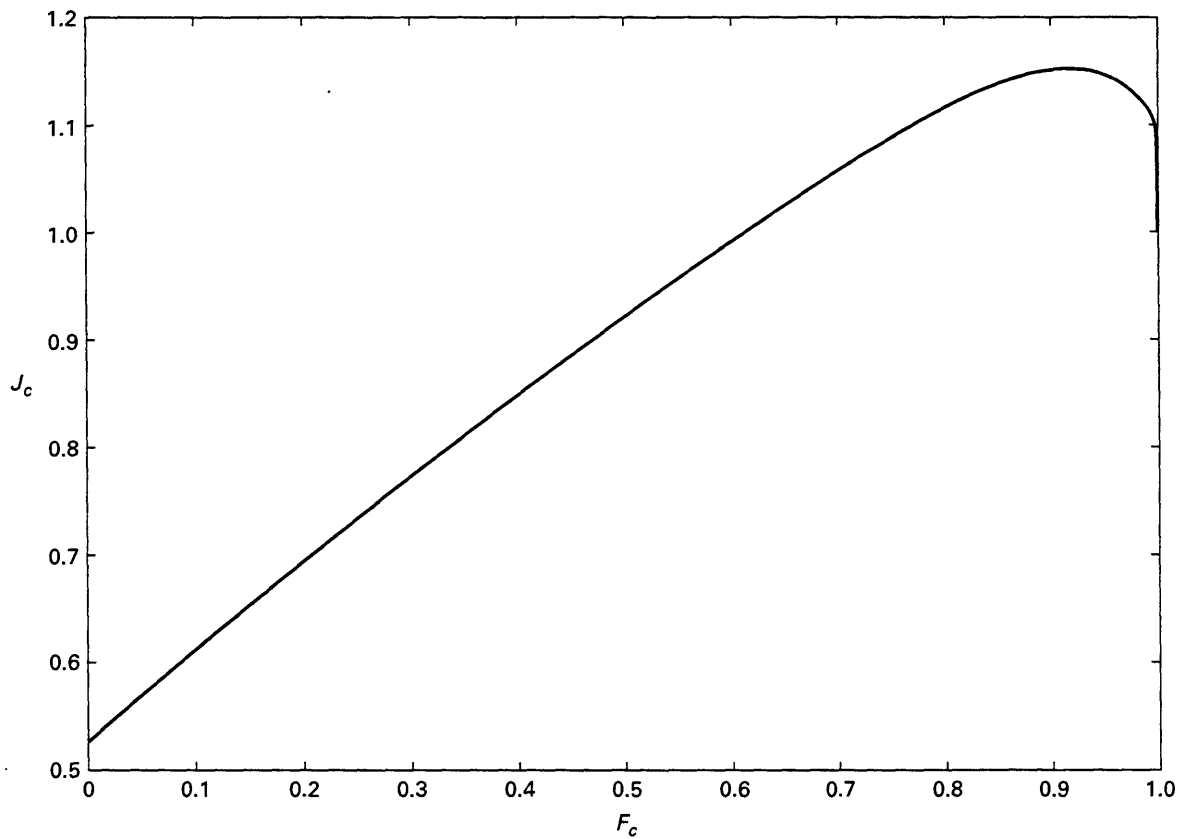


FIG. C.4-2 CORRECTION FACTOR FOR BAFFLE CONFIGURATION EFFECTS  
(Courtesy of Kenneth J. Bell)

$f_i$  = friction factor for flow across an ideal tube bank  
 $g_c$  = gravitational conversion constant,  $4.17 \times 10^8$  lbm-ft/lb-hr<sup>2</sup>  
 $h_f$  = height of fin of low-finned tube  
 $h_{ideal}$  = shell-side heat transfer coefficient for ideal tube bank  
 $h_s$  = shell-side heat transfer coefficient for exchanger  
 $J_b$  = correction factor on the shell-side heat transfer coefficient for bundle bypass effects  
 $J_c$  = correction factor on the shell-side heat transfer coefficient to account for baffle configuration effects  
 $J_\ell$  = correction factor on the shell-side heat transfer coefficient to account for baffle leakage  
 $J_r$  = correction factor on the shell-side heat transfer coefficient to account for build-up of adverse temperature gradient

$J_r^*$  = base correction factor on the shell-side heat transfer coefficient to account for build-up of adverse temperature gradient  
 $J_s$  = correction factor on the shell-side heat transfer coefficient to account for unequal baffle spacing  
 $j_i$  = colburn j-factor for an ideal tube bank  
 $k_s$  = thermal conductivity of shell-side fluid  
 $k_w$  = thermal conductivity of tube wall  
 $\ell$  = effective tube length (between tube sheets)  
 $\ell_c$  = baffle cut distance from baffle tip to shell inside diameter  
 $\ell_s$  = baffle spacing, center-to-center of consecutive baffles  
 $\ell_{s,i}$ ,  $\ell_{s,o}$  = baffle spacing at inlet and exit of the exchanger, respectively.  $\ell_{s,i}^*$ , and  $\ell_{s,o}^*$  are the corresponding dimensionless values

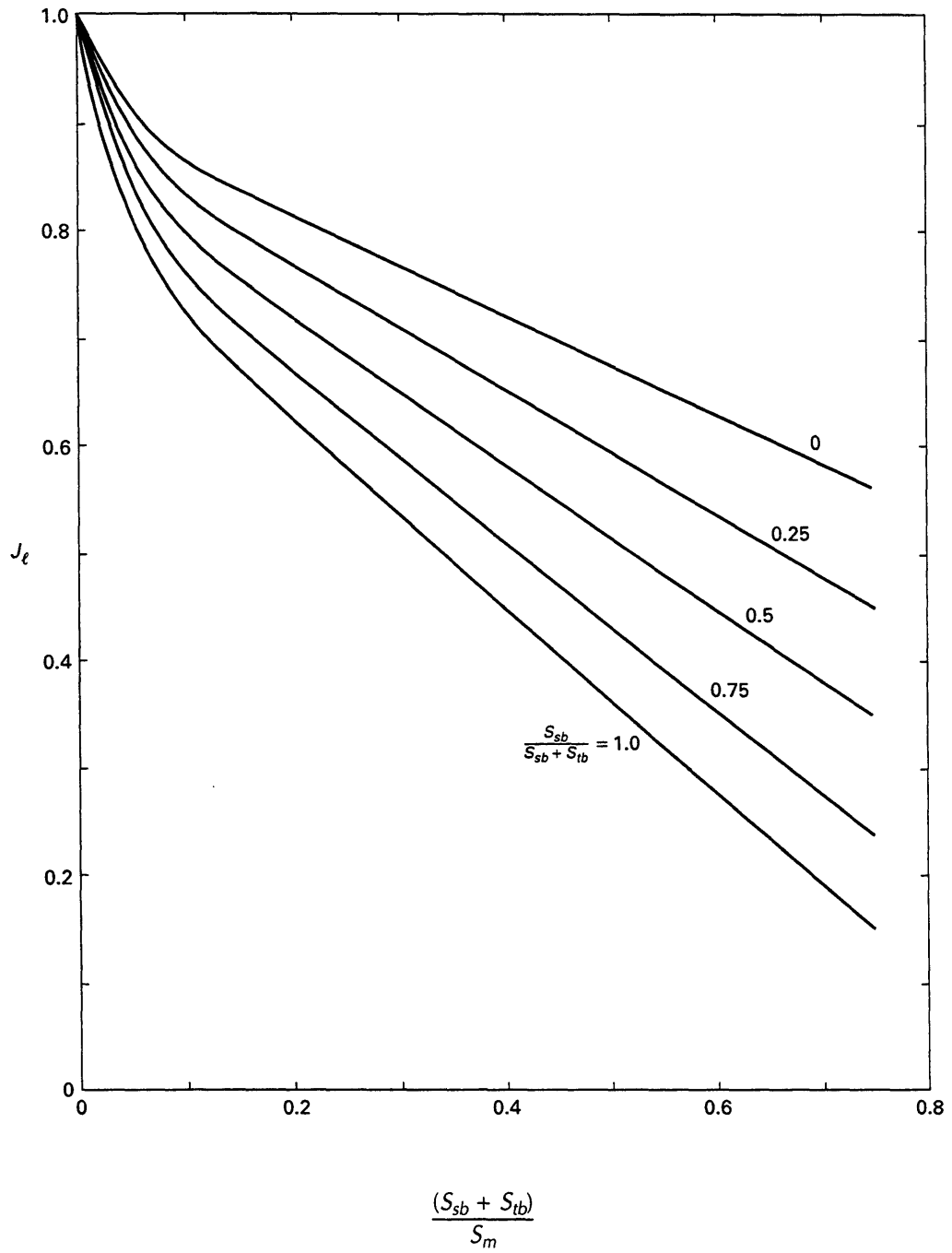


FIG. C.4-3 CORRECTION FACTOR FOR BAFFLE LEAKAGE EFFECTS  
(Courtesy of Kenneth J. Bell)

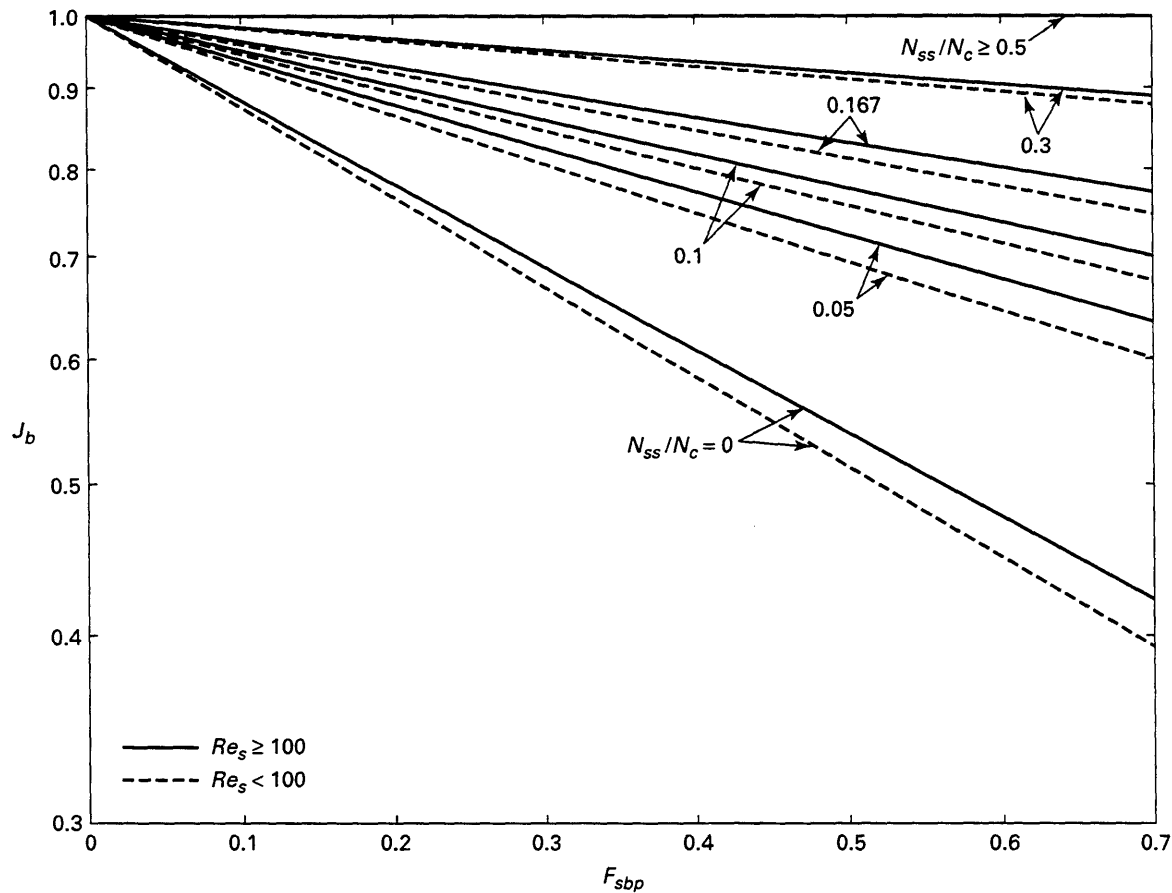
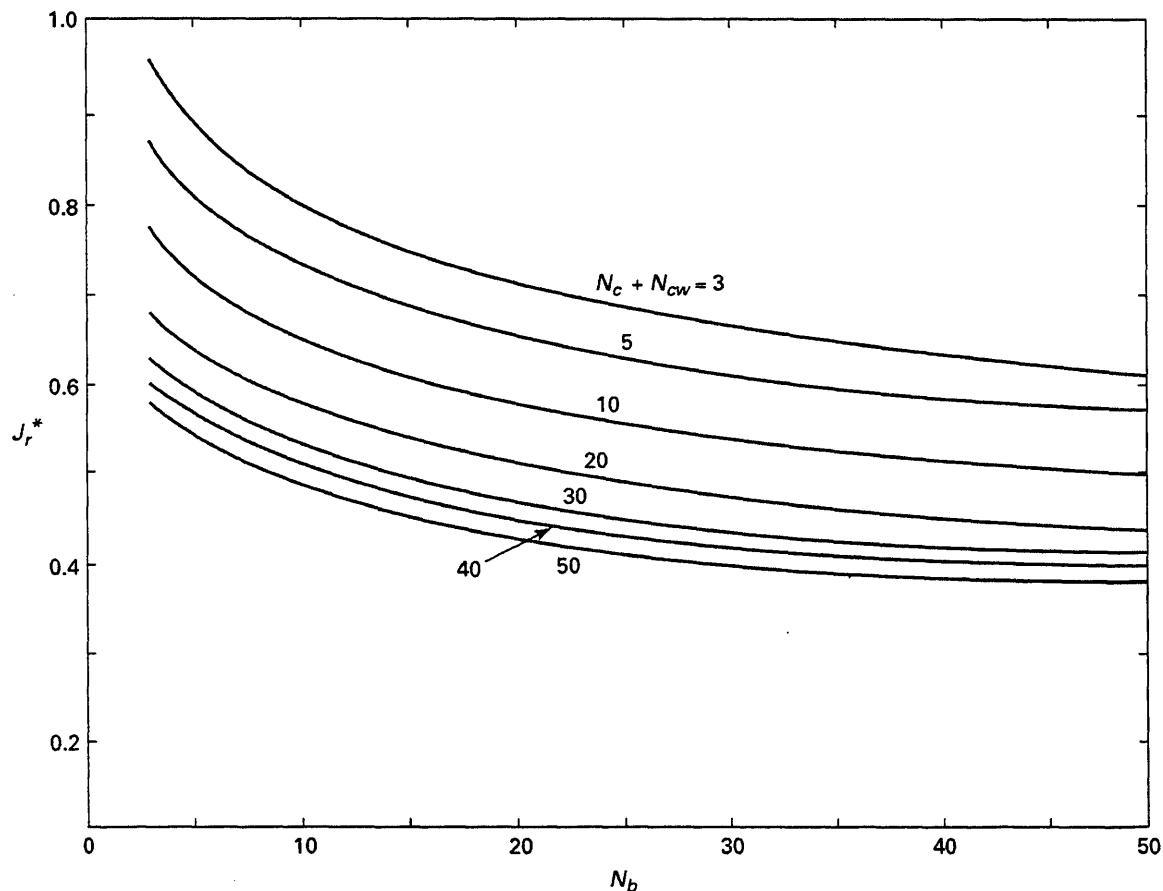


FIG. C.4-4 CORRECTION FACTOR FOR BYPASS FLOW  
(Courtesy of Kenneth J. Bell)

$m_s$  = mass flow rate of shell-side fluid  
 $N_b$  = number of baffles in exchanger  
 $N_c$  = number of tube rows crossed during flow through one crossflow section  
 $N_{cw}$  = effective number of crossflow rows in each window section  
 $N_{ss}$  = number of sealing strips or equivalent obstructions to bypass flow encountered by the stream in one crossflow section  
 $N_t$  = total number of tubes in the exchanger  
 $n, n'$  = exponents for the relationship between  $j_i$  and  $Re_s$  and  $f_i$  and  $Re_s$ , respectively  
 $\Delta P_{b,i}$  = pressure loss during flow across one ideal crossflow section  
 $\Delta P_{w,i}$  = pressure loss through one ideal window section

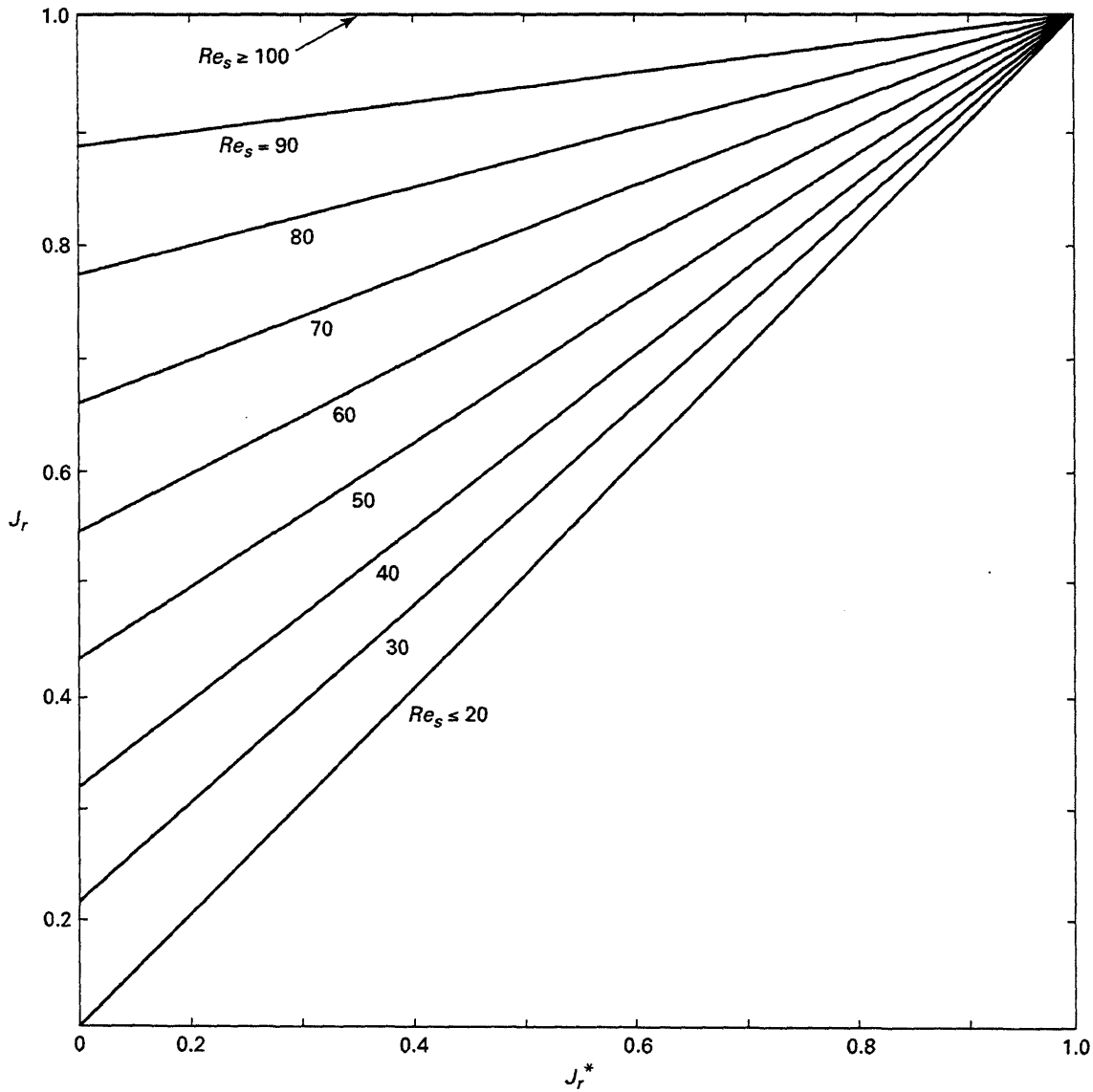
$p$  = tube pitch: distance between centers of nearest tubes in tube layout  
 $p_n$  = tube pitch normal to flow: distance between centers of adjacent tubes normal to the flow  
 $p_p$  = tube pitch parallel to flow: distance between centers of adjacent tube rows in the direction of the flow  
 $R_b$  = correction factor for effect of bundle bypass on pressure loss  
 $R_\ell$  = correction factor for effect of baffle leakage  
 $R_s$  = correction factor for unequal baffle spacing for the inlet and exit section pressure loss  
 $Re_s$  = Reynolds number for shell-side  
 $S_m$  = crossflow area at or near centerline for one crossflow section



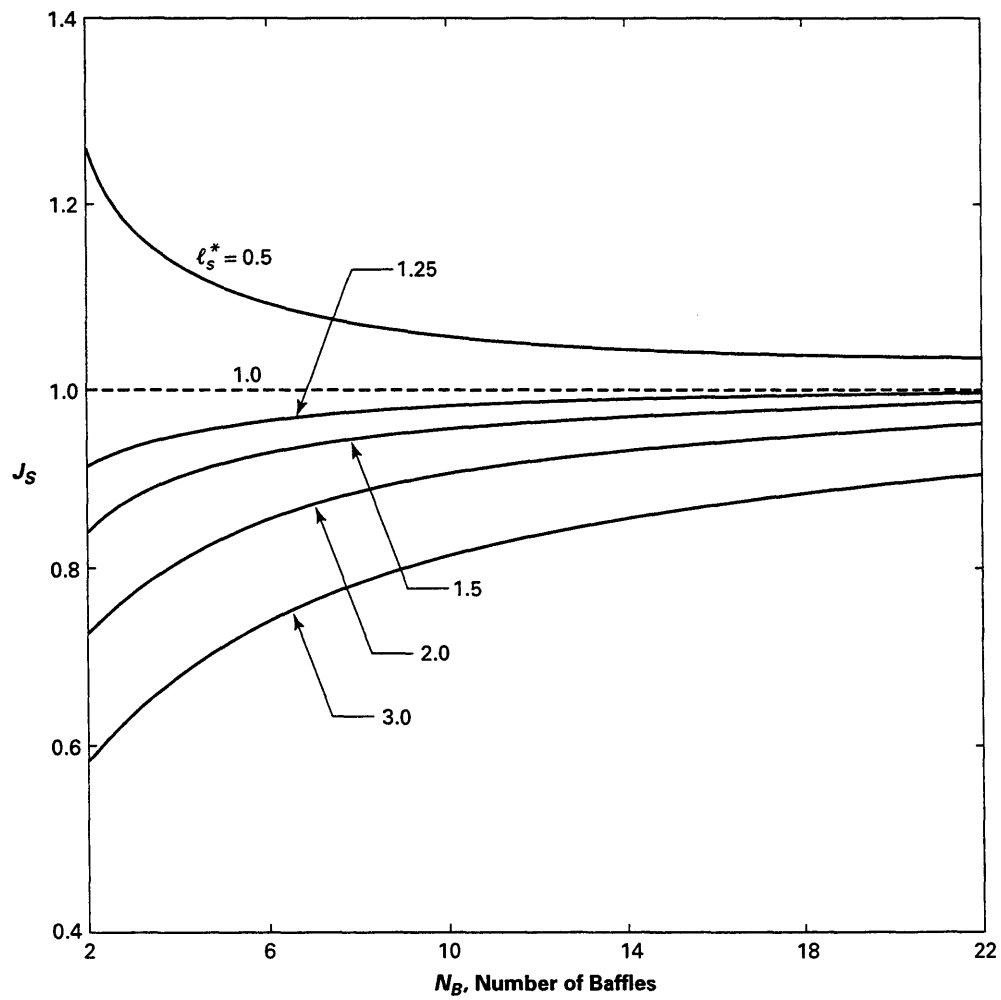
**FIG. C.4-5 CORRECTION FACTOR FOR ADVERSE TEMPERATURE GRADIENT  
AT LOW REYNOLDS NUMBERS**  
(Courtesy of Kenneth J. Bell)

$S_{sb}$  = shell-to-baffle leakage area for single baffle  
 $S_{tb}$  = tube-to-baffle leakage area for one baffle  
 $S_w$  = area for flow through window  
 $S_{wg}$  = window gross cross-sectional area  
 $S_{wt}$  = window area occupied by tubes  
 $W_p$  = width of pass partition clearance in tube field  
 $y_f$  = thickness of fin on low-finned tube

$\delta_{sb}$  = diametral clearance between shell and baffle  
 $\delta_{tb}$  = diametral clearance between tube and baffle  
 $\mu_s$  = viscosity of shell-side fluid at bulk stream temperature  
 $\mu_{s,w}$  = viscosity of shell-side fluid evaluated at surface temperature  
 $\rho_s$  = density of shell-side fluid  
 $\theta$  = baffle cut angle, radians

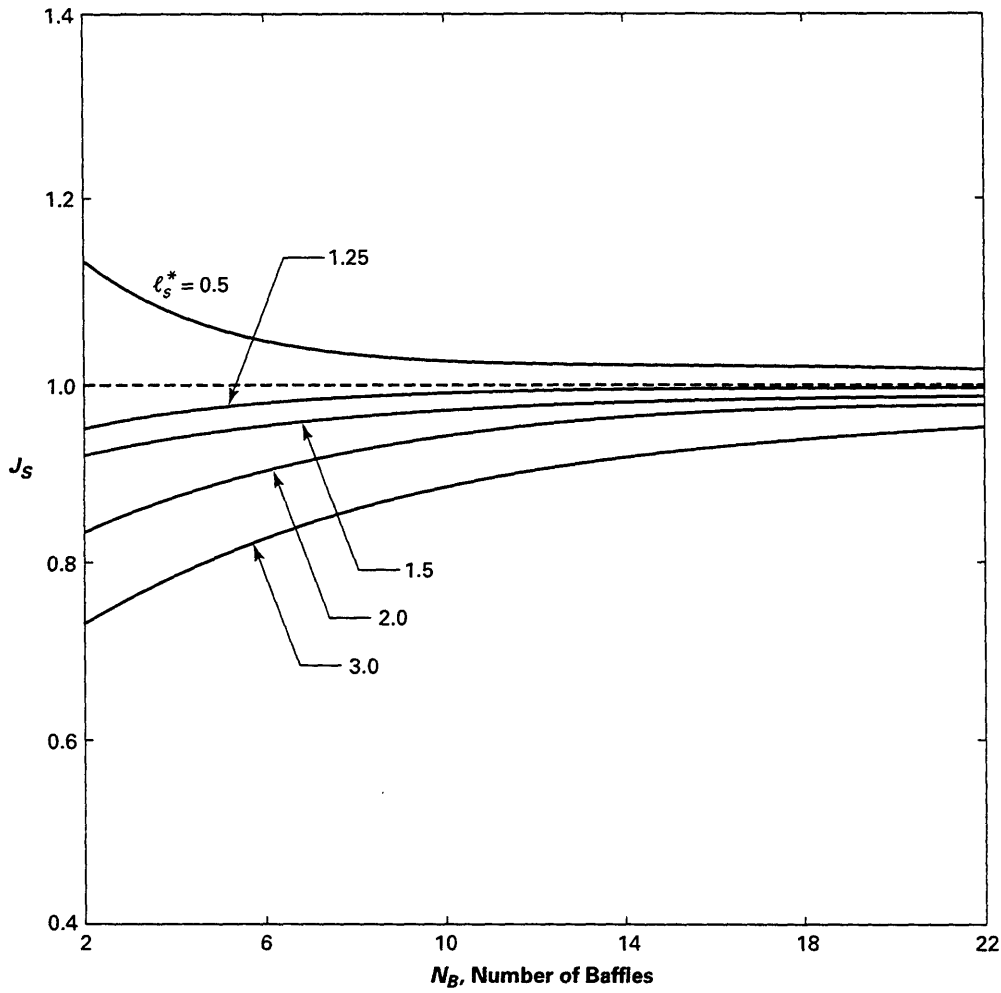


**FIG. C.4-6 CORRECTION FACTORS FOR ADVERSE TEMPERATURE GRADIENT AT INTERMEDIATE REYNOLDS NUMBER**  
 (Courtesy of Kenneth J. Bell)



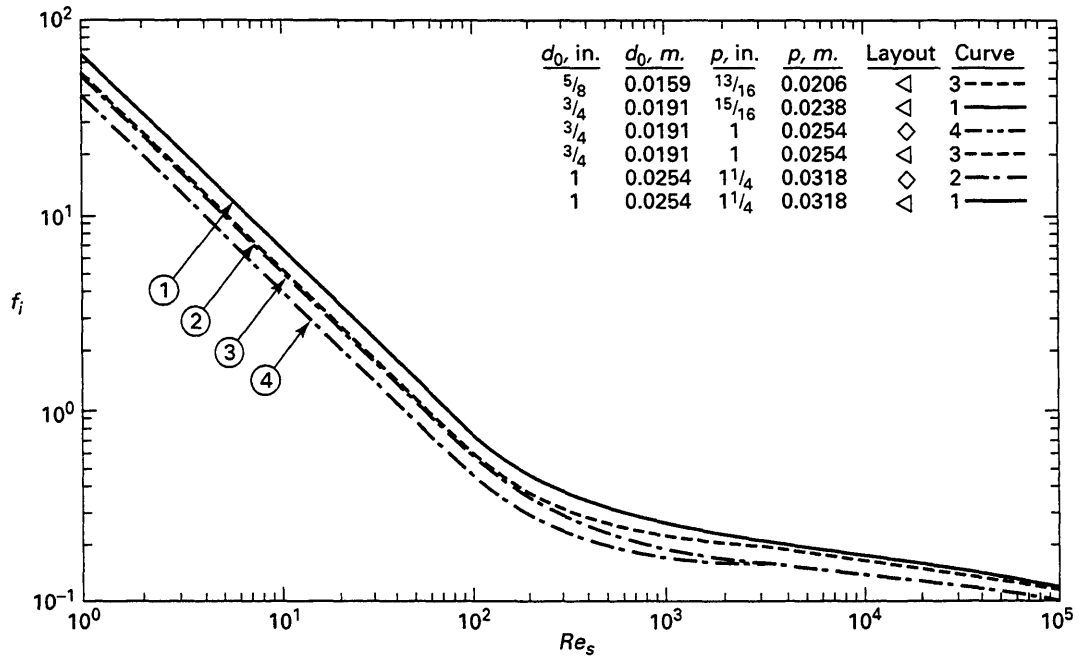
$$J_s = \frac{(N_b - 1) + (l_{s,i}^*)^{0.4} + (l_{s,o}^*)^{0.4}}{(N_b - 1) + l_{s,i}^* + l_{s,o}^*}$$

FIG. C.4-7a  $J_s$  AS A FUNCTION OF  $N_b$  FOR TURBULENT FLOW AND VARIOUS VALUES OF  $l_s^* = l_{s,i}^* = l_{s,o}^*$   
(Courtesy of Kenneth J. Bell)



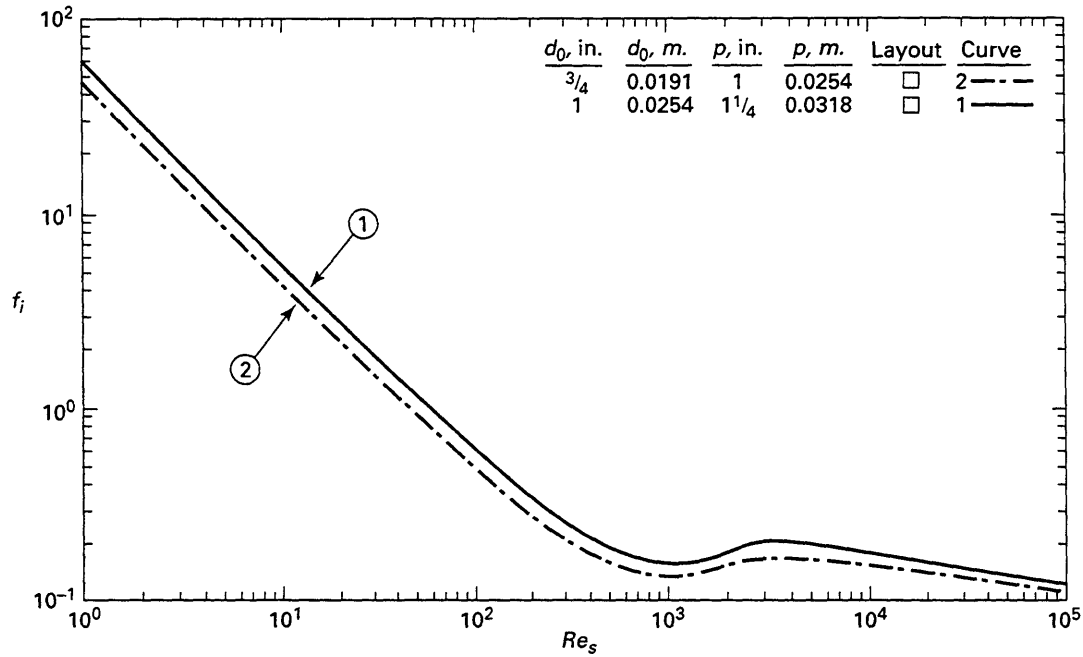
$$J_s = \frac{(N_b - 1) + (l_{s,i}^*)^{0.67} + (l_{s,o}^*)^{0.67}}{(N_b - 1) + l_{s,i}^* + l_{s,o}^*}$$

FIG. C.4-7b  $J_s$  AS A FUNCTION OF  $N_b$  FOR LAMINAR FLOW AND VARIOUS VALUES OF  $l_s^* = l_{s,i}^* = l_{s,o}^*$   
(Courtesy of Kenneth J. Bell)



- Curve 1:  
 $f_i = 68 Re_s^{-1.0} + 0.16$                        $1 \leq Re_s \leq 500$   
 $f_i = 0.97 Re_s^{-0.19}$                                $500 \leq Re_s$
- Curve 2:  
 $f_i = 56 Re_s^{-1.0} + 0.13$                        $1 \leq Re_s \leq 600$   
 $f_i = 0.64 Re_s^{-0.17}$                                $600 \leq Re_s$
- Curve 3:  
 $f_i = 52 Re_s^{-1.0} + 0.17$                        $1 \leq Re_s \leq 500$   
 $f_i = 0.56 Re_s^{-0.14}$                                $500 \leq Re_s$
- Curve 4:  
 $f_i = 42 Re_s^{-1.0} + 0.11$                        $1 \leq Re_s \leq 600$   
 $f_i = 0.37 Re_s^{-0.11}$                                $600 \leq Re_s$

**FIG. C.5-1a CORRELATION OF FRICTION FACTORS FOR IDEAL TUBE BANKS, TRIANGULAR AND ROTATED SQUARE LAYOUTS OF PLAIN TUBES (Courtesy of Kenneth J. Bell)**



Curve 1:

$$f_i = 56 Re_s^{-1.0} + 0.09 \quad 1 \leq Re_s \leq 1000$$

$$f_i = 0.65 Re_s^{-0.14} \quad 4000 \leq Re_s$$

$$f_i = f_{i,1000} + (f_{i,4000} - f_{i,1000})(Re_s - 1000)/3000 \quad 1000 \leq Re_s \leq 4000$$

Curve 2:

$$f_i = 45 Re_s^{-1.0} + 0.09 \quad 1 \leq Re_s \leq 1000$$

$$f_i = 53 Re_s^{-0.14} \quad 4000 \leq Re_s$$

$$f_i = f_{i,1000} + (f_{i,4000} - f_{i,1000})(Re_s - 1000)/3000 \quad 1000 \leq Re_s \leq 4000$$

**FIG. C.5-1b CORRELATION OF FRICTION FACTORS FOR IDEAL TUBE BANKS, INLINE SQUARE LAYOUTS (Courtesy of Kenneth J. Bell)**

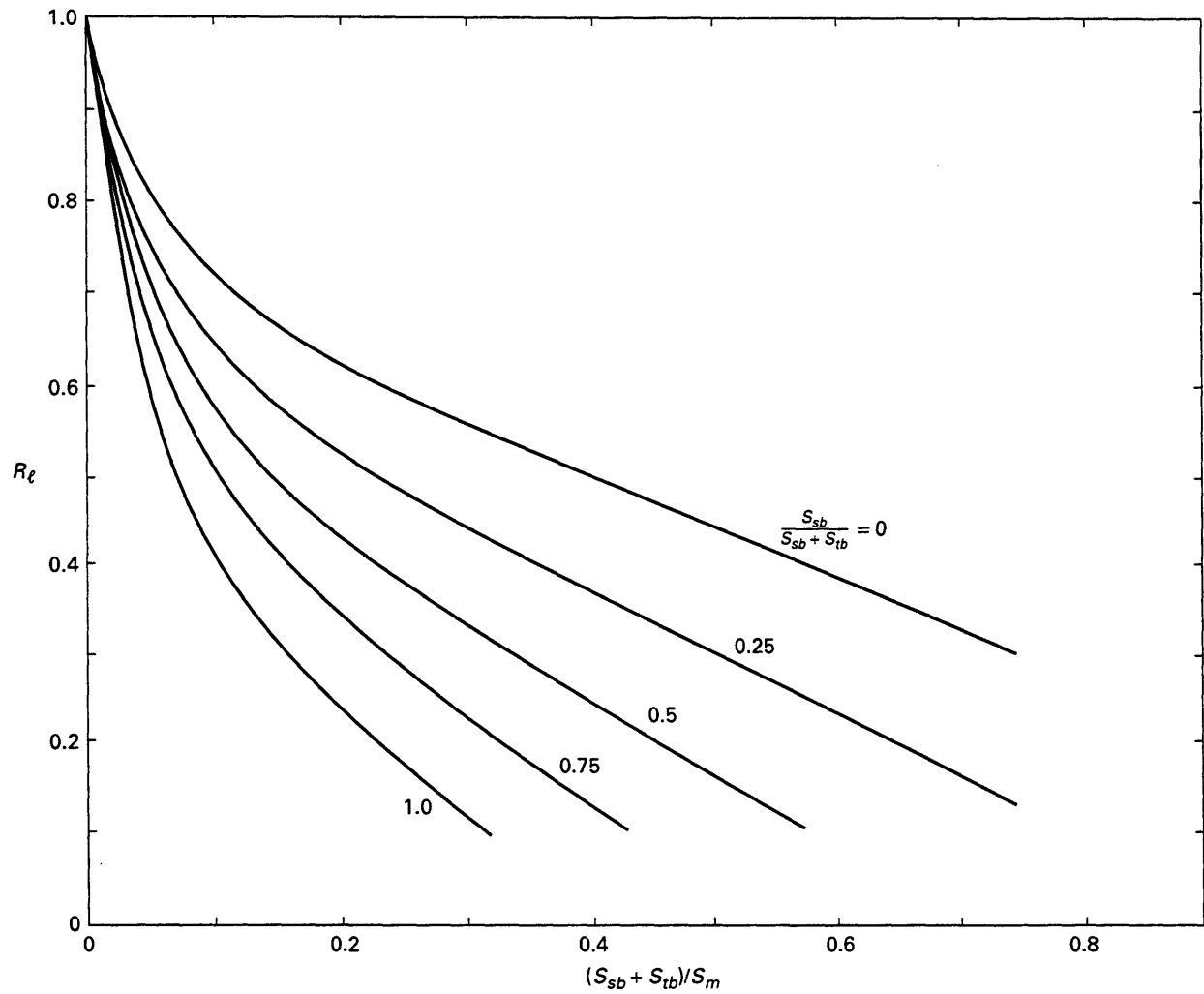


**FIG. C.5-2 CORRECTION FACTOR FOR BAFFLE LEAKAGE  
EFFECT ON PRESSURE DROP  
(Courtesy of Kenneth J. Bell)**

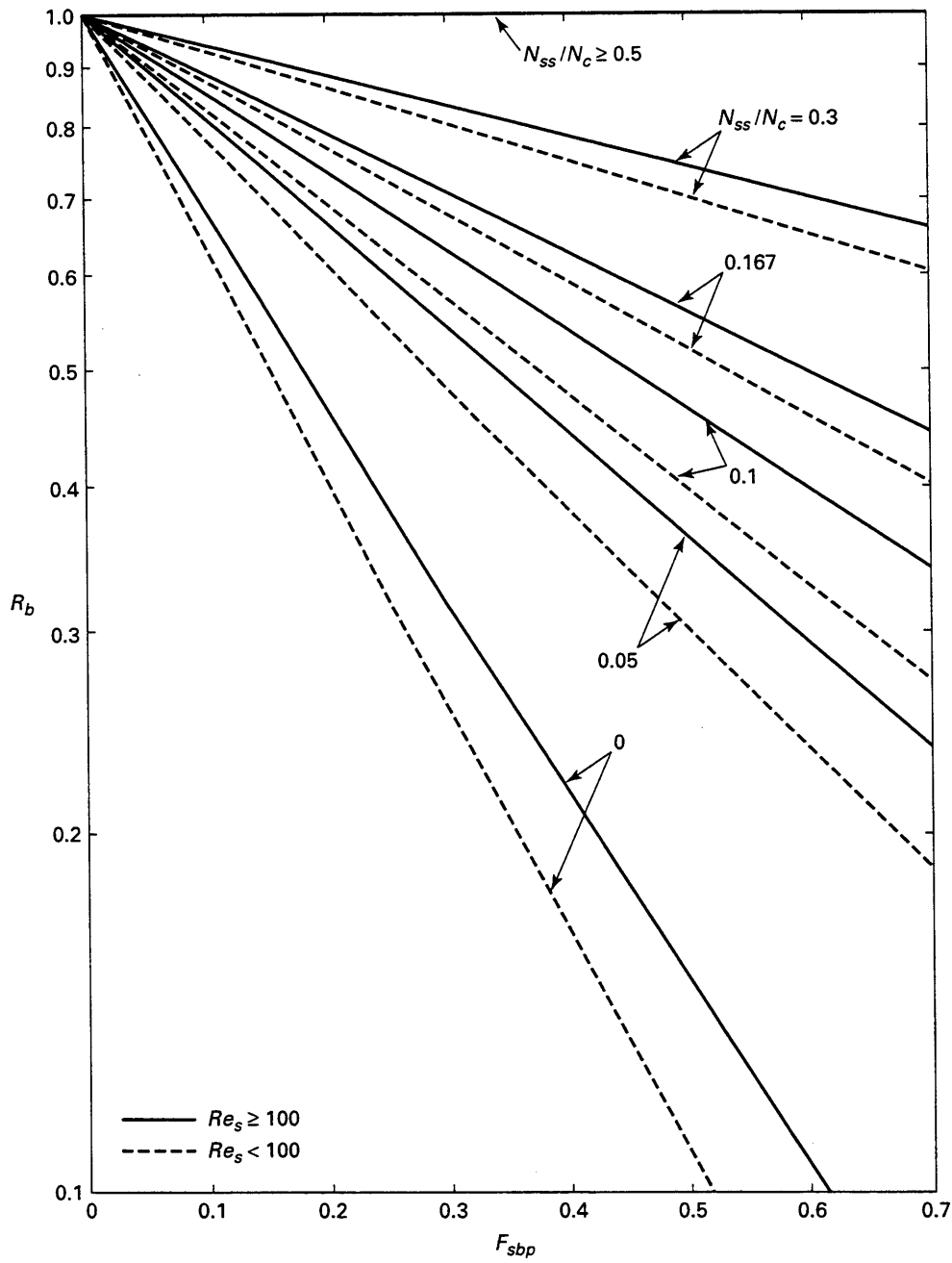


**FIG. C.5-3 CORRECTION FACTOR ON PRESSURE DROP FOR BYPASS FLOW**  
 (Courtesy of Kenneth J. Bell)

This page intentionally left blank.

## NONMANDATORY APPENDIX D — MEAN TEMPERATURE DIFFERENCE

This Appendix describes acceptable methods to calculate the effective mean temperature difference and its associated uncertainty. Since various calculation methods are acceptable, the parties to the test shall agree upon the methods of calculating the mean temperature difference and its associated uncertainty.

$$LMTD_{cc} = \frac{(T_i - t_o) - (T_o - t_i)}{\ln \frac{T_i - t_o}{T_o - t_i}} \quad (D.1)$$

Similarly for true co-current flow, the following log mean temperature difference is derived from Eq. (D.2).

### D.1 DETERMINING THE MEAN TEMPERATURE DIFFERENCE USING THE F-LMTD METHOD

The F-LMTD method of determining mean temperature difference described in this Appendix is based on the development summarized by Bowman, Mueller, and Nagle, Reference 29, and is suitable for evaluating performance test data. Alternative methods of determining mean temperature difference are acceptable as discussed in para. D.2. Using the F-LMTD method, the mean temperature difference is calculated using the terminal temperatures and integrating over the heat transfer area using the following assumptions:

- (a)  $U$  is constant throughout the heat exchanger.
- (b) The rate of flow of each fluid is constant.
- (c) The specific heat of each fluid is constant.
- (d) There is no condensation of vapor or boiling of liquid.
- (e) Heat exchanges with the ambient are negligible.
- (f) For multipass heat exchangers, the temperature of the shell-side fluid in any pass is uniform over any cross section, and the number of tubes in each pass is equal.
- (g) For cross flow heat exchangers, the fluid is either unmixed (non-uniform temperature cross-section) or completely mixed (uniform temperature cross-section) normal to the flow.

For true countercurrent flow arrangement, the well-known log mean temperature difference is derived based on the above assumptions, see Eq. (D.1).

$$LMTD_{co} = \frac{(T_i - t_i) - (T_o - t_o)}{\ln \frac{T_i - t_i}{T_o - t_o}} \quad (D.2)$$

For most heat exchangers in industrial applications, the flow arrangement is not true countercurrent or co-current flow; instead, a combination of countercurrent, crossflow and/or co-current flow arrangements is more typical. To account for these different flow arrangements, a correction factor,  $F$ , is applied to the countercurrent log mean temperature difference, see Eq. (D.3).

$$EMTD = F LMTD_{cc} \quad (D.3)$$

From here on and in other parts of this Code, the term  $LMTD$ , without subscript, refers to the countercurrent log mean temperature difference. Analytic expressions for the mean temperature difference are available in the open literature for only a few flow arrangements. For one-shell-pass/one-tube-pass counterflow arrangements and for most counterflow plate frame arrangements,  $F = 1$  and the mean temperature difference is represented by Eq. (D.1). For one-shell-pass/two-tube-pass arrangements as shown in Fig. D.1, the mean temperature difference is represented by the following from Reference 29.

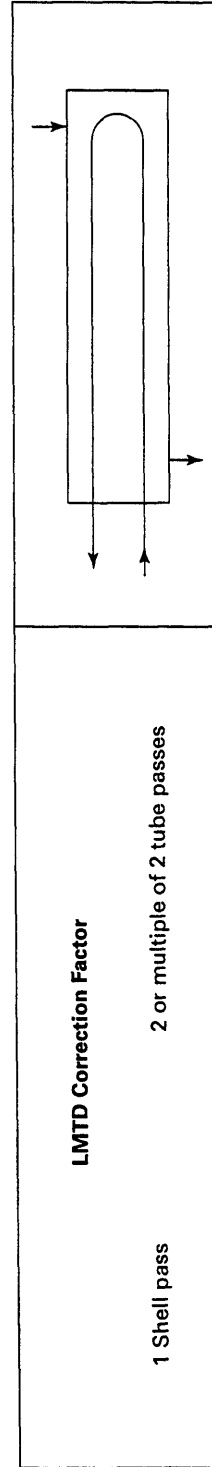
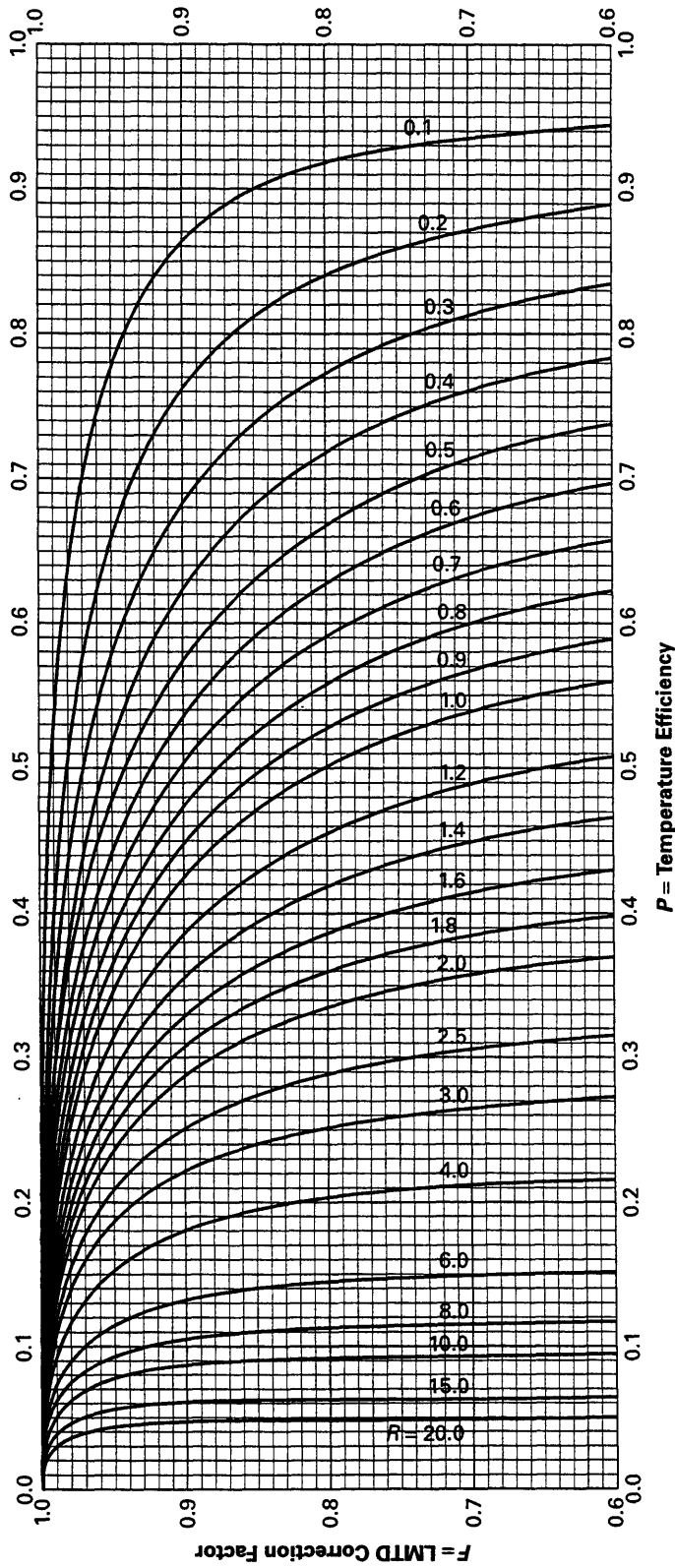


FIG. D.1 LMTD CORRECTION FACTOR FOR TWO OR MULTIPLE OF TWO TUBE PASSES, ONE SHELL PASS (from reference 39)  
 (Reprinted with the permission of Heat Exchange Institute from the HEI Standards for Power Plant Heat Exchangers)

$$\text{EMTD} = \frac{\sqrt{(T_i - T_o)^2 + (t_o - t_i)^2}}{\ln \frac{T_i + T_o - t_i - t_o + \sqrt{(T_i - T_o)^2 + (t_o - t_i)^2}}{T_i + T_o - t_i - t_o - \sqrt{(T_i - T_o)^2 + (t_o - t_i)^2}}} \quad (\text{D.4})$$

Analytic expressions for other arrangements are provided in Reference 29.

Typically, the  $F$  correction factor is shown graphically as function of  $R$  and  $P$  which are defined in Eqs. (D.5) and (D.6).

$$R = \frac{T_i - T_o}{t_o - t_i} \quad (\text{D.5})$$

$$P = \frac{t_o - t_i}{T_i - T_o} \quad (\text{D.6})$$

The correction factors for typical shell-and-tube configurations are shown in Figs. D.1 to D.14.<sup>1</sup> Industry experience indicates that the  $F$  correction factors derived based on the method in Reference 29 provide an adequate estimate of mean temperature difference if the heat exchanger is well designed with minimal bypass flow and sufficient number of baffle plates (for shell and tube designs) and the  $F$  correction factor is greater than 0.75. For many industrial applications, the uncertainty of the effective mean temperature difference is excessive using the terminal temperature measurements and F-LMTD approach. In particular, logarithms of negative values (or other unreasonable results) and uncertainties greater than 25% have occurred for the following circumstances:

(a) *F Correction Factor Less Than 0.75.* For configurations such as one-shell-pass/two-tube-pass design, the  $F$  correction factor is often less than 0.75 under clean conditions. Under such conditions, the  $F$  correction factor is sensitive to variations in terminal temperatures and to variations in the assumptions used to derive the  $F$  correction factor. This sensitivity results in large uncertainties (greater than 10%) for tests where  $F < 0.75$  even with high accuracy temperature measurements.

(b) *Large Variations in  $U$ .* For applications where the change in temperature of a fluid stream is large

and  $U$  varies significantly, the bias in the F-LMTD method is significant. In particular, for fluid streams in the laminar and transition flow regimes, the bias in mean temperature difference using the F-LMTD method can be substantial and the results can be unreasonable.

(c) *Large Measurement Error in Outlet Temperature.* The effective mean temperature difference calculated using the F-LMTD method is more sensitive to variations in outlet temperature than inlet temperature. In general, the error in the outlet temperature measurement is greater than the inlet error due to spatial variation. An excessive error (or uncertainty) in outlet temperatures can produce unreasonable results using the F-LMTD method.

Due to these observations and limitations, alternate methods may be needed to determine mean temperature difference for high-accuracy test analysis for these cases and others where the uncertainty of F-LMTD method is excessive.

## D.2 ALTERNATE METHODS OF DETERMINING THE MEAN TEMPERATURE DIFFERENCE

### D.2.1 General Requirements

Alternate methods of determining mean temperature difference are acceptable as agreed by the parties to the test based on the following guidelines.

(a) Alternative methods should not be used if the total uncertainty of the result increases above acceptable limits.

(b) Assumptions used in the step-wise calculations or derivation should use a heat transfer model consistent with this Code. For example, a heat balance shall be maintained and the individual heat transfer coefficients should be based on the same correlations used to adjust the test conditions to reference conditions (para. 5.3.4).

(c) The uncertainty of all assumptions or idealizations used in the calculation shall be considered in addition to propagating the uncertainties of individual measurements.

### D.2.2 Numerical Methods

Numerical methods typically use commercial and proprietary computer software to calculate the mean temperature difference and its associated uncertainty. In general, numerical methods consist of stepwise calculation of heat transfer rate for thermal elements within the heat exchanger. Variations in overall heat transfer coefficient and mean temperature difference are estimated based on the flow distribution and changes in fluid properties. Due to the interactive

<sup>1</sup> Correction factors other than shown in Figs. D.1 to D.14 may need to be applied to some geometries. For example, a correction for conduction and leakage through a longitudinal baffle of a two pass shell (TEMA F-type) is not included in Fig. D.2. References 40 and 41 develop a correction factor to account for this effect.

effect of overall heat transfer coefficient and mean temperature difference, numerical methods are well suited to determine the mean temperature difference for cases where the mean temperature difference or overall heat transfer coefficient vary substantially throughout the heat exchanger. Examples include flow streams with substantial changes in physical properties (such as specific heat or viscosity), flow arrangements other than counterflow where the outlet temperatures "cross over" or where the temperature difference varies significantly, and geometries where the flow velocity changes substantially throughout the unit (such as with unequal baffle spacing for shell and tube heat exchangers). The use of numerical methods may or may not reduce the overall uncertainty in mean temperature depending on the idealizations used in these methods and the propagation of errors with the stepwise calculation.

### D.2.3 Alternate Analytic Development

The traditional F-LMTD method derives the mean temperature difference based on the four terminal temperatures and the assumptions discussed in para. D.1. Alternate derivations may be considered where the uncertainties of  $Q^*$  and  $U^*$  exceed the values specified in para. 1.3. The following are two examples of alternate approaches to consider:

(a) For tests where the uncertainty of  $T_o$  is very large, an expression for EMTD as a function of  $R$  and  $P$  can be used where  $R = m_h c_{p,h} / m_c c_{p,c}$ . This method is equivalent to the F-LMTD method described in para. D.1.

(b) For tests where the uncertainties of  $T_o$  and  $t_o$  are large, an expression for EMTD may be derived based on the weighted average heat transfer rate,  $Q_{ave}$ , and the inlet temperatures and flow rates of both fluid streams.

The use of alternate derivations requires careful consideration of assumptions and idealizations since additional uncertainty may be introduced with these methods.

## D.3 METHODS OF ASSESSING THE UNCERTAINTY OF MEAN TEMPERATURE DIFFERENCE

As discussed in Section 5, the uncertainty in mean temperature difference shall include contributions due to the measurements of the terminal temperatures (and possibly flowrates) and uncertainty in the analytical model used to calculate the mean temperature difference. The method to determine the uncertainty in mean temperature difference depends

upon the method used to calculate the mean temperature difference.

### D.3.1 Uncertainty of the F-LMTD Method

This paragraph describes the methods to determine the uncertainty of the mean temperature difference using the F-LMTD method. The general approach may be used for alternate methods of determining the mean temperature difference but sensitivity coefficients and bias determination may be somewhat different.

#### D.3.1.1 Analytical and Numerical Expressions.

For arrangements where analytic expressions for the mean temperature difference are available or where commercial and proprietary computer programs are available to determine the mean temperature difference, the uncertainty in mean temperature is calculated in accordance with Eq. (D.7).

$$U_{EMTD} = [(\theta_{EMTD,ti} U_{ti})^2 + (\theta_{EMTD,to} U_{to})^2 + (\theta_{EMTD,Ti} U_{Ti})^2 + (\theta_{EMTD,To} U_{To})^2 + b_{EMTD,U}^2 + b_{EMTD,mixing}^2]^{1/2} \quad (D.7)$$

When computer programs are used, the sensitivity coefficients are calculated using numerical perturbation methods as discussed in ASME PTC 19.1. For the arrangements where analytical expressions are available, the sensitivity coefficients are provided in Tables D.1 and D.2.

**D.3.1.2 Graphical Methods.** For tests where analytical expressions are not available and where computer programs are not used, the uncertainty in mean temperature difference can be estimated using the  $F$  correction factor figures as shown in Figs. D.1 to D.14. The procedure consists of the following steps:

- Calculate the uncertainty of  $R$  and  $P$ .
- Determine the sensitivity coefficients of  $F$  due to a unit variations in  $R$  and  $P$  by graphical methods.
- Calculate the uncertainty of  $F$  based on the uncertainties of  $R$  and  $P$ .
- Calculate the uncertainty of LMTD based on the uncertainties in terminal temperature measurements.
- Calculate the uncertainty of EMTD based on the uncertainties of  $F$  and LMTD.

It should be observed that the following procedure which combines the separate effects of uncertainties of temperature measurements on LMTD and  $F$  overestimates the uncertainty of mean temperature difference since the effects are "double-counted."

**TABLE D.1**  
**SENSITIVITY COEFFICIENTS FOR UNCERTAINTY FOR**  
**MEAN TEMPERATURE DIFFERENCE AT TEST CONDITIONS FOR**  
**COUNTERFLOW ARRANGEMENTS**

Contributing Factor	Sensitivity Coefficient
Uncertainty due to cold stream inlet temperature, $u_{ti}$	$\theta_{EMTD,ti} = -\frac{EMTD [EMTD/\Delta T_2 - 1]}{\Delta T_1 - \Delta T_2}$
Uncertainty due to cold stream outlet temperature, $u_{to}$	$\theta_{EMTD,to} = -\frac{EMTD [1 - EMTD/\Delta T_1]}{\Delta T_1 - \Delta T_2}$
Uncertainty due to hot stream inlet temperature, $u_{Ti}$	$\theta_{EMTD,Ti} = \frac{EMTD [1 - EMTD/\Delta T_1]}{\Delta T_1 - \Delta T_2}$
Uncertainty due to hot stream outlet temperature, $u_{To}$	$\theta_{EMTD,To} = \frac{EMTD [EMTD/\Delta T_2 - 1]}{\Delta T_1 - \Delta T_2}$

where

$$\Delta T_1 = T_i - t_o$$

$$\Delta T_2 = T_o - t_i$$

**TABLE D.2**  
**SENSITIVITY COEFFICIENTS FOR UNCERTAINTY FOR**  
**MEAN TEMPERATURE DIFFERENCE AT TEST CONDITIONS FOR**  
**ONE-SHELL-PASS/TWO-TUBE-PASS ARRANGEMENTS**

Contributing Factor	Sensitivity Coefficient
Uncertainty due to cold stream inlet temperature, $u_{ti}$	$\theta_{EMTD,ti} = \frac{EMTD}{C_1} \left[ \frac{t_o - t_i}{C_1} - \frac{EMTD[-1 - (t_o - t_i)/C_1]}{C_1 + C_2} + \frac{EMTD[-1 + (t_o - t_i)/C_1]}{C_2 - C_1} \right]$
Uncertainty due to cold stream outlet temperature, $u_{to}$	$\theta_{EMTD,to} = \frac{EMTD}{C_1} \left[ \frac{t_o - t_i}{C_1} - \frac{EMTD[-1 + (t_o - t_i)/C_1]}{C_1 + C_2} + \frac{EMTD[-1 - (t_o - t_i)/C_1]}{C_2 - C_1} \right]$
Uncertainty due to hot stream inlet temperature, $u_{Ti}$	$\theta_{EMTD,Ti} = \frac{EMTD}{C_1} \left[ \frac{T_i - T_o}{C_1} - \frac{EMTD[1 + (T_i - T_o)/C_1]}{C_1 + C_2} + \frac{EMTD[1 - (T_i - T_o)/C_1]}{C_2 - C_1} \right]$
Uncertainty due to hot stream outlet temperature, $u_{To}$	$\theta_{EMTD,To} = \frac{EMTD}{C_1} \left[ -\frac{T_i - T_o}{C_1} - \frac{EMTD[1 - (T_i - T_o)/C_1]}{C_1 + C_2} + \frac{EMTD[1 + (T_i - T_o)/C_1]}{C_2 - C_1} \right]$

where

$$C_1 = \sqrt{(T_i - T_o)^2 + (t_o - t_i)^2}$$

$$C_2 = T_i + T_o - t_i - t_o$$

The uncertainty of the temperature change ratio,  $R$ , is given by Eq. (D.8) and Table D.3:

$$u_R = [(\theta_{R,ti}u_{ti})^2 + (\theta_{R,to}u_{to})^2 + (\theta_{R,Ti}u_{Ti})^2 + (\theta_{R,To}u_{To})^2]^{1/2} \quad (D.8)$$

The uncertainty of the temperature effectiveness,  $P$ , is given by Eq. (D.9) and Table D.4:

$$u_P = [(\theta_{P,ti}u_{ti})^2 + (\theta_{P,to}u_{to})^2 + (\theta_{P,Ti}u_{Ti})^2]^{1/2} \quad (D.9)$$

The uncertainty in  $F$  correction factor at test conditions,  $u_F$ , is given in Eq. (D.10).

$$u_F = [(\theta_{F,R}u_R)^2 + (\theta_{F,P}u_P)^2 + u_{F,graph}^2]^{1/2} \quad (D.10)$$

where

$\theta_{F,R}$  and  $\theta_{F,P}$  are determined by estimating the change in  $F$  for a unit change in  $R$  and  $P$  on the plots or by using analytical approximations to the graphs

$u_{F,graph}$  is the uncertainty attributed to determination of sensitivity coefficients  $\theta_{F,R}$  and  $\theta_{F,P}$  using graphical methods<sup>2</sup>

The uncertainty in log mean temperature difference at test conditions,  $u_{LMTD}$  is given by Eq. (D.11) and Table D.5:

<sup>2</sup> With  $F < 0.75$ , the uncertainty attributed the graphical methods is significant since the changes in  $F$  are large for small changes in  $R$  and  $P$ .

**TABLE D.3**  
**SENSITIVITY COEFFICIENTS FOR UNCERTAINTY OF R**

Contributing Factor	Sensitivity Coefficient
Uncertainty due to cold stream inlet temperature, $u_{ti}$	$\theta_{R,ti} = \frac{R}{t_o - t_i}$
Uncertainty due to cold stream outlet temperature, $u_{to}$	$\theta_{R,to} = -\frac{R}{t_o - t_i}$
Uncertainty due to hot stream inlet temperature, $u_{Ti}$	$\theta_{R,Ti} = \frac{1}{t_o - t_i}$
Uncertainty due to hot stream outlet temperature, $u_{To}$	$\theta_{R,To} = -\frac{1}{t_o - t_i}$

**TABLE D.4**  
**SENSITIVITY COEFFICIENTS FOR UNCERTAINTY OF P**

Contributing Factor	Sensitivity Coefficient
Uncertainty due to cold stream inlet temperature, $u_{ti}$	$\theta_{P,ti} = \frac{P(1-P)}{T_i - t_i}$
Uncertainty due to cold stream outlet temperature, $u_{to}$	$\theta_{P,to} = \frac{1}{T_i - t_i}$
Uncertainty due to hot stream inlet temperature, $u_{Ti}$	$\theta_{P,Ti} = -\frac{P}{T_i - t_i}$

**TABLE D.5**  
**SENSITIVITY COEFFICIENTS FOR UNCERTAINTY OF LOG MEAN TEMPERATURE DIFFERENCE**

Contributing Factor	Sensitivity Coefficient
Uncertainty due to cold stream inlet temperature, $u_{ti}$	$\theta_{LMTD,ti} = -\frac{LMTD [LMTD/\Delta T_2 - 1]}{\Delta T_1 - \Delta T_2}$
Uncertainty due to cold stream outlet temperature, $u_{to}$	$\theta_{LMTD,to} = -\frac{LMTD [1 - LMTD/\Delta T_1]}{\Delta T_1 - \Delta T_2}$
Uncertainty due to hot stream inlet temperature, $u_{Ti}$	$\theta_{LMTD,Ti} = \frac{LMTD [1 - LMTD/\Delta T_1]}{\Delta T_1 - \Delta T_2}$
Uncertainty due to hot stream outlet temperature, $u_{To}$	$\theta_{LMTD,To} = \frac{LMTD [LMTD/\Delta T_2 - 1]}{\Delta T_1 - \Delta T_2}$

where

$$\Delta T_1 = T_i - t_o$$

$$\Delta T_2 = T_o - t_i$$

**TABLE D.6**  
**SENSITIVITY COEFFICIENTS FOR UNCERTAINTY OF MEAN TEMPERATURE**  
**DIFFERENCE BASED ON F-LMTD METHOD**

Contributing Factor	Sensitivity Coefficient
Uncertainty due to $F$ correction factor, $u_F$	$\theta_{EMTD,F} = \text{LMTD}$
Uncertainty due to log mean temperature difference, $u_{\text{LMTD}}$	$\theta_{EMTD,\text{LMTD}} = F$
Uncertainty due to variable heat transfer coefficient, $b_{EMTD,U}$	1
Uncertainty due to non-uniform temperature distribution over flow cross section, $b_{EMTD,\text{mixing}}$	1

$$u_{\text{LMTD}} = [(\theta_{\text{LMTD},ti}u_{ti})^2 + (\theta_{\text{LMTD},to}u_{to})^2 + (\theta_{\text{LMTD},Ti}u_{Ti})^2 + (\theta_{\text{LMTD},To}u_{To})^2]^{1/2} \quad (\text{D.11})$$

The uncertainty in mean temperature difference at test conditions,  $u_{EMTD}$ , is given by Eq. (D.12) and Table D.6:

$$u_{EMTD} = [(\theta_{EMTD,F}u_F)^2 + \theta_{EMTD,\text{LMTD}}u_{\text{LMTD}}]^2 + b_{EMTD,U}^2 + b_{EMTD,\text{mixing}}^2]^{1/2} \quad (\text{D.12})$$

**D.3.1.3 Uncertainties in the Analytical Model.** The idealizations and assumptions used in the derivation of mean temperature difference contribute to the uncertainty in mean temperature difference. Some of these effects have been investigated and the results are summarized here.

(a) *Variable Overall Heat Transfer Coefficient.* The variation in  $U$  along the flow length (due to variation in convective heat transfer coefficient and fouling resistance) results in a bias in the mean temperature difference. The magnitude of the bias can be calculated by integrating the differential rate and energy equations along the flow length. Alternatively, the following method may be used for instances where the variation in  $U$  is monotonic. This alternate approach is based on an analytic solution developed by Colburn, Reference 30, for the counterflow heat exchangers where  $U$  is a linear function of temperature of either the hot or cold streams:

$$Q/A = \frac{U_1\Delta T_2 - U_2\Delta T_1}{\ln \frac{U_1\Delta T_2}{U_2\Delta T_1}} \quad (\text{D.13})$$

where

$$\Delta T_1 = T_i - t_o$$

$$\Delta T_2 = T_o - t_i$$

$$U_1 = U \text{ at hot stream inlet}$$

$$U_2 = U \text{ at hot stream outlet}$$

(1) For flow arrangements other than counterflow, a simple approach uses the traditional  $F$  correction factor combined with the above equation as originally suggested by Sieder and Tate, Reference 31, and reiterated by Gardner and Taborek, Reference 32. The error in this approach was estimated to be about 10% by Gardner, Reference 33, for the case of a one-shell-pass/two-tube-pass configuration.

(2) The bias in the mean temperature difference is calculated by comparing the result from the Colburn equation (and the Sieder-Tate modification) with the results using the traditional approach based on an average  $U$ ,  $U_{\text{average}} = (U_1 + U_2)/2$ . This method is similar to the one used by Gardner and Taborek, Reference 32, to determine temperature correction:

$$\frac{b_{EMTD,U}}{EMTD} = 1 - \frac{Q/A_{U_{\text{variable}}}}{Q/A_{U_{\text{average}}}} \quad (\text{D.14})$$

$$\frac{b_{EMTD,U}}{EMTD} = 1 - \frac{2(U_1/U_2 - \Delta T_1/\Delta T_2) \ln(\Delta T_1/\Delta T_2)}{(1 + U_1/U_2)(\Delta T_1/\Delta T_2 - 1) \ln\left(\frac{U_1/U_2}{\Delta T_1/\Delta T_2}\right)} \quad (\text{D.15})$$

where

$$\Delta T_1 = T_i - t_o$$

$$\Delta T_2 = T_o - t_i$$

$U_1 = U$  at hot stream inlet (except for multipass hot stream and single pass cold stream arrangement where  $U_1 = U$  at cold stream outlet)

$U_2 = U$  at hot stream outlet (except for multipass hot stream and single pass cold stream arrangement where  $U_2 = U$  at cold stream inlet)

(b) *Incomplete Thermal Mixing.* Incomplete thermal mixing over a flow cross section may result in a non-uniform temperature distribution and bias in mean temperature difference. Flow maldistribution, bypass flow, and non-uniform distribution of fouling resistance can contribute to the bias. If mixing is adequate along the length of the heat exchanger, the non-uniform distribution of temperatures over the flow cross section is small. As a result, this bias is small for a well designed heat exchanger, without excessive fouling, operating near its design point. However, for thermal performance tests performed at off-design conditions, the bias of this effect may be significant.

(1) For shell and tube heat exchangers, the effect of bypass flow on temperature profile has been investigated previously by Whistler, Reference 34, for one-shell-pass/one-tube-pass counter-flow configuration and by Fisher and Parker, Reference 35, for one-shell pass/two-tube-pass configuration based on the assumption that the main flow stream mixes thoroughly with the bypass stream after each baffle pass. Some investigation of the effect of bypass flow for conditions of partial mixing have been investigated, such as by Bell and Kegler, Reference 36; however, a generalized method to estimate the effect of bypass flow on mean temperature difference has not been developed. To determine the bias due to incomplete thermal mixing for counterflow arrangements in shell-and-tube heat exchangers, the method used by Whistler is considered appropriate if mixing between baffle sections is considered to be good. Assuming a leakage factor of 0.1, a 2% bias bounds most practical applications. This 2% bias is considered to be bounding for other shell-and-tube flow arrangements where  $F > 0.75$  (little or no outlet temperature crossover). When  $F < 0.75$ , the bias due to thermal mixing may be greater, but the overall uncertainty in mean temperature may be bounded by using bounding estimates for the outlet temperature measurements.

(2) A small number of baffles may result in a bias in mean temperature difference as investigated by Gardner and Taborek, Reference 32, and Shah and Pignotti, Reference 37. The results of Gardner and Taborek indicate that more than 11 baffle crossings are needed to ensure that this effect is negligible for one-shell-pass/one-tube-pass counterflow arrangement and that more than 5 baffle crossings are needed for one-shell-pass/two-tube-pass arrangement. The results of Shah and Pignotti indicate that more than 10 baffles are needed to ensure that the effect is negligible for 1-1 TEMA E counterflow heat exchanger and more than 6 baffles are needed for 1-2 TEMA E exchanger.

(3) In summary, for shell and tube heat exchangers, the bias due to incomplete thermal mixing is small and is bounded by 2% uncertainty. However, for tests performed at off-design conditions, where the number of baffles is small, where the ratio of the fluid stream temperature change to mean temperature difference is large (such as for  $F < 0.75$  when outlet temperatures cross-over), or when bypass leakage is large, the bias due to this effect may be significant.

(4) For compact designs such as plate-fin and plate frame, flow maldistribution may result in a non-uniform temperature distribution. Analyses of maldistribution for compact designs reviewed by Mueller and Chiou, Reference 38, typically combine the effects of non-uniform temperatures with the effect of non-uniform heat transfer coefficient. Nevertheless, assuming a 2% bias due to incomplete thermal mixing is reasonable for many configurations. However, conditions where mixing is poor or when the ratio of the fluid stream temperature change to mean temperature difference is large (such as for conditions with a close approach) may result in a significant bias.

### D.3.2 Uncertainty of Alternate Methods

The uncertainty of mean temperature difference calculated by methods different than the F-LMTD methods shall include the effects of uncertainty of the test measurements and the uncertainty of the assumptions and idealizations used in the calculation of mean temperature difference. To meet these requirements, understanding the methods used by computer programs is needed to adequately assess uncertainty. It is noted that the use of stepwise calculation methods does not necessarily eliminate uncertainty due to idealizations in the calculational method.

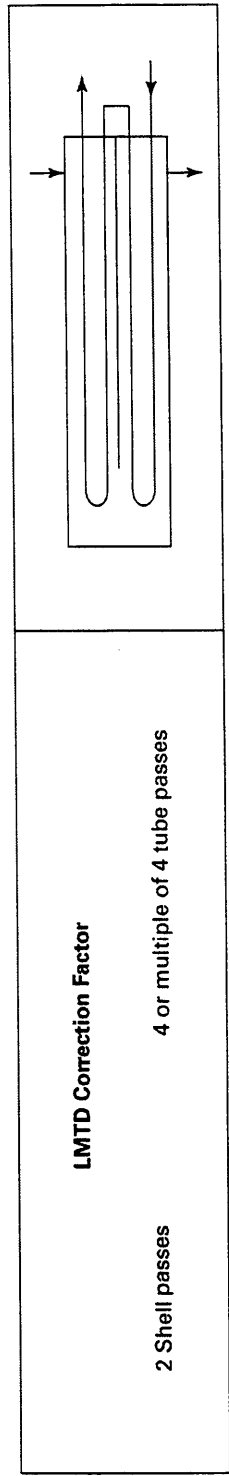
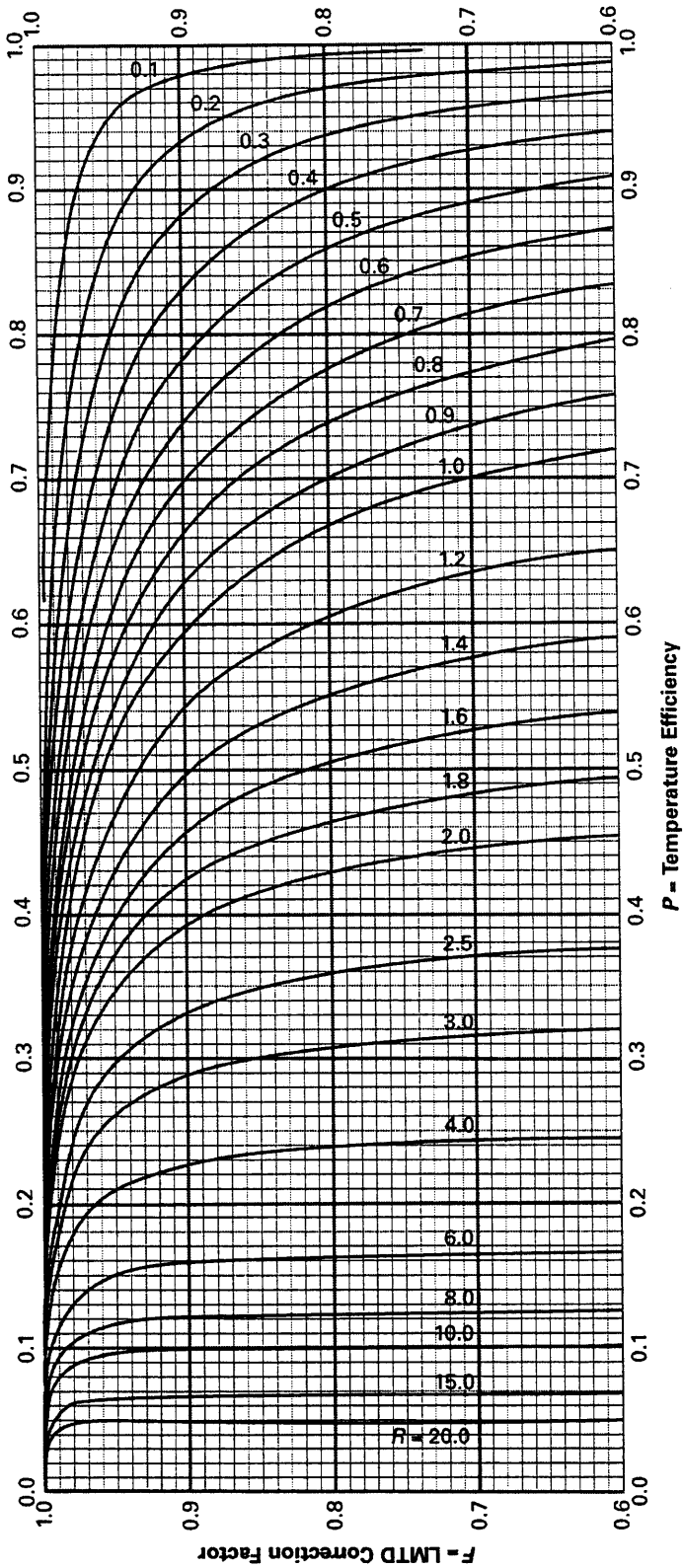
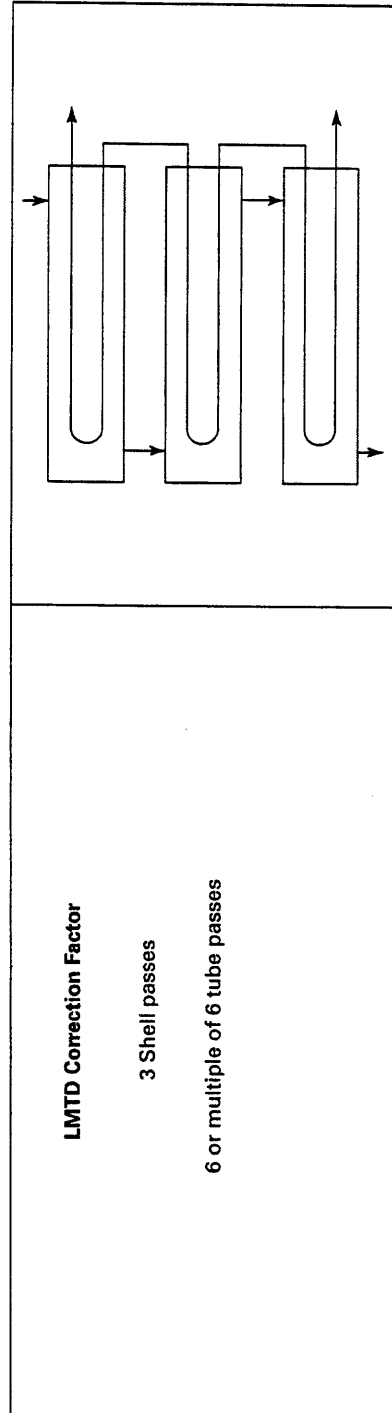
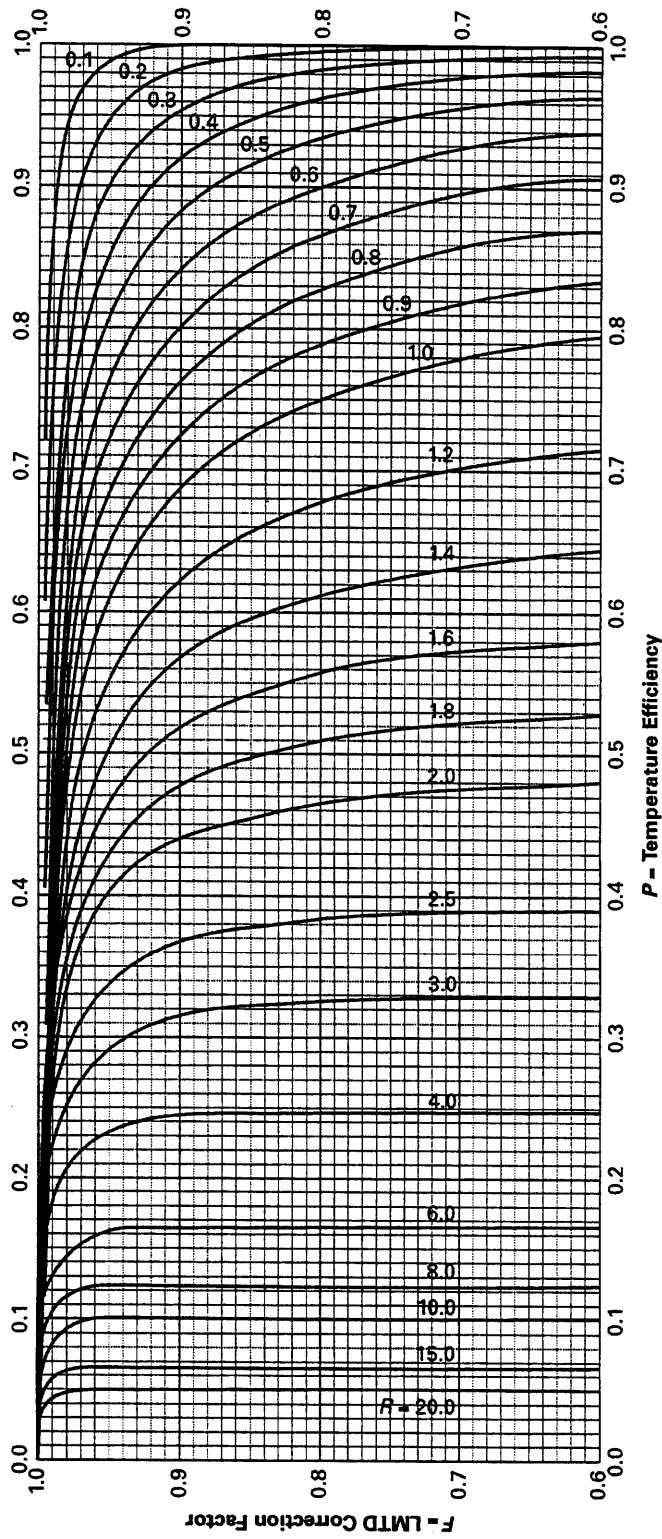


FIG. D.2 LMTD CORRECTION FACTOR FOR FOUR OR MULTIPLE OF FOUR TUBE PASSES, TWO SHELL PASSES (from reference 39)  
 (Reprinted with the permission of Heat Exchange Institute from the HEI Standards for Power Plant Heat Exchangers)



LMTD Correction Factor

3 Shell passes

6 or multiple of 6 tube passes

**FIG. D.3 LMTD CORRECTION FACTOR FOR SIX OR MULTIPLE OF SIX TUBE PASSES, THREE SHELL PASSES (from reference 39)**  
 (Reprinted with the permission of Heat Exchange Institute from the HEI Standards for Power Plant Heat Exchangers)

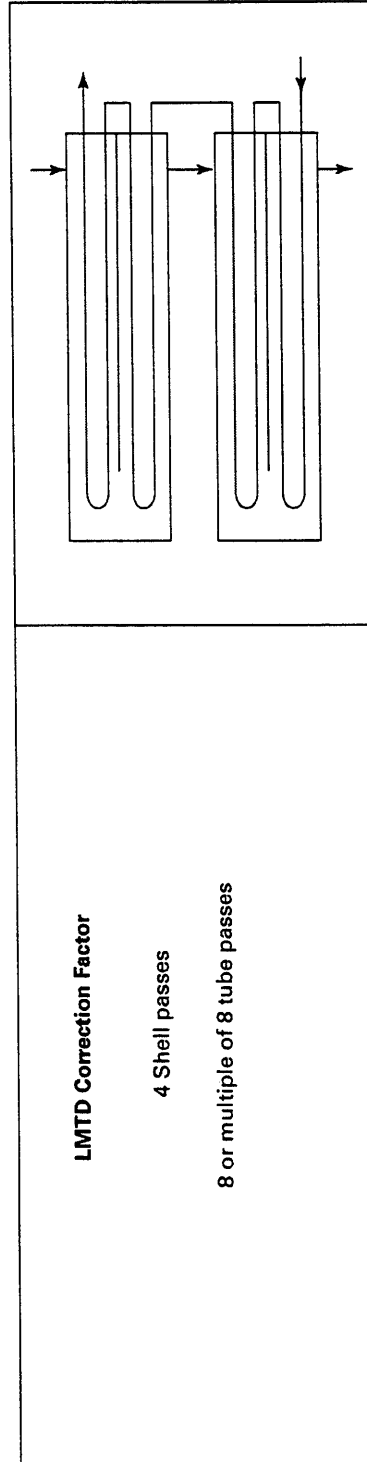
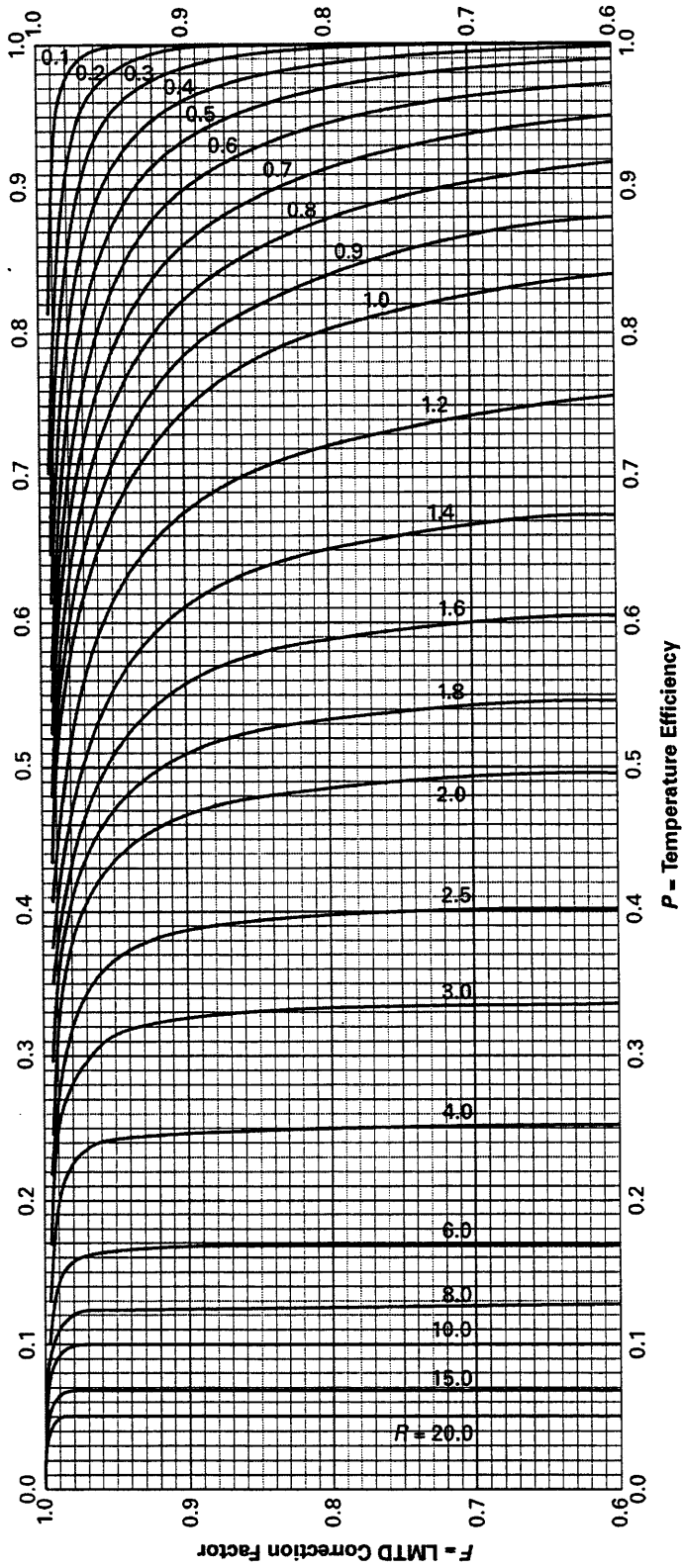


**FIG. D.4 LMTD CORRECTION FACTOR FOR EIGHT OR MULTIPLE OF EIGHT TUBE PASSES, FOUR SHELL PASSES (from reference 39)**  
 (Reprinted with the permission of Heat Exchange Institute from the HEI Standards for Power Plant Heat Exchangers)

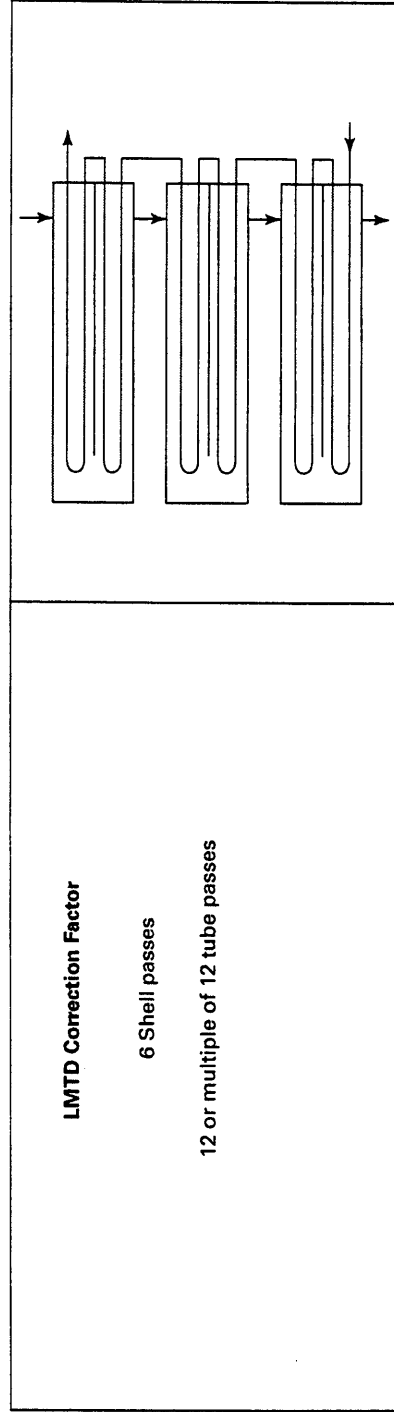
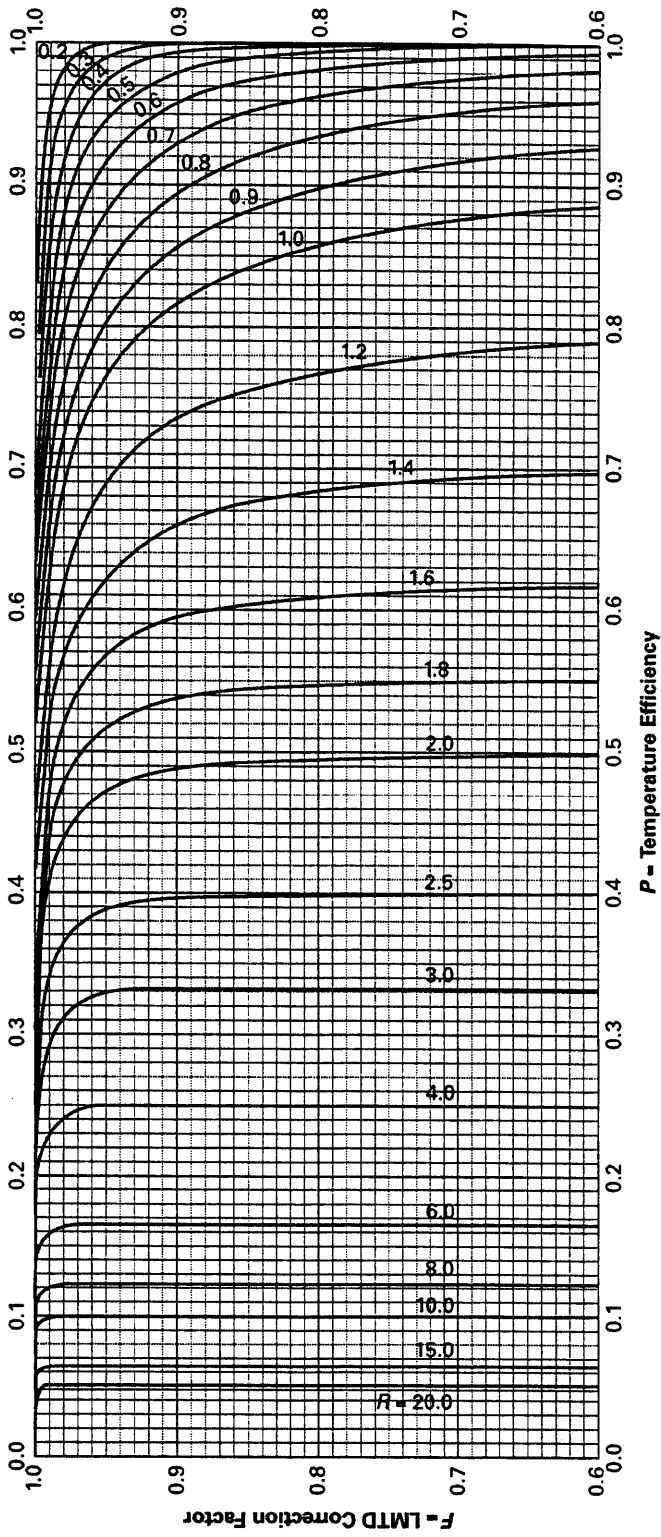


**FIG. D.5 LMTD CORRECTION FACTOR FOR TWELVE OR MULTIPLE OF TWELVE TUBE PASSES, SIX SHELL PASSES (from reference 39)**  
 (Reprinted with the permission of Heat Exchange Institute from the HEI Standards for Power Plant Heat Exchangers)

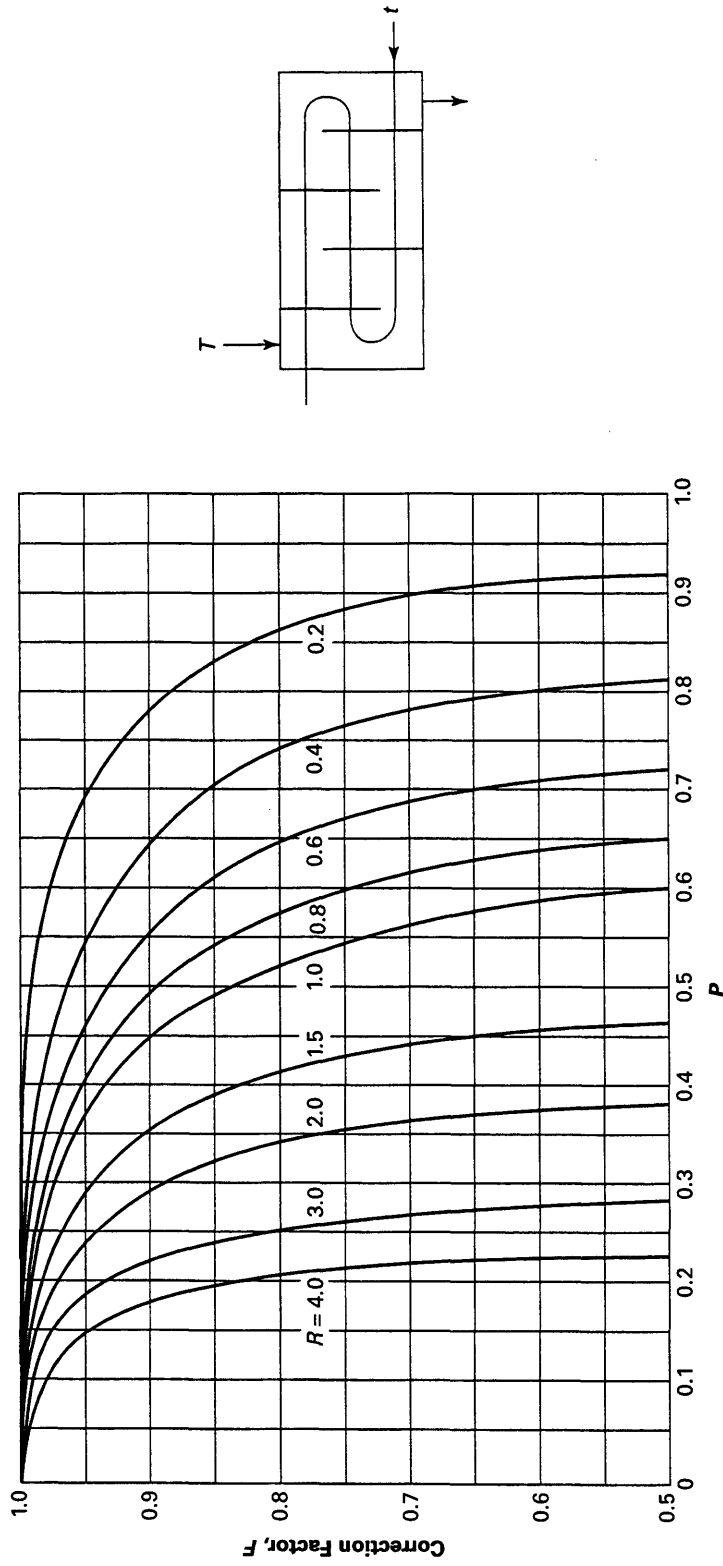


FIG. D.6 LMTD CORRECTION FACTOR FOR THREE OR MULTIPLE OF THREE TUBE PASSES, ONE SHELL PASS (from reference 29)

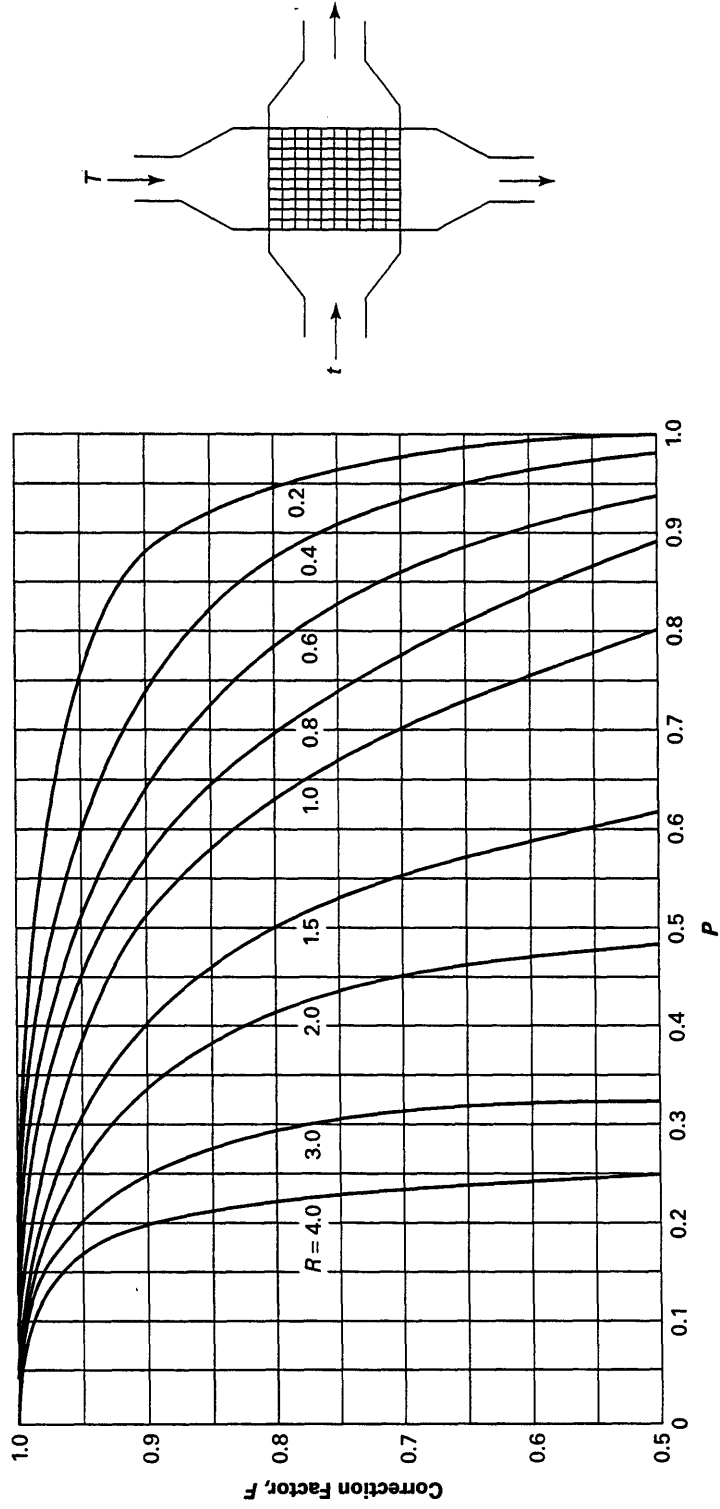


FIG. D.7 LMTD CORRECTION FACTOR FOR SINGLE PASS CROSSFLOW, BOTH FLUIDS UNMIXED (from reference 29)

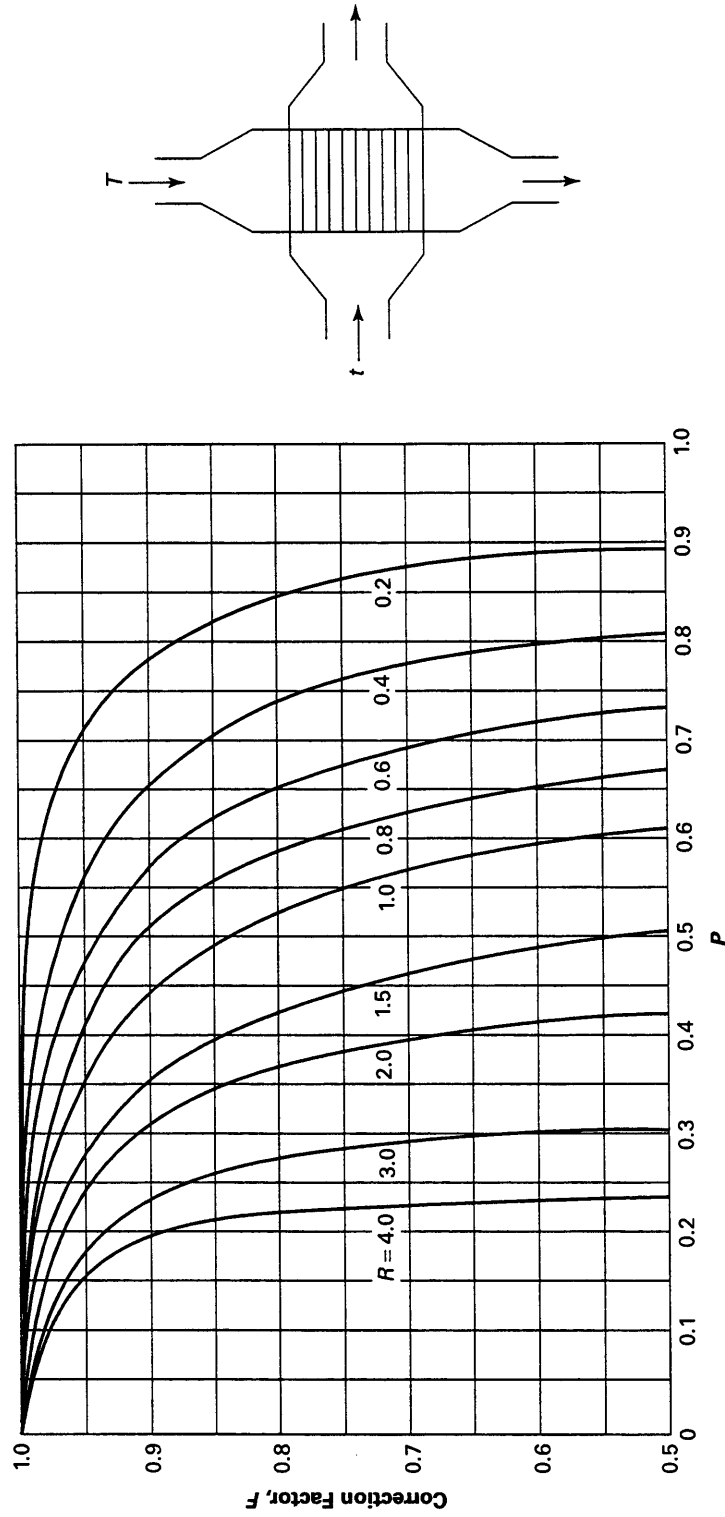


FIG. D.8 LMTD CORRECTION FACTOR FOR SINGLE PASS CROSSFLOW, ONE FLUID MIXED, ONE FLUID UNMIXED (from reference 29)

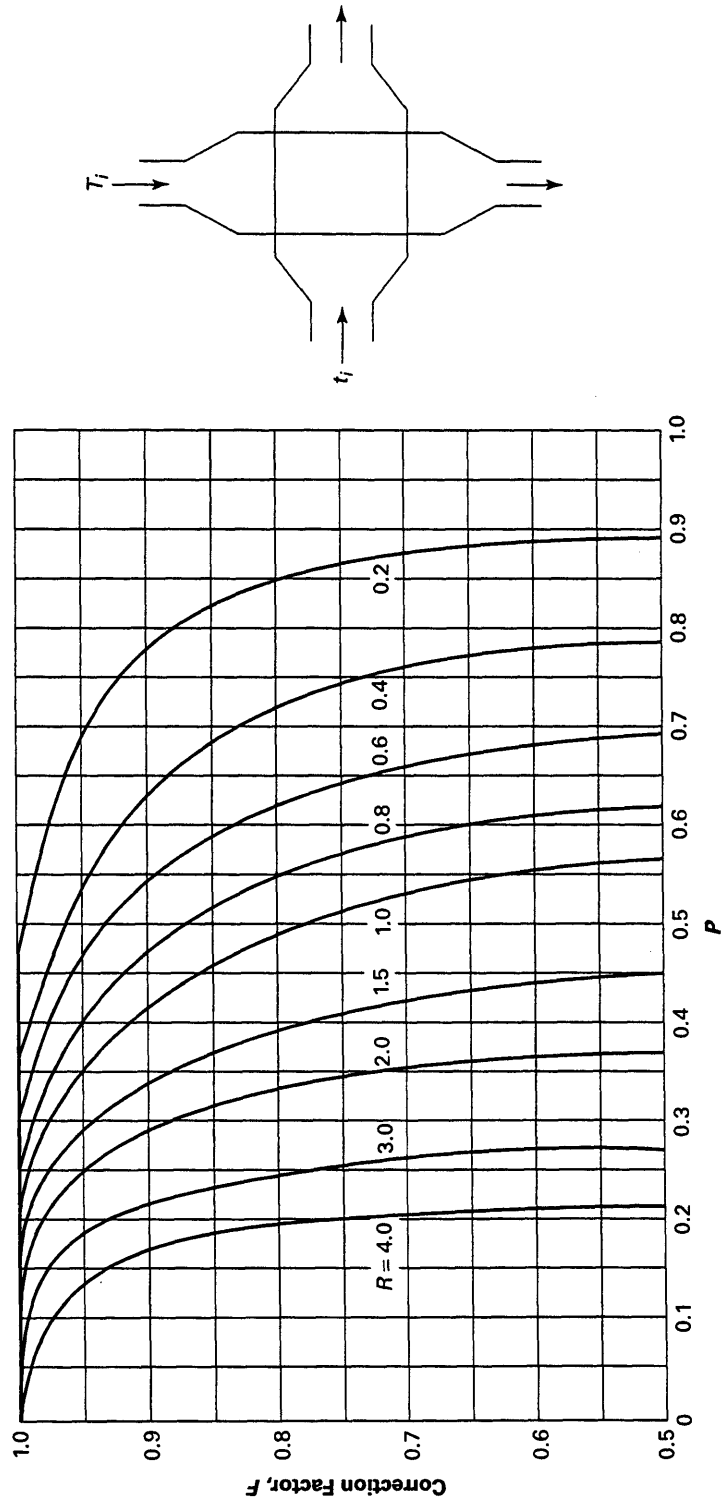


FIG. D.9 LMTD CORRECTION FACTOR FOR SINGLE PASS CROSSFLOW, BOTH FLUIDS MIXED (from reference 29)

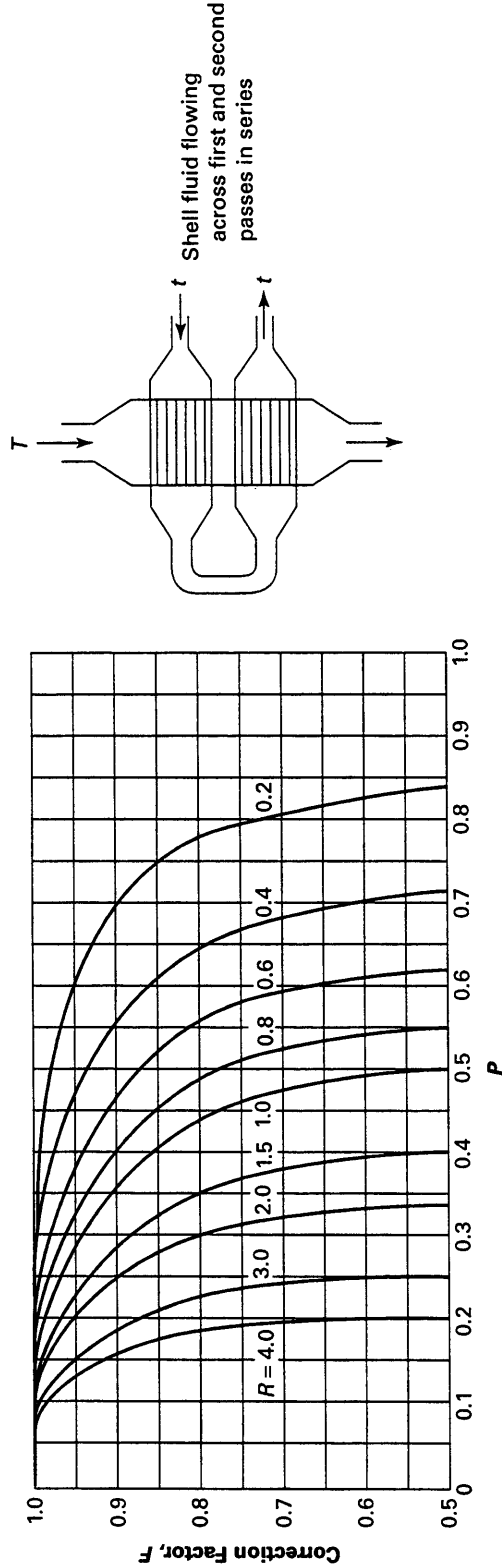
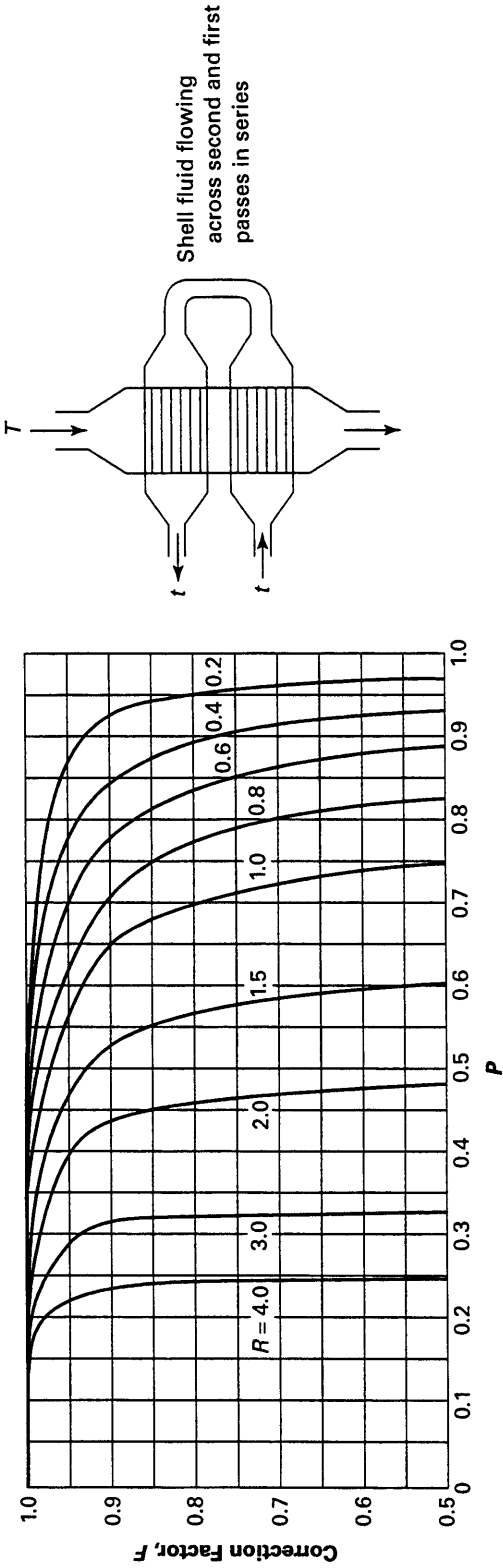
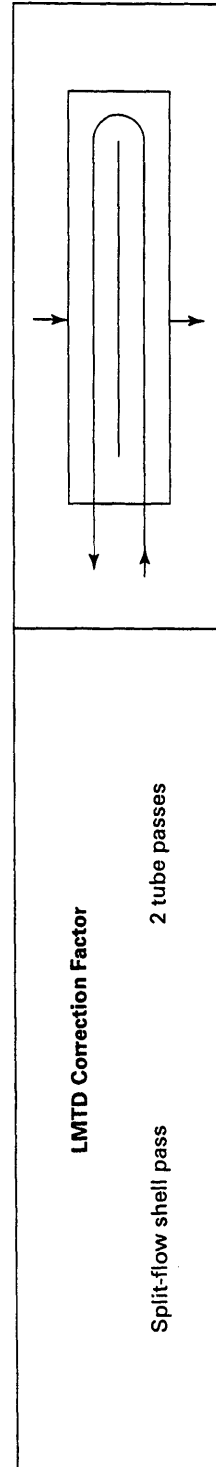
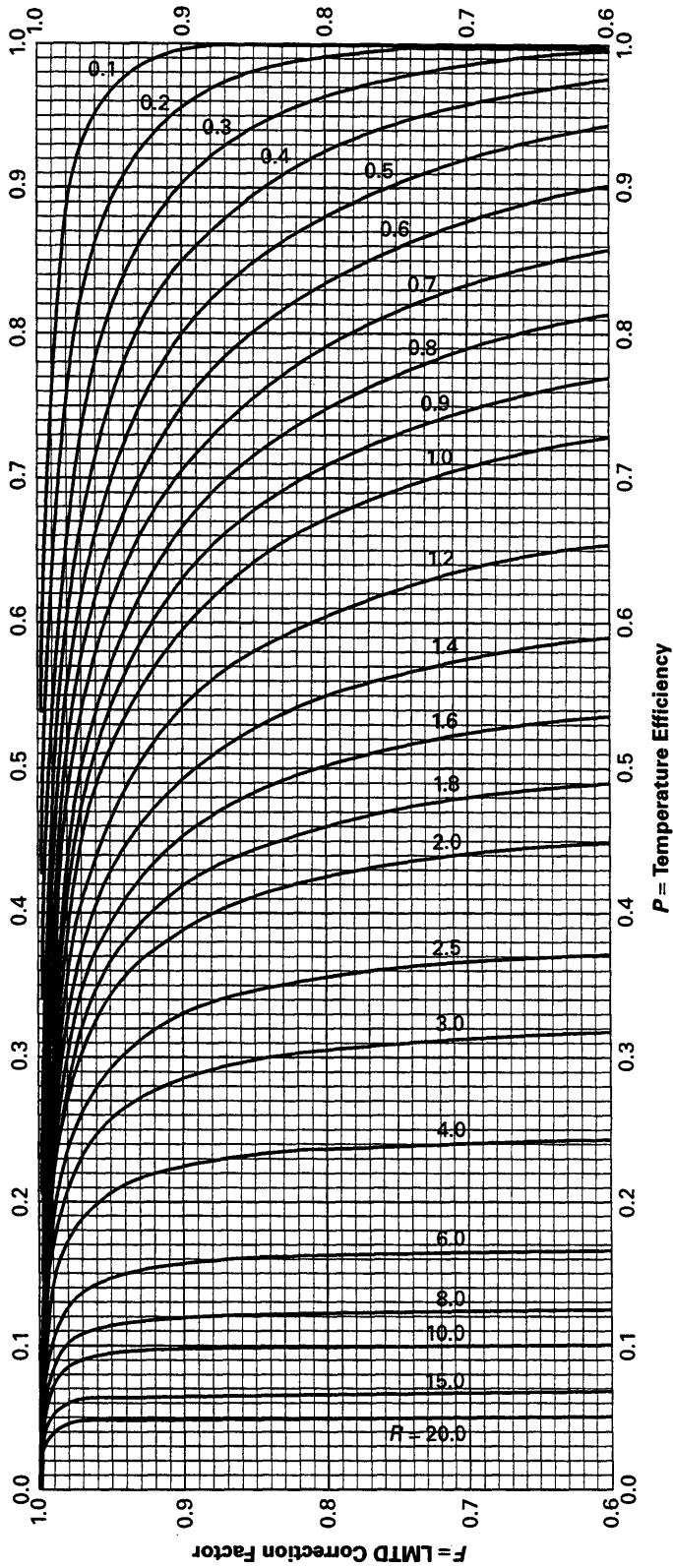
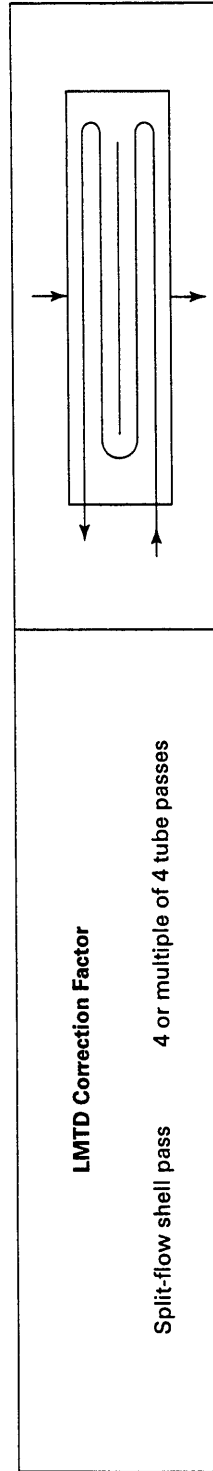
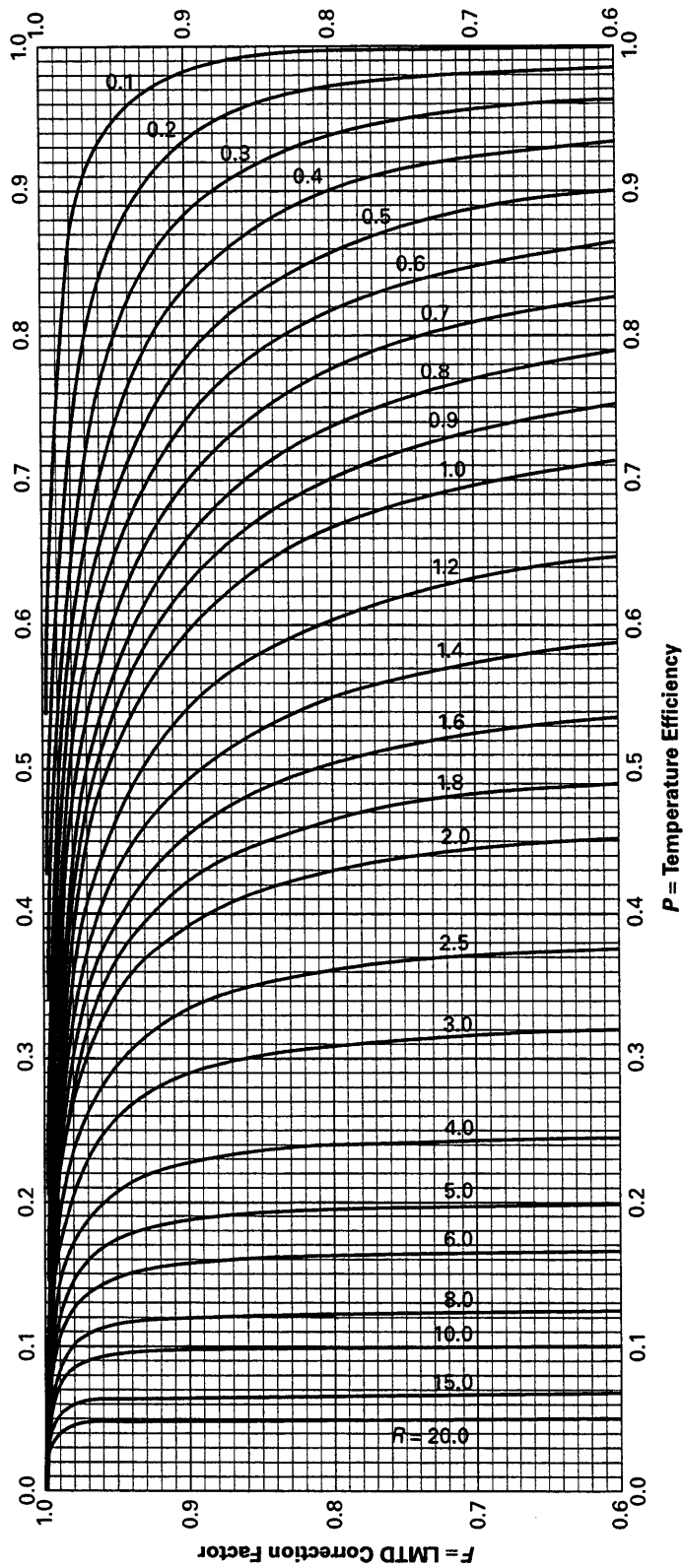


FIG. D.10 LMTD CORRECTION FACTOR FOR TWO SHELL PASS CROSSFLOW, TUBE FLUID UNMIXED (from reference 29)



**FIG. D.11 LMTD CORRECTION FACTOR FOR SPLIT FLOW SHELL PASS  
(G SHELL), TWO TUBE PASSES (from reference 39)  
(Reprinted with the permission of Heat Exchange Institute from the  
HEI Standards for Power Plant Heat Exchangers)**



**FIG. D.12 LMTD CORRECTION FACTOR FOR SPLIT FLOW SHELL PASS (G SHELL), FOUR OR MULTIPLE OF FOUR TUBE PASSES (from reference 39)**  
 (Reprinted with the permission of Heat Exchange Institute from the HEI Standards for Power Plant Heat Exchangers)

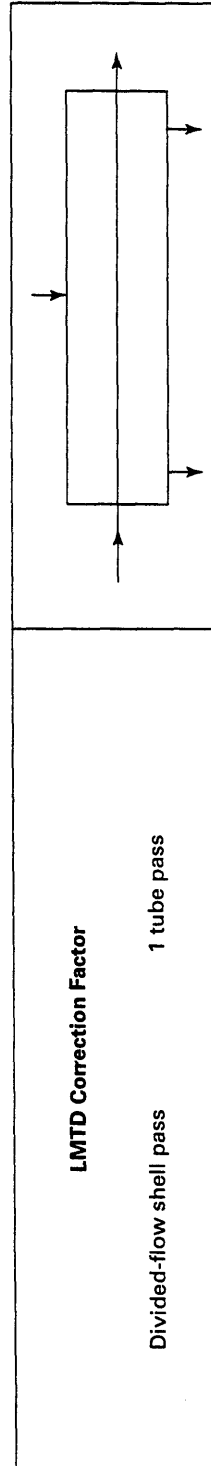
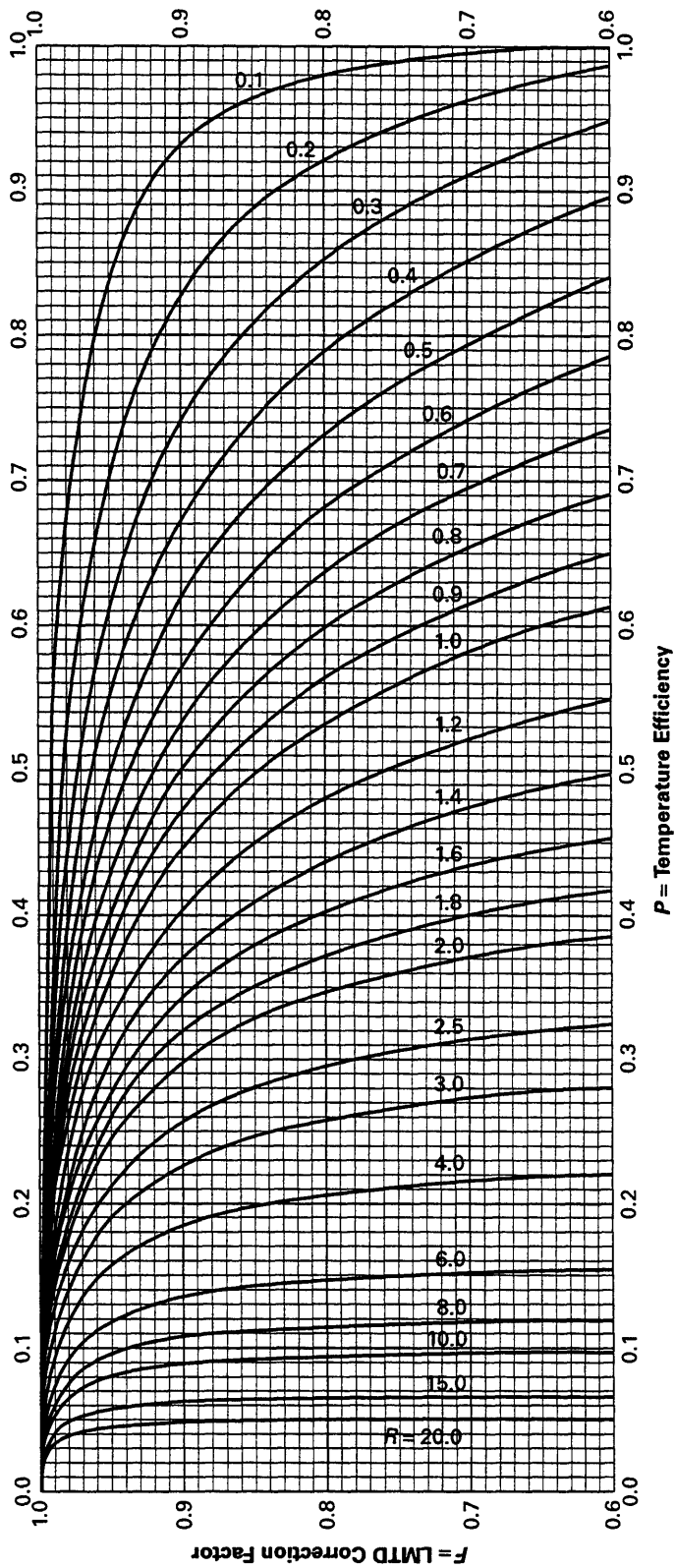
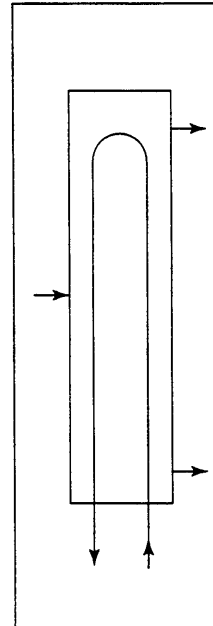
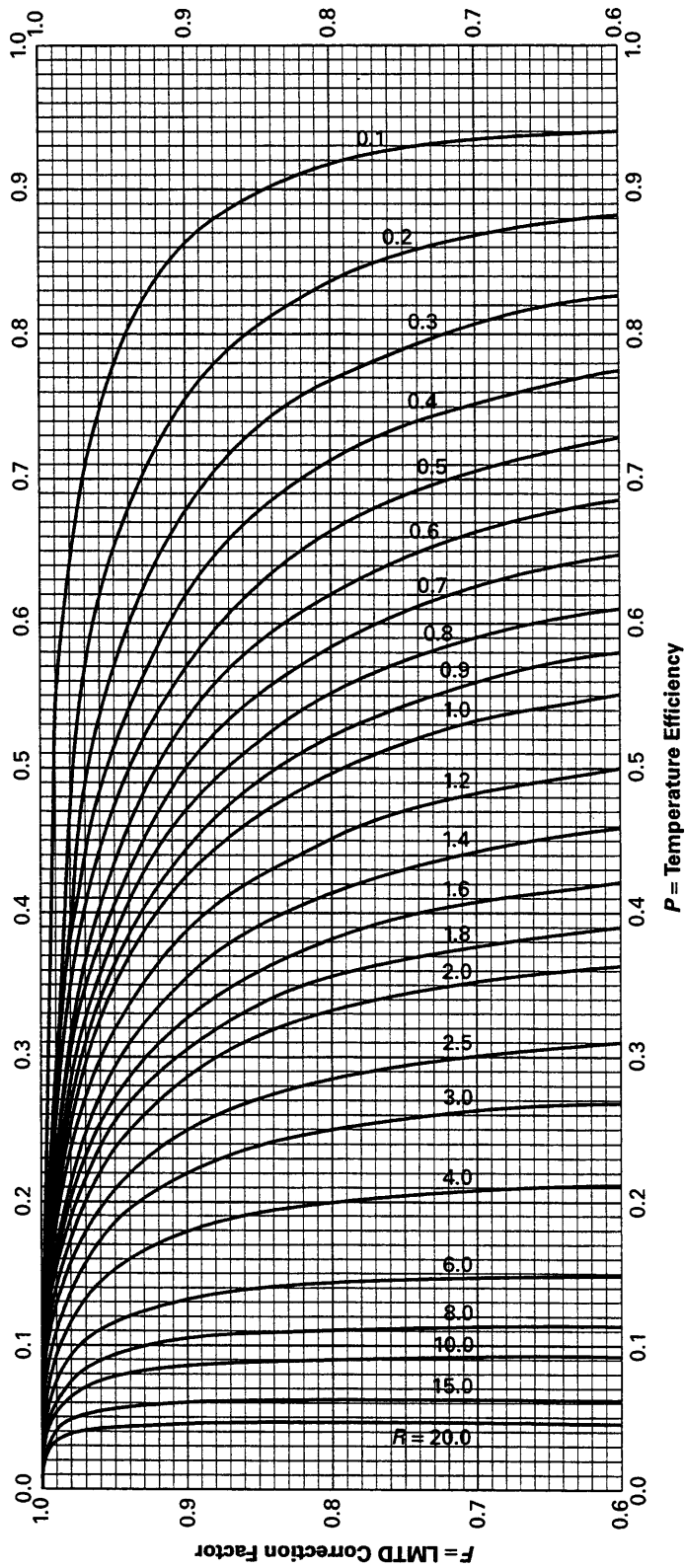


**FIG. D.13 LMTD CORRECTION FACTOR FOR DIVIDED FLOW SHELL PASS (J SHELL), ONE TUBE PASS (from reference 39)**  
 (Reprinted with the permission of Heat Exchange Institute from the HEI Standards for Power Plant Heat Exchangers)



**LMTD Correction Factor**  
 Divided-flow shell pass      2 or multiple of 2 tube passes

**FIG. D.14 LMTD CORRECTION FACTOR FOR DIVIDED FLOW SHELL PASS (J SHELL), TWO OR MULTIPLE OF TWO TUBE PASSES (from reference 39)**  
 (Reprinted with the permission of Heat Exchange Institute from the HEI Standards for Power Plant Heat Exchangers)

This page intentionally left blank.

# NONMANDATORY APPENDIX E — DERIVATION OF PERFORMANCE EQUATIONS

## E.1 THERMAL PERFORMANCE

### E.1.1 General

A thermal performance test consists of measuring six parameters: the inlet and outlet temperatures and the two flow rates. With the six measured parameters, the heat transfer rate,  $Q$ , and overall heat transfer coefficient,  $U$ , can be calculated by solving the energy balance Eqs. (E.1) and (E.2) and the rate Eq. (E.3).

$$Q = m_c c_{p,c}(t_o - t_i) \quad (\text{E.1})$$

$$Q = m_h c_{p,h}(T_i - T_o) \quad (\text{E.2})$$

$$Q = UA(\text{EMTD}) \quad (\text{E.3})$$

With three equations and two unknowns, redundant data is available to solve for  $Q$  and  $U$ . The redundant data is used to confirm a heat balance and calculate a weighted average heat transfer rate. The thermal performance parameters are adjusted to reference conditions for easier comparison to other tests and/or to the system design basis:

$$\frac{1}{U^*} = \frac{1}{U} + \phi_U \quad (\text{E.4})$$

$$Q^* = \phi_Q Q \quad (\text{E.5})$$

The correction factors  $\phi_U$  and  $\phi_Q$  are a function of the heat transfer model and associated assumptions used. This Appendix derives the equations and correction factors used in this Code. The heat transfer model used is based on the description in Reference 42. The nomenclature is described in Section 2 and is consistent with the nomenclature used in Sections 3 and 5.

### E.1.2 Thermal Performance at Test Conditions

Measurement of six terminal parameters and calculation of a weighted mean measured heat duty is

required. The weighted mean measured heat duty is more representative of the actual heat load at the time of the test than either the cold stream heat transfer rate or hot stream heat transfer rate. The cold stream and hot stream heat transfer rates are calculated based on the average (or representative) measurements and specific heat of the fluid streams:

$$Q_c = m_c c_{p,c}(t_o - t_i) \quad (\text{E.6})$$

$$Q_h = m_h c_{p,h}(T_i - T_o) \quad (\text{E.7})$$

Typically,  $Q_c$  and  $Q_h$  are not the same; however, the difference must be attributed to the uncertainties to maintain a heat balance. The weighted mean heat load can be calculated from the hot and cold side heat loads and their associated uncertainties:

$$Q_{ave} = \left( \frac{u_{Q_h}^2}{u_{Q_c}^2 + u_{Q_h}^2} \right) Q_c + \left( \frac{u_{Q_c}^2}{u_{Q_c}^2 + u_{Q_h}^2} \right) Q_h \quad (\text{E.8})$$

The effective mean temperature difference is calculated as discussed in Appendix D. Using the weighted mean heat load, the overall heat transfer coefficient at test conditions is calculated as:

$$U = \frac{Q_{ave}}{A(\text{EMTD})} \quad (\text{E.9})$$

### E.1.3 Adjustment to Reference Conditions

To allow reasonable and valid comparison of heat exchanger performance tests, the results must be adjusted to a set of reference operating conditions.<sup>1</sup> Adjustment to reference conditions is based on a heat

<sup>1</sup> Throughout the remainder of this Appendix, variables reflecting the reference condition will be indicated with an asterisk (\*) while variables without an asterisk will represent the test condition or quantities that are unaffected by the projection to the reference condition.

transfer model consisting of summation of individual thermal resistances. At the test conditions,

$$\frac{1}{UA} = R_w + R_f + R_c + R_h \quad (\text{E.10})$$

and similarly, at the reference conditions:

$$\frac{1}{U^*A} = R_w^* + R_f^* + R_c^* + R_h^* \quad (\text{E.11})$$

where

$U$  = overall heat transfer coefficient at test conditions

$U^*$  = overall heat transfer coefficient at reference conditions

$R_w, R_w^*$  = thermal resistance of the wall at test and reference conditions

$R_f, R_f^*$  = thermal resistance of fouling at test and reference conditions

$R_c, R_c^*$  = thermal resistance of the cold side film at test and reference conditions

$R_h, R_h^*$  = thermal resistance of the hot side film at test and reference conditions

Subtracting Eq. (E.10) from Eq. (E.11) yields:

$$\frac{1}{U^*A} = \frac{1}{UA} + (R_c^* - R_c) + (R_h^* - R_h) + (R_f^* - R_f) + (R_w^* - R_w) \quad (\text{E.12})$$

However, the heat exchanger test described in this Code assumes that the fouling resistance is independent of conditions selected for evaluation (even though it may be a function of time). In other words, it is assumed that the fouling resistance will remain constant if operating conditions are rapidly changed from test to reference conditions. This assumption reduces Eq. (E.12) to:

$$\frac{1}{U^*A} = \frac{1}{UA} + (R_c^* - R_c) + (R_h^* - R_h) + (R_w^* - R_w) \quad (\text{E.13})$$

Substituting for the thermal resistance of the corresponding film layer:

$$R_c = \frac{1}{\eta_c h_c A_c} \quad R_c^* = \frac{1}{\eta_c h_c^* A_c} \quad (\text{E.14})$$

$$R_h = \frac{1}{\eta_h h_h A_h} \quad R_h^* = \frac{1}{\eta_h h_h^* A_h} \quad (\text{E.15})$$

where

$\eta_h, \eta_c$  = surface temperature effectiveness of fins or other enhancements<sup>2</sup>

$h_h, h_h^*$  = hot side film coefficient at test and reference conditions

$h_c, h_c^*$  = cold side film coefficient at test and reference conditions

$A_h, A_c$  = hot side and cold side heat transfer area

$$U^* = \frac{1}{\frac{1}{U} + \frac{A}{\eta_h A_h} \left[ \frac{1}{h_h^*} - \frac{1}{h_h} \right] + \frac{A}{\eta_c A_c} \left[ \frac{1}{h_c^*} - \frac{1}{h_c} \right] + (R_w^* - R_w)} \quad (\text{E.16})$$

The correction factor,  $\phi_U$ , is

$$\phi_U = \frac{A}{\eta_h A_h} \left[ \frac{1}{h_h^*} - \frac{1}{h_h} \right] + \frac{A}{\eta_c A_c} \left[ \frac{1}{h_c^*} - \frac{1}{h_c} \right] + (R_w^* - R_w) \quad (\text{E.17})$$

A similar relationship can be developed for the heat duty at reference conditions ( $Q^*$ ):

$$Q^* = U^*A(\text{EMTD})^* \quad (\text{E.18})$$

Substituting Eqs. (E.18) into (E.17) yields:

$$Q^* = \frac{A(\text{EMTD})^*}{\frac{1}{U} + \frac{A}{\eta_h A_h} \left[ \frac{1}{h_h^*} - \frac{1}{h_h} \right] + \frac{A}{\eta_c A_c} \left[ \frac{1}{h_c^*} - \frac{1}{h_c} \right] + (R_w^* - R_w)} \quad (\text{E.19})$$

Finally, multiplying by  $U/U$  and combining with Eq. (E.3) gives:

<sup>2</sup> The surface temperature effectiveness,  $\eta$ , is a measure of reduction in temperature potential between the extended surface and the fluid. The expression is general and accounts for plain surfaces where  $\eta = 1$ , finned surfaces where  $\eta < 1$ , and other enhancements. The term is related to the fin efficiency,  $\eta_f$ , with the expression  $\eta = 1 - A_f/A(1 - \eta_f)$  where  $A_f$  = fin surface area. The surface temperature effectiveness and fin efficiency are related to the fin resistance as discussed in Reference 43.

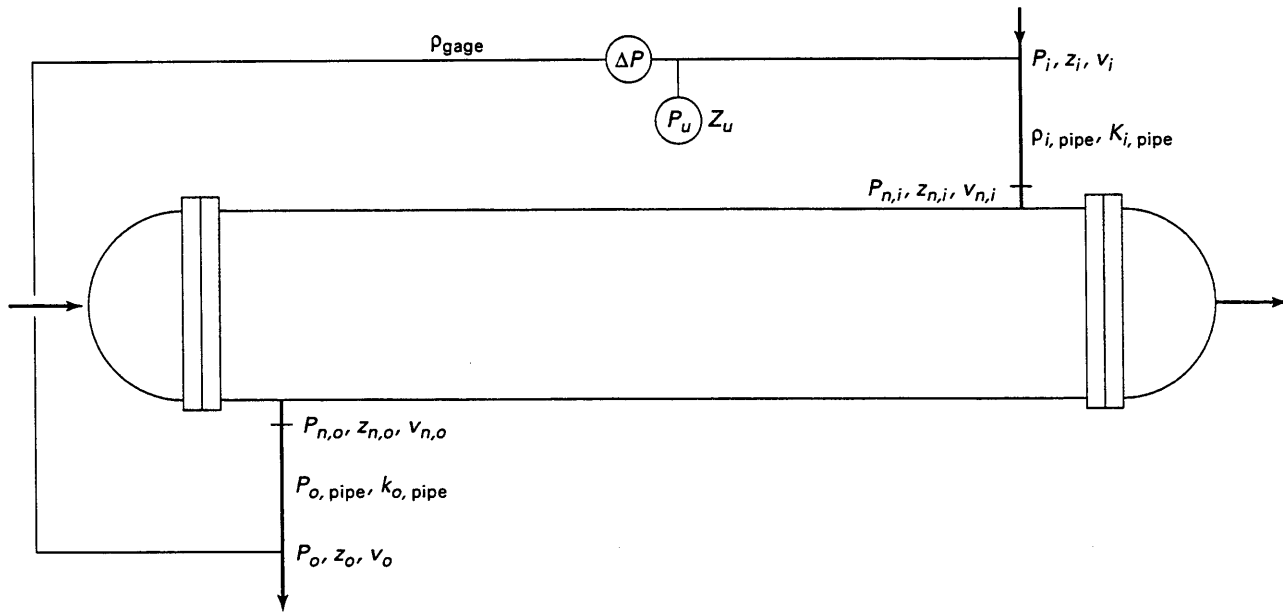


FIG. E.1 TYPICAL CONFIGURATION OF HEAT EXCHANGER DIFFERENTIAL PRESSURE MEASUREMENT

$$Q^* = \frac{Q_{ave} (EMTD)^*/(EMTD)}{1 + U \left( \frac{A}{\eta_h A_h} \left[ \frac{1}{h_h^*} - \frac{1}{h_h} \right] + \frac{A}{\eta_c A_c} \left[ \frac{1}{h_c^*} - \frac{1}{h_c} \right] + (R_w^* - R_w) \right)} \quad (E.20)$$

$$\Delta P_{n-n} = \rho_{ave} \left[ \frac{P_{n,i}}{\rho_{i,pipe}} + \frac{g}{g_c} z_{n,i} + \frac{v_{n,i}^2}{2g_c} - \left( \frac{P_{n,o}}{\rho_{o,pipe}} + \frac{g}{g_c} z_{n,o} + \frac{v_{n,o}^2}{2g_c} \right) \right] \quad (E.22)$$

The correction factor,  $\phi_Q$ , is

$$\phi_Q = \frac{(EMTD)^*/(EMTD)}{1 + U \left( \frac{A}{\eta_h A_h} \left[ \frac{1}{h_h^*} - \frac{1}{h_h} \right] + \frac{A}{\eta_c A_c} \left[ \frac{1}{h_c^*} - \frac{1}{h_c} \right] + (R_w^* - R_w) \right)} \quad (E.21)$$

where

- $\rho_{ave}$  = average density<sup>3</sup>
- $P_{n,i}$  = static pressure at the inlet nozzle
- $P_{n,o}$  = static pressure at the outlet nozzle
- $z_{n,i}$  = elevation at the inlet nozzle
- $z_{n,o}$  = elevation at the outlet nozzle
- $v_{n,i}$  = velocity at the inlet nozzle
- $v_{n,o}$  = velocity at the outlet nozzle

## E.2 TOTAL NOZZLE-TO-NOZZLE PRESSURE LOSS

### E.2.1 Nozzle-to-Nozzle Pressure Loss at Test Conditions

The pressure loss measured using a differential pressure instrument and static wall pressure taps in the upstream and downstream piping must be adjusted to nozzle-to-nozzle conditions. A typical configuration is shown in Fig. E.1.

The total nozzle-to-nozzle pressure loss is defined as follows:

The Bernoulli equation, Reference 16, for the inlet piping, outlet piping, and gage tubing is used to introduce measured data.

<sup>3</sup> For small density variations,  $\rho_{ave} = (\rho_{i,pipe} + \rho_{o,pipe})/2$ . For larger variations where nonlinear variations in density could cause appreciable error, the average density should be determined based on pre-test agreement.

**Inlet Piping**

$$\frac{P_i}{\rho_{i,pipe}} + \frac{g}{g_c} z_i + v_i^2/2g_c = \frac{P_{n,i}}{\rho_{i,pipe}} \quad (E.23)$$

$$+ \frac{g}{g_c} z_{n,i} + v_{n,i}^2/2g_c + K_{i,pipe} v_i^2/2g_c$$

**Outlet Piping**

$$\frac{P_{n,o}}{\rho_{o,pipe}} + \frac{g}{g_c} z_{n,o} + v_{n,o}^2/2g_c = \frac{P_o}{\rho_{o,pipe}} \quad (E.24)$$

$$+ \frac{g}{g_c} z_o + v_o^2/2g_c + K_{o,pipe} v_o^2/2g_c$$

**Differential Pressure Gage Piping**

$$\frac{P_i}{\rho_{gage}} + \frac{g}{g_c} z_i = \frac{P_o}{\rho_{gage}} + \frac{g}{g_c} z_o + \frac{\Delta P}{\rho_{gage}} \quad (E.25)$$

**Upstream Pressure Gage Piping**

$$\frac{P_i}{\rho_{gage}} + \frac{g}{g_c} z_i = \frac{P_u}{\rho_{gage}} + \frac{g}{g_c} z_u \quad (E.26)$$

Using Eqs. (E.23) and (E.24) to eliminate nozzle pressures, elevations and velocities in Eq. (E.22):

$$\Delta P_{n-n} = \rho_{ave} \left[ \frac{P_i}{\rho_{i,pipe}} - \frac{P_o}{\rho_{o,pipe}} + \frac{g}{g_c} (z_i - z_o) \right. \quad (E.27)$$

$$\left. + (1 - K_{i,pipe}) v_i^2/2g_c - (1 + K_{o,pipe}) v_o^2/2g_c \right]$$

The inlet and outlet pipe velocities are related using conservation of mass:

$$\rho_{i,pipe} A_{i,pipe} v_i = \rho_{o,pipe} A_{o,pipe} v_o$$

$$v_o = \frac{\rho_{i,pipe} A_{i,pipe}}{\rho_{o,pipe} A_{o,pipe}} v_i$$

Substituting into Eq. (E.27)

$$\Delta P_{n-n} = \rho_{ave} \left[ \frac{P_i}{\rho_{i,pipe}} - \frac{P_o}{\rho_{o,pipe}} + \frac{g}{g_c} (z_i - z_o) + \right. \quad (E.28)$$

$$\left. \left( 1 - K_{i,pipe} - (1 + K_{o,pipe}) \left( \frac{\rho_{i,pipe} A_{i,pipe}}{\rho_{o,pipe} A_{o,pipe}} \right)^2 \right) v_i^2/2g_c \right]$$

Rearranging Eq. (E.25) to solve for  $P_o$ :

$$P_o = P_i - \Delta P + \rho_{gage} \frac{g}{g_c} (z_i - z_o)$$

Substituting into Eq. (E.28):

$$\Delta P_{n-n} = \rho_{ave} \left[ \frac{\Delta P}{\rho_{o,pipe}} + \left( \frac{1}{\rho_{i,pipe}} - \frac{1}{\rho_{o,pipe}} \right) P_i \right. \quad (E.29)$$

$$\left. + \left( 1 - \frac{\rho_{gage}}{\rho_{o,pipe}} \right) \frac{g}{g_c} (z_i - z_o) + \left( 1 - K_{i,pipe} - (1 + K_{o,pipe}) \left( \frac{\rho_{i,pipe} A_{i,pipe}}{\rho_{o,pipe} A_{o,pipe}} \right)^2 \right) v_i^2/2g_c \right]$$

Substituting for  $P_i$  using Eq. (E.26):

$$\Delta P_{n-n} = \rho_{ave} \left[ \frac{\Delta P}{\rho_{o,pipe}} + \left( \frac{1}{\rho_{i,pipe}} - \frac{1}{\rho_{o,pipe}} \right) \right. \quad (E.30)$$

$$\left. \left( P_u + \rho_{gage} \frac{g}{g_c} (z_u - z_i) \right) + \left( 1 - \frac{\rho_{gage}}{\rho_o} \right) \frac{g}{g_c} (z_i - z_o) + \left( 1 - K_{i,pipe} - (1 + K_{o,pipe}) \left( \frac{\rho_{i,pipe} A_{i,pipe}}{\rho_{o,pipe} A_{o,pipe}} \right)^2 \right) v_i^2/2g_c \right]$$

### E.2.2 Pressure Loss at Reference Conditions

The pressure loss at reference conditions is calculated based on a hydraulic model of the heat exchanger and the ratio of calculated pressure losses:

$$\begin{aligned} \Delta P_{n-n}^* &= \frac{(\Delta P_{n-n})_{\text{calculated at reference conditions}}}{(\Delta P_{n-n})_{\text{calculated at test conditions}}} \Delta P_{n-n}^* \quad (\text{E.31}) \\ &= \phi_{\Delta P} \Delta P_{n-n} \end{aligned}$$

The uncertainty analysis is facilitated if the flow measurement is separated from the terms related to

the hydraulic model (including surface roughness and loss coefficients). Introducing the hydraulic resistance:

$$H_R = \frac{(\Delta P_{n-n})_{\text{calculated}}}{m^n} \quad (\text{E.32})$$

The correction factor for pressure loss becomes:

$$\phi_{\Delta P} = \frac{H_R^* m^{*n}}{H_R m^n} \quad (\text{E.33})$$

This page intentionally left blank.

## NONMANDATORY APPENDIX F — TUBE-SIDE PERFORMANCE METHODS

This Appendix provides guidance to determine the tube-side heat transfer coefficient and pressure loss. Alternate methods to estimate heat transfer coefficient and pressure loss are acceptable as agreed by the parties to the test.

### F.1 DETERMINING GEOMETRICAL PARAMETERS

(a) *Tube Inside Diameter.* For circular plain tubes, the inside diameter,  $d_i$ , is calculated using the nominal outside diameter,  $d_o$ , and nominal tube wall thickness,  $\Delta X_w$ :

$$d_i = d_o - 2\Delta X_w \quad (\text{F.1})$$

Differences between the average inside diameter and the nominal inside diameter (as calculated above) are small, and the resulting bias is included in the uncertainties for the heat transfer coefficient and pressure loss. The calculation of inside diameter may be different from Eq. (F.1) for some enhancements on the inside surface (see para. F.1(d)).

(b) *Number of Tubes.* The number is counted or estimated as discussed in Appendix C.

(c) *Length of Tubes.* The total length of the tubes,  $L$ , is needed for pressure loss calculations. The effective length of the tubes between the tubesheets,  $\ell$ , is needed for calculation of heat transfer area.

(d) *Geometry of Enhancements.* A discussion of geometry of enhancements for the inside surfaces of tubes is considered to be beyond the scope of this Appendix. For heat exchanger tests where enhancements inside tubes are used, specific information regarding the determination of tube-side Reynolds numbers and heat transfer coefficient is needed from the manufacturer. A general discussion of tube-side enhancements is provided in References 44–46.

### F.2 DETERMINING HEAT TRANSFER COEFFICIENT

To calculate the heat transfer performance at reference conditions, the difference in convective thermal

resistance from reference conditions to test conditions ( $1/h_t^* - 1/h_t$ ) is calculated. This paragraph describes a method and appropriate correlations to calculate the heat transfer coefficient for test and reference conditions.

(a) *Flow Regime.* The tube-side Reynolds number is calculated based on the bulk average tube-side properties:

$$Re_t = \frac{4m_t}{\pi d_i N_t \mu} \quad (\text{F.2})$$

where

$m_t$  = tube-side mass flow rate

$\mu$  = dynamic viscosity based on the bulk average conditions of the tube-side fluid

$N_t$  = number of tubes in one pass

(b) *Turbulent Flow Heat Transfer.* For Reynolds numbers in the transition and turbulent regime, forced turbulent convection correlations are used. The three following correlations are based on extensive experimental data and are considered acceptable for use. An overall uncertainty of  $\pm 10\%$  in average tube-side heat transfer coefficient is considered reasonable based on uncertainty of the experimental data and distribution of flow in the tube bundle. For tests where the Reynolds number at test or reference conditions is less than 10,000, the effects of mixed convection should be checked and additional uncertainty may be needed.

(1) From Petukhov, Reference 12,

$$Nu_t = \frac{(f/2) Re_t Pr_t}{1.07 + 12.7(f/2)^{1/2} (Pr_t^{2/3} - 1)} \phi_{\text{prop}} \quad (\text{F.3})$$

where

$Nu_t$  = tube-side Nusselt number =  $(hd_i/k)_t$

$Pr_t$  = tube-side Prandtl number =  $(\mu c/k)_t$

$\frac{1}{\sqrt{f}} = 1.58 \ln Re_t - 3.28$ , see note below

$\phi_{prop} = 1$  for constant properties  
 $= (\mu_b/\mu_w)^n$  for liquids with  $n = 0.11$  when heating the liquid and  $n = 0.25$  when cooling the liquid  
 $= (T_w/T_b)^n$  for gases with  $n = -[a \log(T_w/T_b) + 0.36]$  and  $a = 0.0$  for cooling  
 $= (t_w/t_b)^n$  for gases with  $n = -[a \log(t_w/t_b) + 0.36]$  and  $a = 0.3$  for heating  
 (a)  $10,000 < Re_t < 5,000,000$  with  $Re_t$  evaluated at average bulk conditions  
 (b)  $0.5 < Pr_t < 2000$  with  $Pr_t$  evaluated at average bulk conditions  
 (c) tubes are long and entry effects can be neglected,  $L/d_i > 50$

NOTE: The term  $f$  is the Fanning friction factor defined by Eq. (F.8). The friction factor used by Petukhov is  $\xi = 4f$ . To calculate  $\xi$ , Petukhov uses an expression developed by Filonenko, Reference 47, for isothermal flow in smooth tubes and the equivalent expression using  $f$  is shown here.

Petukhov's evaluation with experimental data indicates that this correlation is within 5–6% of the most accurate experimental data over a range of 10,000 to 5,000,000 for  $Re_t$  and 0.5–200 for  $Pr_t$  and a 10% accuracy for  $0.5 < Pr_t < 2000$  and the same range of  $Re_t$ .

(2) Gnielinski, Reference 48, modified Petukhov's correlation to represent experimental values at lower Reynolds numbers and added a correction to account for short tube lengths:

$$Nu_t = \frac{(f/2)(Re_t - 1000)Pr_t}{1 + 12.7(f/2)^{1/2}(Pr_t^{2/3} - 1)} [1 + (d_i/L)^{2/3}] \phi_{prop} \quad (F.4)$$

where

$$\frac{1}{\sqrt{f}} = 1.58 \ln Re_t - 3.28, \text{ see note below}$$

$\phi_{prop} = 1$  for constant properties  
 $= (Pr_b/Pr_w)^{0.11}$  for liquids with  $0.05 < Pr_b/Pr_w < 20$   
 $= (T_b/T_w)^{0.45}$  for gases with  $0.5 < T_b/T_w < 1.5$   
 (a)  $2300 < Re_t < 5,000,000$  with  $Re_t$  evaluated at average bulk conditions  
 (b)  $0.5 < Pr_t < 2000$  with  $Pr_t$  evaluated at average bulk conditions

NOTE: The term  $f$  is the Fanning friction factor defined by Eq. (F.8). The expression for  $f$  is the same as used with the Petukhov correlation.

Gnielinski's evaluation indicates that 90% of the experimental data differ by less than  $\pm 20\%$  from the calculated values using this correlation.

(3) The following classical correlation is based on a method developed by Colburn, Reference 49,

using the film properties (average of wall and bulk conditions). Sieder and Tate, Reference 31, modified the Colburn correlation to make it easier to use by using bulk fluid conditions and the viscosity correction  $(\mu_b/\mu_w)^{0.14}$  to account for variable properties. The correlation is still in wide use.

$$Nu_t = 0.023 Re_t^{0.8} Pr_t^{1/3} (\mu_b/\mu_w)^{0.14} \quad (F.5)$$

where

- (a)  $10,000 < Re_t < 100,000$  using average bulk conditions  
 (b)  $0.5 < Pr_t < 250$  using average bulk conditions  
 (c)  $L/d_i > 60$   
 (d)  $0.01 < \mu_b/\mu_w < 10$

(c) *Mixed Convection Heat Transfer.* At Reynolds numbers less than 10,000, effects of gravitational body forces may be significant and mixed convection heat transfer may dominate. The flow regime for mixed convection is determined by comparing the Reynolds number with the parameter  $GrPr(d/L)$ . Metz and Eckert, Reference 50, developed figures of flow regime limits for horizontal and vertical tubes. The figures were originally provided for preliminary information but are used extensively today. Some modifications in these flow regime figures have been proposed based on more recent data, Reference 51. General correlations based on a wide body of experimental data are not available for all flow regimes. Over selected flow regimes, the following correlations are widely used and are based on substantial amount of experimental data.

(1) *Horizontal Tubes.* For liquid flow in horizontal tubes with high Prandtl number, Palen and Taborek, Reference 52, developed the following:

$$Nu_t = 2.5 + 4.55(Re^{**})^{0.37}(d/L)^{0.37} Pr_t^{0.17} (\mu_b/\mu_w)^{0.14} \quad (F.6)$$

where

$$Re^{**} = Re_t + 0.8 Gr^{0.5} \exp[-42/Gr^2]$$

$$Gr = \frac{\beta |t_w - t_b| d_i^3 \rho_t^2 g}{\mu_t^2} = \text{Grashof number}$$

$\beta$  = the volumetric coefficient of thermal expansion

- (a)  $0.1 < Re_t < 2000$  using bulk average properties  
 (b)  $20 < Pr_t < 10,000$  using bulk average properties  
 (c)  $0 < Gr < 30,000,000$  using bulk average properties  
 (d)  $0 < \mu_b/\mu_w < 55$   
 (e)  $L/d_i > 40$

For liquids with lower Prandtl numbers, a correlation by Depew and August, Reference 53, based on experimental data using water, ethyl alcohol, glycerol/water mixture, and oil can be used:

$$Nu_t = 1.75[Gz + 0.12 (GzGr^{1/3}Pr_t^{0.36})^{0.88}]^{1/3}(\mu_b/\mu_w)^{0.14} \quad (F.7)$$

where

$$Gz = \frac{m_t c_p}{kL} = \text{Graetz Number}$$

- (a)  $10 < Gz < 440$
- (b)  $2700 < Gr < 4,900,000$
- (c)  $5 < Pr_t < 1900$
- (d)  $L/d_i > 28$

In general, the uncertainty in the average heat transfer coefficient in the mixed convection regime is greater than in the turbulent and transition regimes depending on the validity of the experimental data (i.e., similarity of the Reynolds number, Prandtl number, and Grashof number with conditions inside the heat exchanger). Within the range of applicability of the correlations, an uncertainty of 10 to 40% is reasonable.

(2) *Vertical Tubes.* For vertical tubes the heat transfer coefficient is a function of the direction of fluid flow. A general discussion of mixed convection heat transfer is beyond the scope of this Appendix. Discussions, some correlations and comparisons with experimental data for a few instances are provided in References 54–57.

### F.3 DETERMINING PRESSURE LOSS

To calculate the nozzle-to-nozzle pressure loss at reference conditions, the pressure loss at test conditions is multiplied by the correction factor,  $\phi_{\Delta P} = \Delta P_{n-n}^*/\Delta P_{n-n}$ . This paragraph describes a method to calculate the pressure loss correction.

(a) *Flow Regime.* The flow regime is based on the tube-side Reynolds number as calculated in Eq. (F.2).

(b) *Friction Factor and Roughness Regime.* For this Appendix, the Fanning friction factor,  $f$ , is used as defined in accordance with the following formula:

$$\frac{f}{2} = \frac{\Delta P g_c d_i}{\rho v_t^2 4L} \quad (F.8)$$

where

$\Delta P$  = pressure loss along tube length  $L$

$\rho$  = fluid density

$g_c$  = units conversion constant

$v_t$  = bulk fluid velocity in tube

$d_i$  = inside tube diameter

$L$  = tube length

The Fanning friction factor is commonly used for heat exchanger performance and is different than the Darcy friction factor which is commonly used for pipe flow, Reference 16. The Darcy friction factor is 4 times the Fanning friction factor, i.e.,  $4f_{\text{Fanning}} = f_{\text{Darcy}}$ .

(1) *Friction Factor for Laminar Flow.* For Reynolds numbers less than 2000, the flow is considered laminar and the friction factor is independent of pipe roughness:

$$f = \frac{16}{Re_t} \quad (F.9)$$

where  $Re_t < 2000$ .

(2) *Friction Factor for Turbulent Flow.* For Reynolds numbers greater than 4000, the friction factor is a function of the Reynolds number and the roughness. The correlation of friction factor with roughness and Reynolds number is attributed to work performed by Colebrook and White, Reference 58, using commercial pipe. Based on this work, turbulent flow in rough pipe is divided into smooth, fully rough and transition roughness regimes. The roughness regime is determined by the roughness Reynolds number,  $Re_\epsilon$ .

$$Re_\epsilon = \frac{\rho v_t \epsilon}{\mu} = \sqrt{\frac{f}{2}} \frac{\epsilon}{d_i} Re_t \quad (F.10)$$

where

$$v_\tau = \sqrt{\frac{\tau}{\rho}} = \text{shear force velocity}$$

$\tau$  = the shear stress at the wall

$\epsilon/d_i$  = the relative roughness of the inside surface of the tube

(a)  $Re_\epsilon < 0.5$  for flow in smooth pipe;

(b)  $Re_\epsilon > 60$  for flow in fully rough pipe;

(c)  $0.5 < Re_\epsilon < 60$  for flow in transition region between smooth and full rough pipe.

For smooth pipe ( $Re_\epsilon < 0.5$ ),

$$\frac{1}{\sqrt{f}} = 4 \log_{10} \frac{Re_t \sqrt{f}}{1.255} \quad (\text{F.11})$$

For fully rough pipe ( $Re_\epsilon > 60$ ),

$$\frac{1}{\sqrt{f}} = 4 \log_{10} \left( 3.7 \frac{d_i}{\epsilon} \right) \quad (\text{F.12})$$

For the transition region ( $0.5 < Re_\epsilon < 60$ ),

$$\frac{1}{\sqrt{f}} = -4 \log_{10} \left( \frac{\epsilon}{3.7 d_i} + \frac{1.255}{Re_t \sqrt{f}} \right) \quad (\text{F.13})$$

The Colebrook and White correlation, Eq. (F.13), is difficult to use since the friction factor is included on both sides of the equation. As a result, friction factor data are traditionally plotted on a diagram developed by Moody, Reference 59, which is in wide use today.

The roughness of clean commercial tubing is reported in the industry literature such as Reference 16; however, estimating the roughness of inservice tubing results in some uncertainty. The bounds of estimated roughness should be considered when calculating the uncertainty of the adjustment in pressure loss,  $\phi_{\Delta P}$ .

(c) *Tube-Side Pressure Loss and Correction Factor.* The total nozzle-to-nozzle pressure loss for the tube-side of a heat exchanger is given by the following:

$$\Delta P_t = \Delta P_{\text{entry}} + 4f\rho \frac{L}{d_i} \frac{v_t^2}{2g_c} + \Delta P_{\text{exit}} \quad (\text{F.14})$$

where

$\Delta P_t$  = tube-side pressure loss from inlet nozzle to outlet nozzle

$\Delta P_{\text{entry}}$  = entrance pressure loss associated with channel head and tube entry

$\Delta P_{\text{exit}}$  = exit pressure loss associated with channel head and tube exit

(1) Methods to determine each of the terms in Eq. (F.14) are provided in Reference 60. For many heat exchangers, the pressure loss is dominated by the losses in the tubes and many of the other terms can be neglected. The pressure loss correction is given by:

$$\phi_{\Delta P} = \left( \frac{\Delta P_{n-n}^*}{\Delta P_{n-n}^{\text{calculated}}} \right) \quad (\text{F.15})$$

$$= \frac{\left[ \Delta P_{\text{entry}} + 4f\rho \frac{L}{d_i} \frac{v_t^2}{2g_c} + \Delta P_{\text{exit}} \right]^*}{\Delta P_{\text{entry}} + 4f\rho \frac{L}{d_i} \frac{v_t^2}{2g_c} + \Delta P_{\text{exit}}}$$

(2)  $\phi_{\Delta P}$  is a strong function of the assumptions used for friction factor and loss coefficients used for  $\Delta P_{\text{entry}}$  and  $\Delta P_{\text{exit}}$ . To estimate the uncertainty in  $\phi_{\Delta P}$ , upper and lower bound corrections should be calculated.

## NONMANDATORY APPENDIX G — FOULING RESISTANCE

The most accurate assessment of heat exchanger performance is measured with new or clean conditions. Under these conditions, the fouling resistance is small and may be neglected. For industrial heat exchangers, it is difficult and often not practical to verify the fouling condition on the hot and cold stream sides of the heat transfer surface. Furthermore, testing has shown that visual inspection of heat exchanger surfaces does not always provide an accurate assessment of fouling resistance. As a result, some fouling is expected for most heat exchanger tests.

The calculation of average fouling resistance as the performance parameter is not recommended. This conclusion is based on the assessment of uncertainty of fouling resistance using the following.

- (a) measured temperatures and flow rates and;
- (b) estimated convective thermal resistances and wall resistances.

Assumptions regarding the fouling resistance are required to calculate overall heat transfer coefficient and heat transfer rate at reference conditions. This Appendix discusses the characteristics of fouling resistance so that the test engineer may better assess the overall uncertainty due to the assumptions regarding fouling resistance.

### G.1 MEASUREMENT OF FOULING RESISTANCE

The total heat transfer resistance,  $r_{\text{total}}$  is given by Eq. (G.1).

$$r_{\text{total}} = \frac{A \text{ EMTD}}{Q} \quad (\text{G.1})$$

$Q$  and EMTD are determined based on measured temperatures and flow rates of the hot and cold fluid streams. If it is possible to test the heat exchanger under clean conditions,  $r_{\text{total}} = r_{\text{clean}} = 1/U_{\text{clean}}$ . The fouling resistance,  $r_f$  is determined by Eq. (G.2).

$$r_f = r_{\text{total}} - r_{\text{clean}} \quad (\text{G.2})$$

Experience indicates that the uncertainty of the fouling resistance calculated in accordance with Eq. (G.2) may be large relative to the uncertainty of other performance parameters such as  $U$  and  $Q$ . The uncertainty of the fouling resistance can be assessed by introducing the fouling Biot number,  $Bi_f = r_f U_{\text{clean}}$ , Reference 61. The fouling Biot number is a measure of the relative magnitude of fouling on a heat transfer surface. Fouling Biot numbers for typical gas-gas, liquid-gas, and water-water heat exchangers are shown in Table G.1.

Investigations by Somerscales et al., Reference 62, have shown that the uncertainty of the fouling resistance is inversely proportional to the fouling Biot number. A summary of their results is shown in Figs. G.1 and G.2 for a counterflow heat exchanger where the uncertainty in heat transfer coefficient is neglected (the test conditions at clean conditions are very similar to fouled conditions so that the convective heat transfer coefficients are the same for both conditions). Even with measurements having uncertainties in the ranges specified in Section 4, the uncertainty in fouling resistance may be 20–50% or even larger for many industrial applications. For example, for test data where  $r_{\text{total}}$  is almost equal to  $r_{\text{clean}}$  (i.e., almost clean conditions), the uncertainty in the calculated fouling resistance is high because the fouling Biot number is very low as shown in Fig. G.2. For instances where  $r_{\text{clean}}$  is not known, the uncertainty in fouling resistance may be high since the uncertainty in the individual heat transfer coefficients is high.

Since the uncertainty in measured fouling resistance can be large relative to the uncertainty of other observed performance parameters for many industrial tests, measurement of fouling resistance is not recommended.

### G.2 FOULING RESISTANCE ASSUMPTIONS

#### G.2.1 Variation in Fouling Resistance Over Heat Transfer Area

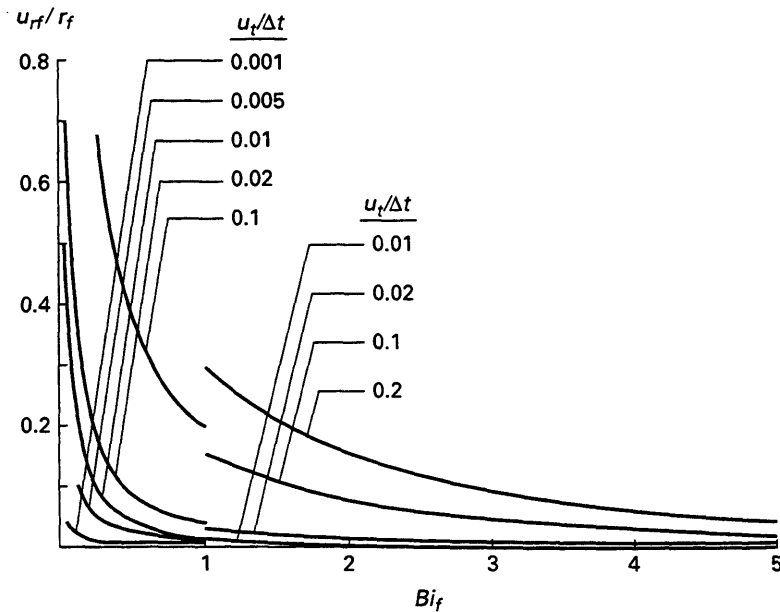
Non-uniform distribution of fouling is expected for industrial heat exchangers since the flow is often

**TABLE G.1**  
**TYPICAL VALUES OF THE FOULING BIOT NUMBER [Note (1)]**

Heat Exchanger Type	$U_{clean}$ (Btu/hr-ft <sup>2</sup> -°F)	$r_f$ (hr-ft <sup>2</sup> -°F/Btu)	$Bi_f$
Gas-gas	10	0.003	0.03
Liquid-gas	30	0.003	0.09
Water-water	450	0.003	1.35

## NOTE:

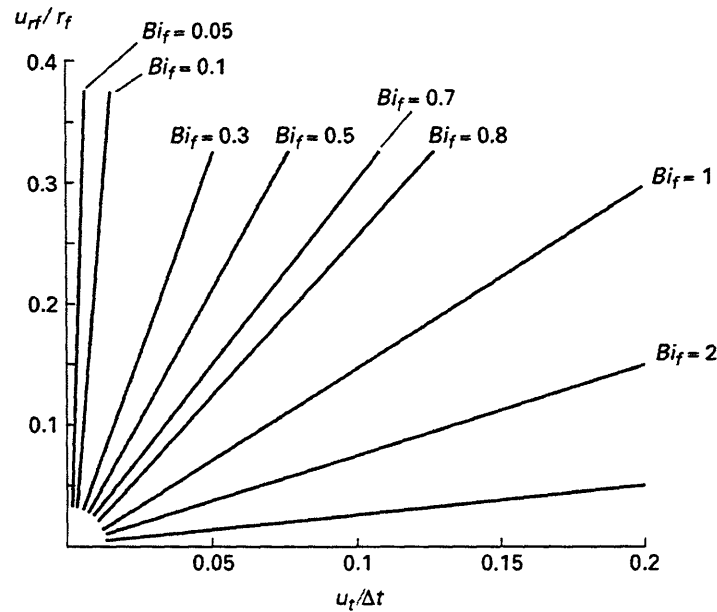
- (1) The fouling Biot numbers shown are typical for plain unfinned surfaces inside and outside of tubes. For finned surfaces, these may represent low fouling conditions.



GENERAL NOTE: The dependence of the relative uncertainty ( $u_{rf}/r_f$ ) of the measured fouling thermal resistance on the fouling Biot number ( $Bi_f$ ) and the relative uncertainty ( $u_t/\Delta t$ ) of the temperature measurements. The following expressions are used in constructing this figure:  $u_{rf}/r_f = (K/Bi_f)(u_t/\Delta t)$  where  $K = 2$  for  $Bi_f \leq 1$  (sensible heat exchanger) and  $K = \sqrt{2}$  for  $Bi_f \geq 1$  (condenser).

$u_{rf}$  = uncertainty in fouling resistance  
 $r_f$  = unit fouling resistance  
 $u_t$  = uncertainty in temperature measurement  
 $\Delta t$  = rise in cold stream temperature  
 $Bi_f$  = fouling Biot number

**FIG. G.1. UNCERTAINTY IN FOULING RESISTANCE AS A FUNCTION OF FOULING BIOT NUMBER (from reference 62)**  
 (Reprinted with the permission of Euan F.C. Somerscales)



GENERAL NOTE: The dependence of the relative uncertainty ( $u_{rf}/r_f$ ) of the measured fouling thermal resistance on the fouling Biot number ( $Bi_f$ ) and the relative uncertainty ( $u_t/\Delta t$ ) of the temperature measurements. The following expressions are used in constructing this figure:  $u_{rf}/r_f = (K/Bi_f)(u_t/\Delta t)$  where  $K = 2$  for  $Bi_f \leq 1$  (sensible heat exchanger) and  $K = \sqrt{2}$  for  $Bi_f \geq 1$  (condenser).

**FIG. G.2 UNCERTAINTY IN FOULING RESISTANCE AS A FUNCTION OF UNCERTAINTY IN TEMPERATURE MEASUREMENTS (from reference 62)**  
(Reprinted with the permission of Euan F.C. Somerscales)

maldistributed and operating conditions over the heat transfer surface vary. The effect of non-uniform fouling buildup is difficult to predict without detailed information of the distribution of the fouling products and flow distribution in the heat exchanger. Fouling buildup not only restricts heat transfer capability but also may change the flow distribution and average heat transfer coefficient. For example:

(a) buildup of fouling product which blocks bypass flow paths may increase the average heat transfer coefficient for shell-side fluid streams;

(b) buildup of fouling product in the low velocity regions of the heat exchanger may have minimal effect on  $U$ , and;

(c) preferential buildup of fouling product in between fins may substantially reduce  $U$ .

These examples indicate that fouling buildup may or may not provide a substantial change in the average heat transfer coefficient over different operating conditions.

It is assumed that the average fouling resistance at test conditions is the same as the average fouling

resistance at reference conditions. If the fouling resistance is uniform over the heat transfer surface, this assumption is considered reasonable. However, variations in the distribution of the fouling resistance may change the heat transfer coefficient (by changing the flow distribution), and the weighting of the variations in fouling resistance may change for different operating conditions resulting in a change in fouling resistance.

Data available are insufficient to distinguish between effects of variable fouling resistance, measurement uncertainties, and uncertainty of the heat transfer model for the heat exchanger. This is primarily due to the difficulty in making accurate performance measurements over a wide range of flow rates and temperatures, and to the large uncertainty in the application of heat transfer correlations based on experimental data to inservice industrial heat exchangers. As a result, judgment is needed to estimate the effect of variable fouling resistance as discussed in para. G.3.

### G.2.2 Time Variation in Average Fouling Resistance

The thermal performance determined with a test is applicable at the time the test is performed. Trending fouling resistance with time is not within the scope of this Code.

### G.3 UNCERTAINTY IN FOULING RESISTANCE ASSUMPTIONS

Based on the available data, judgment is needed to estimate the effects of spatially variable fouling resistance on the results of the performance test. The following guidelines are intended to assist the test engineer in evaluation of uncertainty in the assumption that the fouling resistance is the same at test conditions as at reference conditions.

(a) *Low Fouling Resistance.* The fouling resistance is considered low if the fouling Biot number is less than 1. Under these conditions, uncertainty in the calculation of heat transfer coefficient will probably be substantially greater than the change in average fouling resistance. In this case, the uncertainty in the assumption that the average fouling resistance is the same at test and reference conditions can be neglected. However, the uncertainty in heat transfer co-

efficient may need to be increased if the fouling buildup affects flow distribution.

(b) *High Fouling Resistance, Test Conditions Near Reference Conditions.* The fouling resistance is considered high if the fouling Biot number is greater than 1. Test conditions are near reference conditions if the uncertainty of the results is dominated by measurement uncertainty (such as temperature and flow rate uncertainties which contribute to the uncertainty in heat transfer rate). In this case, the uncertainty in the assumption that the average fouling resistance is the same at test and reference conditions can be neglected. However, the uncertainty in heat transfer coefficient may need to be increased if the fouling buildup affects flow distribution.

(c) *High Fouling Resistance, Test Conditions Substantially Different Than Reference Conditions.* The fouling resistance is considered high if the fouling Biot number is greater than 1. Test conditions are substantially different than reference conditions if the uncertainty of the results is dominated by the uncertainty in heat transfer coefficient. In this case, the change in average fouling resistance may significantly affect the accuracy of the test. The test conditions should be changed to reduce the contribution of the uncertainty in heat transfer coefficient. Alternatively, calculations of a heat exchanger model can be used to estimate the uncertainty attributed to the change in average fouling resistance.

## NONMANDATORY APPENDIX H — PLATE FRAME PERFORMANCE METHODS

There is no generalized open literature method to calculate the individual heat transfer coefficients for plate frame surfaces. Without data for the particular plate design, estimating the coefficients based on open literature is not recommended. Suitable correlations may be developed using manufacturer data or plant data. This Appendix describes a method to determine a suitable correlation for a plate frame heat exchanger (PHE) based on plant test data.

An algorithm to predict the performance of a PHE may be developed by testing the PHE in the clean condition. Starting with Eq. (H.1).

$$U = \frac{Q}{A(\text{LMTD})F} \quad (\text{H.1})$$

In general, flow through adjacent passages in a PHE is countercurrent (without a cross flow component as with shell-and-tube arrangements). As a result,  $F = 1$  for many PHE applications. However, end effects reduce the mean temperature difference and  $F$  may be less than one for some arrangements, Reference 63.  $F$  may be less than one for designs where very few plates and/or where multiple passes are provided. For the analysis in this Code, it is assumed that  $F = 1$ . The value of  $Q$  and LMTD may be calculated from test results as described in Section 5, and the value of  $A$  may be determined either from vendor data or by measuring the dimensions of a plate. Therefore, the value of  $U$  may be determined and set equal to Eq. (H.2).

$$U = 1/(1/h_h + 1/h_c + r_w + r_{fh} + r_{fc}) \quad (\text{H.2})$$

where

$r_w$  = thermal resistance of wall based on heat transfer per unit area =  $\Delta X/k_w$

$r_{fh}$  = heat transfer resistance due to fouling on the hot side of the plate based on heat transfer per unit area

$r_{fc}$  = heat transfer resistance due to fouling on the cold side of the plate based on heat transfer per unit area

For a given plate of known material and thickness, the value for  $r_w$  is known. If the PHE is clean when tested,  $r_{fh}$  and  $r_{fc}$  are both zero. Therefore, the problem is reduced to finding an expression for  $h_h$  and  $h_c$  which is correlated to the Nusselt number,  $Nu$ , by the following expression:

$$h = Nu(k/D_e) \quad (\text{H.3})$$

where

$D_e$  = equivalent hydraulic diameter

The problem is thus reduced to finding a relationship for  $Nu$  as a function of  $Re$  where:

$$Re = D_e G / \mu \quad (\text{H.4})$$

where

$G$  = mass velocity =  $\rho V$

The Colburn Analogy,

$$Nu = C Re^n Pr^m (\mu_b / \mu_w)^{0.14} \quad (\text{H.5})$$

is applicable where  $C$ ,  $n$ , and  $m$  are constants and

$\mu_b$  = bulk average dynamic viscosity

$\mu_w$  = dynamic viscosity at the plate wall

The last term can be neglected for applications where variation in fluid properties is small. Note that for PHEs the geometry of the plate is the same on both sides of the plate, so the same equation for  $Nu$  applies to both sides. For turbulent heat transfer through a flat plate, the Nusselt number is directly proportional to the Reynolds number to the 0.75 power, and to the Prandtl number to the 0.333 power for gases, liquids, and viscous oils where  $Pr > 1$  (Reference 64). Therefore:

$$h_h = C Re_h^{3/4} Pr_h^{1/3} \left( \frac{k_h}{D_e} \right) \left( \frac{\mu_b}{\mu_w} \right)^{0.14} \quad (\text{H.6})$$

$$h_c = C Re_c^{3/4} Pr_c^{1/3} \left( \frac{k_c}{D_e} \right) \left( \frac{\mu_b}{\mu_w} \right)^{0.14} \quad (\text{H.7})$$

$C$  may be determined by conducting a test with the PHE clean so that

$$r_{fh} = r_{fc} = 0 \quad (\text{H.8})$$

by setting the Eqs. (H.1) and (H.2) equal to each other.

$$U = \frac{Q}{A(\text{LMTD}) F} = 1/(1/h_h + 1/h_c + r_w) \quad (\text{H.9})$$

the value for  $C$  may be computed by substituting for  $h_h$  and  $h_c$  and solving for  $C$  as indicated in Eq. (H.10).

$$C = \frac{\frac{D_e}{Re_h^{3/4} Pr_h^{1/3} \left( \frac{\mu_b}{\mu_w} \right)^{0.14} k_h} + \frac{D_e}{Re_c^{3/4} Pr_c^{1/3} \left( \frac{\mu_b}{\mu_w} \right)^{0.14} k_c}}{\frac{A(\text{LMTD})}{Q} - r_w} \quad (\text{H.10})$$

Alternately,  $C$  may be determined from manufacturer's data. By trial and error, the value of  $C$  may be found that provides the best agreement with vendor predictions of  $U$  for an array of two or more Reynolds numbers (Reference 65).

# NONMANDATORY APPENDIX I — THERMAL PHYSICAL PROPERTIES

Accurate information of thermal physical properties of fluids and of the wall, which separates the hot and cold streams, is needed for a test. This Appendix provides guidance in determining property values and estimating their uncertainties.

## I.1 FLUID PROPERTIES REQUIRED FOR A TEST

The following fluid properties for the hot and cold fluid streams are needed for a test:

Fluid Property	Test Parameter Calculated
density, $\rho$	mass flow rate of the hot and cold streams at test conditions, $m_c$ and $m_h$ heat transfer coefficient of the hot and cold streams at test and reference conditions, $h_h$ , $h_c$ , $h_h^*$ , and $h_c^*$ pressure loss of the hot and cold streams at test and reference conditions, $\Delta P_{n-n}$ , $\Delta P_{n-n}^*$
specific heat, $c_p$	heat transfer rate of the hot and cold streams at test conditions, $Q_h$ and $Q_c$ . heat transfer coefficient of the hot and cold streams at test and reference conditions, $h_h$ , $h_c$ , $h_h^*$ , and $h_c^*$
absolute viscosity, $\mu$	heat transfer coefficient of the hot and cold streams at test and reference conditions, $h_h$ , $h_c$ , $h_h^*$ , and $h_c^*$ pressure loss of the hot and cold streams at test and reference conditions, $\Delta P_{n-n}$ , $\Delta P_{n-n}^*$
thermal conductivity, $k$	heat transfer coefficient of the hot and cold streams at test and reference conditions, $h_h$ , $h_c$ , $h_h^*$ , and $h_c^*$

## I.2 OPEN LITERATURE SOURCES OF FLUID PROPERTY DATA

As discussed in Section 3, the parties to the test shall agree to the method of determining fluid properties. The following sources of open literature data are provided for Reference:

Data Source	Fluids
ASME Steam Tables, Reference 66 TEMA Standards, Section 8, Reference 28	water, steam  liquid petroleum fractions, organic liquids, petroleum vapors, hydrocarbon gases and other miscellaneous liquids and gases
Chapter 5 of HEDH by M. Schunck, R.N. Maddox, Z.P. Shulman, Reference 26	pure liquids, gases and mixtures (including organics, oils, halogens)
reid, R.C., Prausnitz, J.M., and Poling, B.E., Reference 67	pure liquids, gases and mixtures including an extensive bibliography
Handbook of Physical Properties of Liquids and Gases, Reference 68	pure compounds (including organic compounds and halogens), binary gas mixtures, liquid fuel and oils
ASHRAE Handbook of Fundamentals, Reference 69	air, halogens

The uncertainty of specific heat for the hot and cold streams shall be considered. Using the ASME Steam Tables, an uncertainty in the specific heat of  $\pm 1\%$  is considered reasonable and bounding for water. For other liquids, an uncertainty in the specific heat of  $\pm 5\%$  is considered reasonable for most instances based on the discussion in Reid, Prausnitz, and Poling. For steam and dry air, an uncertainty of  $\pm 1\%$  is considered bounding for operating conditions not near the critical point. For other gases, an uncertainty of  $\pm 2\%$  is considered appropriate based on the discussion in Reid, Prausnitz and Poling. In general, larger uncertainties should be considered when fluids are operating near the critical point since the accuracy of the standard correlation methods is reduced.

The uncertainty of fluid density, viscosity, specific heat and thermal conductivity should be considered in determination of heat transfer coefficients. In general, the uncertainty limits for heat transfer coefficients in Section 6 include the effects of uncertain properties for many engineering applications. Judgment is needed to apply the appropriate uncertainty for a particular test.

### I.3 FLUID SAMPLING PROCEDURES

For fluids whose properties are known to change significantly within in a heat exchanger or for fluids whose properties are not known with sufficient confidence, sampling and analysis should be performed. Sampling should be performed when the uncertainty attributed to generalized correlations of fluid property data dominates the overall uncertainty of the performance analysis.

The objective of gas and liquid sampling is to obtain a small volume of fluid which has the same properties as the bulk fluid in the process stream. Considerable planning and effort are needed to obtain and analyze fluid samples, which are representative of the bulk fluid stream without leakage to the environ-

ment. A description of factors, which need to be considered, is beyond the scope of this Code and is included in References 70–73. The pretest uncertainty analysis may be used to determine the need and precision of any fluid sample analysis for a Code test.

### I.4 THERMAL RESISTANCE OF WALL

Thermal conductivity of the wall, which separates the hot and cold streams, may vary with temperature. This variation may result in a significant change in the thermal resistance of the wall between test and reference conditions. The thermal conductivity as a function of temperature for metals commonly used in heat exchangers is provided in TEMA Standards, Reference 28.

# NONMANDATORY APPENDIX J — ROOM COOLER PERFORMANCE METHODS

## J.1 INTRODUCTION

Room coolers are tube-in-plate fin heat exchangers that remove equipment and lighting loads from open spaces and transfer the heat to other heat exchange systems or cooling systems. The tubes can be in-line or staggered, and the fins can be flat, corrugated, or discontinuous. Room coolers are often referred to as chilled or heated water coils, and air-side performance data is often proprietary. The test methods described in this Appendix are based on sensible heat transfer with minimal condensation.

## J.2 PREPARATION AND TESTING

Field testing of room coolers requires special attention to ensure accurate results. Recommended test practices are discussed in this Appendix. Required measurements include:

- (a) Inlet water temperature
- (b) Outlet water temperature
- (c) Water flow rate
- (d) Inlet air dry-bulb temperature
- (e) Outlet air relative humidity or wet-bulb temperature
- (f) Inlet air barometric pressure
- (g) Outlet air dry-bulb temperature
- (h) Air flow rate (actual or converted to standard conditions)

### J.2.1 Water Measurements

Room coolers often have modular coil arrangements, where additional capacity has been gained by adding coils in parallel with each other. Inlet and outlet liquid enters or discharges from tubes to a block header, which then splits or joins into the common feed line. Although temperatures to individual coils can be measured separately, water flows typically cannot. Water temperatures and flows should be measured on inlet headers upstream and downstream of the heat exchanger.

Water measurements are performed with the methods discussed in Section 4.

### J.2.2 Air Measurements

Inlet and outlet air-to-room coolers may be ducted or unducted. The inlet face is often unducted, and the entering air is unconditioned. The coils may be constructed into one face or as adjacent faces (similar to sides of a box). Inlet air flows are usually measured with propeller or vane anemometers. Inlet temperatures are measured with low profile RTDs, thermistors, thermocouples, or other temperature devices. As with water conditions, air temperatures and flows should be measured to represent the entire cooler and not individual coils.

Air-side measurements are usually taken using an instrument traverse because large numbers of measurements are often required to improve test accuracy. An individual sensor may be used to measure each location, or an array of sensors may be used with a movable grid. Air flow and temperature are assumed to remain steady during the measurement period. Inlet air is typically not stratified but can have large spatial variations in temperature. Depending on the individual application and sensitivity of heat load to inlet air temperature, thirty or more measurements may be required.

Outlet air (gas) temperatures taken downstream of the fan or fan/motor assembly may require correction for fan or motor losses, depending on how the coils were originally rated and on whether motor heat is discharged into the conditioned air stream or into the room environment. These losses and the resulting rise in outlet air temperature can be estimated from motor current, voltage, and fan speed.

### J.2.3 Fan Motor Power

Motor power is measured, when necessary, using a true RMS power meter. The motor power and fan efficiency are used to estimate rise in outlet temperature attributed to fan inefficiency.

### J.2.4 Measurement Constraints

It is critical to integrate uncertainty analysis into room-cooler test design. Small temperature differences will result in unacceptably high errors in

measured heat transfer rates. Expected or available test loads must be determined and used in pre-test analysis. Accurate and repeatable tests depend upon the following:

(a) Accurate water temperature measurements and flow measurements (for example, total water temperature measurement uncertainties less than  $\pm 0.5^\circ\text{F}$  and water flow rate uncertainty less than  $\pm 3\%$  are often needed to meet the uncertainty ranges specified in para. 1.3 for  $U^*$  and  $Q^*$ ).

(b) Large mean temperature differences (for example, EMTD greater than  $10^\circ\text{F}$  is often needed to meet the uncertainty ranges in para. 1.3 for  $U^*$  and  $Q^*$ ).

(c) Operating the fan at the same speed as at reference conditions, which eliminate air flow as a critical variable.

(d) Water-side heat load should be measured accurately and used to analyze room cooler performance. Under these conditions, the uncertainty in air flow measurements do not have a significant effect on the results since the uncertainty in heat transfer rate is determined by water measurements (i.e., the weighting factor for air side heat transfer rate is small). The uncertainty in air temperature measurements has a small effect on the uncertainty in EMTD since the mean temperatures difference is large, and the uncertainty in air-side heat transfer coefficient has very little impact on overall uncertainty because the volumetric flow rate at test and reference conditions is about the same.

(e) Other things to consider include:

(1) Coolers with composite loads from heavy mass systems or structures should be preconditioned for 12 hours or more prior to testing.

(2) Electric resistance space heaters may be used to boost room loads and provide higher temperature differences.

(3) Field verification of drain pans or valves should be completed to confirm dry coil conditions.

## J.3 EVALUATION OF RESULTS

### J.3.1 Coil Geometry

(a) Evaluation of a cooling or heating coil may require the following design data:

- (1) Length and width of coil frame
- (2) Total external coil surface
- (3) Straight tube length per pass
- (4) Equivalent length of coil per return bend
- (5) Tube outside diameter
- (6) Tube wall thickness

- (7) Total number of tubes in coil
- (8) Coil depth in number of tube rows
- (9) Tube material/thermal conductivity
- (10) Number of tube circuits in coil
- (11) Transverse tube spacing
- (12) Longitudinal tube spacing
- (13) Fin thickness
- (14) Fin spacing
- (15) Fin depth in direction of air flow
- (16) Fin length perpendicular to direction of tubes

(17) Fin root radius

(18) Fin material/thermal conductivity

(b) Other information that may be necessary includes:

(1) Turbulators (none, spiral, or other)

(2) Fin type (flat, corrugated, discontinuous)

(3) Coil type (serpentine, etc.)

### J.3.2 Correlations

**J.3.2.1 Tube-Side.** Many room coolers are designed for low fluid velocities, and turbulators are sometimes used to increase the effective Reynolds number in these exchangers. Performance curves for turbulators are not available in this Code. Tube-side film and friction coefficients are provided in Appendix F.

**J.3.2.2 Air-Side.** Air-side heat transfer performance is typically determined using commercial heat exchanger software or manufacturer coil-selection software. Some data has been correlated in the open literature, and a recent publication, Reference 76, identifies the following formula by correlating data from several previous researchers:

$$j = 0.163 Re_{\max}^{-0.369} \left( \frac{p_n}{p_p} \right)^{0.106} \left( \frac{w_f}{d_o} \right)^{0.0138} \left( \frac{p_n}{d_o} \right)^{0.13} \quad (J.1)$$

where

$Re_{\max}$  = Reynolds number based on the maximum air velocity (gap velocity) =  $\rho v_{\max} d_o / \mu$

$d_o$  = outside tube diameter

$v_{\max}$  = maximum velocity based on minimum flow area

$p_n$  = tube spacing normal to flow direction

$p_p$  = tube spacing parallel to flow direction

$w_f$  = spacing between adjacent fins

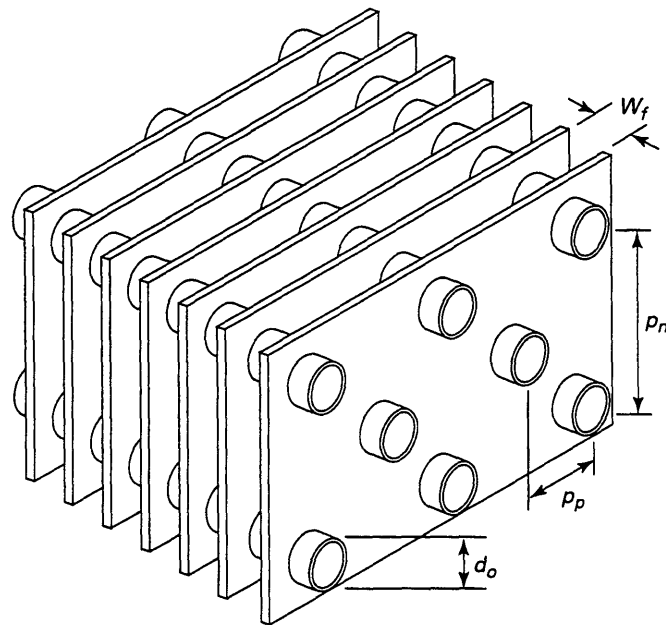


FIG. J.1 TYPICAL GEOMETRY OF TUBE-IN-PLATE  
FIN AIR COOLER HEAT EXCHANGER

(a) This correlation is considered applicable for:

- (1) number of tube rows  $\geq 3$
- (2)  $505 < Re_{\max} < 24707$
- (3)  $0.857 \geq p_n/p_p \geq 1.654$
- (4)  $1.996 \leq p_n/d_o \leq 2.881$
- (5)  $0.081 \leq w_f/d_o \leq 0.641$

(b) Figure J.1 shows the schematic arrangement for a typical tube bundle.

### J.3.3 Analytical Constraints

As with other types of heat exchangers, steady-state conditions should be obtained prior to testing.

Gas-to-liquid heat exchangers have a slower thermal response than liquid-to-liquid exchangers, and pre-test operation should be long enough to develop steady conditions (approximately 15 to 30 minutes).

Also, the sensible heat ratio (sensible load divided by total load) should be greater than 95% to minimize the error associated with condensation heat transfer, ARI 410, Reference 74. Field verification of drain pans or valves can be made to confirm this requirement.

Accurate air properties should be obtained. Air specific heat and other properties vary with absolute moisture content and can impact calculated heat loads by several percentage points.

This page intentionally left blank.

## NONMANDATORY APPENDIX K — EXAMPLES

This Appendix contains several example calculations of performance based on the requirements and guidance in this Code.

### K.1 THERMAL PERFORMANCE OF A SHELL-AND-TUBE HEAT EXCHANGER

Figure K.1 shows a water-to-water heat exchanger in a commercial power plant. The shell side contains modified double segmental baffles and the flow arrangement is considered to be counterflow with  $F = 1$ .

(a) *Review Raw Data (para. 5.2.1).* More than an hour prior to the test period, steady plant conditions are established. During the test period, the data acquisition system recorded data from the instruments at a rate of once per second. Traces of the data over a one hour test period are reviewed and the test conditions appear to be consistent with the test plan and other pre-test agreements. No gross errors in the data are identified. A 15 min window is selected where the inlet temperature and flow conditions do not appear to change 15 min prior to and throughout the duration of the test window.

(b) *Average Selected Data and Calculate Standard Deviation (para. 5.2.2).* The average and standard deviation is calculated for the data at each measurement station in accordance with the definitions in PTC 19.1, Reference 1:

$$\bar{x} = \frac{1}{N} \sum_{i=1}^N x_i \quad s_x = \sqrt{\frac{\sum_{i=1}^N (x_i - \bar{x})^2}{N - 1}}$$

where

- $x_i$  = a measurement of parameter  $x$
- $\bar{x}$  = average of parameter  $x$  over the test window
- $s_x$  = standard deviation of  $x$  over the test window
- $N$  = number of measurements over the test window

$$N = \left( \frac{60 \text{ measurements}}{1 \text{ minute}} \right) (15 \text{ minutes}) = 900$$

**TABLE K.1**  
AVERAGE AND STANDARD DEVIATION FOR  $t_i$

Location	$\bar{x}$ (°F)	$s_x$ (°F)
Top	79.95	0.05
Right	79.92	0.03
Bottom	79.90	0.06
Left	79.88	0.07

**TABLE K.2**  
AVERAGE AND STANDARD DEVIATION FOR  $T_i$

Location	$\bar{x}$ (°F)	$s_x$ (°F)
Top	95.40	0.07
Right	95.30	0.05
Bottom	95.15	0.04
Left	95.22	0.06

The averages and standard deviations for each measurement station are shown in Tables K.1 to K.5.

The mass flow rate is calculated using the density of water based on the average inlet temperatures:

$$m_c = (20475 \text{ gpm})(62.23 \text{ lbm/ft}^3) \left( \frac{1 \text{ ft}^3}{7.4805 \text{ gal}} \right) \left( \frac{60 \text{ minutes}}{1 \text{ hour}} \right) = 10.22(10)^6 \text{ lbm/hr}$$

$$m_h = (12055 \text{ gpm})(62.05 \text{ lbm/ft}^3) \left( \frac{1 \text{ ft}^3}{7.4805 \text{ gal}} \right) \left( \frac{60 \text{ minutes}}{1 \text{ hour}} \right) = 6.000(10)^6 \text{ lbm/hr}$$

(c) *Evaluate the Uncertainty of Temperature and Flow Measurements (para. 5.2.3).* The measurement uncertainties include effects due to instrument calibra-

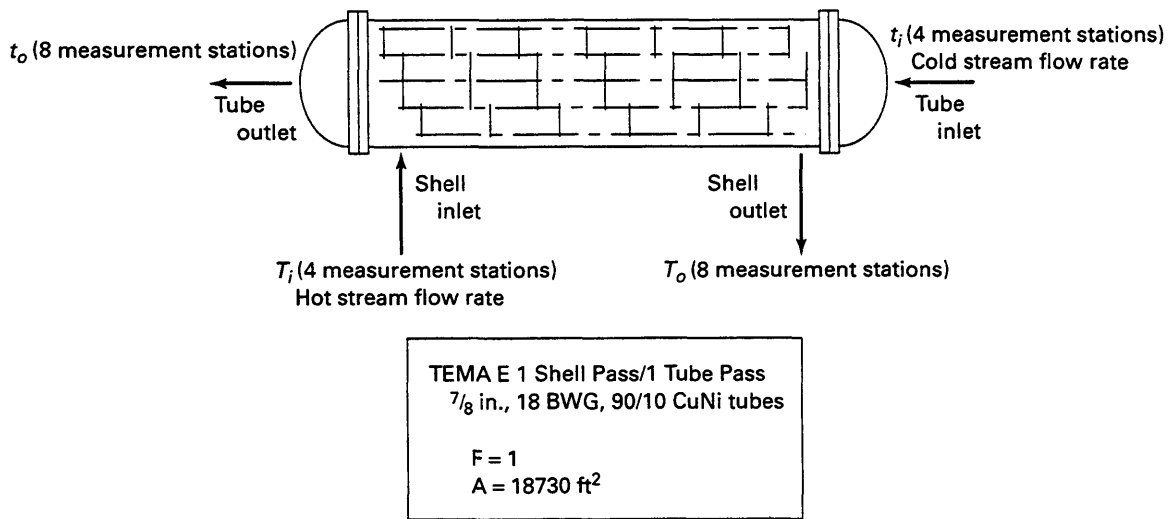


FIG. K.1 CONFIGURATION FOR WATER-WATER HEAT EXCHANGER TEST IN A POWER PLANT

TABLE K.3  
AVERAGE AND STANDARD DEVIATION FOR  $t_o$

Location	$\bar{x}$ (°F)	$s_x$ (°F)
Top	86.80	0.08
Top-Right	86.52	0.10
Right	86.05	0.05
Bottom-Right	85.26	0.10
Bottom	84.65	0.15
Bottom-Left	84.95	0.07
Left	85.75	0.15
Top-Left	86.03	0.06

TABLE K.4  
AVERAGE AND STANDARD DEVIATION FOR  $T_o$

Location	$\bar{x}$ (°F)	$s_x$ (°F)
Top	86.18	0.10
Top-Right	85.70	0.05
Right	85.55	0.08
Bottom-Right	85.13	0.08
Bottom	84.85	0.12
Bottom-Left	85.36	0.06
Left	85.48	0.07
Top-Left	86.01	0.10

tion, spatial variation, installation, data acquisition, and random error based on 95% confidence.

(1) *Temperature Calibration Uncertainty.* The temperature measurements are performed using type T thin film thermocouples mounted to the outside surface of the pipe. Four thermocouples are mounted at equally spaced locations at the inlets, and eight thermocouples are mounted at equally spaced locations at the outlets. Prior to the test, the thermocouples are calibrated as a matched pair (measuring and reference junctions) to within  $\pm 0.2^\circ\text{F}$ . The calibration is performed using the same data acquisition equipment as used in the test (and therefore the uncertainty attributed to data acquisition is neglected). The calibration is performed as a check against a standard tolerance;

TABLE K.5  
AVERAGE AND STANDARD DEVIATION FOR HOT AND COLD STREAM FLOW RATES

Location	$\bar{x}$ (gpm)	$s_x$ (gpm)
Cold Stream Inlet	20475	410
Hot Stream Inlet	12055	280

adjustments are made only when the result is outside the tolerance interval. As such, the uncertainties in temperature calibration for different instruments may be considered independent. In addition, random error attributed to the instrument and data acquisition system variations while system conditions are constant is small and is neglected.

(2) *Temperature Installation Uncertainty.* The thermocouple junctions and six inches of wire are mounted under a blanket of insulation with a thermal resistance more than 4000 times the resistance between the fluid and thermocouple. A calculation of heat transfer from the fluid to the environment estimates that the systematic error is 0.05°F.

(3) *Temperature Spatial Variation Uncertainty.* The temperature distribution is not uniform at the pipe cross sections. Using surface temperature measurements, the bulk average fluid temperature is calculated by applying weighting factors to the surface temperature measurements and adding the contribution of each weighted temperature. The weighting factors can be determined using available data for the internal temperature distribution or based on assumptions regarding the distribution. Data regarding the shape of the fluid temperature distribution in the pipe is not available for this application. As a result, it is assumed that each surface temperature measurement represents the temperature of an equal fraction of fluid mass, and the bulk average fluid temperature is estimated by averaging the surface temperature measurements around the pipe circumference. The estimate of the inherent systematic error attributed to the difference between the numerical average temperature and the true bulk average temperature is the spatial variation uncertainty.

(a) For this test, the spatial variation of the outlet temperatures is substantial over the pipe cross section. The temperature at the top of the pipe is higher than at the bottom of the pipe and it is concluded that the bulk average temperature is somewhere near the middle of the spread between the maximum and minimum temperature. Without internal temperature data, it is not clear if the distribution is uniformly stratified (with horizontal isotherms) or if the distribution is distorted from this ideal case. For this example with eight equally spaced measurement stations for each outlet location, it is assumed that the error associated with equal weighting factors is randomly distributed.<sup>1</sup> As

<sup>1</sup> Test experience indicates that it is reasonable to assume random errors with equal weighting factors provided that the number of measurement stations is 10 or less. For more stations, the measurement errors at adjacent locations may be correlated so that the spatial error of two adjacent stations may be approxi-

**TABLE K.6**  
**BULK AVERAGE TEMPERATURES AND**  
**ASSOCIATED SPATIAL VARIATION**  
**UNCERTAINTIES**

Parameter	$\bar{\bar{x}}$ (°F)	$b_{\text{SpatVar}}$ (°F)
$t_i$	79.91	0.05
$t_o$	85.75	0.63
$T_i$	95.27	0.17
$T_o$	85.53	0.37

such, the method described in PTC 19.1, Reference 1, is adapted to estimate the systematic uncertainty due to spatial variation:

$$b_{\text{SpatVar}} = \hat{t} \sqrt{\frac{1}{J} \sum_{i=1}^J \frac{(\bar{x}_i - \bar{\bar{x}})^2}{J-1}} \quad (\text{K.1})$$

where

$\bar{x}$  = time weighted average at a measurement station

$\bar{\bar{x}}$  = estimate of the bulk average at a flow cross-section

$J$  = number of measurement stations at a flow cross-section

$\hat{t}$  = Student  $t$  for  $J-1$  degrees of freedom = 3.182 for inlet temperatures and 2.365 for outlet temperatures

(b) For the inlet temperatures, the spatial variation in the temperature is less than for the outlet temperatures. The assumption regarding the random distribution of spatial errors is the same as with the outlet temperature measurements and therefore Eq. (K.1) is used to estimate the uncertainty in spatial variation for inlet temperatures.

The estimates of the bulk average temperatures and the associated uncertainties in spatial variation are shown in Table K.6.

(4) *Temperature Process Variation Uncertainty.* During the test period, random variations in the process temperatures are observed. Since the one Hertz sampling rate is greater than the frequency of the process variations, successive temperature measurements

are approximately equal. Since the method described in this example applies where spatial error is random for each measurement station, additional information regarding the internal temperature distribution would be needed to reduce the uncertainty for more than 10 measurement stations.

**TABLE K.7**  
**TEMPERATURE UNCERTAINTY**  
**ATTRIBUTED TO PROCESS VARIATIONS**

Parameter	$u_{pv}$ (°F)
$t_i$	0.028
$t_o$	0.052
$T_i$	0.029
$T_o$	0.044

are not independent of process variations. The uncertainty attributed to process variations is calculated based on independent time intervals such that process variations in successive time intervals are not correlated. The uncertainty attributed to random process variations is calculated in accordance with the guidelines in Appendix A based on 15 one-minute intervals. A qualitative evaluation of the data indicates that changes in these 1 minute average temperatures are random and are less than the standard deviations in Table K.1 to K.4. As such, it is concluded that the process is stationary. Based on 15 one-minute intervals, the standard deviation for the process variations may be estimated by adapting Eq. (A.3) as follows:

$$s_{\bar{x}} = \sqrt{\sum_{i=1}^J \frac{1}{J} \frac{(s_x^2)_i}{15}} \quad (\text{K.2})$$

where

$J$  = number of measurement stations

Since the process is stationary, drift is negligible and based on Eq. (A.4),  $u_{pv} = 2s_{\bar{x}}$ . The uncertainty due to process variations are shown in Table K.7:

(5) *Overall Temperature Measurement Uncertainty.* The overall measurement uncertainty is calculated by combining the uncertainties for calibration, installation, spatial variation and process variations by a root-sum-squares as identified in Eq. (B.4), (noting that random errors of the instrument and data acquisition are included in the calibration uncertainty). The results are summarized in Table K.8.

(6) *Flow Measurement Uncertainty Attributed to Calibration, Installation, Data Acquisition, Spatial Variation and Random Error.* The calibration of the flow instrument was performed by the manufacturer prior to the test. Based on data from the manufacturer, the flowmeter is accurate to within 3% of reading if installation requirements are met. The experience of the test personnel (from previous tests performed in a

flow test laboratory) indicates that the manufacturer accuracy data includes effects due to calibration, installation practices, spatial variation (flow profile effects), and random instrument error. Furthermore, this experience indicates the data acquisition uncertainty is small compared to these other factors and can be neglected. The combined uncertainty attributed to calibration, installation, data acquisition, spatial variation and random instrument error,  $u_{cal}$ , is  $\pm 3\%$  of reading as shown in Table K.9.

(7) *Flow Measurement Process Variation Uncertainty.* As with the temperature data, the uncertainty attributed to drift is neglected and the uncertainty due to random variations is twice the standard deviation of process variations for 15 one-minute intervals. (Based on Eq. (K.2) where  $J = 1$  flow measurement station and applicable density and units conversion are applied). Table K.10 shows the uncertainty in flow measurement process variations based on Eq. (K.2).

(8) *Uncertainty of Inlet Fluid Density Used to Calculate Mass Flow Rate.* The uncertainty of the fluid density is a function of the uncertainty of the compressed water data in the Steam Tables, Reference 66, and the uncertainty of the inlet water temperature measurements. The uncertainty of inlet fluid density is bounded by the hot stream density uncertainty which is given by:

$$u_{\rho} = \sqrt{b^2_{\rho, \text{steam tables}} + \left(\frac{\partial \rho}{\partial T} u_{T_i}\right)^2} \quad (\text{K.3})$$

The uncertainty of the specific volume data for compressed water in the Steam Tables is estimated to be about  $\pm 0.01\%$ . The sensitivity coefficient for the temperature measurement is  $\partial \rho / \partial T = 0.01$  (lbm/ft<sup>3</sup>)/°F and the uncertainty of the hot stream inlet temperature is  $\pm 0.27^\circ\text{F}$ . The resulting uncertainty in density,  $u_{\rho}$  is less than 0.1% and is not considered further since it is a negligible contribution to the overall flow measurement uncertainty.

(9) *Overall Flow Measurement Uncertainty.* The overall flow measurement uncertainty is calculated by combining the uncertainties by a root-sum-squares. The results are summarized in Table K.11:

The measurement data is summarized as follows:

$$\begin{aligned} t_i &= 79.91 \pm 0.21^\circ\text{F} \\ t_o &= 85.75 \pm 0.66^\circ\text{F} \\ T_i &= 95.27 \pm 0.27^\circ\text{F} \\ T_o &= 85.53 \pm 0.43^\circ\text{F} \\ m_c &= 10.22(10)^6 \pm 0.33(10)^6 \text{ lbm/hr} \\ m_h &= 6.00(10)^6 \pm 0.19(10)^6 \text{ lbm/hr} \end{aligned}$$

**TABLE K.8**  
**OVERALL MEASUREMENT UNCERTAINTY FOR TEMPERATURES**

Parameter	$b_{cal}$ (°F)	$b_{install}$ (°F)	$b_{SpatVar}$ (°F)	$u_{pv}$ (°F)	$u_{overall}$ (°F)
$t_i$	0.2	0.05	0.05	0.028	0.21
$t_o$	0.2	0.05	0.63	0.052	0.66
$T_i$	0.2	0.05	0.17	0.029	0.27
$T_o$	0.2	0.05	0.37	0.044	0.43

**TABLE K.9**  
**FLOW MEASUREMENT UNCERTAINTY**  
**ATTRIBUTED TO CALIBRATION,**  
**INSTALLATION, SPATIAL VARIATION, AND**  
**RANDOM INSTRUMENT VARIATIONS**

Parameter	$u_{cal}$ (lbm/hr)
$m_c$	$0.307(10)^6$
$m_h$	$0.180(10)^6$

**TABLE K.10**  
**FLOW MEASUREMENT UNCERTAINTY**  
**ATTRIBUTED TO PROCESS VARIATIONS**

Parameter	$u_{pv}$ (lbm/hr)
$m_c$	$0.106(10)^6$
$m_h$	$0.072(10)^6$

**TABLE K.11**  
**OVERALL MEASUREMENT UNCERTAINTY FOR FLOW**

Parameter	$u_{cal}$ (lbm/hr)	$u_{pv}$ (lbm/hr)	$u_{overall}$ (lbm/hr)
$m_c$	$0.307(10)^6$	$0.106(10)^6$	$0.325(10)^6$
$m_h$	$0.180(10)^6$	$0.072(10)^6$	$0.194(10)^6$

(d) Compute the Heat Transfer Rate at Test Conditions (para. 5.3.1). The average temperature of the cold stream is  $(79.91 + 85.75)/2 = 82.83^\circ\text{F}$  and the average temperature of the hot stream is  $(95.27 + 85.53)/2 = 90.40^\circ\text{F}$ . The specific heat of the hot and cold streams are based on these average temperatures using data from the Steam Tables, Reference 66:

$$c_{p,h} = 0.998 \text{ Btu/lbm} - ^\circ\text{F}$$

$$c_{p,c} = 0.998 \text{ Btu/lbm} - ^\circ\text{F}$$

The hot and cold stream heat transfer rates are calculated based on Eqs. (5.1) and (5.2):

$$\begin{aligned} Q_h &= m_h c_{p,h} (T_i - T_o) \\ &= 6.000(10)^6 (0.998)(95.27 - 85.53) \\ &= 58.32(10)^6 \text{ Btu/hr} \end{aligned}$$

$$\begin{aligned} Q_c &= m_c c_{p,c} (t_o - t_i) \\ &= 10.22(10)^6 (0.998)(85.75 - 79.91) \\ &= 59.57(10)^6 \text{ Btu/hr} \end{aligned}$$

The uncertainty is calculated based on Eqs. (B.5) and (B.6) and sensitivity coefficients in Table B.2. The results are summarized in Tables K.12 and K.13.

The heat balance is assessed by evaluating the overlap of uncertainty bars. This example meets the conditions of complete overlap as shown in case a for Fig. 5.1. As such, a heat balance is confirmed and the weighted average heat transfer rate is calculated in accordance with Eq. (5.3):

**TABLE K.12**  
**UNCERTAINTY IN HOT STREAM HEAT-TRANSFER RATE**

Contributing Factor	Uncertainty, $u$	Sensitivity, $\theta$	Uncertainty Contribution, $(\theta u)^2$ (Btu/hr) <sup>2</sup>
Inlet hot stream temperature, $T_i$	0.27°F	5.988(10) <sup>6</sup> Btu/hr-°F	2.614(10) <sup>12</sup>
Outlet hot stream temperature, $T_o$	0.43°F	-5.988(10) <sup>6</sup> Btu/hr-°F	6.630(10) <sup>12</sup>
Hot stream flow rate, $m_h$	0.194(10) <sup>6</sup> lbm/hr	9.721 Btu/lbm	3.557(10) <sup>12</sup>
Hot stream specific heat, $c_{p,h}$	0.00998 Btu/lbm-°F	58.44(10) <sup>6</sup> lbm-°F/hr	0.340(10) <sup>12</sup>
Total uncertainty in hot stream heat transfer rate = 3.625(10) <sup>6</sup> Btu/hr.			

**TABLE K.13**  
**UNCERTAINTY IN COLD STREAM HEAT-TRANSFER RATE**

Contributing Factor	Uncertainty, $u$	Sensitivity, $\theta$	Uncertainty Contribution, $(\theta u)^2$ (Btu/hr) <sup>2</sup>
Inlet cold stream temperature, $t_i$	0.21°F	-10.20(10) <sup>6</sup> Btu/hr-°F	4.588(10) <sup>12</sup>
Outlet cold stream temperature, $t_o$	0.66°F	10.20(10) <sup>6</sup> Btu/hr-°F	45.32(10) <sup>12</sup>
Cold stream flow rate, $m_c$	0.327(10) <sup>6</sup> lbm/hr	5.828 Btu/lbm	3.632(10) <sup>12</sup>
Cold stream specific heat, $c_{p,c}$	0.00998 Btu/lbm-°F	59.68(10) <sup>6</sup> lbm-°F/hr	0.355(10) <sup>12</sup>
Total uncertainty in cold stream heat transfer rate = 7.341(10) <sup>6</sup> Btu/hr.			

$$\begin{aligned}
 Q_{ave} &= \left( \frac{u_{Qh}^2}{u_{Qc}^2 + u_{Qh}^2} \right) Q_c + \left( \frac{u_{Qc}^2}{u_{Qc}^2 + u_{Qh}^2} \right) Q_h \\
 &= \left( \frac{3.625^2}{7.341^2 + 3.625^2} \right) 59.57(10)^6 \\
 &\quad + \left( \frac{7.341^2}{7.341^2 + 3.625^2} \right) 58.32(10)^6 \\
 &= 58.57(10)^6 \text{ Btu/hr}
 \end{aligned}$$

The uncertainty of the average heat transfer rate is calculated using Eq. (B.7):

$$\begin{aligned}
 u_{Qave} &= \frac{[u_{Qc}^4 u_{Qh}^2 + u_{Qh}^4 u_{Qc}^2]^{1/2}}{u_{Qc}^2 + u_{Qh}^2} \\
 &= \frac{[(7.341)^4 (3.625)^2 + (3.625)^4 (7.341)^2]^{1/2}}{7.341^2 + 3.625^2} (10)^6 \\
 &= 3.25(10)^6 \text{ Btu/hr}
 \end{aligned}$$

where

$$Q_{ave} = 58.57 \pm 3.25 (10)^6 \text{ Btu/hr}$$

(e) Compute the Effective Mean Temperature Difference at Test Conditions (para. 5.3.2). The flow arrangement is considered counterflow so that  $F = 1$ . Therefore, the effective mean temperature difference is the same as the log mean temperature difference which is calculated using Eq. (D.1):

$$\begin{aligned}
 \text{EMTD} &= \frac{(T_i - t_o) - (T_o - t_i)}{\ln \left( \frac{(T_i - t_o)}{(T_o - t_i)} \right)} \\
 &= \frac{(95.27 - 85.75) - (85.53 - 79.91)}{\ln \left( \frac{(95.27 - 85.75)}{(85.53 - 79.91)} \right)} = 7.40^\circ\text{F}
 \end{aligned}$$

The uncertainty of the mean temperature difference at test conditions is based on the uncertainties of the measured terminal temperatures, biases for variable  $U$  and non-uniform temperature distribution over a flow cross section in accordance with Eq. (D.7):

$$U_{EMTD} = \left[ \theta_{EMTD,ti}^2 u_{ti}^2 + (\theta_{EMTD,to} u_{to})^2 + (\theta_{EMTD,Ti} u_{Ti})^2 + (\theta_{EMTD,To} u_{To})^2 + b_{EMTD,U}^2 + b_{EMTD,mixing}^2 \right]^{1/2}$$

The method to estimate the bias terms is based on pre-test agreements. To determine the bias attributed to variable  $U$ ,  $b_{EMTD,U}$ , a variation of fouling resistance on the inside surface of the tubes is assumed based on heat exchanger inspections and previous plant experience. It is observed that silt attachment in the biofilm layer varies along the tube length with additional silt attached to the inlet end of the tubes. Bounding estimates for the variation of fouling resistance are typical fouling Biot numbers for water-water heat exchangers (see Appendix G for the definition of fouling Biot number). It is assumed that the outlet end of the tubes are clean and the fouling Biot number is 0, and that inlet conditions are fouled such that the fouling Biot number is 1. (At the end of this example it is shown that these assumptions bound the fouling range for this test). Under these conditions,  $U_1/U_2 = 0.5$  and Eq. (D.15) is used to estimate  $b_{EMTD,U}$ .

$$\begin{aligned} \frac{b_{EMTD,U}}{EMTD} &= 1 - \frac{2(U_1/U_2 - \Delta T_1/\Delta T_2) \ln \left( \frac{\Delta T_1}{\Delta T_2} \right)}{(1 + U_1/U_2)(\Delta T_1/\Delta T_2 - 1) \ln \left( \frac{U_1/U_2}{\Delta T_1/\Delta T_2} \right)} \\ &= 1 - \frac{2(0.5 - 1.69) \ln 1.69}{(1 + 0.5)(1.69 - 1) \ln \left( \frac{0.5}{1.69} \right)} = 0.0092 \end{aligned}$$

The resulting bias,  $b_{EMTD,U} = 7.4(0.0092) = 0.07^\circ\text{F}$

For non-uniform temperature distribution, the bias,  $b_{EMTD,mixing}/EMTD = 2\%$  from the discussion in para. D.3:1.3 (corresponding to  $b_{EMTD,mixing} = 0.15^\circ\text{F}$ ). The uncertainty in mean temperature difference and at test conditions is calculated based on Eq. (D.7) and sensitivity coefficients in Table D.1. The results are summarized in Table K.14.

(f) *Compute the Overall Heat Transfer Coefficient at Test Conditions (para. 5.3.3).* The overall heat transfer coefficient at test conditions is calculated based on Eq. (5.5).

$$U = \frac{Q_{ave}}{A(EMTD)} = \frac{58.57(10)^6}{(18730)(7.40)} = 422.6 \frac{\text{Btu}}{\text{hr-ft}^2\text{-}^\circ\text{F}}$$

The associated uncertainty is calculated based on Eq. (B.8) and sensitivity coefficients in Table B.3. The results are shown in Table K.15.

(g) *Determine Individual Heat Transfer Coefficients at Test Conditions (para. 5.3.4).* Based on a pre-test agreement, the heat transfer coefficients are determined using a proprietary computer code. The heat transfer coefficients at test conditions are calculated as follows:

$$h_c = 1411.1 \text{ Btu}/(\text{hr-ft}^2\text{-}^\circ\text{F})$$

$$h_h = 1215.8 \text{ Btu}/(\text{hr-ft}^2\text{-}^\circ\text{F})$$

The uncertainty in convective thermal resistance is based on a 10% uncertainty in tube-side heat transfer coefficient and 50% uncertainty in shell-side heat transfer coefficient. The large uncertainty in shell-side uncertainty is attributed to the unusual baffle arrangement and the associated ability to predict heat transfer coefficient.

(h) *Determine the Wall Resistance at Test Conditions (para. 5.3.5).* The wall resistance at test conditions is given by expression which is adapted based on Eq. 5.6:

$$R_w = \frac{d_o \ln(d_o/d_i)}{2k_w A} \quad (\text{K.4})$$

where  $k_w$  is the thermal conductivity of 90-10 Cu-Ni tubes based on the average wall temperature. For this example, the wall temperature is approximated at the midpoint between the hot and cold fluid streams. Therefore;

$$t_w = \frac{79.91 + 85.75 + 95.27 + 85.53}{4} = 86.6^\circ\text{F}$$

where

$$k_w = 29 \text{ Btu}/\text{hr-ft-}^\circ\text{F, Reference 28}$$

$$d_o = 0.875 \text{ in.} = 0.0729 \text{ ft}$$

$$d_i = 0.875 - 2(0.049) = 0.777 \text{ in.}$$

The wall resistance at test conditions becomes:

$$\begin{aligned} R_w &= \frac{d_o \ln(d_o/d_i)}{2k_w A} = \frac{0.0729 \ln(0.875/0.777)}{2(29)18730} \\ &= 8(10)^{-9} \text{ hr-}^\circ\text{F}/\text{Btu} \end{aligned}$$

(i) *Solve the Heat Transfer Equations at Reference Conditions (para. 5.4.1).* The thermal performance parameters are calculated using methods based on pre-test agreements. The reference conditions are defined by the following parameters:

$$T_i^* = 171.6^\circ\text{F}$$

$$m_h^* = 3.22(10)^6 \text{ lbm}/\text{hr}$$

**TABLE K.14**  
**UNCERTAINTY IN EMTD AT TEST CONDITIONS**

Contributing Factor	Uncertainty, $u$	Sensitivity, $\theta$ (dimensionless)	Uncertainty Contribution, $(\theta u)^2$ (°F) <sup>2</sup>
Inlet hot stream temperature, $T_i$	0.27°F	0.42	0.0129
Outlet hot stream temperature, $T_o$	0.43°F	0.60	0.0666
Inlet cold stream temperature, $t_i$	0.21°F	-0.60	0.0159
Outlet cold stream temperature, $t_o$	0.66°F	-0.42	0.0768
Variation in overall heat transfer coefficient, $b_{EMTD,U}$	0.07°F	1	0.0049
Incomplete thermal mixing, $b_{EMTD,mixing}$	0.15°F	1	0.0225
Total uncertainty in EMTD at test conditions = 0.45°F.			

**TABLE K.15**  
**UNCERTAINTY IN OVERALL HEAT TRANSFER COEFFICIENT AT TEST CONDITIONS**

Contributing Factor	Uncertainty, $u$	Sensitivity, $\theta$	Uncertainty Contribution, $(\theta u)^2$ (Btu/hr-ft <sup>2</sup> -°F) <sup>2</sup>
Average heat transfer rate, $Q_{ave}$	3.25(10) <sup>6</sup> Btu/hr	7.22(10) <sup>-6</sup> ft <sup>-2</sup> °F <sup>-1</sup>	550.6
Mean temperature difference, EMTD	0.45°F	57.1 Btu/hr-ft <sup>2</sup> -°F <sup>2</sup>	660.2
Total uncertainty in overall heat transfer coefficient at test conditions = 34.8 Btu/hr-ft <sup>2</sup> -°F.			

$$t_i^* = 87.0^\circ\text{F}$$

$$m_c^* = 8.34(10)^6 \text{ lbm/hr}$$

The performance at reference conditions is calculated by solving Eqs. (5.9), (5.10), (5.11) and (5.12) using an iterative approach. First, average hot stream, cold stream and wall temperatures are assumed, and the individual heat transfer coefficients, specific heats and wall resistance are calculated. (The individual heat transfer coefficients are calculated using the computer program, the specific heats are calculated using the Steam Tables, and the wall resistance is calculated using Eq. (K.4).) The results of these calculations are as follows:

$$h_h^* = 981.2 \text{ Btu}/(\text{hr}\cdot\text{ft}^2\cdot^\circ\text{F})$$

$$h_c^* = 1314.2 \text{ Btu}/(\text{hr}\cdot\text{ft}^2\cdot^\circ\text{F})$$

$$c_{p,c}^* = 0.998 \text{ Btu}/\text{lbm}\cdot^\circ\text{F}$$

$$c_{p,h}^* = 0.999 \text{ Btu}/\text{lbm}\cdot^\circ\text{F}$$

$$R_w^* = 8(10^{-9}) \text{ hr}\cdot^\circ\text{F}/\text{Btu}$$

The overall heat transfer coefficient is calculated using Eq. (5.15):

$$\begin{aligned}
 U^* &= \frac{1}{\frac{1}{U} + \frac{A}{\eta_h A_h} \left[ \frac{1}{h_h^*} - \frac{1}{h_h} \right] + \frac{A}{\eta_c A_c} \left[ \frac{1}{h_c^*} - \frac{1}{h_c} \right] + (R_w^* - R_w)} \\
 &= \left[ \frac{1}{422.6} + \left[ \frac{1}{981.2} - \frac{1}{1215.8} \right] + 1.13 \left[ \frac{1}{1314.2} - \frac{1}{1411.1} \right] \right]^{-1} \\
 &= 381.4 \frac{\text{Btu}}{\text{hr}\cdot\text{ft}^2\cdot^\circ\text{F}}
 \end{aligned}$$

where

$\eta = 1$  since the tubes are plain without enhancement

**TABLE K.16**  
**UNCERTAINTY IN HEAT TRANSFER COEFFICIENT AT REFERENCE**  
**CONDITIONS**

Contributing Factor	Uncertainty, $u$	Sensitivity, $\theta$	Uncertainty Contribution, $(\theta u)^2$ (Btu/hr-ft <sup>2</sup> -°F) <sup>2</sup>
Overall heat transfer coefficient at test conditions, $U$	34.8 Btu/hr-ft <sup>2</sup> -°F	0.815	804.4
Adjustment in hot stream heat transfer coefficient, $(1/h^* - 1/h)_h$	$9.83(10)^{-5}$ hr-ft <sup>2</sup> -°F/Btu	$1.45(10)^5$ (Btu/hr-ft <sup>2</sup> -°F) <sup>2</sup>	203.2
Adjustment in cold stream heat transfer coefficient, $(1/h^* - 1/h)_c$	$5.23(10)^{-6}$ hr-ft <sup>2</sup> -°F/Btu	$1.64(10)^5$ (Btu/hr-ft <sup>2</sup> -°F) <sup>2</sup>	0.7
Total uncertainty in overall heat transfer coefficient at reference conditions = 31.8 Btu/hr-ft <sup>2</sup> -°F.			

$$A/(\eta A)_h = 1$$

$$A/(\eta A)_c = d_o/d_i = 0.875/(0.875 - 2(0.049)) = 1.13$$

$$R_w^* - R_w = 0$$

Based on the design data for the heat exchanger, the overall heat transfer coefficient for clean conditions is 610 Btu/hr-ft<sup>2</sup>-°F. Therefore, the fouling Biot number for this example is:

$$Bi_f = r_i U_{\text{clean}} = \frac{U_{\text{clean}}}{U^*} - 1 = \frac{610}{381} - 1 = 0.6$$

This fouling Biot number is typical and the assumption used to calculate  $b_{U, \text{EMTD}}$  is bounding.

The outlet temperatures and heat transfer rate are calculated by solving Eqs. (5.9), (5.10), and (5.11) simultaneously.

$$T_o^* = 101.8^\circ\text{F}$$

$$t_o^* = 114.0^\circ\text{F}$$

$$\text{EMTD}^* = 31.5^\circ\text{F}$$

$$Q^* = 224.7 (10^6) \text{ Btu/hr}$$

Using these outlet temperatures, the individual heat transfer coefficients are recalculated to confirm that the solution has converged.

(d) Determine the Uncertainty of Overall Heat Transfer Coefficient and Heat Transfer Rate at Reference Conditions. The uncertainty in the adjustment in individual heat transfer coefficients is calculated using Eq. (5.14):

$$(u_{1/h^* - 1/h})_h = (u_{1/h})_h(1 - X) = 0.50 \left( \frac{1}{981.2} \right) \left( 1 - \frac{981.2}{1215.8} \right)$$

$$= 9.83(10)^{-5} \frac{\text{hr-ft}^2\text{-}^\circ\text{F}}{\text{Btu}}$$

$$(u_{1/h^* - 1/h})_c = (u_{1/h})_c(1 - X) = 0.10 \left( \frac{1}{1314.2} \right) \left( 1 - \frac{1314.2}{1411.1} \right)$$

$$= 5.23(10)^{-6} \frac{\text{hr-ft}^2\text{-}^\circ\text{F}}{\text{Btu}}$$

The uncertainty of overall heat transfer coefficient at reference conditions is based on Eq. (B.9) and sensitivity coefficients in Table B.4. The results are shown in Table K.16.

The uncertainty of the heat transfer rate at reference conditions is based on Eq. (B.10) and sensitivity coefficients in Table B.5. The results are shown in Table K.17.

$$U^* = 381 \pm 32 \text{ Btu}/(\text{hr-ft}^2\text{-}^\circ\text{F})$$

$$Q^* = 225 \pm 20 (10^6) \text{ Btu/hr}$$

## K.2 TOTAL TUBE-SIDE PRESSURE LOSS

Figure K.2 shows a lube oil-to-water heat exchanger. The heat exchanger is a TEMA E shell with a single tube pass. The test engineer has reviewed the raw test data and averaged a set of data under steady state conditions (paras. 5.2.1 and 5.2.2). Average differential pressure and flow rate data and reference conditions are shown along with the applicable geometry data.

(a) Evaluate Measurement Uncertainties (para. 5.2.3). The differential pressure measurement is mea-

**TABLE K.17**  
**UNCERTAINTY IN HEAT TRANSFER RATE AT REFERENCE CONDITIONS**

<b>Contributing Factor</b>	<b>Uncertainty, <math>u</math></b>	<b>Sensitivity, <math>\theta</math></b>	<b>Uncertainty Contribution, <math>(\theta u)^2</math> (Btu/hr)<sup>2</sup></b>
Mean temperature difference at test conditions, EMTD	0.45°F	-30.4(10) <sup>6</sup> Btu/hr-°F	187(10) <sup>12</sup>
Heat transfer rate at test conditions, $Q_{ave}$	3.25(10) <sup>6</sup> Btu/hr	3.84	156(10) <sup>12</sup>
Overall heat transfer coefficient at test conditions, $U$	34.8 Btu/hr-ft <sup>2</sup> -°F	0.0518(10) <sup>6</sup> ft <sup>2</sup> -°F	3(10) <sup>12</sup>
Adjustment in hot stream heat transfer coefficient, $(1/h^* - 1/h)_h$	9.83(10) <sup>-5</sup> hr-ft <sup>2</sup> -°F/Btu	85700(10) <sup>6</sup> Btu <sup>2</sup> /hr <sup>2</sup> -ft <sup>2</sup> -°F	71(10) <sup>12</sup>
Adjustment in cold stream heat transfer coefficient, $(1/h^* - 1/h)_c$	5.23(10) <sup>-6</sup> hr-ft <sup>2</sup> -°F/Btu	96800(10) <sup>6</sup> Btu <sup>2</sup> /hr <sup>2</sup> -ft <sup>2</sup> -°F	0.3(10) <sup>12</sup>

Total uncertainty in heat transfer rate at reference conditions = 20.4 Btu/hr-ft<sup>2</sup>-°F.

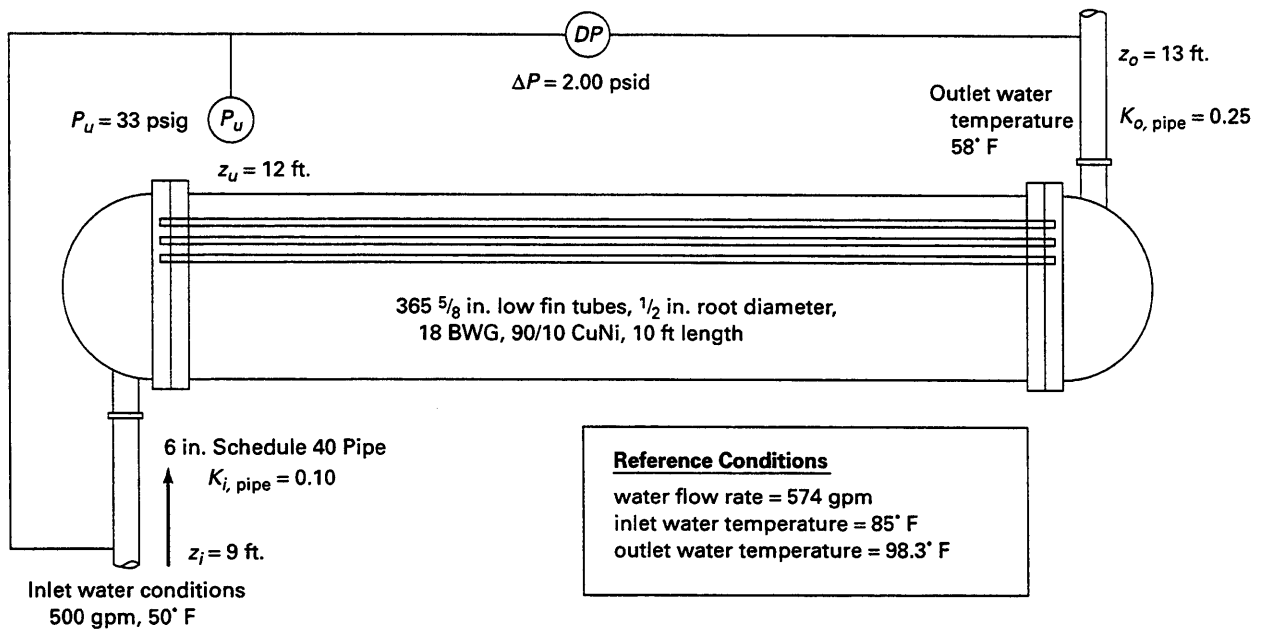


**FIG. K.2 EXAMPLE TUBE-SIDE PRESSURE DROP DATA FOR A LUBE OIL COOLER**

sured using a differential pressure transducer and static pressure taps with an overall uncertainty of  $\pm 1\%$  of reading. The upstream pressure is measured with a pressure gage with an overall uncertainty of  $\pm 0.25$  psi. The water flow rate is measured at the inlet end of the heat exchanger with an overall uncertainty of  $\pm 2\%$  of reading (volumetric or bulk average velocity). The temperature measurements are used to estimate water property data only and the overall uncertainty is estimated to be  $\pm 0.5^\circ\text{F}$ .

(b) *Determine the Nozzle-to-Nozzle Total Pressure Loss (para. 5.3.6).* The total nozzle to nozzle pressure loss is calculated based on Eq. (5.8):

$$\Delta P_{n-n} = \rho_{ave} \left[ \frac{\Delta P}{\rho_{o,pipe}} + \left( \frac{1}{\rho_{i,pipe}} - \frac{1}{\rho_{o,pipe}} \right) \left( P_u + \rho_{gage} \frac{g}{g_c} (z_u - z_i) \right) \right. \\ \left. + \left( 1 - \frac{\rho_{gage}}{\rho_{o,pipe}} \right) \frac{g}{g_c} (z_i - z_o) \right. \\ \left. + \left( 1 - K_{i,pipe} - (1 + K_{o,pipe}) \left( \frac{\rho_{i,pipe} A_{i,pipe}}{\rho_{o,pipe} A_{o,pipe}} \right)^2 \right) \frac{v_i^2}{2g_c} \right]$$

where

- $\Delta P_{n-n}$  = nozzle-to-nozzle pressure loss
- $\Delta P$  = measured differential pressure = 2.00 psid = 288 lbf/ft<sup>2</sup>
- $P_u$  = measured upstream pressure = (33 + 14.7) psia = 6869 lbf/ft<sup>2</sup> absolute
- $\rho_{i,pipe}$  = inlet water density = 62.42 lbm/ft<sup>3</sup> @ 50°F, Reference 66
- $\rho_{o,pipe}$  = outlet water density = 62.38 lbm/ft<sup>3</sup> @ 58°F, Reference 66
- $\rho_{ave}$  = average water density =  $(\rho_{i,pipe} + \rho_{o,pipe})/2$  = 62.40 lbm/ft<sup>3</sup>
- $\rho_{gage}$  = water density in gage tubing = 62.28 lbm/ft<sup>3</sup> @ 70°F, Reference 66
- $g$  = gravitational acceleration = 32.2 ft/s<sup>2</sup> = 4.17(10<sup>8</sup>) ft/hr<sup>2</sup>
- $g_c$  = units conversion constant = 32.2 lbm-ft/lbf-s<sup>2</sup> = 4.17(10<sup>8</sup>) lbm-ft/lbf-hr<sup>2</sup>
- $z_u$  = elevation of upstream pressure instrument = 12 ft.
- $z_i$  = elevation of the inlet pressure tap = 9 ft.
- $z_o$  = elevation of the outlet pressure tap = 13 ft.
- $K_{i,pipe}$  = loss coefficient for the fittings and pipe between the inlet pressure instrument and nozzle = 0.10 based on 6 in. Schedule 40 pipe
- $v_i$  = inlet pipe flow velocity
- $K_{o,pipe}$  = loss coefficient for the fittings and pipe between the outlet pressure instrument

and nozzle = 0.25 based on 6 in. Schedule 40 pipe

$$A_{i,pipe} = \text{flow area of the inlet piping} = \left( \frac{\pi}{4} \right) 6.065^2 = 28.89 \text{ in.}^2 = 0.2006 \text{ ft}^2$$

$$A_{o,pipe} = \text{flow area of the outlet piping} = \left( \frac{\pi}{4} \right) 6.065^2 = 28.89 \text{ in.}^2 = 0.2006 \text{ ft}^2$$

The inlet velocity is calculated based the inside diameter of 6 in. Schedule 40 pipe and the measured volumetric flow rate:

$$v_i = (500 \text{ gpm}) \left( \frac{1}{\frac{\pi}{4} 6.065^2 \text{ in.}^2} \right) \left( \frac{1 \text{ ft}^3}{7.4805 \text{ gal}} \right) \left( \frac{144 \text{ in.}^2}{1 \text{ ft}^2} \right) \left( \frac{1 \text{ min}}{60 \text{ s}} \right) \\ = 5.553 \text{ ft/s} = 19990 \text{ ft/hr}$$

The total nozzle-to-nozzle pressure loss at test conditions is:

$$\Delta P_{n-n} = 62.40 \left[ \begin{array}{l} \frac{288}{62.38} + \left( \frac{1}{62.42} - \frac{1}{62.38} \right) \\ \left( 6869 + 62.28 \frac{32.2}{32.2} (12 - 9) \right) \\ + \left( 1 - \frac{62.28}{62.38} \right) \frac{32.2}{32.2} (9 - 13) \\ + \left( 1 - 0.10 - (1 + 0.25) \right) \\ \left( \frac{62.42(0.2006)}{62.38(0.2006)} \right)^2 \frac{5.553^2}{2(32.2)} \end{array} \right] \\ = 272.7 \text{ lbf/ft}^2 = 1.894 \text{ psid}$$

The uncertainty of the total nozzle-to-nozzle pressure drop is calculated based on uncertainties in the measured pressure, estimated loss coefficients for the upstream and downstream pipe, and uncertainty in flow rate measurement. The uncertainty in elevation measurements and density determination is neglected.

$$u_{\Delta P} = \text{uncertainty of differential pressure measurement} = 0.01(2.00) = 0.02 \text{ psi}$$

$$u_{P_u} = \text{uncertainty of upstream pressure measurement} = 0.25 \text{ psi}$$

$$u_{K_{pipe i}} = \text{uncertainty of upstream piping loss coefficient} = 0.20(0.10) = 0.02 \text{ assuming a 20\% uncertainty in the loss coefficient data in Reference 16}$$

$$u_{K_{pipe o}} = \text{uncertainty of downstream piping loss coefficient} = 0.20(0.25) = 0.05 \text{ assuming a 20\% uncertainty in the loss coefficient data in Reference 16}$$

$$u_{v_i} = 0.02(5.553) = 0.1111 \text{ ft/s}$$

The uncertainty of the total nozzle-to-nozzle pressure loss is calculated based on Eq. (B.12) and sensitivity coefficients in Table B.6. The results are shown in Table K.18.

$$\Delta P_{n-n} = 1.894 \pm 0.023 \text{ psi}$$

**TABLE K.18**  
**UNCERTAINTY IN TOTAL NOZZLE-TO-NOZZLE PRESSURE LOSS AT TEST**  
**CONDITIONS**

Contributing Factor	Uncertainty, $u$	Sensitivity, $\theta$	Uncertainty Contribution, $(\theta u)^2$ (psi) <sup>2</sup>
Differential pressure measurement, $\Delta P$	0.02 psi	1.000	4.00(10) <sup>-4</sup>
Upstream pressure measurement, $P_u$	0.25 psi	-6.41(10 <sup>-4</sup> )	0.00026(10 <sup>-4</sup> )
Loss coefficient for inlet pipe and fittings, $K_{pipe,i}$	0.02	-0.207 psi	0.17(10) <sup>-4</sup>
Loss coefficient for outlet pipe and fittings, $K_{pipe,o}$	0.05	-0.208 psi	1.08(10) <sup>-4</sup>
Inlet pipe velocity, $V_i$	0.1111 ft/s	0.0263 psi-s/ft	0.09(10) <sup>-4</sup>
Total uncertainty in total nozzle-to-nozzle pressure loss at test conditions = 0.023 psi.			

(c) Calculate the Total Pressure Loss at Reference Conditions (para. 5.4.7). The total pressure loss at reference conditions is determined by Eq. (5.17):

$$\Delta P_{n-n}^* = \phi_{\Delta P} \Delta P_{n-n}$$

where

$\phi_{\Delta P}$  = correction factor calculated using Eq. (F.15)

$$\phi_{\Delta P} = \left( \frac{\Delta P_{n-n}^*}{\Delta P_{n-n} \text{ calculated}} \right)$$

$$= \frac{\left[ \Delta P_{\text{entry}} + 4f \rho_{\text{ave}} \frac{L}{d_i} \frac{v_i^2}{2g_c} + \Delta P_{\text{exit}} \right]^*}{\Delta P_{\text{entry}} + 4f \rho_{\text{ave}} \frac{L}{d_i} \frac{v_i^2}{2g_c} + \Delta P_{\text{exit}}}$$

Equation (F.15) can be rewritten as follows to facilitate the use of hydraulic handbook data to estimate the entry and exit losses:

$$\phi_{\Delta P} = \frac{\left[ m_t^2 \left( \frac{1}{\rho_i} K_i + \frac{1}{\rho_{\text{ave}}} 4f \frac{L}{d_i} + \frac{1}{\rho_o} K_o \right) \right]^*}{m_t^2 \left( \frac{1}{\rho_i} K_i + \frac{1}{\rho_{\text{ave}}} 4f \frac{L}{d_i} + \frac{1}{\rho_o} K_o \right)} \quad (\text{K.5})$$

$$= \frac{H_R^*}{H_R} \left( \frac{m_t}{m_t} \right)^2$$

where

$m_t^*$  = tube side mass flow rate at reference conditions

$m_t$  = tube side mass flow rate at test conditions

$H_R^*$  = hydraulic resistance at reference conditions

$H_R$  = hydraulic resistance at test conditions

$K_i$  = contraction loss coefficient associated with the tube entry

$K_o$  = expansion loss coefficient associated with tube exit

$f$  = Fanning friction factor as defined by Eq. (F.8)

$L$  = tube length = 10 ft = 120 in.

$d_i$  = inside tube diameter = 0.500 - 2(0.049) = 0.402 in.

$\rho_i^*$  = inlet water density at reference conditions = 62.17 lbm/ft<sup>3</sup>@85°F

$\rho_o^*$  = outlet water density at reference conditions = 62.02 lbm/ft<sup>3</sup>@98.3°F

$\rho_{\text{ave}}^*$  = average water density at reference conditions =  $(\rho_i^* + \rho_o^*)/2$  = 62.10 lbm/ft<sup>3</sup>

$\rho_i$  = inlet water density at test conditions = 62.42 lbm/ft<sup>3</sup>@50°F

$\rho_o$  = outlet water density at test conditions = 62.38 lbm/ft<sup>3</sup>@58°F

$\rho_{\text{ave}}$  = average water density at test conditions =  $(\rho_i + \rho_o)/2$  = 62.40 lbm/ft<sup>3</sup>

The mass flow rate and associated ratio are given by:

$$m_t^* = \rho_i^* (574 \text{ gpm})$$

$$= \left( 62.17 \frac{\text{lbm}}{\text{ft}^3} \right) (574 \text{ gpm}) \left( \frac{1 \text{ ft}^3}{7.4805 \text{ gal}} \right) \left( \frac{60 \text{ min}}{1 \text{ hr}} \right)$$

$$\begin{aligned}
 &= 2.862(10)^5 \text{ lbm/hr} \\
 m_t &= \rho_i(500 \text{ gpm}) \\
 &= \left(62.42 \frac{\text{lbm}}{\text{ft}^3}\right) (500 \text{ gpm}) \left(\frac{1 \text{ ft}^3}{7.4805 \text{ gal}}\right) \left(\frac{60 \text{ min}}{1 \text{ hr}}\right) \\
 &= 2.503(10)^5 \text{ lbm/hr} \\
 \frac{m_t^*}{m_t} &= \frac{\rho_i^*(574 \text{ gpm})}{\rho_i(500 \text{ gpm})} = \frac{62.17(574)}{62.42(500)} = 1.143
 \end{aligned}$$

The ratio of the hydraulic resistances is a function of the tube side Reynolds number, roughness, and heat exchanger geometry. While an inspection of the water boxes prior to the test indicated that none of the tubes were plugged and tubes were not blocked by macrofouling, the tube surface was not cleaned to bare metal. In addition, the water supply typically contains substantial biological activity and some particulate. Without additional data (such as intermediate pressure data within the tubes or previous-pressure-loss-versus-flow-rate data correlated with inspection results) bounding estimates for the hydraulic resistance ratio need to be developed.

Based on pre-test agreements, the following approach is used to estimate the maximum and minimum hydraulic resistance ratio. Equation (K.5) is used as the basis for the following expression of the hydraulic resistance ratio:

$$\frac{H_R^*}{H_R} = \frac{\rho_{ave}}{\rho_{ave}^*} \frac{\left(\frac{\rho_{ave}}{\rho_i} K_i + 4f \frac{L}{d_i} + \frac{\rho_{ave}}{\rho_o} K_o\right)^*}{\left(\frac{\rho_{ave}}{\rho_i} K_i + 4f \frac{L}{d_i} + \frac{\rho_{ave}}{\rho_o} K_o\right)} \quad (\text{K.6})$$

The maximum hydraulic resistance ratio is estimated by assuming that the inside surface of the tubes is sufficiently roughened so that the Fanning friction factor  $f$  is independent of Reynolds number in the region of complete turbulence (as shown on the Moody diagram, Reference 16). Under these conditions, the following approximations are considered reasonable:

$$\begin{aligned}
 \text{Maximum } H_R^*/H_R: f^* &= f, K_i^* = K_i, K_o^* = K_o, \\
 \frac{\rho_{ave}^*}{\rho_i^*} &\approx \frac{\rho_{ave}}{\rho_i}, \frac{\rho_{ave}^*}{\rho_o^*} \approx \frac{\rho_{ave}}{\rho_o}
 \end{aligned}$$

Equation (K.6) is reduced to the following:

$$\left(\frac{H_R^*}{H_R}\right)_{\max} = \frac{\rho_{ave}}{\rho_{ave}^*} = \frac{62.40}{62.10} = 1.005$$

The minimum hydraulic resistance ratio is estimated by assuming that the total pressure loss is dominated by frictional losses in the tubes, and the tubes are smooth so that the friction factor changes with Reynolds number. With these assumptions, the following bounding approximations are considered:

$$\begin{aligned}
 \text{Minimum } H_R^*/H_R: &\left(\frac{\rho_{ave}}{\rho_i} K_i\right. \\
 &+ \left.\frac{\rho_{ave}}{\rho_o} K_o \ll 4f \frac{L}{d_i}\right)^*, \frac{\rho_{ave}}{\rho_i} K_i + \frac{\rho_{ave}}{\rho_o} K_o \ll 4f \frac{L}{d_i}
 \end{aligned}$$

The minimum hydraulic resistance ratio becomes:

$$\left(\frac{H_R^*}{H_R}\right)_{\min} = \frac{\rho_{ave} f^*}{\rho_{ave}^* f}$$

The friction factor is estimated using Eq. (F.11):

$$\frac{1}{\sqrt{f}} = 4 \log_{10} \frac{Re_t \sqrt{f}}{1.255}$$

where

$$Re_t = \text{tube-side Reynolds number defined in Eq. (F.2)}$$

The results of friction-factor calculations are in Table K.19.

$$\left(\frac{H_R^*}{H_R}\right)_{\min} = \frac{\rho_{ave} f^*}{\rho_{ave}^* f} = \frac{62.40}{62.10} \frac{0.00683}{0.00802} = 0.856$$

The best estimate of the hydraulic resistance ratio is the average of the maximum and minimum:

$$\begin{aligned}
 H_R^*/H_R &= \frac{\left(\frac{H_R^*}{H_R}\right)_{\max} + \left(\frac{H_R^*}{H_R}\right)_{\min}}{2} \\
 &= \frac{1.005 + 0.856}{2} = 0.931
 \end{aligned}$$

**TABLE K.19**  
**FRICTION FACTORS AT TEST AND REFERENCE CONDITIONS FOR**  
**SMOOTH TUBES**

Conditions	$m_t$ (lbm/hr)	$\mu$ (lbm/hr-ft)	$Re_t$	$f$
Test	2.503(10) <sup>5</sup>	3.01	8660	0.00802
Reference	2.862(10) <sup>5</sup>	1.85	16100	0.00683

**TABLE K.20**  
**UNCERTAINTY IN TOTAL NOZZLE-TO-NOZZLE PRESSURE LOSS AT**  
**REFERENCE CONDITIONS**

Contributing Factor	Uncertainty, $u$	Sensitivity, $\theta$	Uncertainty Contribution, $(\theta u)^2$ (psi) <sup>2</sup>
Total pressure loss at test conditions, $\Delta P_{n-n}$	0.023 psi	1.216	7.8(10) <sup>-4</sup>
Mass flow rate, $m_t$	5006 lbm/hr	1.841 (10) <sup>-5</sup> psi/(lbm/hr)	84.9(10) <sup>-4</sup>
Hydraulic resistance ratio, $H_R^*/H_R$	0.0745	2.474 psi	339.7(10) <sup>-4</sup>
Total uncertainty in total nozzle-to-nozzle pressure loss at reference conditions = 0.208 psi.			

The pressure loss at reference conditions is estimated to be:

$$\begin{aligned}\Delta P_{n-n}^* &= \frac{H_R^*}{H_R} \left( \frac{m_t^*}{m_t} \right)^2 \Delta P_{n-n} \\ &= (0.931)(1.143)^2(1.894) = 2.304 \text{ psi}\end{aligned}$$

The uncertainty in mass flow rate is estimated as  $0.02 m_t = 0.02(250,300) = 5006$  lbm/hr. The uncertainty in hydraulic resistance ratio is estimated as:

$$\begin{aligned}&\frac{\left( H_R^*/H_R \right)_{\max} - \left( H_R^*/H_R \right)_{\min}}{2} \\ &= \frac{(1.005 - 0.856)}{2} = 0.0745\end{aligned}$$

The uncertainty is evaluated using Eq. (B.13) and the sensitivity coefficients in Table B.7. The results are summarized in Table K.20.

$$\Delta P_{n-n}^* = 2.30 \pm 0.21 \text{ psi}$$

### K.3 THERMAL PERFORMANCE OF AN AIR COOLER

A room cooler in an industrial facility has been designed to remove heat dissipated from electrical equipment, piping, and motors and to maintain ambient room temperatures and adequate air circulation. Room air is pulled across coils through an unducted inlet and discharged back into the room through a ducted outlet. River water splits into separate headers and passes through two stacked coils.

In this example, the cooler is tested to determine air- and water-side temperatures, heat loads, and uncertainties. A pre-test uncertainty analysis specifies that thirty-two inlet and twenty-four outlet air temperature locations, and six inlet water and eight outlet water temperature locations, are to be used using a 30 second sampling frequency. Flow rates and uncertainties are provided to allow calculation of heat load and heat load uncertainty. The coolers are placed in operating mode 12 hr prior to testing. Adjacent

systems are held fixed over the test period to reduce load variation. Figures K.3 and K.4 show the air-side and water-side geometry and measurement locations, respectively.

### K.3.1 Measurements

(a) *Inlet Air Temperature Data.* Inlet air temperatures are sampled using a movable rack. The rack has 4 sensors fastened at equal distances along its width and is moved vertically to 8 different locations for a total of 32 measurements. Because reducing high spatial variation on inlet air requires a large number of measurement points, a moveable rack can reduce the number of sensors used in tests. A key assumption in using a moveable rack, however, is that the measurements remain steady over the test period. Air measurements were taken from top to bottom across the two coil sections, Fig. K.3. Rows are labeled "1" through "8." Measurements across the width of the cooler are labeled "A" through "D."

A time trace for each of the 8 rows (rack locations) is presented in Fig. K.5. Average inlet air temperature for each location is presented in Table K.21. The temperatures for each row vary significantly across the face showing spatial variation. By looking at the outlet air or water temperature traces (Fig. K.6), which were collected continuously over the entire test period, the test engineer can see that the maximum change in temperature is less than 0.3°F, suggesting that steady conditions prevailed over the entire test period.

(b) *Outlet Air Temperature Data.* Outlet air temperature sensors are placed in a 3x8 circular grid pattern at the entrance to the exhaust ductwork, Fig. K.3. Outlet air measurements were collected over the entire test period. Average spatial temperatures for each of the 24 locations are presented in Table K.22. A composite average temperature is plotted versus time in Fig. K.6.

(c) *Water Temperature Data.* Inlet and outlet water temperatures were measured with surface mounted RTD's placed at equally spaced locations around the circumference of the pipe. Six inlet and eight outlet locations were measured. Two separate insulation blankets of 1 in., thickness were fastened snugly over the sensors. The joints from each blanket were staggered from each other and centered between sensors. The configuration of the inlet water measurement stations is shown in Fig. K.4. Inlet water temperatures were obtained with surface mounted sensors placed beneath two inches of insulation. Water temperature data is shown in Table K.23 and in Fig. K.6.

(d) *Other Data.* The details of other measurement practices are not provided in this example. Other data needed to calculate the heat transfer rate includes air flow rate, water flow rate and relative humidity:

Air flow rate = 75,000 cfm

Water flow rate = 150,000 lbm/hr

Inlet air relative humidity = 35%

(e) *Air Temperature Uncertainty.* The calibration uncertainty of the air temperature instruments is  $\pm 0.2^\circ\text{F}$ . The uncertainties attributed to installation, data acquisition and random instrument effects are considered negligible. Data traces in Fig. K.6 show small process variations during the test period. Since a movable rack is used for the inlet air measurements, only a small window of data is available for each row and the error attributed to these variations cannot be reduced by averaging data over the test period (using methods discussed in Appendix A). Instead, a bounding estimate of the process variations is applied to all the temperatures. The bounding estimate of process variations is  $\pm 0.2^\circ\text{F}$ .

The uncertainty attributed to spatial variation is calculated based on equal weighting of each temperature measurement in the calculation of the bulk average. The spatial precision of the inlet temperature is the standard deviation of the measurements at each location, and the uncertainty due to spatial variation is given by Eq. (K.1):

$$b_{\text{SpatVar}} = \hat{t} \sqrt{\frac{s_x^2}{J}}$$

where

$s_x$  = spatial precision of the air measurements =  
0.698°F for the inlet air measurements and  
1.382°F for the outlet air measurements

$J$  = number of measurement locations = 32  
for inlet air and 24 for outlet air

$\hat{t}$  = Student  $t$  for  $J-1$  degrees of freedom =  
2.042 for inlet air measurements and 2.069  
for outlet air measurements

The uncertainty of the air temperature measurements is summarized in Table K.24

In evaluating the air-side uncertainty values, the outlet uncertainty is substantially higher than that for the inlet. This suggests that the variation in actual outlet conditions was substantially different than suggested by pre-test data. In future tests of this cooler, increasing the number of outlet measurements can reduce the uncertainty.

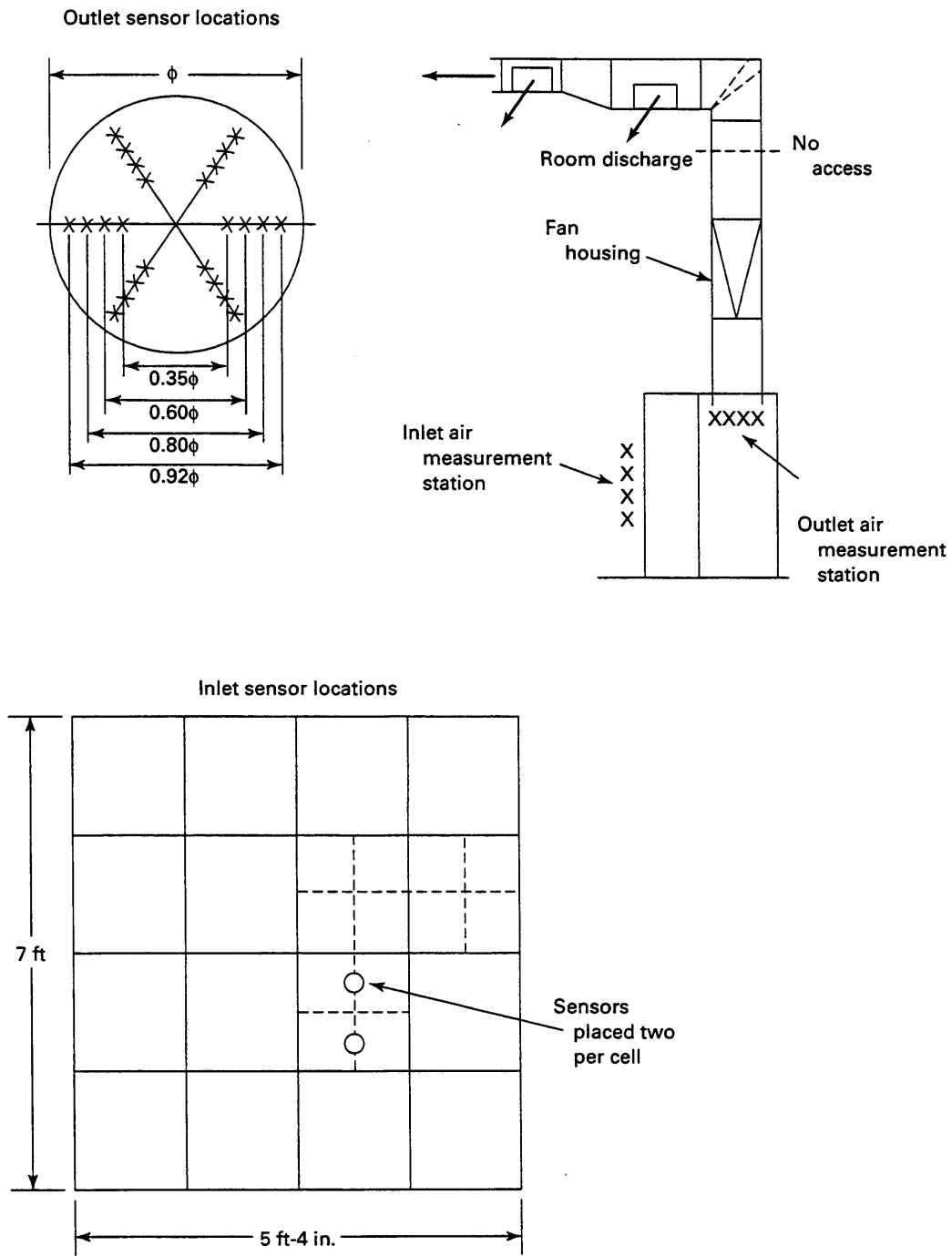


FIG. K.3 AIR MEASUREMENT LOCATIONS

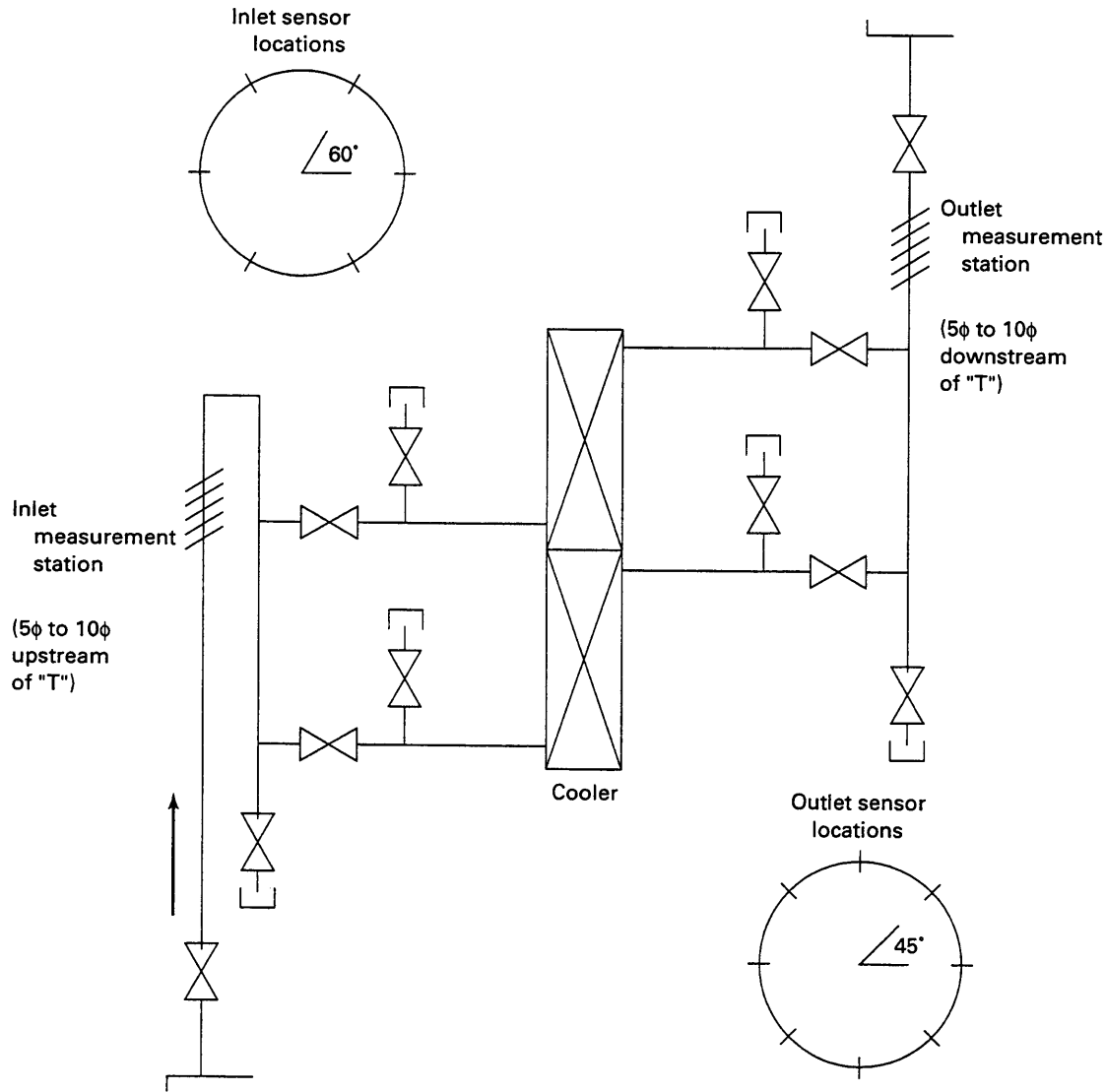


FIG. K.4 WATER MEASUREMENT LOCATIONS

(f) *Water Temperature Uncertainty.* The calibration uncertainty of the water temperature instruments is  $\pm 0.2^\circ\text{F}$ . The uncertainties attributed to installation, data acquisition and random instrument effects are considered negligible. Data traces in Fig. K.6 show small process variations during the test period. The standard deviation of the mean of these process variations is negligible for this test.

The uncertainty attributed to spatial variation is calculated based on equal weighting of each temperature measurement in the calculation of the bulk average. The spatial precision of the inlet temperature is the standard deviation of the measurements at

each location, and the uncertainty due to spatial variation is given by Eq. (K.1):

$$b_{\text{SpatVar}} = \hat{t} \sqrt{\frac{s_x^2}{J}}$$

where

$s_x$  = spatial precision of the water measurements =  $0.172^\circ\text{F}$  for the inlet water measurements and  $0.074^\circ\text{F}$  for the outlet water measurements,

$J$  = number of measurement locations

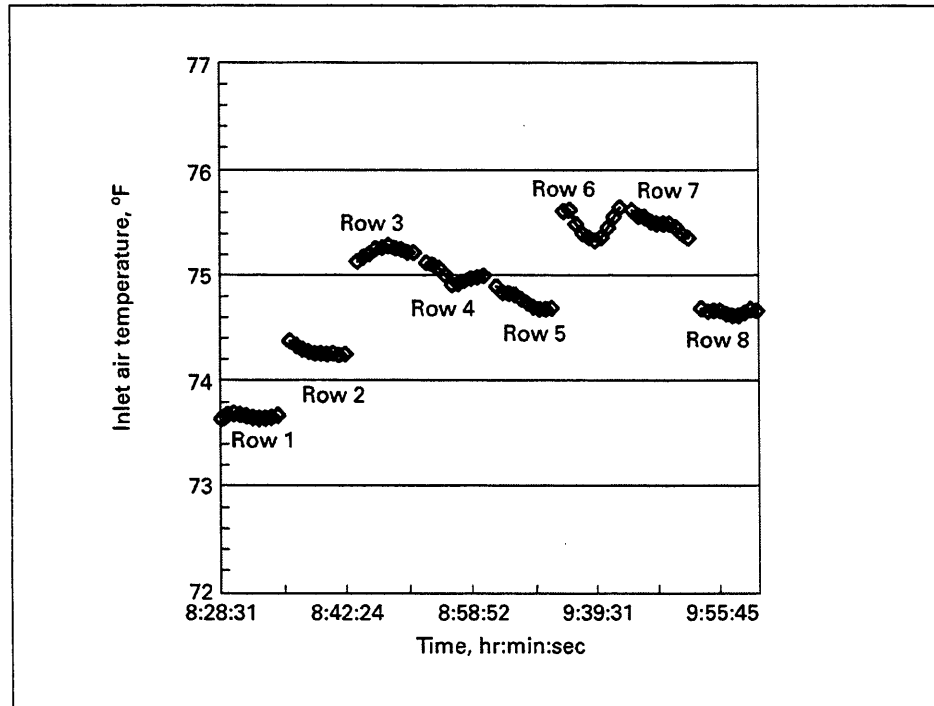


FIG. K.5 TIME TRACE OF AIR INLET TEMPERATURE

TABLE K.21  
TIME-AVERAGED INLET AIR TEMPERATURES BY LOCATION, °F

Rack Position	A	B	C	D	Average
Row 1	73.60	73.64	73.91	73.53	73.67
Row 2	73.97	74.04	74.61	74.50	74.28
Row 3	74.84	74.85	75.66	75.53	75.22
Row 4	74.61	74.81	75.40	75.13	74.99
Row 5	74.56	75.20	74.34	74.89	74.75
Row 6	75.73	75.78	74.54	75.79	75.46
Row 7	75.31	75.41	75.60	75.55	75.47
Row 8	74.15	73.90	75.27	75.18	74.63
Column Average	74.60	74.70	74.92	75.01	74.81

**TABLE K.22**  
**TIME-AVERAGED OUTLET AIR TEMPERATURES**  
**BY LOCATION, °F**

	A	B	C	Average
1	64.43	68.27	66.41	66.37
2	63.94	64.18	66.44	64.85
3	64.26	65.70	64.14	64.70
4	65.50	67.95	64.16	65.87
5	68.39	64.41	64.62	65.81
6	64.71	64.28	65.39	64.79
7	63.85	64.23	65.60	64.56
8	63.93	65.20	64.48	64.54
Column Average	64.88	65.53	65.16	65.19

**TABLE K.23**  
**TIME-AVERAGED INLET AND OUTLET WATER**  
**TEMPERATURES BY LOCATION, °F**

Position	Inlet	Outlet
1	60.30	65.19
2	60.42	65.20
3	60.31	65.33
4	60.52	65.13
5	60.49	65.23
6	60.05	65.24
7	...	65.20
8	...	65.08
Column Average	60.35	65.20

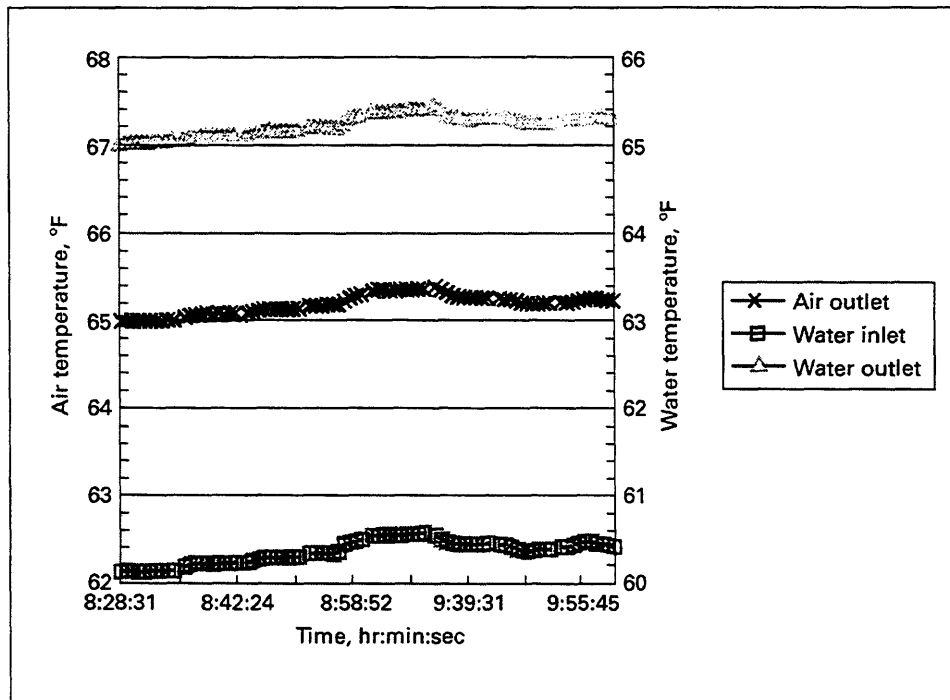


**FIG. K.6 TIME TRACE OF TEMPERATURES**

**TABLE K.24**  
**AIR TEMPERATURE UNCERTAINTIES**

Parameter	$b_{cal}$ (°F)	$u_{pv}$ (°F)	$b_{SpatVar}$ (°F)	$u_{overall}$ (°F)
$T_i$	0.2	0.2	0.252	0.38
$T_o$	0.2	0.2	0.584	0.65

**TABLE K.25**  
**WATER TEMPERATURE UNCERTAINTIES**

Parameter	$b_{cal}$ (°F)	$b_{SpatVar}$ (°F)	$u_{overall}$ (°F)
$t_i$	0.2	0.180	0.27
$t_o$	0.2	0.062	0.21

$\hat{t}$  = Student  $t$  for  $J-1$  degrees of freedom =  
2.571 for inlet water measurements and  
2.365 for outlet water measurements

The uncertainty of the water temperature measurements is summarized in Table K.25

(g) *Uncertainty of Other Measurements.* The uncertainties of the other measurements are not investigated in this example. The overall uncertainty of the air flow measurement is estimated as  $\pm 6\%$  of reading. The overall uncertainty of the water flow measurement is estimated as  $\pm 4\%$  of reading. The uncertainty of the relative humidity measurement is  $\pm 3\%$ .

The measurement data can be summarized as follows:

$$T_i = 74.81 \pm 0.38^\circ\text{F}$$

$$T_o = 65.19 \pm 0.65^\circ\text{F}$$

$$\text{Air flow rate} = 75,000 \pm 4500 \text{ cfm}$$

$$RH = 35 \pm 3\%$$

$$t_i = 60.35 \pm 0.27^\circ\text{F}$$

$$t_o = 65.20 \pm 0.21^\circ\text{F}$$

$$m_c = 150,000 \pm 6,000 \text{ lbm/hr}$$

### K.3.2 Heat Transfer Calculations

(a) *Air Side Heat Transfer Rate.* The air side heat transfer rate is calculated based on Eq. (5.1):

$$Q_h = m_h c_{p,h} (T_i - T_o)$$

The specific heat of moist air is calculated using ASHRAE psychrometric charts, Reference 69. At the inlet conditions of  $74.81^\circ\text{F}$  at 35% relative humidity, the humidity ratio is 0.0064 lbm moisture/lbm dry air. The inlet enthalpy is 24.96 Btu/lbm(dry air). Since no moisture condenses, the humidity remains constant and the outlet enthalpy is 22.62 Btu/lbm(dry air). The average specific heat is:

$$c_{p,h} = \frac{h_i - h_o}{T_i - T_o} = \frac{24.96 - 22.62}{74.81 - 65.19} \\ = 0.243 \text{ Btu/lbm(dry air)-}^\circ\text{F}$$

The uncertainty of the specific heat is estimated to be  $\pm 1\%$  based on para. 5.3.1.1. The mass flow rate is calculated based on a specific volume of 13.62  $\text{ft}^3/\text{lbm(dry air)}$ .

$$m_h = \left(75,000 \frac{\text{ft}^3}{\text{min}}\right) \left(\frac{1 \text{ lbm(dry air)}}{13.62 \text{ ft}^3}\right) \left(60 \frac{\text{min}}{\text{hr}}\right) \\ = 330,400 \text{ lbm/hr}$$

The heat transfer rate becomes:

$$Q_h = (330,400)(0.243)(74.81 - 65.19) \\ = 7.724(10^5) \text{ Btu/hr}$$

The uncertainty is calculated based on Eq. (B.6) and the sensitivity coefficients in Table B.2. The results are summarized in Table K.26.

$$Q_h = 772,000 \pm 77,000 \text{ Btu/hr}$$

(b) *Water Side Heat Transfer Rate.* The water side heat transfer rate is calculated based on Eq. (5.2):

$$Q_c = m_c c_{p,c} (t_o - t_i)$$

The average specific heat of water is 0.998 Btu/lbm- $^\circ\text{F}$  from Reference 66. The uncertainty of the specific heat is estimated to be  $\pm 1\%$  based on para. 5.3.1.1. The heat transfer rate becomes:

**TABLE K.26**  
**UNCERTAINTY IN HOT STREAM HEAT TRANSFER RATE**

Contributing Factor	Uncertainty, $u$	Sensitivity, $\theta$	Uncertainty Contribution, $(\theta u)^2$ (Btu/hr) <sup>2</sup>
Inlet temperature, $T_i$	0.38°F	80,300 Btu/hr-°F	931(10 <sup>6</sup> )
Outlet temperature, $T_o$	0.65°F	-80,300 Btu/hr-°F	2720(10 <sup>6</sup> )
Mass flow rate, $m_h$	19,800 lbm/hr	2.34 Btu/lbm	2150(10 <sup>6</sup> )
Specific heat, $c_{p,h}$	0.00243 Btu/lbm-°F	3.18(10 <sup>6</sup> ) lbm-°F/hr	59.7(10 <sup>6</sup> )
Total uncertainty in hot stream heat transfer rate = 77,000 Btu/hr			

**TABLE K.27**  
**UNCERTAINTY IN COLD STREAM HEAT TRANSFER RATE**

Contributing Factor	Uncertainty, $u$	Sensitivity, $\theta$	Uncertainty Contribution, $(\theta u)^2$ (Btu/hr) <sup>2</sup>
Inlet temperature, $t_i$	0.27 °F	-150,000 Btu/hr-°F	1640(10 <sup>6</sup> )
Outlet temperature, $t_o$	0.21°F	150,000 Btu/hr-°F	992(10 <sup>6</sup> )
Mass flow rate, $m_c$	6000 lbm/hr	4.84 Btu/lbm	843(10 <sup>6</sup> )
Specific heat, $c_{p,c}$	0.00998 Btu/lbm-°F	0.728(10 <sup>6</sup> ) lbm-°F/hr	52.8(10 <sup>6</sup> )
Total uncertainty in cold stream heat transfer rate = 59,000 Btu/hr.			

$$Q_h = (150,000)(0.998)(65.20 - 60.35) \\ = 7.26(10^5) \text{ Btu/hr}$$

The uncertainty is based on Eq. (B.5) and the sensitivity coefficients in Table B.2. The results are summarized in Table K.27.

$$Q_c = 726,000 \pm 59,000 \text{ Btu/hr}$$

(c) *Weighted Average Heat Transfer Rate.* The heat balance is assessed by evaluating the overlap of uncertainty bars. This example meets the conditions of complete overlap as shown in case a for Fig. 5.1. A heat balance is confirmed and the weighted average heat transfer rate is calculated in accordance with Eq. (5.3):

$$Q_{ave} = \left( \frac{u_{Qh}^2}{u_{Qc}^2 + u_{Qh}^2} \right) Q_c + \left( \frac{u_{Qc}^2}{u_{Qc}^2 + u_{Qh}^2} \right) Q_h \\ = \left( \frac{77^2}{59^2 + 77^2} \right) 726,000 + \left( \frac{59^2}{59^2 + 77^2} \right) 772,000 \\ = 743,000 \text{ Btu/hr}$$

The uncertainty of the average heat transfer rate is calculated using Eq. (B.7):

$$u_{Qave} = \frac{[u_{Qc}^4 u_{Qh}^2 + u_{Qh}^4 u_{Qc}^2]^{1/2}}{u_{Qc}^2 + u_{Qh}^2} \\ = \frac{[59^4 77^2 + 77^4 59^2]^{1/2}}{59^2 + 77^2} (10)^3 = 47,000 \text{ Btu/hr}$$

The weighted average heat transfer rate is

$$Q_{ave} = 743,000 \pm 47,000 \text{ Btu/hr}$$

#### K.4 HYPOTHESIS TESTS TO EVALUATE HEAT BALANCE

The evaluation of a heat exchanger heat balance asks the fundamental question: Is there a significant difference between the observed heat loads of the hot and the cold fluid streams, when the observations are made under nominally identical conditions? If

the answer is in the affirmative, then the relevant data points should be rejected and the observations replicated, and/or the test procedure should be examined for faults.

The methodology for evaluating the question posed above involves the comparison of the difference between the heat load values and the estimated (sample) standard deviation of the difference. The computed ratio of these two quantities is compared to the value of the ratio if the probability (chosen by the test engineer before running the test) of its occurrence could be ascribed to a chance effect. This requires the assumption that there is no significant difference, that is, the observed values of the hot ( $Q_h$ ) and the cold ( $Q_c$ ) heat loads come from the same statistical populations of individual measurements of heat load and that the corresponding mean values ( $\bar{Q}_h$ ,  $\bar{Q}_c$ ) come from statistical populations of (sample) mean heat loads that have, at least, identical population means ( $\hat{\mu}_h = \hat{\mu}_c$ ). The implication that the population means are equal ( $\hat{\mu}_h = \hat{\mu}_c$ ), is known as the null hypothesis. The whole technique of posing the question and investigating its answer using statistical and probabilistic concepts is known as hypothesis testing.

Logic suggests that there must be an alternative to the null hypothesis, and it is called the alternate hypothesis. In the case of the heat balance test, the question raised by the test engineer concerns the difference between the observed mean values of the heat loads, so the alternate hypothesis assumes that the observed difference between the mean values is significant. That is, it can be assumed that the individual values of the hot and cold stream heat loads, and the corresponding (sample) mean values are associated with statistical populations that have different mean values<sup>1</sup> ( $\hat{\mu}_h \neq \hat{\mu}_c$ ).

**Example K.4.1:** Two replications, under nominally constant conditions, of a heat transfer test have been carried out. The mean values of the two observations of the hot ( $h$ ) and cold ( $c$ ) stream heat loads ( $Q$ ) are as follows:

$$\begin{aligned}\bar{Q}_h &= 5.10 \times 10^5 \text{ W} \\ \bar{Q}_c &= 4.85 \times 10^5 \text{ W}\end{aligned}$$

<sup>1</sup> To those unfamiliar with the methodology of statistical hypothesis testing, the statement of the alternate hypothesis may appear to be a statement of the obvious. In spite of its possible obviousness, the proper formulation of the alternate hypothesis is related critically to the question posed by the test engineer. The further discussion of these matters must be referred to some other source. See Reference 77.

where the overbar indicates the sample mean values. The standard deviations ( $s_h$ ,  $s_c$ ) of the samples of two heat load observations are:

$$\begin{aligned}s_h &= \pm 0.05 \times 10^5 \text{ W} \\ s_c &= \pm 0.05 \times 10^5 \text{ W}\end{aligned}$$

The test engineer wishes to ascertain if the difference between the mean values of the heat loads is due to some significant effect (systematic error of the measurement) or can be treated as a chance effect associated with the inevitable random variability of the measurements.

The difference between the hot and cold heat loads is compared to the variability of the data using the observed test statistic ( $\hat{t}_o$ ) given by:

$$\hat{t}_o = \frac{|\bar{Q}_h - \bar{Q}_c|}{s_{\Delta Q}}$$

where<sup>2</sup>

$$s_{\Delta Q} = s_p \sqrt{\frac{1}{n_h} + \frac{1}{n_c}}$$

and

$$s_p^2 = \frac{(n_h - 1)s_h^2 + (n_c - 1)s_c^2}{n_h + n_c - 2}$$

In this case

$$s_p = \pm 0.05 \times 10^5 \text{ W}$$

and

<sup>2</sup> The indicated form of  $s_{\Delta Q}$  assumes that the standard deviations ( $\sigma_h, \sigma_c$ ) of the populations of individual observations are identical. Statistical tests (Fisher's F-test) are available to investigate this point formally. In addition or alternatively, the test engineer can make such an assumption on the grounds that, for example, the temperature and flow rate sensors are of the same type in the hot and cold streams, that their calibration procedures are the same, and that they have been installed in the heat exchanger in an identical manner. If the test engineer does not feel justified in making such assumptions and/or statistical tests do not support such a conclusion, then the  $s_{\Delta Q}$  used in the observed test statistic is  $s_{\Delta Q} = \sqrt{\frac{s_h^2}{n_h} + \frac{s_c^2}{n_c}}$  and the applicable degrees of freedom ( $d$ ) are given by

$$d = \frac{\left(\frac{s_h^2}{n_h} + \frac{s_c^2}{n_c}\right)}{\frac{(s_h/n_h)^2}{n_h + 1} + \frac{(s_c/n_c)^2}{n_c + 1}} - 2$$

$$s_{\Delta Q} = \pm 0.05 \times 10^5 \text{ W}$$

Then

$$\hat{t}_o = \frac{|5.10 \times 10^5 - 4.85 \times 10^5|}{\pm 0.05 \times 10^5} \\ = \pm 5$$

The observed test statistic ( $\hat{t}_o$ ) is compared with or tested against the expected value ( $\hat{t}_e$ ) of the same statistic if the difference between the heat loads was to be the consequence of a chance event of a probability that is assigned by the test engineer. This probability is known as the level of significance<sup>3</sup> of the comparison or test.

Suppose in this case that the test engineer judges that the observed difference ( $5.10 \times 10^5 - 4.85 \times 10^5 = 0.25 \times 10^5$ ), or a greater difference, would occur by chance in the test situation under consideration in about 10% of the cases of a long series of such heat balance determinations. In this case the expected value ( $\hat{t}_e$ ) of the test statistic obtained from standard statistical tables<sup>4</sup> is  $t_e = \pm 2.92$ . Since the observed value of the test statistic ( $\hat{t}_o = \pm 5$ ) is much larger than its expected value ( $\hat{t}_e = \pm 2.92$ ), then the probability that the difference between the observed mean heat load values or a larger difference, is due to chance is much less (about 3%) than that (10%) assumed by the test engineer. In these circumstances it would be reasonable to assume that the difference is a consequence of a systematic influence, such as an error associated with the flow rate measurement in one or both streams. The heat balance, as a consequence, can be considered unsatisfactory, and the corresponding weighted mean heat load ( $Q_{ave}$ ) should be discarded. The test should be repeated and/or the instrumenta-

<sup>3</sup> The choice of the level of significance depends fundamentally on two factors: (a) the manufacturer's desire to minimize the cost of a heat exchanger; (b) the customer's desire to avoid the purchase of equipment that does not perform according to the design specification. Roughly speaking, the two desires are complementary i.e., the more one desire is satisfied the less the other desire can be met. In practice, one desire tends to predominate over the other. For example, where a heat exchanger is a critical component of a plant then the desire under item (b) should predominate over item (a). In that case the level of significance of the heat balance test should be comparatively large, say 20%. That is, a comparatively small difference in hot and cold stream heat loads relative to the variability of the data should result in the rejection of the heat balance, with the possible result that the heat exchanger is condemned. This of course can be expected to result in an increase in the cost of a heat exchanger, but that is the price of meeting the imposed critical condition.

<sup>4</sup> Tables of Student's t-distribution were used with degrees of freedom ( $d$ ) given by  $d = n_h + n_c - 2$ , so in this case  $d = 2$ .

tion should be examined for the presence of systematic errors.

**Examples K.4.2 and K.4.3:** The following examples illustrate the two other possible outcomes, in addition to that presented in Example K.4.1, of a significance test applied to a heat exchanger heat balance. Since the methodology is identical to that of Example K.4.1, the relevant calculations are given in Table K.28.

## K.5 THERMAL PERFORMANCE OF A PLATE HEAT EXCHANGER

Three water-to-seawater plate heat exchangers (PHE) arranged in parallel are tested in the clean condition with the same test results as the shell-and-tube heat exchanger described in Example K.1.

(a) The geometric parameters for each PHE are as follows:

Number of heat exchangers,  $NHX = 3$   
 Plate width,  $L_w = 33.25$  in.  
 Compressed length of plates,  $L_c = 31.375$  in.  
 Number of plates,  $N_p = 179$   
 Number of channel passes,  $N_{cp} = 89$   
 Thickness of plate,  $\Delta X = 0.024$  in.  
 Effective area,  $A = 6134.79$  ft<sup>2</sup>  
 Wall resistance,  $r_w = 0.0002$  hr-ft<sup>2</sup>-°F/Btu

(b) Based on the average cold-side and hot-side fluid temperatures, the properties of the fluids are as follows (recalling that the cold-side fluid is seawater):

Cold water density,  $\rho_c = 63.99$  lbm/ft<sup>3</sup>  
 Cold water specific heat,  $c_{pc} = 0.96$  Btu/lbm °F  
 Cold water viscosity,  $\mu_c = 2.18$  lbm/ft-hr  
 Cold water thermal conductivity,  $k_c = 0.354$  Btu/hr-ft-°F  
 Hot water density,  $\rho_h = 62.11$  lbm/ft<sup>3</sup>  
 Hot water specific heat,  $c_{ph} = 1.0$  Btu/lbm-°F  
 Hot water viscosity,  $\mu_h = 1.74$  lbm/ft-hr  
 Hot water thermal conductivity,  $k_h = 0.358$  Btu/hr-ft-°F

(c) The following values may be calculated:  
 Channel plate spacing,  $b$

$$b = \left( \frac{L_c}{N_p} \right) - \Delta X = 0.1513 \text{ in.}$$

**TABLE K.28**  
**HEAT EXCHANGER HEAT BALANCE HYPOTHESIS TESTS**

Ex	$\bar{Q}_h$ [W]	$\bar{Q}_c$ [W]	$ \bar{Q}_h - \bar{Q}_c $ [W]	$\hat{t}_e$	$\hat{t}_e$ @ 10% L of $S(d = 2)$	Significance of $ Q_h - Q_c $	Action taken by the test engineer
K.4.2	$4.50 \times 10^5$	$4.60 \times 10^5$	$0.10 \times 10^5$	$\pm 2$	$\pm 2.92$	Not significant	Valid heat balance
K.4.3	$5.70 \times 10^5$	$5.55 \times 10^5$	$0.15 \times 10^5$	$\pm 3$	$\pm 2.92$	Uncertain	Repeat test. Anticipating unambiguous value of $t_o$

GENERAL NOTE: In both examples:  $s_h = \pm 0.05 \times 10^5$  W =  $s_c$  and  $\sigma_h = \sigma_c$  is assumed.

Hydraulic diameter,  $D_e$

$$D_e = \frac{4L_w b}{(2L_w + 2b)12} = 0.0251 \text{ ft.}$$

$$Re_h = \frac{D_e G_h}{\mu_h} = 9,280$$

Cold stream and hot stream mass velocities,  $G_c$  and  $G_h$

$$Pr_h = \frac{\mu_h C_{ph}}{k_h} = 4.85$$

$$G_c = \frac{m_c}{N_{cp} \left( \frac{b}{12} \right) \left( \frac{L_w}{12} \right) NHX} = 1,095,800 \left( \frac{\text{lbm}}{\text{ft}^2 \cdot \text{hr}} \right) \quad \text{and}$$

$$Re_c = \frac{D_e G_c}{\mu_c} = 12,600$$

$$G_h = \frac{m_h}{N_{cp} \left( \frac{b}{12} \right) \left( \frac{L_w}{12} \right) NHX} = 643,300 \left( \frac{\text{lbm}}{\text{ft}^2 \cdot \text{hr}} \right)$$

$$Pr_c = \frac{\mu_c C_{pc}}{k_c} = 5.92$$

The PHE is pure counterflow, so the log mean temperature difference, LMTD, may be calculated as:

$$LMTD = \frac{(T_i - t_o) - (T_o - t_i)}{\ln \left( \frac{T_i - t_o}{T_o - t_i} \right)} = 7.38^\circ \text{F}$$

Since the PHE was clean when tested, the overall heat transfer coefficient,  $U$ , is:

$$U = \frac{1}{\frac{1}{h_h} + \frac{1}{h_c} + r_w}$$

The heat transfer rate,  $U$ , may be calculated from the results of the test as:

$$U = \frac{Q}{A \text{ LMTD}} = 1,281 \left( \frac{\text{Btu}}{\text{hr} \cdot \text{ft}^2 \cdot ^\circ \text{F}} \right)$$

For a PHE the Colburn Analogy

$$Nu = \frac{h D_e}{k} = C Re^n Pr^m \left( \frac{\mu_b}{\mu_w} \right)^{0.14}$$

The Reynolds numbers and Prandtl numbers for the hot stream and cold streams are calculated from the fluid properties as follows:

is applicable where  $C$ ,  $n$ , and  $m$  are constants and  $\mu_b$  and  $\mu_w$  are the dynamic viscosity of the average bulk fluid and at the plate wall, respectively. The last term in the above equation may be neglected for nearly constant properties. Note that for PHE's

the geometry of the plate is the same on both sides of the plate, so the same equation for  $Nu$  applies to both sides. For turbulent heat transfer through a flat plate, the Nusselt number is directly proportional to the Reynolds number to the 0.75 power, and to the Prandtl number to the 0.333 power for gases, liquids, and viscous oils where  $Pr > 1$ . Therefore:

$$h_h = C Re_h^{3/4} Pr_h^{1/3} \left( \frac{k_h}{D_e} \right)$$

$$h_c = C Re_c^{3/4} Pr_c^{1/3} \left( \frac{k_c}{D_e} \right)$$

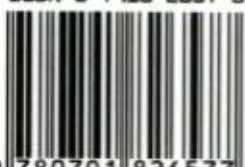
The value for  $C$  may be calculated by substituting these values for  $h_h$  and  $h_c$  into the equation for  $U$  above and setting it equal to  $U$  to yield the following equation:

$$C = \frac{\frac{D_e}{Re_h^{3/4} Pr_h^{1/3} k_h} + \frac{D_e}{Re_c^{3/4} Pr_c^{1/3} k_c}}{\frac{A LMTD}{Q} - r_w} = 0.132$$

Therefore, the values for  $h_h$  and  $h_c$  may be calculated following subsequent tests and the performance at reference conditions may be calculated as shown in Example K.1.



ISBN 0-7918-2657-0



9 780791 826577



C06500